RESERVOIR APPLICATIONS OF ARCED LABYRINTH WEIRS

by

Seth D. Thompson

A thesis submitted in partial fulfillment
of the requirements for the degree

of

MASTER OF SCIENCE

in

Civil and Environmental Engineering

Approved:

_____	_____
Blake P. Tullis, Ph.D. Major Professor	Brian M. Crookston, Ph.D. Committee Member
_____	_____
Joseph A. Caliendo, Ph.D. Committee Member	Richard S. Inouye, Ph.D. Vice Provost for Graduate Studies

UTAH STATE UNIVERSITY
Logan, Utah

2019

ABSTRACT

Reservoir Applications of Arced Labyrinth Weirs

by

Seth D. Thompson, Master of Science

Utah State University, 2019

Major Professor: Dr. Blake P. Tullis
Department: Civil and Environmental Engineering

In recent years, magnitudes of flood estimates used in hydraulic design have increased for many reservoirs. Consequently, many existing spillways are now deficient as they do not meet current discharge capacity requirements. To rehabilitate existing, fixed-width spillways, labyrinth weirs are often viable solutions. For reservoir applications, arcing labyrinth weirs into the reservoir increases hydraulic efficiency. This results from better cycle orientation to the approaching flow field.

This study supplements available arced labyrinth weir hydraulic data by observing flow characteristics of three laboratory-scale arced labyrinth weirs (α=16°, θ=10°, 20°, 30°, where α is sidewall angle and θ is arc angle); two numerical models (α=16°, θ=10°, 30°) were also developed using CFD software. The purpose of the CFD analysis was to assess the appropriateness of CFD as a design tool for arced labyrinth weir rating curve development.

Rating curves were developed using the physical models; velocity head, nappe behavior, and weir submergence were also evaluated. Results determined that velocity's contribution to total head was negligible; therefore, rating curves employ piezometric head alone. Arced labyrinth weirs with θ=30° were most efficient at dimensionless upstream head ratios (H/P)<~0.4, where H/P is upstream piezometric head divided by weir height. However, as θ increases, effects of downstream submergence increase, which, with increasing upstream head, decrease efficiency at H/P>~0.5. The θ=20° weirs were more efficient than θ=30° weirs at H/P>~0.3 and more efficient than θ=10° weirs at all discharges. Increasing θ improves discharge efficiency for $H/P \geq 0.3$.

The numerical model results were evaluated against the physical model data. Six discharges for both models were tested using five grid configurations. Good agreement between physical and numerical rating curves was found. The numerical models accurately demonstrated nappe behavior and submergence for θ=30° when compared with the physical model. The θ=10° numerical model showed an aerated nappe for $0.4<H/P<0.7$ while the physical model demonstrated drowned behavior. For arced labyrinth weirs, CFD can be a useful tool for implementing site-specific conditions; however, CFD models should be calibrated to reliable laboratory or field data.

This study's data may be used, with sound engineering judgement, to aid in the design of arced labyrinth weirs.

(158 pages)

PUBLIC ABSTRACT

Reservoir Applications of Arced Labyrinth Weirs

Seth D. Thompson, Master of Science

In recent years, magnitudes of flood estimates used in hydraulic design have increased for many reservoirs. Consequently, many existing spillways are now deficient as they do not meet current discharge capacity requirements. To rehabilitate existing, fixed-width spillways, labyrinth weirs are often viable solutions. For reservoir applications, arcing labyrinth weirs into the reservoir increases hydraulic efficiency. This results from better cycle orientation to the approaching flow field.

This study supplements available arced labyrinth weir hydraulic data by observing flow characteristics of three laboratory-scale physical models and two numerical (CFD) models. Physical model results provide head (energy)-discharge data and empirical coefficients for hydraulic design. Results also show that increasing the arc angle improves efficiency at $H/P<0.3$, where H/P is upstream piezometric head divided by weir height; after which, efficiency improvements diminish as downstream submergence also increases.

The purpose of the CFD analysis was to assess the appropriateness of CFD as a design tool for arced labyrinth weir head-discharge relationship development. The CFD model results found good agreement with the physical model data indicating CFD's usefulness as a hydraulic design tool; however, it is recommended that CFD models be calibrated to reliable laboratory or field data.

This study's data may be used, with sound engineering judgement, to aid in hydraulic design of arced labyrinth weirs

ACKNOWLEDGMENTS

The opportunity to research at the Utah Water Research Laboratory will forever be a cherished time in my life. There are several people that have helped lead me to this point that I would like to thank. Initially, Kyle Spencer, a professional civil engineer from my hometown, took the time to let me ride along with him for a day as we visited multiple local projects that he was working on. This solidified my decision to become a civil engineer. I transferred to Utah State University (USU) the next semester.

After a few semesters at Utah State, I attended a seminar organized by Dr. Ning Fang, and the USU NSF-STEM Scholarship team. The speaker was Mitchell Dabling; he spoke of an extremely interesting project related to pipeline hydraulics and hydropower generation. Mitch also spoke of the vital role that his research at the Utah Water Research Laboratory (UWRL) had in the development of his career. Without the advice Mitch gave, I would have never pursued undergraduate research nor a master's degree.

Shortly after attending the seminar I reached out to Mitch's previous major professor, Dr. Blake Tullis. Dr. Tullis hired me as an undergraduate researcher and has made this research possible. He has since been an excellent advisor, mentor, and friend.

I would also like to thank those who personally aided in the completion of this project: Dr. Brian Crookston for his mentorship and aid regarding numerical and physical modeling and his previous work in laying the foundation for arced labyrinth weir research; Dr. Zac Sharp, Andy Lee, Ethan Sunderland, Wyatt Lantz, and Taylor Vaughn for their aid in fabrication and installation of the physical models. Dr. Brian Crookston and Nathan Christensen also helped provide a starting point for this research through their graduate research relating to the hydraulic performance of arced labyrinth weirs.

Lastly, I would like to thank my beautiful wife, Chelsea; our son, Henry; my family, and God. Chelsea has always supported me and has spent countless late nights and Saturday's at the UWRL helping me collect data and survey the weir crests (best weir surveyor in the valley). Henry has given me added strength and motivation to do my best work with the purpose of providing our family with a better future. Our family has helped us take care of Henry, and always supported me in my education. Finally, God has blessed me with the strength, will, and knowledge necessary to finish this worthy endeavor.

– Seth Thompson

CONTENTS

Page

Page

LIST OF TABLES

Table Page

Table Page

LIST OF FIGURES

Figure Page

Figure Page

Figure Page

NOMENCLATURE

a, b, c, d	Empirically calculated coefficients
A	Upstream interior apex length
A_i	Grid surface interface area
b_{X_i}	Systematic standard error
C_d	Discharge coefficient
$C_{d\text{-}phys}$	Discharge coefficient calculated directly from physical data
$C_{d\text{-}emp}$	Discharge coefficient calculated from empirical fit to physical data
f_i	CFD solution of interest
F	Froude Number
F_s	Factor of safety
GCI	Grid Convergence Index
g	Gravitational constant
h	Piezometric head
H	Total head
H/P	Headwater ratio
l_c	Centerline length of sidewall
L_c	Centerline length of weir, L_c=$L_{c\text{-}cycle}$ *N
$L_{c\text{-}cycle}$	Centerline length of one complete cycle
N	Number of cycles
p	Fluid pressure
p_c	Order of convergence
P	Weir height

Q	Discharge or volumetric flow rate
ρ	Fluid density
r	Segment height from channel opening to center of imaginary arc circle
r'	Segment height from channel opening to perpendicular downstream apex
r_g	Grid refinement ratio, $r_g=\Delta_2/\Delta_1$
R	Arced radius, $R=(W^2/4 + r'^2)^{1/2}$
R_{crest}	Radius of crest shape
RM	CFD reservoir mesh
s_{X_i}	Random standard error
t_w	Wall thickness at crest
u	Local velocity in the y direction
u_{C_d}	Combined standard uncertainty in C_d
$U_{C_d 95}$	Standard uncertainty of C_d with 95% confidence intervals
v	Local velocity in the y direction
V	Depth averaged velocity
w	Local velocity in the z direction
w'	Cycle arc width, $w'=W'/N$
W	Downstream channel width
W'	Arced labyrinth weir arc width ($R\Theta$)
WM	CFD weir mesh
x	Horizontal cartesian coordinate direction perpendicular to channel outlet
y	Horizontal cartesian coordinate direction parallel to channel outlet
y_c	Critical depth

z	Vertical cartesian coordinate direction
α	Sidewall angle
α'	Upstream sidewall angle, $\alpha'=\alpha + \theta/2$
Δ_i	Representative CFD grid size
ε	Relative error between CFD grid size
ε	Turbulent dissipation term in numerical turbulence model
ε_{C_d}	Relative error in C_d between CFD and physical models
ε'	Cycle efficiency $\varepsilon'=C_d * L_{c\text{-}cycle}/w$
k	Turbulent kinetic energy in numerical turbulence model
ω_{X_i}	Sensitivity coefficient for each measured variable
θ	Cycle arc angle, $\theta=\Theta/N$
Θ	Central arc angle, $\Theta=W'/R$

INTRODUCTION

Weirs are hydraulic structures that are typically used for measuring flow rate, altering flow regime in channel applications, and controlling reservoir discharge. Weirs are often installed as the crest of a spillway to act as a passive discharge control structure. In recent years, magnitudes of inflow design floods (IDF) such as the probable maximum flood (PMF) have increased for many reservoir systems. The revised hydrologic analyses often result in hydraulically deficient spillways. As a countermeasure, non-linear weirs are often installed to rehabilitate a spillway by increasing discharge capacity.

Weir flow can be described using a standard form of the weir head-discharge equation (Eq. [1]). In Eq. [1], Q is the discharge over the weir's crest, C_d is an empirically determined discharge coefficient, L is the weir's crest length, H is the total head measured relative to the weir's crest elevation, and g is the acceleration of gravity.

$$Q = \frac{2}{3} C_d L \sqrt{2g}\, H^{\frac{3}{2}} \quad [1]$$

As seen in Eq. [1], the discharge (Q) is proportional to the weir's crest length (L). Therefore, as L increases, for a given constant upstream total head (H), Q also increases. Increasing spillway width (W) is often not a feasible solution to inadequate discharge capacity; however, folding a linear weir in plan view (see Fig. 1a and b) increases the allowable weir length without increasing W. The nonlinear weir shown in Fig. 1b is referred to as a labyrinth weir. Past research shows that labyrinth weirs can approximately double the discharge capacity relative to linear weirs at a constant H (Tullis et al. 1995).

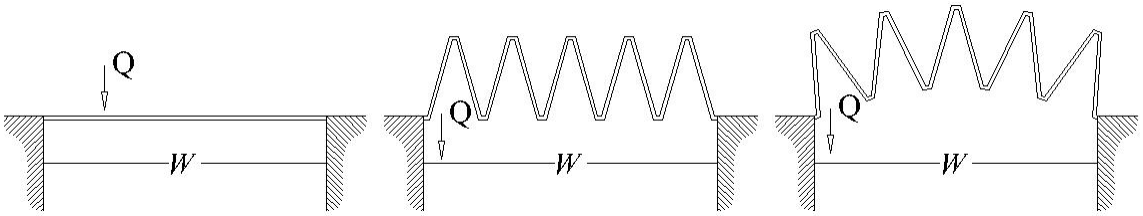

(a) (b) (c)

Fig. 1 Plan view of a (a) linear weir, (b) labyrinth weir, and (c) arced labyrinth weir.

Typically, labyrinth weirs are built in a linear configuration (see Fig. 1b) and have been researched extensively using laboratory flumes where flow is channelized and perpendicular to the weir. Labyrinth weir research dates to the initial efforts of Gentilini (1940) and Kozák and Sváb (1961). Since then, multiple studies have produced methods for linear labyrinth weir design: Taylor (1968), Hay and Taylor (1970) , Darvas (1971), Hinchliff and Houston (1984), Lux and Hinchliff (1985), Magalhães and Lorena (1989), Tullis et al. (1995), Melo et al. (2002), Tullis et al. (2007), Lopes et al. (2006, 2008), and Crookston and Tullis (2013). Moreover, Falvey (2003) compiled and summarized several key studies and design methods, including some of the afore-mentioned. The broad database of non-arced labyrinth weir research and design methods have provided practicing engineers a foundation upon which to hydraulically design labyrinth weirs. However, labyrinth weirs often behave differently in reservoir applications due to converging flow patterns, varying approach bathymetry and upstream spillway abutment shape.

For reservoir labyrinth weir applications, arcing the weir (see Fig. c) into the reservoir can increase the hydraulic efficiency of labyrinth weirs by ~5–11% (Crookston 2010). When a reservoir spillway is engaged, the approach flow patterns tend to converge toward the spillway. By arcing a labyrinth weir (with suitable approach flow conditions), the labyrinth cycles are better oriented to efficiently handle these flow patterns. Arcing the

labyrinth weir also increases the sidewall angle in the inlet cycles improving their hydraulic capacity. Therefore, an arced labyrinth weir retrofit can improve dam safety and long-term sustainability by preserving the dam structure during extreme flood events. Fig. 2 shows an example of an arced labyrinth weir used as the emergency spillway for the Maguga Dam in Hhohho, Swaziland.

Fig. 2 Maguga Dam arced labyrinth spillway, Hhohho, Swaziland.

(image courtesy Mr. Dawid Van Wyke)

While ample design guidance and research is available on non-arced labyrinth weirs, limited research has been performed on arced labyrinth weirs. Crookston (2010)/Crookston and Tullis (2012) and Christensen (2012) researched the effects of cycle number, sidewall angle, and arc angle on arced labyrinth weir discharge efficiency (Q at a

given upstream *H*). Their results represent the primary empirical data source used to predict the hydraulic performance of prototype arced labyrinth weirs; physical models are typically used to verify performance. The current study provides additional design reference data for practicing engineers by supplementing the Crookston (2010)/Crookston and Tullis (2012), and Christensen (2012) research; to achieve this, physical laboratory models and numerical/computational fluid dynamics (CFD) models will be utilized.

LITERATURE REVIEW

For labyrinth weir reservoir applications, arcing the weir into the reservoir can further increase the labyrinth weir's hydraulic efficiency. When a spillway is engaged, the approach flow patterns converge toward the spillway. By arcing a labyrinth weir, the cycles are better oriented to efficiently handle these flow patterns. Arcing the labyrinth weir also increases the sidewall angle in the inlet cycles, which also improves their hydraulic capacity. This literature review discusses previous research on arced labyrinth weirs, current design practices, and the use of CFD in numerically modeling non-linear weirs.

Previous Arced Labyrinth Weir Research

Falvey (2003) compiled data on many existing labyrinth spillways. He identified four spillways that suffered from non-ideal approach flow conditions: Prado, Kizilcapinar, Sarioglan, and Avon. These non-ideal conditions resulted in lower discharge capacity, turbulent flow at the weir crest, flow separation, and unstable nappe aeration. Falvey suggests that if the Prado spillway alignment had been curved, to orient labyrinth cycles perpendicular to approaching streamlines, the spillway would have been more efficient. The Kizilcapinar, and Avon weirs were later arced to address these concerns.

In an effort to better understand arced labyrinth weirs in reservoir applications, Crookston (2010)/Crookston and Tullis (2012), studied eight laboratory-scale labyrinth weir geometries in a reservoir headbox, six of which were arced. Crookston (2010)/Crookston and Tullis (2012) also established a nomenclature for arced labyrinth weirs (see Fig. 3); this nomenclature will be used throughout this study.

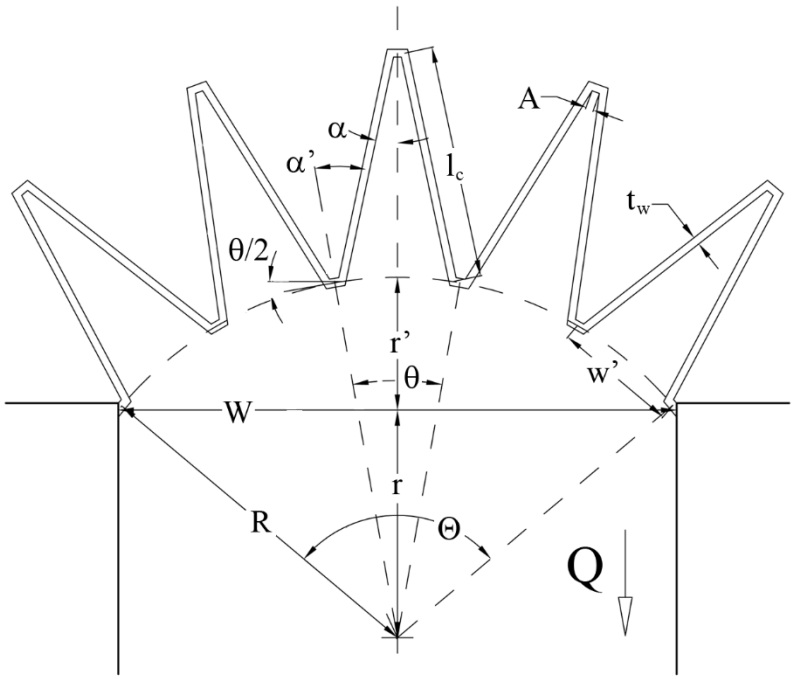

Fig. 3 Arced labyrinth weir nomenclature (Crookston 2010).

Arced labyrinth weir geometric parameters include:

A	Upstream interior apex length
l_c	Centerline length of the sidewall
L_c	Centerline length of weir
$L_{c\text{-}cycle}$	Centerline length of one complete cycle
N	Number of cycles or trapezoidal folds
Q	Discharge or volumetric flow rate
r	Segment height from channel opening to center of imaginary arc circle
r'	Segment height from channel opening to perpendicular downstream apex
R	Arced radius, $R=(W^2/4 + r'^2)^{1/2}$
t_w	Wall thickness at crest
w'	Cycle arc width, $w'=W'/N$

W	Downstream channel width
α	Sidewall angle
α'	Upstream sidewall angle, $\alpha'=\alpha + \theta/2$
θ	Cycle arc angle, $\theta=\Theta/N$
Θ	Central arc angle, $\Theta=W'/R$

The arced labyrinth weirs that Crookston (2010)/Crookston and Tullis (2012) tested had sidewall angles of α=6° and 12° each with cycle arc angles of θ=10°, 20°, and 30°. They generally found that arced labyrinth configurations increase discharge capacity when compared to an in-channel linear labyrinth configuration; this increase is due to better orientation of the cycles to the approaching flow conditions. However, this increase is limited by local submergence. Arcing a labyrinth weir increases the upstream sidewall angle (α') relative to the downstream sidewall angle (α). This increased upstream area available for flow increases discharge efficiency (quantified using C_d from Eq. [1]), but with less available area downstream local submergence potential also increases. In other words, the improved upstream orientation and increased cycle inlet area increases discharge per-unit weir length at a given H. However, the increase in discharge capacity exceed the outlet cycle free-flow capacity at smaller H/P when compared to the non-arced labyrinth weir.

This is best illustrated in Fig. 4 that shows a snapshot of the Crookston (2010)/Crookston and Tullis (2012) data for arced and non-arced labyrinth weirs with α=6° at various cycle arc angles (θ). In Fig. 4, local submergence effects were first observed at H/P>0.15 for the θ=30° arced labyrinth weir, which is represented by the rapid decline in efficiency when compared to the linear labyrinth configurations. This phenomenon is also

present for other sidewall angles and occurs more prominently at larger θ due to the large ratio of inlet cycle area to outlet cycle area.

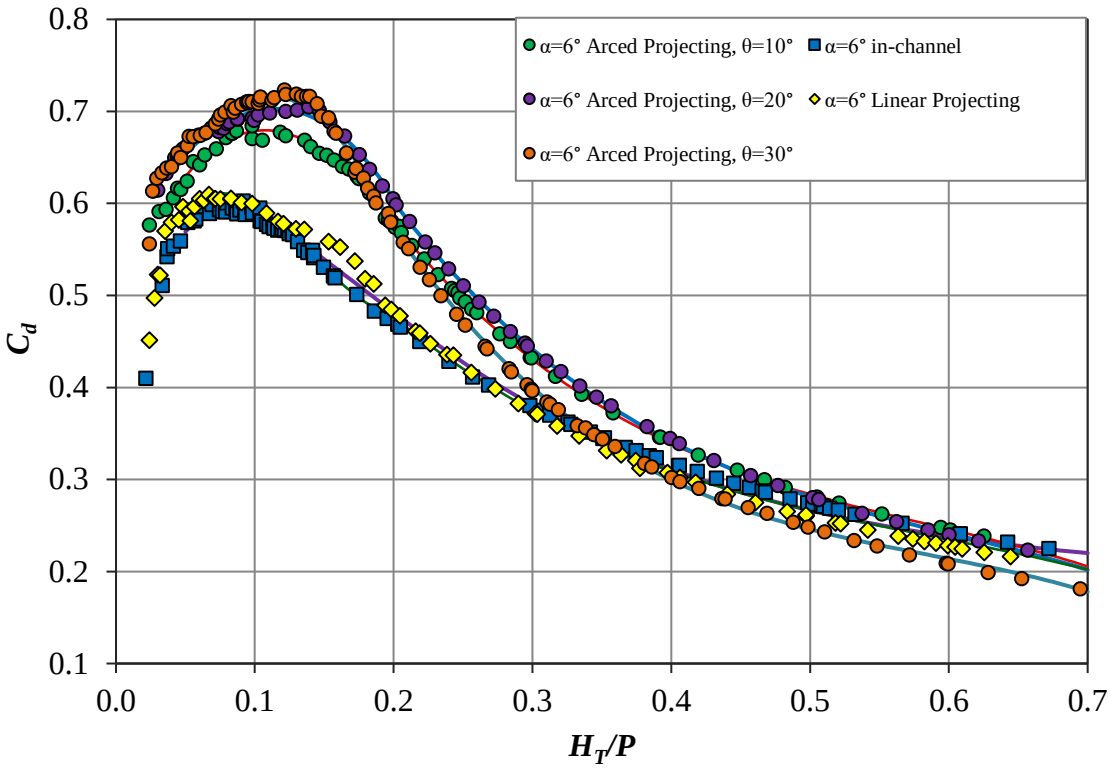

Fig. 4 Discharge efficiency comparison between α=6°labyrinth weirs in reservoirs (Crookston 2010).

Sangsefidi et al. (2015) used computational fluid dynamic to validate the Crookston (2010)/Crookston and Tullis (2012) data. While observing the increased presence of local submergence for arced labyrinth weirs, Sansefidi et al. (2015) decided to lower the downstream invert of the labyrinth apron to increase the free flow capacity of the outlet cycles. They found that by lowering the downstream apron by the weir's height (P), C_d linearly increases with increasing H/P in comparison to the weirs of Crookston (2010)/Crookston and Tullis (2012); at H/P=0.7 (the maximum discharge simulated) C_d

increases by ~120%. While lowering the downstream invert may be applicable at some reservoir sites, it is likely that using a taller weir (common upstream and downstream apron elevations), requiring less fill/excavation, will be more suitable.

Christensen (2012) furthered the research performed by Crookston (2010)/Crookston and Tullis (2012) by testing arced labyrinth weirs of α=12° and 20° at θ=10°, 20°, and 30° and testing various cycle numbers (N=5, 7, and 10). Christensen (2012) observed that altering cycle number causes little effect in discharge efficiency (discharge increased proportionally to the increase in weir length). He also studied the effects of sidewall angle on nappe behavior; he found that at larger sidewall angles nappe aeration conditions were unsteady with temporal and spatial variability. Nappe conditions oscillated between clinging and aerated at low heads, and aerated and drowned at high heads. These conditions and their relative *H/P* values are shown in Fig. 5; for the arced labyrinth weirs modeled no *H/P* value resulted in steady aeration.

In order to improve the stability of the nappe, Christensen (2012) installed nappe breakers, triangular columns placed at the downstream apexes of each cycle. Nappe breakers vent the nappe to atmospheric pressure and improve stability. While Christensen (2012) observed that stability improved, discharge efficiency dropped by 5 to 8% for α=20° and 3 to 4% for α=12°.

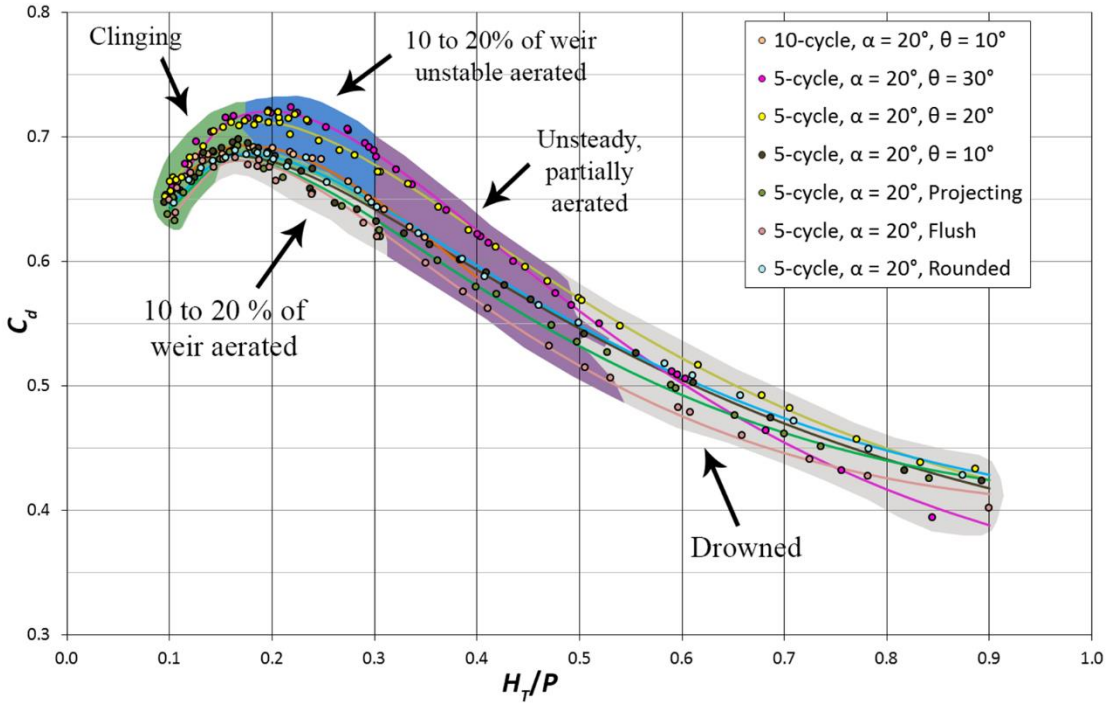

Fig. 5 C_d versus H/P showing nappe aeration conditions for arced labyrinth weirs of α=20° (Christensen 2012).

Moreover, Christensen (2012) made comparisons between arced and non-arced in-reservoir labyrinth weirs and found that the arced labyrinth weir of α=12° increased discharge efficiency, when compared to a non-arced weir of the same α, by as much as ~19% (θ=20°). However, the α=20° only increased discharge efficiency by ~8% (θ=20°); these data are shown in Fig. 6. From this observation Christensen (2012) states that the relative increase in discharge efficiency between arced and non-arced labyrinth weirs in reservoirs decreases with increasing α.

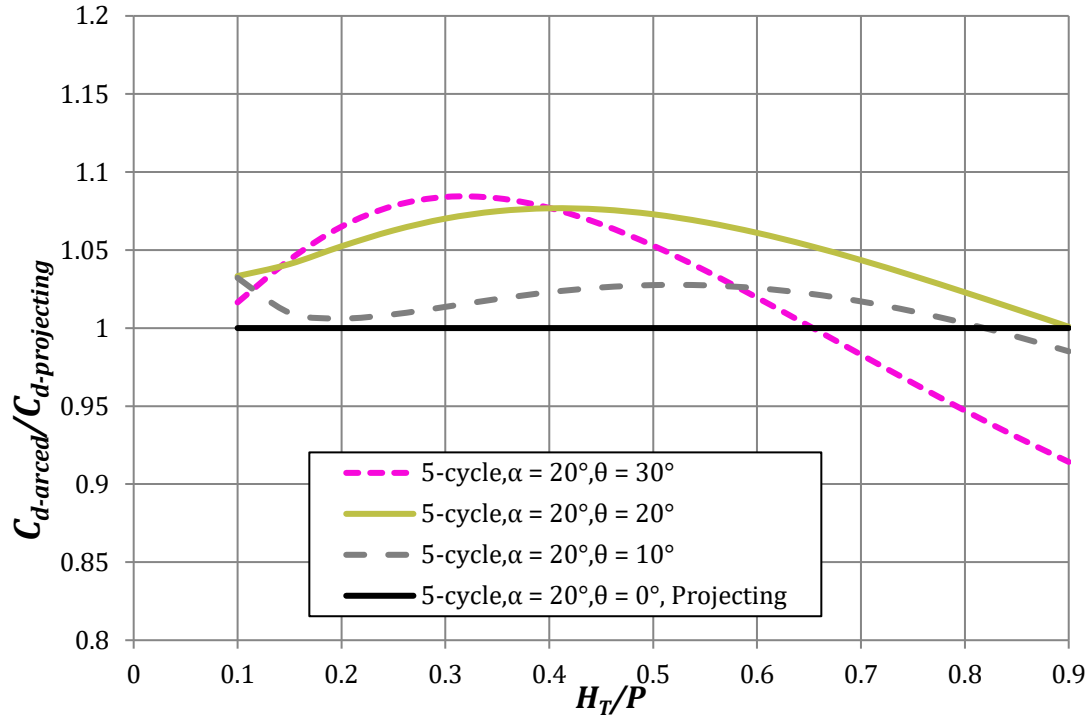

(a)

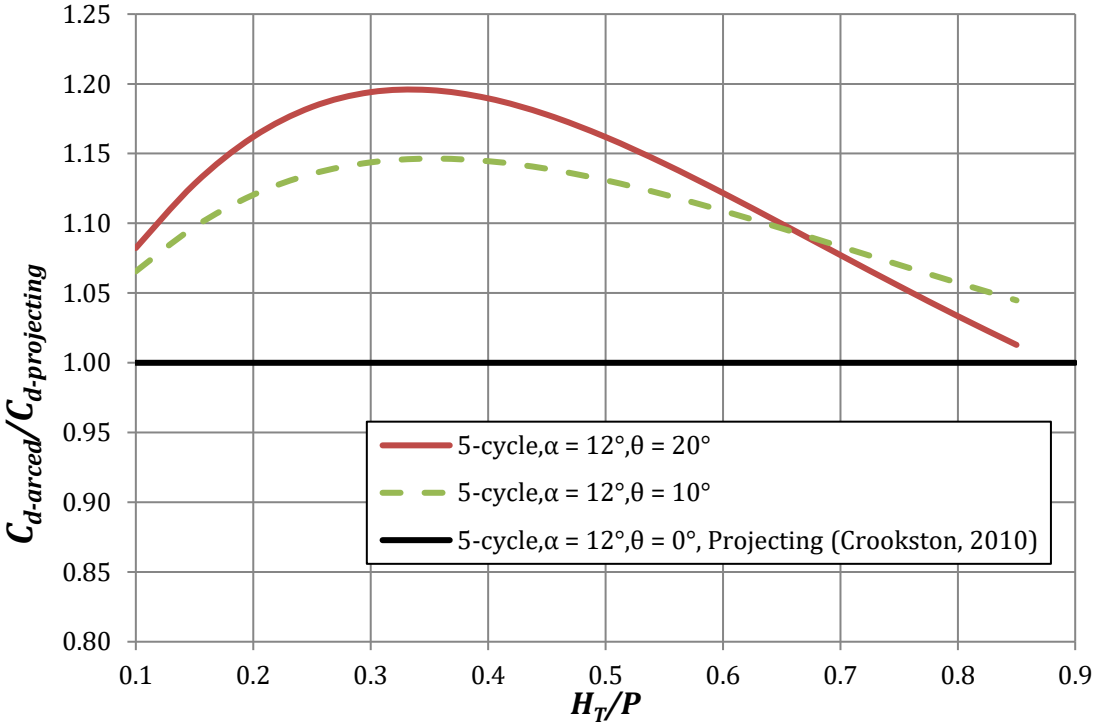

(b)

Fig. 6 Relative discharge efficiency between arced labyrinth weirs and non-arced, in-reservoir labyrinth weirs: (a) α=12° and (b) α=20° (Christensen 2012).

For labyrinth weirs, the discharge coefficient (C_d), and the centerline weir length (L_c), are both functions of the sidewall angle (α). Previous research (mentioned in the Introduction) suggests that C_d decreases with decreasing α; however, L_c increases. Willmore (2004) developed a relationship to compare flow capacity of labyrinth weirs of different α and L_c but identical cycle width (w). Because discharge is proportional to C_d and L_c (see Eq. [1]), Willmore's (2004) relationship multiplies C_d by the ratio, L/W. Crookston (2010) adapted this method to determine cycle efficiency (ε'), which is defined in Eq. [2]

Cycle efficiency is a representation of the discharge per cycle width and allows for labyrinth weir design optimization of the two afore-mentioned opposing factors: (1) C_d decreases with decreasing α and (2) $L_{c\text{-}cycle}$ increasing with decreasing α for a constant cycle width, w.

$$\varepsilon' = C_d * \frac{L_{c-cycle}}{w'} \quad [2]$$

Christensen (2012) compiled ε' data for arced labyrinth weirs of α=6°, 12°, and 20° at w'=40.8 cm and found that ε' decreases with increasing α and increasing H/P as shown in Fig. 7. These data suggest that the increase in cycle length with smaller α are more significant than the decrease in C_d. However, with smaller α, as previously mentioned, effects of local submergence have a greater impact and restrict discharge capacity; this is shown again in the rapid decline of ε' of the α=6° weirs.

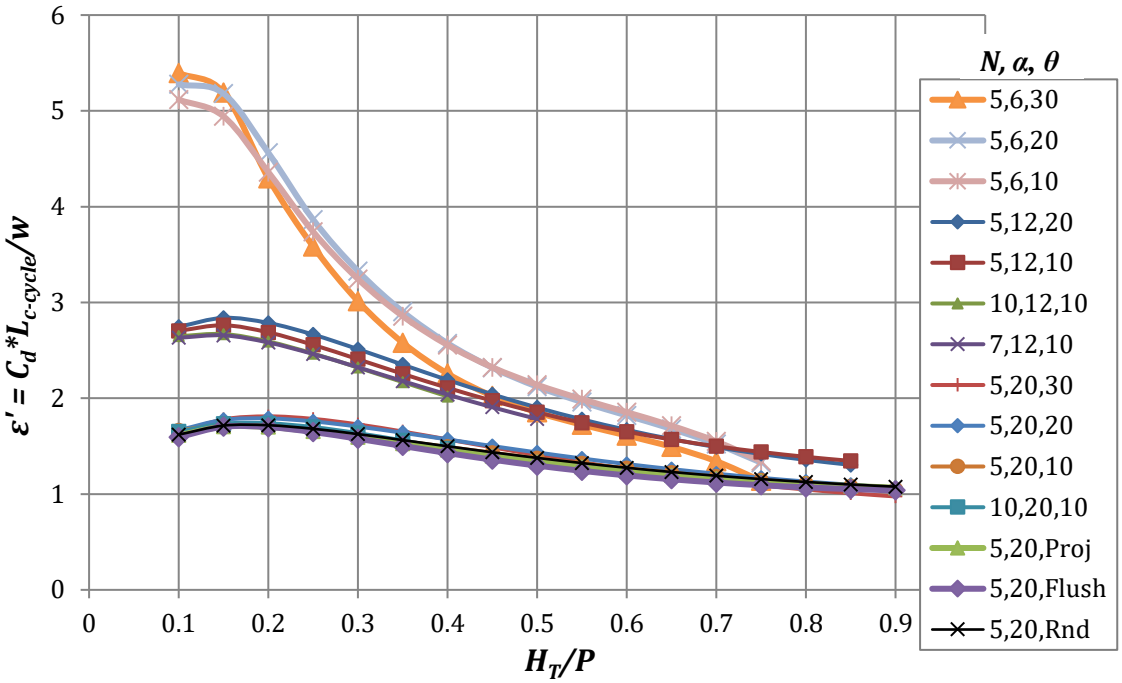

Fig. 7 Comparison of cycle efficiency, ε' for α=6°, 12°, and 20° and w'=40.8 cm (Christensen, 2012).

Arced Labyrinth Weir Design

In the design of arced labyrinth weirs, site specific features and hydraulic requirements predominantly influence weir geometry (i.e. sidewall angles, arc angles, etc.). To select an initial weir geometry, the head-discharge rating curve must be estimated; this is typically accomplished using empirical data. The reservoir system is then reanalyzed to confirm performance; this is typically an iterative process before a labyrinth weir geometry satisfies all project requirements and is finalized. The results from the Crookston (2010)/Crookston and Tullis (2012) and Christensen (2012) research represent the primary empirical data source used to predict the hydraulic performance of prototype arced labyrinth weirs and a refined rating curve may be developed using physical and/or numerical models. For arced labyrinth weir geometries differing from the published data

sets, consideration of uncertainties and engineering judgment is needed to determine if design efforts require site-specific modeling. Multiple arced labyrinth weirs have been designed using empirical data and modeling; a specific example is the Isabella Dam (Kern County, CA, USA), which is currently under construction.

Based on site-specific constraints, the US Army Corps of Engineers (USACE) selected a 12-cycle, α=16º, θ=10° arced labyrinth weir as the new emergency spillway for the Isabella Dam. Preliminary hydraulic performance estimates were developed by interpolating between the published α=12º and 20º data by Crookston (2010)/Crookston and Tullis (2012) and Christensen (2012); the performance was further refined using a physical and numerical model that incorporated reservoir bathymetric influences and the influence of an adjacent service spillway. The physical model was conducted at the Utah Water Research Laboratory (UWRL) as shown in Fig. 8.

The interpolated rating curve data were compared to the laboratory model data and reasonably good agreement was found. The physical model was then verified through CFD modeling with the purpose of verifying the spillway rating curves, addressing concerns about scale and reservoir truncation effects in the physical model, and providing increased hydraulic condition resolution that is not attainable through the physical model (Thompson et al. 2016).

Fig. 8 Isabella Dam laboratory model at the UWRL.

(image courtesy Dr. Blake P. Tullis)

Due to the limits of empirical arced labyrinth weir data and in an effort to reduce the amount of uncertainty inherent in the interpolation process, the current study was undertaken to provide additional design reference data for arced labyrinth weirs. Three α=16º, laboratory-scale arced labyrinth weirs with θ=10º, 20°, and 30º were evaluated for hydraulic performance in physical and numerical models with an idealized upstream reservoir condition (flat-bottomed reservoir with 180º flow convergence approaching the weir similar to Crookston 2010 and Christensen 2012). The results contained herein reduce the uncertainty associated with designing arced labyrinth weirs for $12^o<\alpha<20^o$ when using interpolation.

Numerical Modeling

The use of CFD modeling in hydraulic structure design, including arced labyrinth weirs, has become increasingly more common. Similar to the use of CFD in the design of the Isabella Dam spillway, CFD models are often used to validate against empirical and interpolated data. CFD can also be used for design when empirical data are not available; however, models used without empirical or interpolated data for comparison still need to be validated. The ASCE Task Committee on 3D Free-Surface Flow Model Verification and Validation compiled numerous studies on CFD Models' validation, verification, error estimation, quantification of uncertainty, etc.; the major conclusion from these studies is that verification and validation of numerical models using the best available data is a must (ASCE 2009). This task committee specifies the use of the Grid Convergence Index (GCI) as defined by Roache (1998) for numerical calculation verification.

The GCI provides a method of reporting grid convergence, based on asymptotic theory, using the desired solution (f), the grid refinement ratio ($r_g=\Delta_2/\Delta_1$ where Δ is a representative size of grid elements), the order of convergence (p_c), and an empirically based factor of safety (F_s). An F_s of 1.25 is typically recommended for convergence studies of three mesh sizes and F_s=3 for two-grid studies; these recommendations correlate with providing numerical 95% error bounds (ASCE 2009). The GCI is defined in Eq. [3].

$$GCI = F_s \frac{|\varepsilon|}{r_g^{p_c}-1} \quad [3]$$

In Eq. [3], ε is the relative or absolute error between grid size solutions (i.e. relative: $|f_2-f_1|/f_1$ or absolute: $|f_2-f_1|$). While the GCI helps provide criteria for convergence based on grid size, it is still best to compare CFD results with physical laboratory data. The

remainder of this section will summarize two examples where CFD modeling for non-linear weirs was compared with empirical data.

Crookston et al. (2018) numerically modeled two piano-key (PK) weir geometries that were modeled physically by Anderson and Tullis (2013). While studies have been performed showing that no turbulence models are required for head-discharge measurements (Lefebvre et al. 2014; Pralong et al. 2011), Crookston et al. (2018) sought to determine the effect of two separate turbulence models (LES and RNG k-ε models) on head-discharge measurements. Using the correct turbulence model is necessary in determining solutions for adjacent structures such as, spillway chutes, energy dissipaters and downstream channels.

Crookston et al. (2018) found that both turbulence models (LES and RNG k-ε) are suitable for estimating hydraulic conditions with average errors between 3 and 4%. The numerical model also showed some deviations in the downstream flow field such as a longer nappe trajectory than the physical model Crookston et al. (2018) also state that CFD can be a higher order design tool when compared to empirically derived design methods due to its ability to incorporate site specific conditions. However, the uncertainties of results are critical and physical models and laboratory data are needed for numerical calibration and validation (Crookston et al. 2018).

Savage et al. (2016) state the need to research labyrinth weir hydraulic performance at $H/P>1.0$ to provide design guidance for project sites that may not allow for sufficient weir height to achieve $H/P<1.0$ and to optimize a labyrinth spillway that experiences relatively frequent storms but also has enough capacity to pass extreme floods. To achieve this, Savage et al. extended the research of Crookston and Tullis (2013) for an $\alpha=15°$ in-

channel, non-arced labyrinth weir from H/P=1.0 to 2.0 using physical and numerical modeling. Similar to Crookston et al. (2018), Savage et al. (2016) tested two turbulence models (LES and RNG k-ε) and found that the different turbulence models had little effect on discharge estimation since the upstream flow can be categorized as hydraulically smooth.

Savage et al. (2016) used the ASCE (2009) GCI method to report grid convergence and found that their solutions were independent of grid size. However, they did find that grid refinement slightly increased the relative error between physical and numerical results with all results within ±3%. This error trend is credited to the fractional area/volume obstacle representation (FAVOR) algorithm used to resolve solid geometries, which represents obstacles (i.e. the labyrinth weir, apron, and channel bed) numerically by the volume of obstacle to volume of cell ratio and the ratio of obstacle area to cell face area. Therefore, solid obstacles change slightly with changes to the mesh (Savage et al. 2016).

Similar to Crookston et al. (2018) and Savage et al. (2016) and in an effort to provide some insight into the ability of CFD to accurately represent arced labyrinth weir hydraulic performance, the same α= 16º arced labyrinth weirs (for θ=10° and 30°) tested physically were evaluated using commercial CFD software (Flow-3D®). The overreaching purpose of this CFD analysis was to assess the appropriateness of CFD modeling as a design tool for arced labyrinth weir rating curve development. A good correlation between the empirical and numerical data would suggest that CFD modeling likely can be used for other sidewall angles and decrease the dependency on interpolated empirical data in design.

Research Objectives

The following represent the key research objectives in this study:

- Observe hydraulic behavior and anomalies on various arced labyrinth weir models to further understand their advantages and disadvantages.
- Establish a broader understanding of discharge and efficiency in relation to varying cycle arc angle (θ=10°, 20°, and 30°) for α=16° and compare these findings with the results of Christensen (2012), and Crookston (2010)/Crookston and Tullis (2012).
- Develop best-fit empirical C_d vs *H/P* equations for the weir geometries tested to facilitate ease of use in design.
- Explore the influence of upstream velocity head (or lack thereof) on the hydraulic efficiency of arced labyrinth weirs. In reservoir applications, velocity heads are typically negligible and assumed to be zero, making the upstream total and piezometric heads equivalent. Uncertainties associated with this assumption will be explored and quantified.
- Explore the feasibility of using CFD as a design tool for arced labyrinth weirs by comparing physical and numerical hydraulic performance data for arced labyrinth weirs of α=16°: θ=10° and 30°. Quantitative and qualitative results will be compared.

PHYSICAL MODEL SETUP

The physical modeling of the current study involved fabricating, installing, and collecting data on three arced labyrinth weir, laboratory scale models in a headbox that simulates ideal reservoir flow conditions (180° converging flow towards spillway). This section will describe the testing facilities, weir fabrication and installation, and the instrumentation used in data collection.

Testing Facilities

The physical modeling for the three arced labyrinth weirs tested in this study was performed at the Utah Water Research Laboratory (UWRL) at Utah State University in Logan, Utah, USA (https://uwrl.usu.edu/) in an elevated, steel headbox/reservoir (5.8 x 6.5 x 1.5 m) as shown in Fig. 9. The weirs were installed on an acrylic platform/apron, 9.0 x 4.0 ft (2.8 x 1.2 m), 3.5 in. (8.9 cm) above the reservoir bed projecting into the reservoir. Sloped ramps (7.3%) were used to transition the upstream approach flow between the reservoir and apron.

The headbox is supplied with water from an adjacent reservoir via gravity flow through a 15.2 cm (6 in.) or 50.8 cm (20 in.) diameter supply line depending on the required discharge. The headbox is elevated to allow these supply lines to enter from beneath the headbox. Water is then channeled through a diffuser pipe within a plenum chamber, which is separated from the reservoir by a baffle wall; this chamber lines three sides of the headbox to allow for reservoir-type, uniform flow conditions converging from 180° (see Fig. 9).

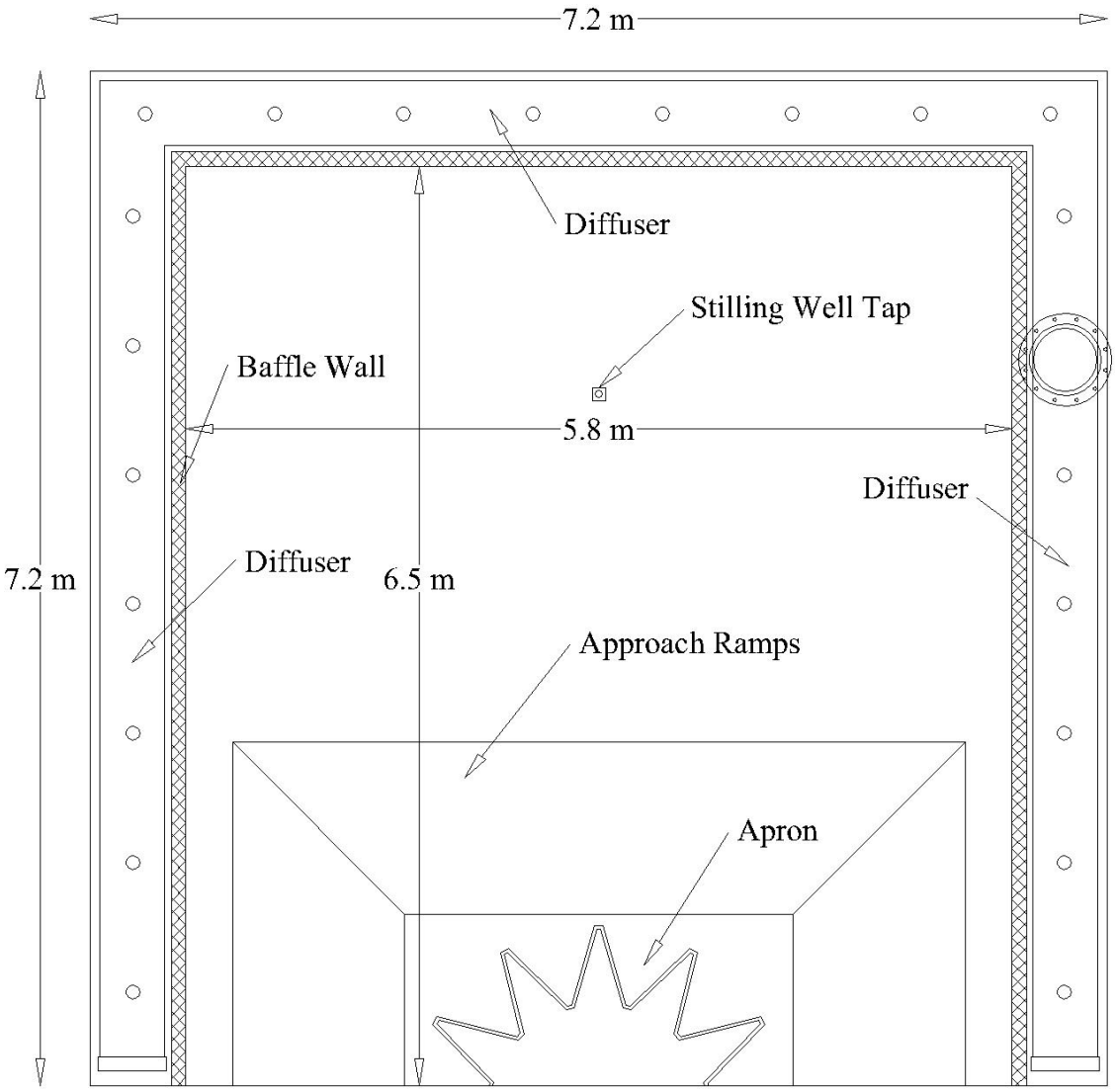

Fig. 9 Plan view of reservoir headbox with diffuser, baffle wall, stilling well tap, apron and approach ramps labeled.

Arced Labyrinth Weir Fabrication and Installation

Three arced labyrinth weir models were fabricated out of polyvinyl chloride (PVC) sheeting with a weir wall height (P), of 20 cm and a nominal wall thickness (t_w), of 2.54 cm. The three weirs each had α=16°, N=5 and θ=10°, 20°, or 30°, respectively (see Fig. 10). Each weir had a half-round crest shape, due to this shape's hydraulic efficiency

(Crookston 2010); the crest radius (R_{crest}) is equal to one half of t_w. The weirs were assembled with PVC adhesive and fastened to the apron. The designed and as-built dimensions for each weir such as centerline length (L_c), channel width (W), cycle centerline length ($L_{c\text{-}cycle}$) cycle width (w'), cycle length to cycle width ratio ($L_{c\text{-}cycle}/w'$), and cycle width to weir height ratio (w'/P) are given in Table 1. Complete drawing details of each weir are given in Appendix A.

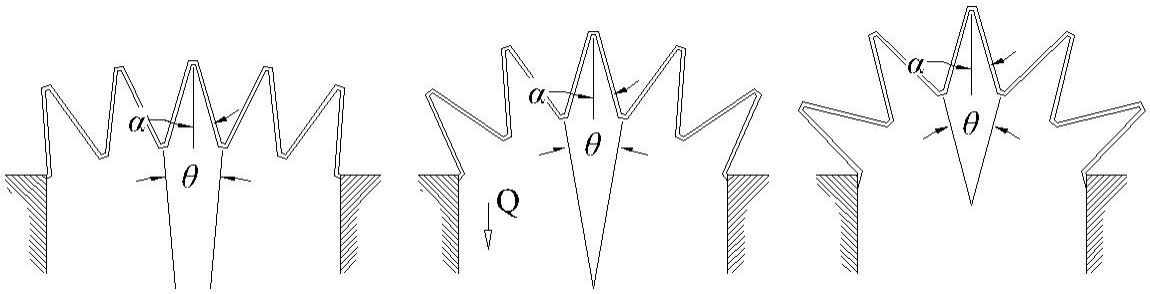

(a) (b) (c)

Fig. 10 Arced labyrinth weirs: α=16° and θ=10° (a), 20° (b), and 30° (c).

Ensuring the levelness of the weir crest is critical for accurately measuring H and calculating C_d, especially at low heads, where slight variations in the crest elevation can compose a significant portion of H. In determining the crest elevation, a surveying level was used, and 30-40 points were collected across the weir crest. These points were averaged and the range of variation between each point was noted. The variation was not permitted to exceed ± 0.794 mm; if this tolerance was not achieved, metal shims were placed under the weir, and the crest was re-surveyed until each point was within the specified tolerance.

Table 1 Arced labyrinth weir model dimensions.

As Designed Dimensions									
Model	α	θ	P	L_c	W	$L_{c\text{-}cycle}$	w'	$L_{c\text{-}cycle}/w'$	w'/P
	[°]	[°]	[cm]	[m]	[m]	[m]	[cm]	[cm/cm]	[cm/cm]
1	16	10	20.32	6.246	1.989	1.247	40.58	3.073	1.997
2	16	20	20.32	6.274	1.819	1.249	40.36	3.095	1.986
3	16	30	20.32	6.284	1.547	1.252	40.14	3.119	1.975
As Built Dimensions									
Model	α	θ	P	L_c	W	$L_{c\text{-}cycle}$	w'	$L_{c\text{-}cycle}/w'$	w'/P
	[°]	[°]	[cm]	[m]	[m]	[m]	[cm]	[cm/cm]	[cm/cm]
1	16	10	20.46	6.249	1.983	1.242	40.67	3.054	1.988
2	16	20	20.35	6.301	1.797	1.249	40.70	3.069	2.000
3	16	30	20.48	6.321	1.547	1.255	41.12	3.052	2.008

Instrumentation

Each supply line utilized a calibrated electromagnetic flow meter (6- and 20-inch diameter ABB MagMaster® flow meters) with an average uncertainty of ±0.25% (see Fig. 11). Multimeters were connected to each flow meter to record output frequency in Hz. This reading was then converted into a discharge using each meters' calibration data. For one data point, a 5 min average discharge was measured twice and recorded; if the two 5 min averages differed, another average was measured until steady state was present.

To measure piezometric head, a stilling well was hydraulically connected to the headbox and equipped with a precision point gauge (accurate within ± 0.152 mm). the piezometer in the reservoir was located at the center of the weir installation (center of middle cycle's upstream apex) and 4.89 m upstream from the downstream edge of the weir apron.

(a) (b)

Fig. 11 –15.2 cm (a) and 50.8 cm (b) diameter supply lines with butterfly control valves (1), magnetic flow meters (2), and multimeter (3).

Two-dimensional (2D) velocity measurements were collected at the location of the piezometer tap. These data were collected via a Sontek Flow Tracker 2D acoustic dopple velocimeter (ADV); two to four 20 second averages were measured at each point (if there was not good agreement between the first two averages, additional measurements were taken) at the theoretical depth of average velocity (0.4*total depth). The purpose of these velocity data is to measure velocity head ($V^2/2g$) at the piezometer tap to understand its contribution to the total head (H), and to make comparisons between the physical and numerical models.

Flow conditions were documented using still and video photography. Nappe aeration characteristics were also noted. Each dataset is composed of ~50-70 data points with multiple repeated datapoints to ensure data accuracy and repeatability. Microsoft Excel® was used for data management and calculations.

NUMERICAL MODEL SETUP

The numerical modeling of the current study involves modeling the θ=10° and 30° arced labyrinth weirs using a commercially available computational fluid dynamic (CFD) package, Flow-3D. This section provides a description of the equations solved and algorithms used to render the solid and track the free surface; moreover, an explanation of how the numerical models of the current study were constructed is given.

Numerical Model

Flow-3D solves the Reynolds-Averaged Navier Stokes (RANS) equations, which describe fluid motion by applying the momentum principle or Newton's Second Law, in differential form to relate the forces that are acting on a finite element or volume (Flow-3D). These forces include gravitational, pressure, and viscous (or frictional) (Finnemore and Franzini 2002). In Cartesian coordinates and for an incompressible fluid with constant viscosity (common assumptions for water in free surface applications) and *z* increasing vertically the RANS equations in the *x*, *y*, and *z* directions are defined in Eq. [4].

$$x\text{: } -\frac{dp}{dx}+\mu\left(\frac{\partial^2 u}{\partial x^2}+\frac{\partial^2 u}{\partial y^2}+\frac{\partial^2 u}{\partial z^2}\right)=\rho\left(\frac{\partial u}{\partial t}+u\frac{\partial u}{\partial x}+v\frac{\partial u}{\partial y}+w\frac{\partial u}{\partial z}\right) \quad [4a]$$

$$y\text{: } -\frac{dp}{dy}+\mu\left(\frac{\partial^2 v}{\partial x^2}+\frac{\partial^2 v}{\partial y^2}+\frac{\partial^2 v}{\partial z^2}\right)=\rho\left(\frac{\partial v}{\partial t}+u\frac{\partial v}{\partial x}+v\frac{\partial v}{\partial y}+w\frac{\partial v}{\partial z}\right) \quad [4b]$$

$$z\text{: } -\rho g-\frac{dp}{dz}+\mu\left(\frac{\partial^2 w}{\partial x^2}+\frac{\partial^2 w}{\partial y^2}+\frac{\partial^2 w}{\partial z^2}\right)=\rho\left(\frac{\partial w}{\partial t}+u\frac{\partial w}{\partial x}+v\frac{\partial w}{\partial y}+w\frac{\partial w}{\partial z}\right) \quad [4c]$$

In Eq. [4], the force terms are on the left side of the equation, with the convective and local acceleration terms on the right. In the numerical models of this study, the computational domain is composed of two hexahedral (cube) meshes, in Cartesian coordinates. Each mesh is subdivided into small hexahedral cells, with finer cells in closer

proximity to the weir. For each cell, the RANS equations (Eq. [4]) are used to calculate flow parameters such as the average pressure (p) and velocities (u, v, w). The mesh is also used to render the arced labyrinth weir, apron, and downstream wing walls.

Flow-3D uses an algorithm, which they call the fractional area/volume obstacle representation (FAVOR) method. The FAVOR method numerically defines the region of a cell that contains an obstacle by computing the ratio of the obstacle area to cell face area and the obstacle volume to cell volume. If this ratio is one, the cell is completely filled with the solid; a ratio of zero defines a cell that is completely available for fluid flow, and a ratio between zero and one represents a partially filled cell (Flow-3D). This method defines the surface by a series of interconnected, flat planes. Therefore, curved surfaces are approximated as flat surfaces in each cell using this first-order technique. Savage et al. (2016) note that the FAVOR renderings are very similar to a triangulated irregular network (TIN) commonly used in geospatial surveys for geographic information system (GIS) applications. The FAVOR algorithm is run during preprocessing, which allows rendering of the weir and reservoir prior to the simulation. The location of these objects is then held stationary throughout the simulation.

In tracking the free surface, which varies temporally and spatially, Flow-3D uses an algorithm called the modified volume-of-fluid (VOF) method (Hirt and Nichols 1981). The Hirt and Nichols (1981) modified VOF method, similar to the FAVOR method, uses a ratio to calculate the fraction of a cell that is filled with the fluid, the surface interface area (A_x, A_y, A_z) is also calculated; these two parameters allow for water surface tracking with respect to time and space.

For open channel water flow applications, it is typically suitable to neglect the inertia of the air adjacent to the water surface. Becaues water is much heavier than air, the impacts of the air are negligible. The volume of air is replaced with empty space, void of mass. This empty space is only represented by constant pressure (atmospheric) and temperature (Flow-3D). These assumptions reduce the computational demand required in tracking the free surface. Furthermore, Savage et al. (2016) note that the strict application of the VOF method creates a misty region within the cells where the free surface ought to be contained. Therefore, the modified VOF method allows for small volume correction of these misty regions at the end of each time step to create a better defined free surface. While this adjustment violates the principle of conservation of mass, the sum of corrections throughout a simulation are generally less than ±0.01%. Such small adjustments are considered insigfnicant to the solution.

Flow-3D gives the user six turbulence closure schemes to choose between. Commonly used in open-channel flow problems are the Renormalized Group (RNG) k-ε and Large Eddie Simulation (LES) models; this study implemented the RNG k-ε turbulence model. The RNG k-ε model utilizes two transport equations: one for turbulent kinetic energy (k) and another for turbulent dissipation (ε). k determines the energy of the turbulence while ε determines the scale. The standard k-ε model is dependent upon a single turbulence length scale, and the RNG k-ε model mathematically accounts for turbulent mixing occurring at various scales of motion. The RNG k-ε model works well with free-surface flows and rotating turbulent patterns with small mean pressure gradients. However, accuracy is reduced for flows with large pressure gradients (CFD Online Wiki 2011).

Model Creation

In modeling the two arced labyrinth weirs (α=16°; θ=10° and 30°), three-dimensional (3D) steriolithography (stl) files of the two weirs and headbox were exported from 3D drawing files drafted in AutoCAD 2018®. In order for the FAVOR algorithm to accurately render the wing walls in the comuptational domain, the stl files were translated 1.524 cm in the *y* direction; to render the fluid at the outflow (downstream boundary) the headbox stl was extended 30.48 cm down. Relative to the right (looking downstream) lower corner of the stl, the domain's origin is (0,-0.015,0 m) (see Fig. 12) . While the stl files include the complete headbox and weir, the flow is symmetrical about the upstream apex of the third or middle cycle (see Fig. 10); therefore, the computation domain was confined to only the right half of the weir and headbox. Two mesh blocks were used to resolve the flow (see Fig. 12): a coarse upstream reservoir mesh (RM) (shown in green in Fig. 12), and a finer weir mesh (WM), nested within the reservoir mesh (shown in yellow in Fig. 12).

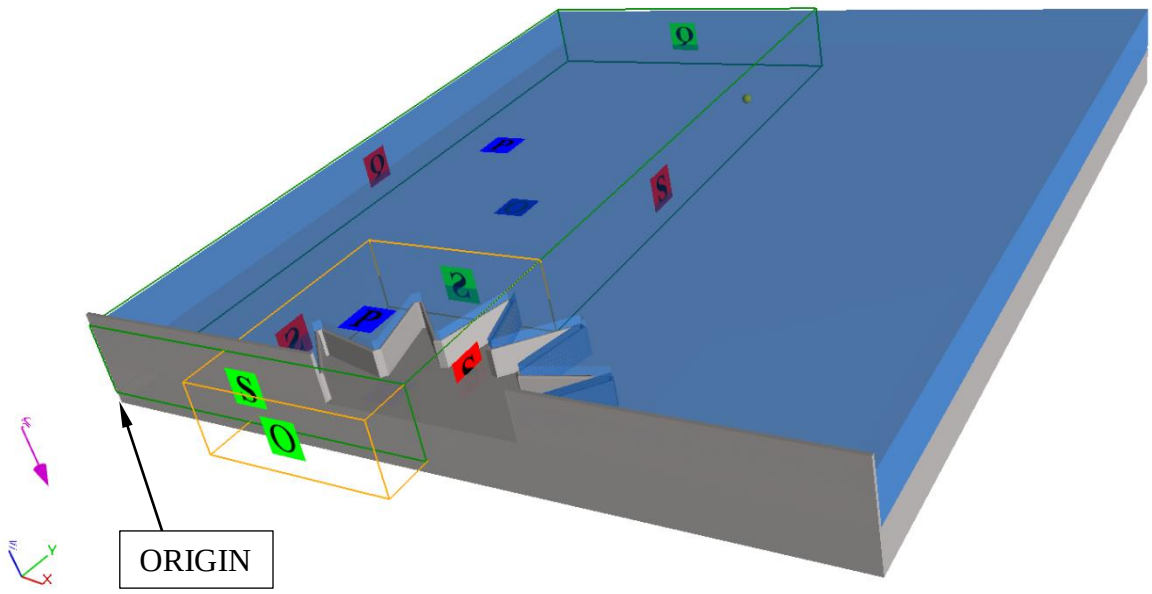

Fig. 12 CFD reservoir and weir model showing domain origin, mesh boundaries, boundary conditions, history probe, and initial fluid region.

The reservoir mesh varied between two grid sizes (Δ_{RM}), 36.6 mm and 27.4 mm. To ensure grid alignment at inter-mesh boundaries, the 36.6 mm grid size was tested with two finer weir mesh grid sizes (Δ_{WM}), 12.2 mm and 9.14 mm, being 1/3 and 1/4 the size of the reservoir mesh, respetively. The 27.4 mm mesh was tested along side weir meshes of 13.7 mm, 9.14 mm, and 6.86 mm, being 1/2, 1/3, and 1/4 the size of the reservoir mesh, respectively. Therefore, each discharge was simulated using five independent mesh configurations; nomenclature for these configurations is defined and mesh sizes are summarized in Table 2. To normalize the grid size, it is divided by the weir crest width (t_w): for the reservoir meshes Δ/t_w=1.44 and 1.08; for the weir meshes Δ/t_w=0.54, 0.48, 0.36, and 0.27. The nested block mesh boundary and FAVOR rendering of the weir looking at the *x*-max. plane (profile view) are shown in Fig. 13. Dimensions for each RM and WM configuration are given in Table 3.

Table 2 CFD mesh configuration summary.

Mesh Configuration	Reservoir Mesh Size (Δ_{RM})	Relative Reservoir Mesh Size (Δ_{RM}/t_w)	Weir Mesh Size (Δ_{WM})	Relative Weir Mesh Size (Δ_{WM}/t_w)	Δ_{RM}/Δ_{WM}
	[mm]	[-]	[mm]	[-]	[-]
RM0-WM1	36.6	1.44	12.2	0.48	3
RM0-WM2	36.6	1.44	9.14	0.36	4
RM1-WM0	27.4	1.08	13.7	0.54	2
RM1-WM2	27.4	1.08	9.14	0.36	3
RM1-WM3	27.4	1.08	6.86	0.27	4

Table 3 CFD mesh block extents and mesh planes.

α=16°: θ=10°							
Plane:	*x-min*	*x-max*	*y-min*	*y-max*	*z-min*	*z-crest*	*z-max*
Mesh Block	[m]	[m]	[m]	[m]	[m]	[m]	[m]
RM0	0.013	2.921	0.000	6.51	0.0848	0.597	0.670-0.789
WM1-2	1.385	2.921	-0.378	1.43	0.0848	0.597	0.670-0.789
RM1	0.013	2.921	0.000	6.53	0.1031	0.597	0.679-0.761
WM0 2, 3	1.385	2.921	-0.384	1.29	0.1031	0.597	0.679-0.761
α=16°: θ=30°							
Plane:	*x-min*	*x-max*	*y-min*	*y-max*	*z-min*	*z-crest*	*z-max*
Mesh	[m]	[m]	[m]	[m]	[m]	[m]	[m]
RM0	0.013	2.921	0.000	6.51	0.0848	0.597	0.670-0.789
WM1-2	1.385	2.921	-0.378	1.57	0.0848	0.597	0.670-0.789
RM1	0.013	2.921	0.000	6.53	0.1031	0.597	0.679-0.761
WM0 2, 3	1.385	2.921	-0.384	1.56	0.1031	0.597	0.679-0.761

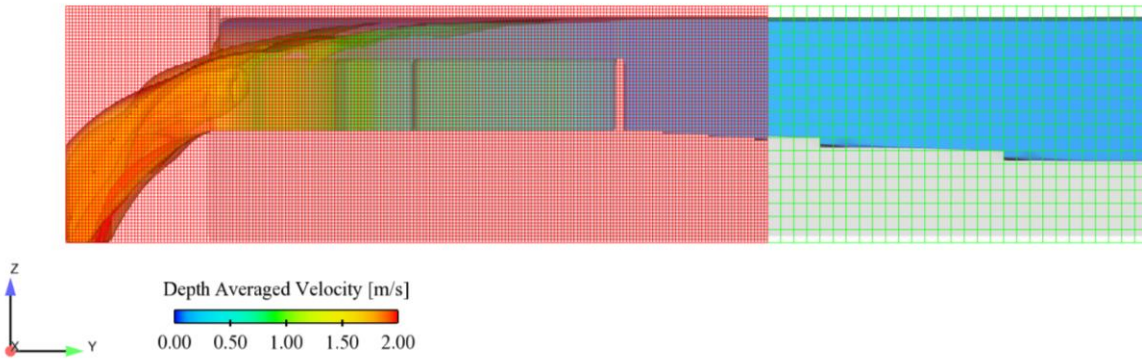

Fig. 13 Nested mesh block boundary for the RM0-WM2 configuration with FAVOR rendering of α=16°: θ=30° weir and reservoir floor at *H/P*=0.6.

In order to capture the converging flow field in the headbox, *Q* was specified as a constant at the minimum *x* (*x*-min) and maximum *y* (*y*-max) boundaries (see Q in Fig. 12). The chosen discharges corresponded to *H/P* increments of 0.1 between 0.3 and 0.8 based on physical model results. Because the physical model as-built weir length slightly differs from the designed model a unit inflow was calculated: using the physical data, C_d was used to calculate *Q* based on the numerical model weir length resolved by the weir mesh; this *Q* was then proportioned to the lengths of the *x*-min, and *y*-max boundaries in order to apply the correct discharge for a given *H/P*.

Symmetry or free-slip (S) boundaries were placed between the inter-block mesh boundaries and at the *x*-max plane (see S in Fig. 12); the symmetry boundaries create a free-slip interaction between the meshes by setting the velocity derivative at the boundary face to zero. Outflow boundaries (O) were placed at the free discharging boundary (*y*-min), downstream of the weir to create a free outfall condition. Atmospheric pressure (P) boundaries were applied at the *z*-max plane (see P in Fig. 12) with a specified VOF fluid fraction of zero. A summary of each boundary condition for both meshes is given in Table 4, and the location of each boundary condition is displayed in Fig. 12.

Table 4 Summary of CFD mesh boundary conditions.

Boundary	Reservoir Mesh	Weir Mesh
x-min.	constant *Q*	symmetry
x-max.	symmetry	symmetry
y-min.	symmetry	outflow
y-max.	constant *Q*	symmetry
z-min.	outflow	outflow
z-max.	constant *P*	constant *P*

The piezometric (*h*) and total (*H*) heads were computed using a history probe (used to report hydraulic variables at a specific location in the x-y plane) located at the exact location of the piezometer tap in the physical model (4.89 m upstream from the downstream edge of the weir apron) shown as a yellow sphere in Fig. 12**.**

To facilitate initialization of the simulation, a 3D initial fluid region was drafted in AutoCAD and imported to Flow-3D as a stl file (see Fig. 12**).** This fluid region fits upstream of the weir and above the reservoir floor and weir apron. The initial fluid region depth is set for each simulation flowrate at multiples of 0.1 *H/P*.

The main goal of the CFD modeling was to compare rating curve data (C_d data) between the numerical and physical models of the current study. Savage et al. (2016) and Crookston et al. (2018) each found that the selection of turbulence model has little effect on C_d relative to non-linear weirs (i.e. labyrinth and piano key). Therefore, the RNG k-ε turbulence model, which is common among open channel problems, was chosen as the turbulence model for this simulation. The RNG k-ε model is dependent upon a maximum turbulent mixing length that was set to be dynamically computed by the solver. The model utilized the split-lagrangian VOF advection to track the free surface coupled with a second order approximation for the momentum advection scheme; for computational stability a monotonicity preserving scheme was used for the α=16°: θ=10° at the RM0-WM1

configuration. Pressures in each cell were solved using the generalized minimal residual (GMRES) method algorithm (Saad and Schults 1986)). The fluid flow solver solved the full momentum and continuity equations.

Numerical Simulations

A total of 60 simulations were modeled. That includes H/P=0.3, 0.4, 0.5 ,0.6, 0.7, and 0.8 at each mesh configuration (see

Table 2). Initially, each simulation modeled 60 s of time; however, 30 s duration restart simulations were added to some models to optimize runtime. Data were then extracted via text files to Microsoft Excel. Once the time series reached steady-state conditions, fifteen second averages were calculated in order to compute time-averaged C_d values and corresponding relative errors (ε) between the numerical and physical results. Flow-3D's model viewer and postprocessing visualization tool, FlowSight® were used to create figures and further understand qualitative flow characteristics.

Velocity and Total Head

To determine hydraulic efficiency, C_d was calculated via Eq. [1] at each datapoint. In Eq. [1], the energy gradient driving flow is characterized by the total head ($H=h+V^2/2g$) relative to the weir crest. In order to determine the effect of the velocity head ($V^2/2g$) on H, 2D velocity vector measurements were made for $0.1 \leq H/P \leq 0.7$ for the α=16°: θ=20° and 30° weirs. Velocity head was also calculated using the CFD models for the α=16°: θ=10° and 30° weirs for $0.3 \leq H/P \leq 0.8$.

The current reservoir model has shallow approach flow depths of ~1.5P, which cause relatively higher velocities compared to most reservoirs. With the available data collected on each physical model, the velocity head ranges between 0.014% and 1.0% of H. The CFD models support this observation with velocity head values from 0.13% to 0.28% for all models and H/P values simulated. These values are likely to be much lower in actual reservoir applications.

The relative error when calculating C_d without the inclusion of velocity head varies between 0.02% for H/P=0.1 and 1.5% for H/P=0.7. Due to the low contribution of velocity head and low error in C_d calculation, the uncertainty associated with using the piezometric head (reservoir water surface elevation) to characterize the upstream driving head instead of the total head is minimal and justified; In many reservoir applications, identifying the appropriate velocity head, specific to the piezometric head measurement location, is typically impractical without the aid of physical or numerical modeling. This difficulty is due to varying reservoir bathymetry, 3D flow patterns, and secondary currents.

Based on these observations, C_d has been determined to be a function of piezometric head, h. The Crookston (2010)/Crookston and Tullis (2012), and Christensen (2012) C_d data shown herein have been modified to only include piezometric head.

Head – Discharge Relationship

In the current study, C_d data were collected for $0.05 \leq H/P \leq 0.8$ for the α=16°: θ=10°, 20°, 30°: N=5 arced labyrinth weirs (tabular data found in Appendix B). Using these data and the software LAB Fit®, best-fit curves were generated for this study's results, and those of previous arced labyrinth weir studies (Crookston 2010/Crookston and Tullis (2012) and Christensen 2012). Eq. [5] for α=6° and Eq. [6] for α=12°, 16°, and 20°, using h as the driving head, represent the best-fit equations for the tested arced labyrinth weirs, with a, b, c, and d being empirically calculated coefficients via LAB Fit.

for α=6°: $$C_d = ab^{\frac{H}{P}}\left(\frac{H}{P}\right)^c + d \quad [5]$$

for α=12°, 16°, and 20°: $$C_d = \frac{1}{a\left(\frac{H}{P}+b\right)^2+c} + d\ln\left(\frac{H}{P}\right) \quad [6]$$

Fig. 14 shows the C_d vs. H/P experimental data and empirical curve fits for the α=16°: θ=10°, 20°, 30° arced labyrinth weirs, and Fig. 15, Fig. 16, and Fig. 17 present the data for all α geometries organized by θ. Values for a, b, c, and d, to be used in Eqs. [5] and [6], and the correlation coefficient (R^2) for each fit (~0.984 – 0.999) are given in **Error! Reference source not found.**.

In Fig. 14, and as observed by Crookston (2010)/Crookston and Tullis (2012), and Christensen (2012), discharge efficiency increases when increasing θ from 10° to 20° at all discharges tested ($H/P<0.8$); however, when increasing θ to 30° efficiency starts to drop below the θ=20° geometry for $H/P \geq 0.35$ and below the θ=10° for $H/P \geq 0.55$. At lower

heads the increase in θ (i.e. θ=30° compared to θ=10°) better orients the labyrinth cycles to the approaching flow. However, as H increases, approach velocity increases, and streamlines become more oriented parallel to the channel outlet centerline. This causes the weir to act as a form-loss element, and the control point shifts further downstream; these factors decrease efficiency at H>0.55. Christensen (2012) observed this decrease in efficiency by collecting velocity vector data on the α=20°: θ=30° arced labyrinth weir at H/P=0.3 and 0.6 and observing the shift in vector orientation for the two discharges tested (a similar comparison is made in the numerical models discussed in the Numerical Model Results section). The α=16°: θ=20° provides a good middle ground, by improving efficiency at H/P>0.3 while not sacrificing low head (H/P<0.3) efficiency.

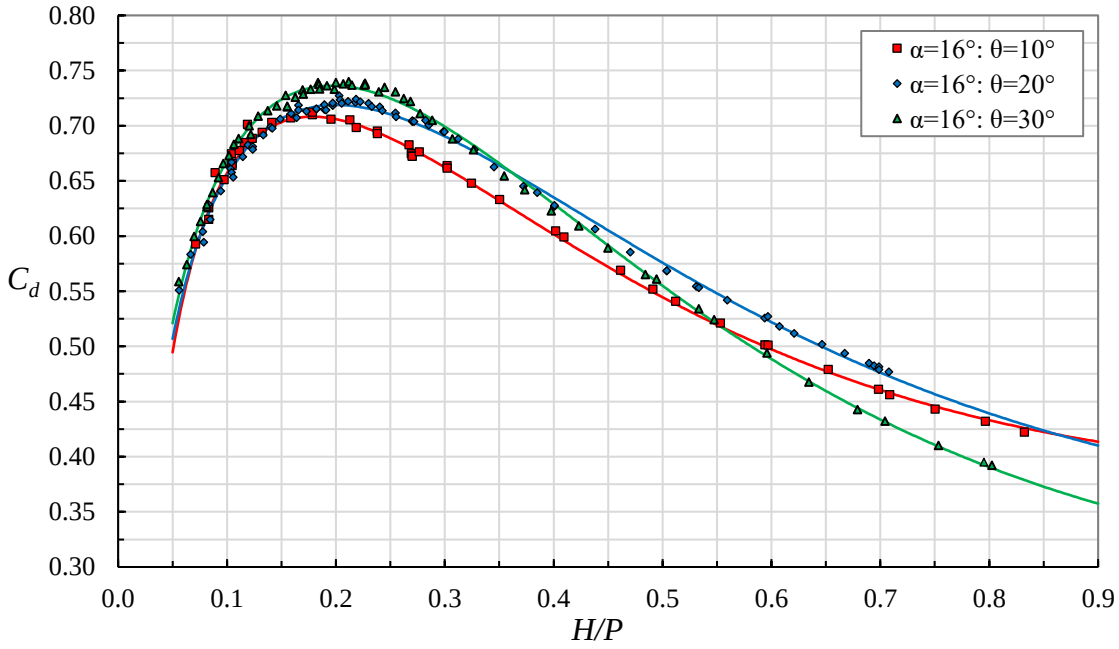

Fig. 14 C_d vs. H/P for α=16° arced labyrinth weirs (current study).

It should be noted in Fig. 15, Fig. 16, and Fig. 17 that the α=16° weirs have very similar C_d vs. H/P curves as the α=20° weirs. It was expected, based on interpolation that the α=16° weir curves would lie directly in between the α=12° and 20° curves. However,

a log-scale type relationship may exist where between α=12° and 20° as α increases linearly, the corresponding efficiency curve increases exponentially until matching the α=20° curve. This theory requires additional modeling of arced labyrinth weirs with α between 12° and 20°. Differences may also be attributed to alterations in the physical model setup, such as reservoir size, apron size, approach ramps, and apron elevation.

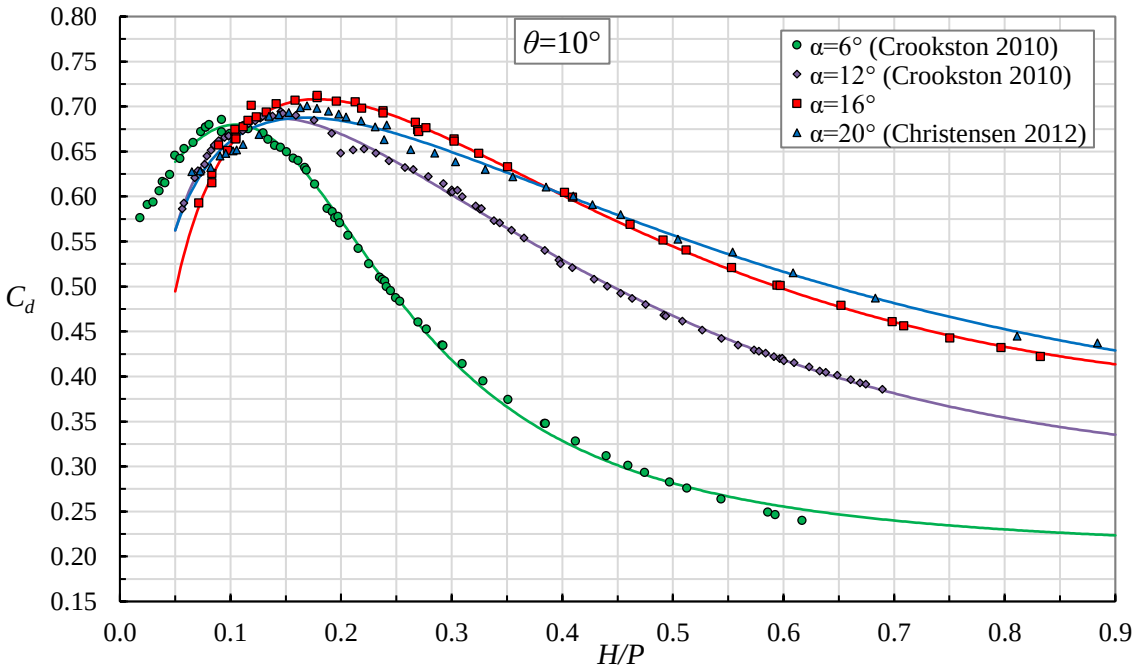

Fig. 15 C_d vs. H/P for θ=10°: α=6°, 12°, 16°, and 20° arced labyrinth weirs.

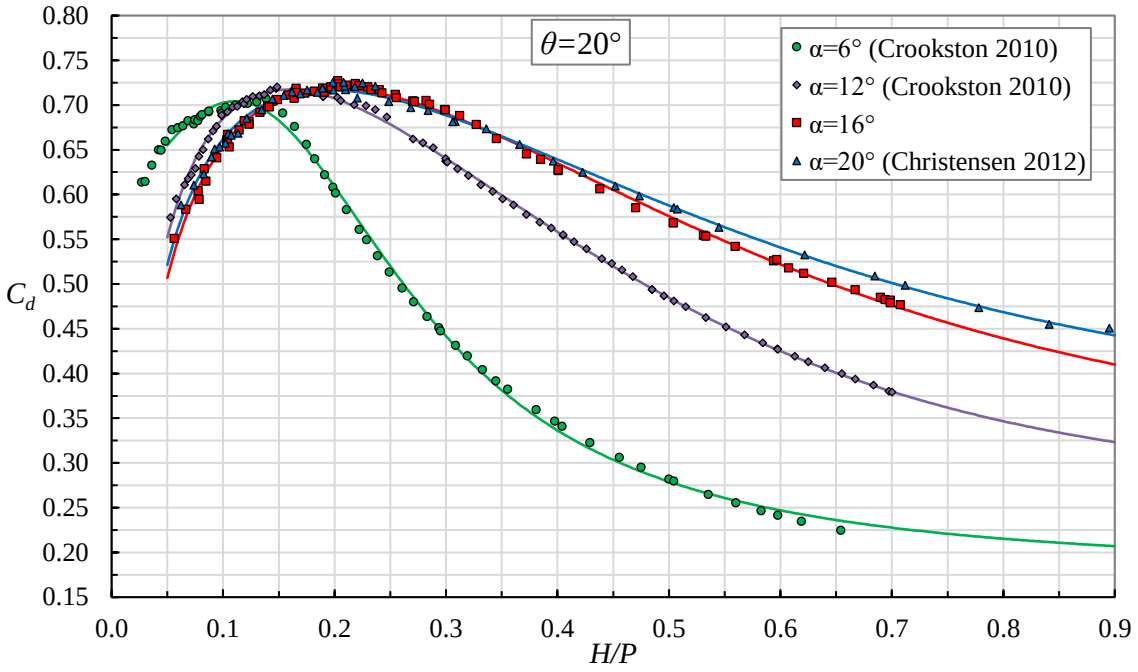

Fig. 16 C_d vs. H/P for θ=20°: α=6°, 12°, 16°, and 20° arced labyrinth weirs.

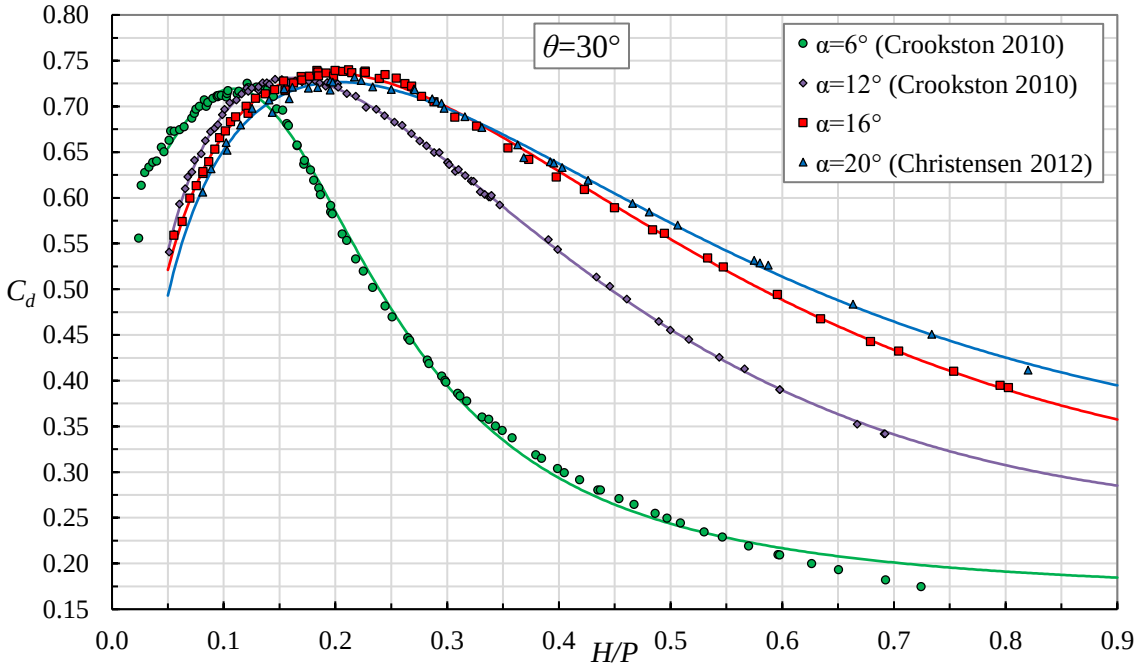

Fig. 17 C_d vs. H/P for θ=30°: α=6°, 12°, 16°, and 20° arced labyrinth weirs.

Table 5 Half-round crested arced labyrinth weir curve fit coefficients for Eqs. [5] and [6] valid for $0.05 \leq H/P \leq 0.8$.

Geometry		Eq.	Empirical Coefficients				Correlation Coefficient
θ [°]	α [°]		a	b	c	d	R^2
10	6	5	65.7156	-0.1048	2.0860	0.2005	0.997
	12	6	1.6633	0.2532	0.4867	0.3342	0.998
	16	6	1.2573	0.2784	0.4420	0.4128	0.995
	20	6	0.8774	0.5045	0.4539	0.2735	0.984
20	6	5	52.9460	-0.1108	1.9018	0.1784	0.998
	12	6	2.1060	0.1227	0.5972	0.3214	0.999
	16	6	1.43872	0.1636	0.6310	0.3100	0.996
	20	6	1.0847	0.3008	0.5319	0.3276	0.995
30	6	5	68.6077	-0.1088	1.7951	0.1623	0.996
	12	6	2.7769	0.0482	0.6341	0.3244	0.992
	16	6	2.1022	0.0410	0.7260	0.2751	0.998
	20	6	1.6654	0.1040	0.6576	0.3142	0.996

In applying these data, designers may be required to interpolate between datasets to accommodate site-specific constraints. When interpolating between α datasets for design purposes, common θ values should be used when possible. When design constraints require θ to be something other than 10°, 20°, or 30° double interpolation may be required.

While the presented data above are for arced labyrinth weirs with cycle number (N) equaling five, these data can be applied to arced labyrinth weirs with varying N. As mentioned in the Literature Review, Christensen (2012) studied the effects of cycle number on discharge efficiency. The distal cycles are likely less efficient due to abutment effects and possible flow separation; therefore, increasing cycle number could slightly increase efficiency by increasing the number of interior cycles. Otherwise the data can be applied with negligible effects due to cycle number.

Nappe Behavior and Submergence

For each of the α=16° geometries modeled, only the nappes for the distal half cycles aerated between 0.2<*H/P*<0.3 (see Fig. 18). At 0.3<*H/P*<0.4 this aeration became unstable and oscillated between aerated and drowned. At *H/P*<0.2 all cycles experienced a clinging nappe behavior, and at *H/P*>0.4 all cycles were drowned. For *H/P*>0.6, small air cavities would occasionally travel upstream from the aerated tailwater flow into the downstream cycles. These cavities would rapidly be filled with water and forced downstream.

(a) (b) (c)

Fig. 18 Distal half cycle nappe aeration at *H/P*=0.2 for α=16°: θ=10°(a), 20°(b), and 30°(c).

Due to the short radius (*R*) of the θ=30° geometry and convergent flow momentum, the θ=30° weir experiences more severe submergence compared to θ=10° and 20°, initially forming immediately downstream of the upstream apexes. A mound also formed due to converging flow. Fig. 19 compares the downstream behavior of the α=16°, arced labyrinth weirs at *H/P*=0.3 and 0.6. With the milder arc of θ=10°, the downstream cycles of the arced labyrinth weir can easily discharge the incoming fluid from the upstream cycles; this can be seen by the jets of whitewater discharging from the center of each downstream cycle (Fig. 19a).

On the contrary, the θ=30° arced labyrinth weir (Fig. 19c) experienced a downstream standing wave or flow mound due to converging flow (shown in red in Fig.

19c), like that of an arced-ogee spillway. This mound submerges the weir at lower *H/P* when compared to the θ=10° and 20° weirs, which decreases the weirs free flow capacity and, consequently, the weir's discharge efficiency. Designers need to consider under what *H/P* ratios their prototype will operate and select the appropriate design, giving special consideration to site-specific constraints and the cycle arc angle (θ) with its accompanying submergence effects.

For nappe behavior and submergence information on the α=6°, 12°, and 20° arced labyrinth weirs see the Literature Review, and Crookston (2010) and Christensen (2012).

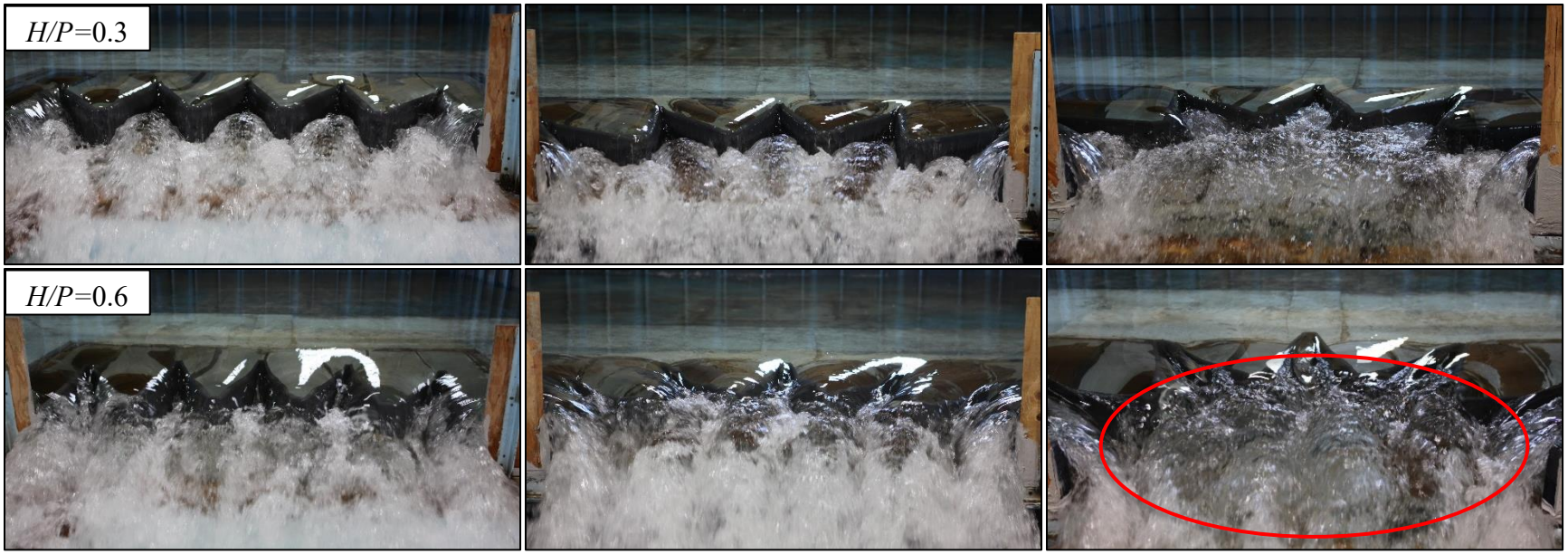

(a) (b) (c)

Fig. 19 Comparison of tailwater submergence at H/P=0.3 and 0.6 for α=16°: θ=10°(a), 20°(b), and 30°(c). Downstream mound shown in red for θ=30°.

Physical Data Uncertainty Analysis

Using the methods described in ASME PTC 19.1 (ASME 2006) an uncertainty analysis was performed on each datapoint to quantify the confidence interval of the C_d results. Eq. [1] was solved for C_d as shown in.Eq. [7], which resultes in C_d being a function of Q, L_c, g, and H. Because g is a known constant, the uncertainty in C_d results from random standard (s_{X_i}) and systematic standard (b_{X_i}) errors in Q, L_c, and H; each of these errors are quantified in Table 6.

$$C_d = \frac{3}{2} \cdot \frac{Q}{L_c\sqrt{2g}H^{\frac{3}{2}}} \quad [7]$$

Table 6 Random and systematic standard errors for each measured variable.

Variable	Description	Units	Random Standard Uncertainty (s_{X_i})	Systematic Standard Uncertainty (b_{X_i})
Q	Volumetric flow rate	m^3/s	±0.25%	0
L_c	Weir crest length	mm	0	±0.794
H	Total head	mm	±0.305	±0.152

Partial derivatives of Eq. [7] were then taken for each variable (i.e. $\frac{\partial C_d}{\partial X_i}$ where X_i represents each measured variable) to calculate sensitivity coefficients (ω_{Xi}) as per ASME (2006). The equations for each sensitivity coefficient are given in Eqs. [8], [9], and [10].

$$\omega_Q = \frac{3}{4} \cdot \frac{\sqrt{2}}{L_c\sqrt{g} \cdot H^{\frac{3}{2}}} \quad [8]$$

$$\omega_{L_c} = -\frac{3}{4} \cdot \frac{\sqrt{2} \cdot \mathrm{Q}}{[\![(L]\!]_c)^2\sqrt{g} \cdot H^{\frac{3}{2}}} \quad [9]$$

$$\omega_H = -\frac{9}{8} \cdot \frac{\sqrt{2} \cdot \mathrm{Q}}{L_c\sqrt{g} \cdot H^{\frac{5}{2}}} \quad [10]$$

ω_{X_i} was then related to s_{X_i} and b_{X_i} via Eqs. [11] and [12]. s_{C_d} and b_{C_d} were then used to calculate combined standard uncertainty in C_d (u_{C_d}) using Eq. [13]. u_{C_d} was then multiplied by a T value of 2 to represent confidence intervals of 95% and is symbolized by $U_{C_{d\,95}}$.

$$s_{C_d} = \sqrt{\sum\left(\omega_{X_i} \cdot s_{X_i}\right)^2} \quad [11]$$

$$b_{C_d} = \sqrt{\sum\left(\omega_{X_i} \cdot b_{X_i}\right)^2} \quad [12]$$

$$u_{C_d} = \sqrt{\left(b_{C_d}\right)^2 + \left(s_{C_d}\right)^2} \quad [13]$$

$U_{C_{d\,95}}$ is visualized in Fig. 20 where 95% confidence intervals are shown for each collected C_d datapoint; each datapoint is also normalized by an empirically calculated C_d using Eq. [6]. A maximum error of 5% occurs at the lowest head tested while the minimum error of 0.3% occurs at the highest head tested. Higher uncertainty is present at low head datapoints because slight errors in determining H (e.g.; slight error in the crest elevation reference, etc.) can result in a significant error in C_d. Physical model tabular uncertainty data are shown alongside tabular datapoints in Appendix B

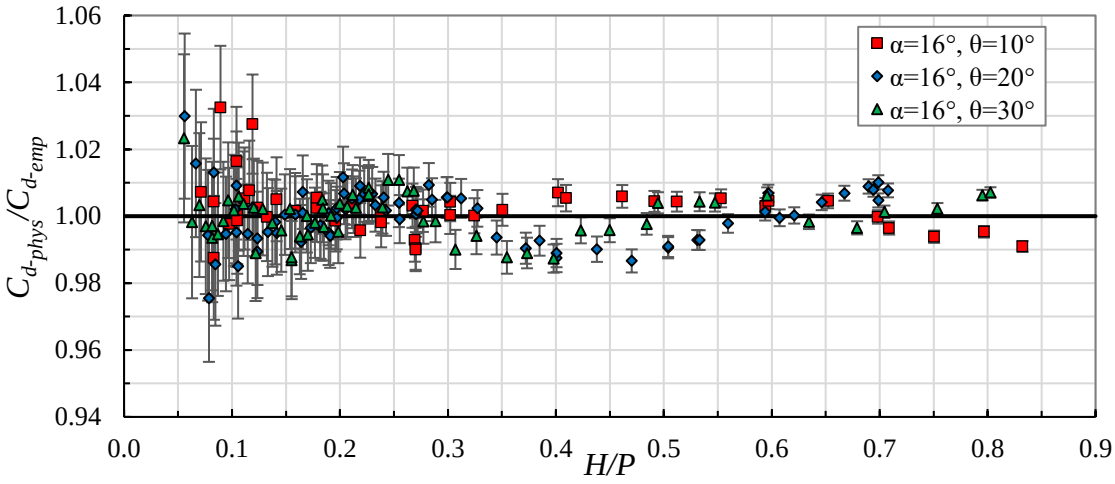

Fig. 20 Representation of $U_{C_{d\,95}}$ with C_d normalized by Eq. [6] (i.e. $C_{d\text{-}phys}/C_{d\text{-}emp}$).

NUMERICAL MODEL RESULTS

The results presented in this section are time-averaged over 10-15 seconds. Time series data and plots and specified Q and time average H values are found in Appendix C.

Grid Convergence Index

Using the mesh configurations in Table 2, a grid convergence index (GCI) (ASCE 2009) was calculated using Eq. [3] with p_c=2 and F_s=1.25 as per ASCE (2009). These results are shown in Table 7. While two reservoir meshes were tested, the GCI focuses on the grid refinement of the weir mesh alone. To normalize slight variations in discharge, the relative error in C_d between the physical and numerical data was used in the analysis and produced GCI values less than 2% for nearly all discharges. These results ensure that the numerical solutions are within the asymptotic range of a true solution, independent of grid size.

However, at H/P=0.6 for the θ=10° weir and at $H/P \geq 0.6$ for the θ=30° weir the solution diverged at the finest mesh with 3%<GCI<5%. It is the author's opinion that this behavior is due to the large quantity of cells associated with resolving the velocity profile at the weir crest. At $H/P \geq 0.6$ and at the finest weir mesh tested (Δ_{WM}/t_w=0.27), 10.7 to 12.2 cells are used to resolve flow depth at the crest. Flow-3D utilizes a log-law estimation of the velocity profile near wall boundaries and just outside of the viscous sub-layer. In their documentation Flow-3D states the following:

> *The first cells along the wall should be sized so that they include the viscous sub-layer and end well within the log-law region of the boundary layer. If the first cell outer edge falls in the viscous sub-layer or extends into the outer, or free-stream, region, then the calculated near-wall velocity and shear stress deviate from the physical case, where they do not correspond to the log-law relation.*

Due to the high velocities and increased critical depths associated with $H/P \geq 0.6$, it is assumed that the finest mesh uses multiple cells to resolve the viscous sub-layer, which can cause the numerical solution to deviate from physical observations. The GCI only shows divergence at $H/P = 0.6$ for the $\theta = 10°$; however, at $H/P \geq 0.6$, for both weirs, solutions for the RM1-WM3 mesh configuration slightly deviated from the physical data, which is discussed in the following section.

Table 7 Calculated GCI for α=16°: θ=10° and 30° as per ASCE (2009).

				θ=10°			θ=30°		
	Mesh	Δ_{WM}/t_w	r (Δ_2/Δ_1)	ε_{C_d}	ε ($\lvert f_2-f_1\rvert$)	**GCI (%)**	ε_{C_d}	ε ($\lvert f_2-f_1\rvert$)	**GCI (%)**
H/P=0.3	RM1-WM0	0.54	–	0.0575	–	**–**	0.0744	–	**–**
	RM0-WM1	0.48	1.13	0.0227	0.0349	**16.41%**	0.0362	0.0383	**18.02%**
	RM0-WM2	0.36	1.33	0.0049	0.0178	**2.86%**	0.0020	0.0341	**5.49%**
	RM1-WM2	0.36	1.33	0.0055	0.0172	**2.76%**	0.0114	0.0248	**3.98%**
	RM1-WM3	0.27	1.33	0.0069	0.0014	**0.23%**	0.0028	0.0086	**1.39%**
H/P=0.4	RM1-WM0	0.54	–	0.0185	–	**–**	0.0246	–	**–**
	RM0-WM1	0.48	1.13	-0.0508	0.0693	**32.62%**	0.0123	0.0123	**5.79%**
	RM0-WM2	0.36	1.33	-0.0229	0.0280	**4.49%**	-0.0038	0.0161	**2.59%**
	RM1-WM2	0.36	1.33	-0.0254	0.0254	**4.08%**	-0.0029	0.0152	**2.44%**
	RM1-WM3	0.27	1.33	-0.0186	0.0068	**1.09%**	0.0037	0.0065	**1.05%**
H/P=0.5	RM1-WM0	0.54	–	0.0365	–	**–**	0.0154	–	**–**
	RM0-WM1	0.48	1.13	-0.0409	0.0774	**36.42%**	0.0095	0.0058	**2.75%**
	RM0-WM2	0.36	1.33	-0.0181	0.0228	**3.67%**	0.0154	0.0058	**0.94%**
	RM1-WM2	0.36	1.33	-0.0195	0.0214	**3.43%**	0.0111	0.0016	**0.26%**
	RM1-WM3	0.27	1.33	-0.0109	0.0086	**1.39%**	0.0121	0.0010	**0.16%**
H/P=0.6	RM1-WM0	0.54	–	0.0453	–	**–**	0.0142	–	**–**
	RM0-WM1	0.48	1.13	0.0112	0.0340	**16.02%**	-0.0003	0.0145	**6.80%**
	RM0-WM2	0.36	1.33	0.0193	0.0081	**1.30%**	0.0104	0.0107	**1.71%**
	RM1-WM2	0.36	1.33	0.0150	0.0038	**0.61%**	0.0135	0.0138	**2.22%**
	RM1-WM3	0.27	1.33	0.0351	0.0201	**3.23%**	0.0452	0.0317	**5.09%**
H/P=0.7	RM1-WM0	0.54	–	0.0344	–	**–**	0.0226	–	**–**
	RM0-WM1	0.48	1.13	-0.0074	0.0418	**19.66%**	0.0128	0.0098	**4.62%**
	RM0-WM2	0.36	1.33	0.0187	0.0261	**4.19%**	0.0206	0.0078	**1.25%**
	RM1-WM2	0.36	1.33	0.0283	0.0357	**5.74%**	0.0197	0.0069	**1.11%**
	RM1-WM3	0.27	1.33	0.0321	0.0038	**0.61%**	0.0447	0.0250	**4.01%**
H/P=0.8	RM1-WM0	0.54	–	0.0271	–	**–**	0.0401	–	**–**
	RM0-WM1	0.48	1.13	0.0140	0.0131	**6.15%**	0.0295	0.0107	**5.02%**
	RM0-WM2	0.36	1.33	0.0136	0.0004	**0.07%**	0.0319	0.0024	**0.39%**
	RM1-WM2	0.36	1.33	0.0212	0.0071	**1.14%**	0.0357	0.0062	**1.00%**
	RM1-WM3	0.27	1.33	0.0187	0.0025	**0.40%**	0.0545	0.0188	**3.01%**

Comparison to Physical Data

Good agreement was found when comparing the numerical results to the physical model data. Due to variations in the numerically calculated *H*, the numerical results will be directly compared to the physical data via Eq. [6] at the same *H;* these comparisons, along with physical data points, are shown in Fig. 21 and Fig. 22 for the α=16°: θ=10° and 30° weirs, respectively.

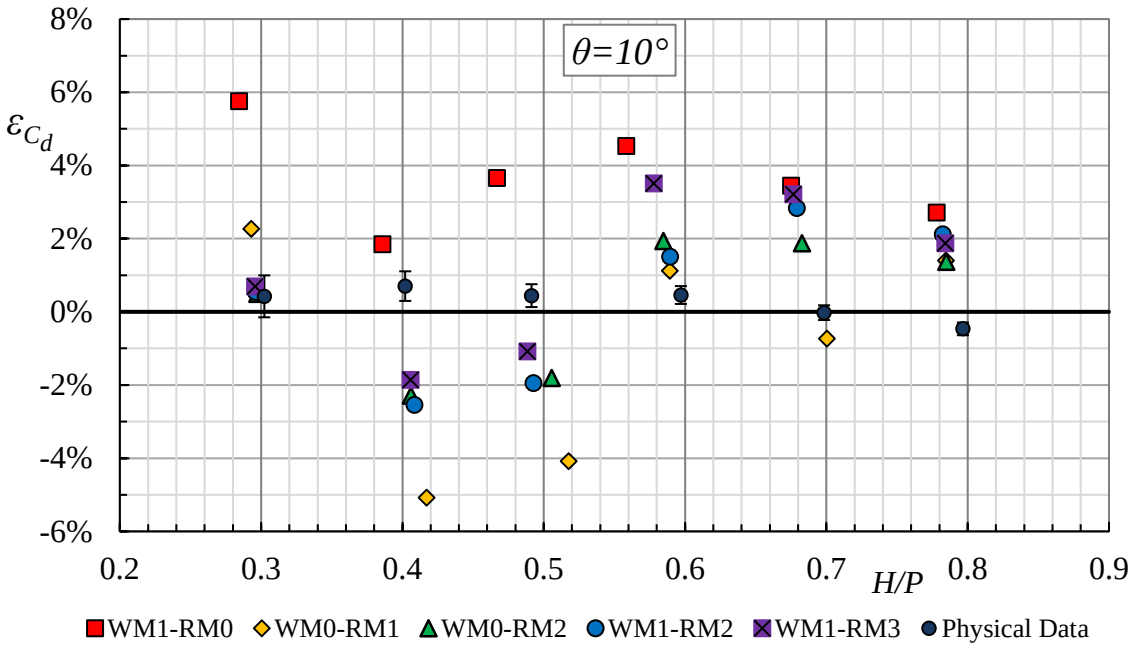

Fig. 21 Relative errors (ε_{C_d}) between numerical and empirical (Eq. [6]) results for all mesh configurations for the α=16°: θ=10° weir.

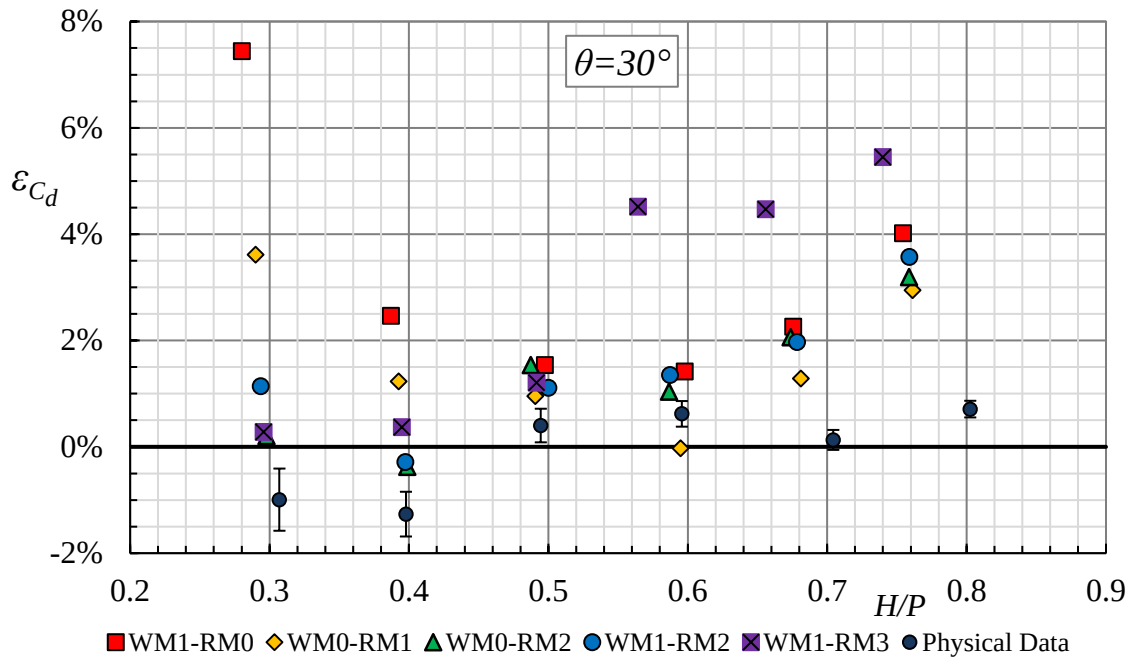

Fig. 22 Relative errors (ε_{C_d}) between numerical and empirical (Eq. [6]) results for all mesh configurations for the α=16°: θ=30° weir.

The WM2 mesh provided results closest to the physical data independent of it being paired with either RM0 or RM1. All results of the WM2 mesh had relative errors (error between numerical and Eq. [6]) in C_d of -2.5% to 2.8% for the α=16°: θ=10° weir and relative errors of -0.4% to 3.6% for θ=30°. The C_d values of the physical, Eq. [6], and numerical data are displayed in Fig. 23 and Fig. 24 for θ=10° and 30°, respectively. The WM1-RM3 mesh configuration also produced accurate results at $H/P \leq 0.5$ with relative errors between -1.9% and 0.7% for θ=10° and 0.3% and 1.2% for θ=30°.

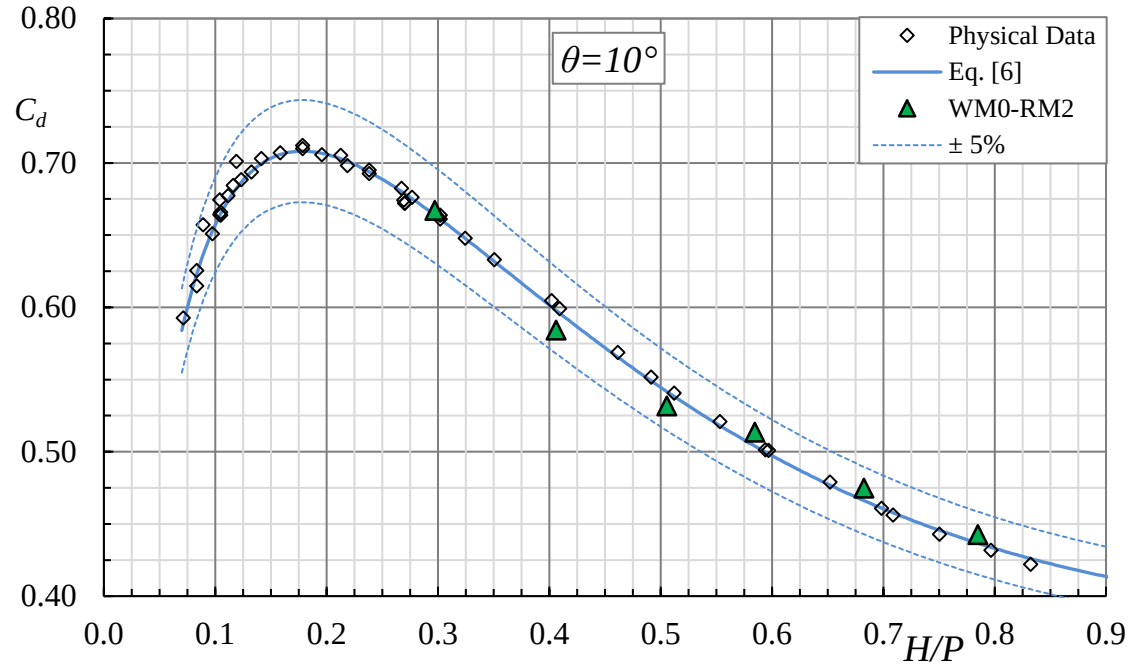

Fig. 23 C_d vs. H/P comparison between physical results, Eq. [6], and WM0-RM2 results for the α=16°: θ=10° weir.

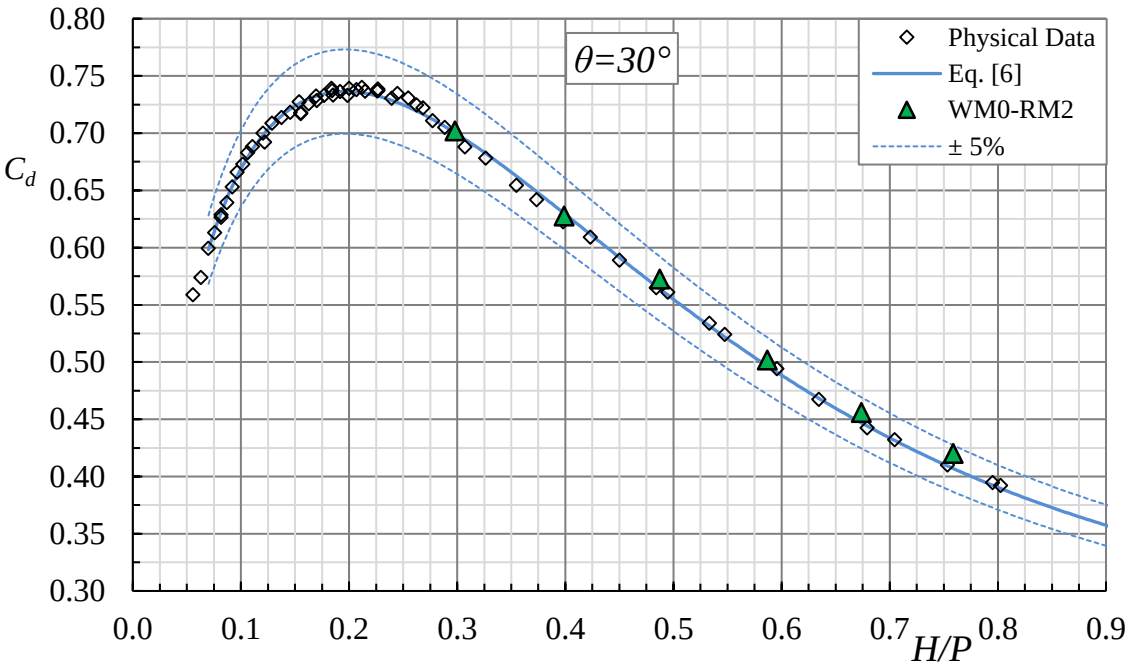

Fig. 24 C_d vs. H/P comparison between physical results, Eq. [6], and WM0-RM2 results for the α=16°: θ=30° weir.

The good behavior of the CFD models suggests that both physical and numerical models are accurately representing the hydraulic behavior of the arced labyrinth weir geometry tested, and that CFD could be a useful tool for predicting hydraulic performance for other geometric variations of arced labyrinth weirs. The use of CFD modeling is recommended when designing arced labyrinth weirs due to its ability to implement site-specific conditions and give a level of assurance when using and interpolating between the available empirical data. The author does, however, recommend that the results of CFD models be validated through empirical data or, ideally, a physical model. This validation allows the modeler to identify and avoid errors like those discussed in the Grid Convergence Index section that were experienced at the finest mesh resolution tested (WM3).

Nappe and Downstream Behavior

For the α=16°: θ=30° weir the CFD results generally replicated the nappe behavior and tailwater submergence observations seen during physical data collection at all discharges tested. Examples of this are given in Fig. 25 and Fig. 26. Fig. 25 provides a downstream view of the θ=30° weir at H/P=0.5 that displays local submergence forming at the interior of the upstream apexes; the numerical model also accurately resolved the nearly complete drowned condition of the weir with some aeration forming at the distal downstream apexes. Fig. 26 demonstrates the accurate numerical resolution of the drowned behavior of the θ=30° weir at H/P=0.8.

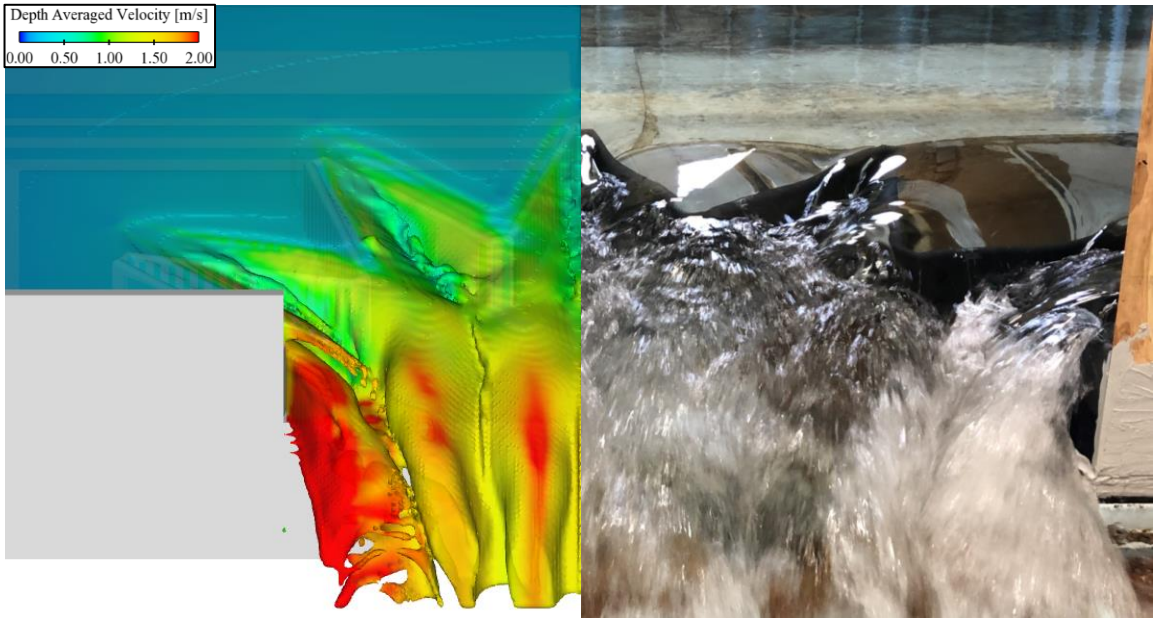

Fig. 25 α=16°: θ=30° H/P=0.5 comparison between numerical and physical model tailwaters.

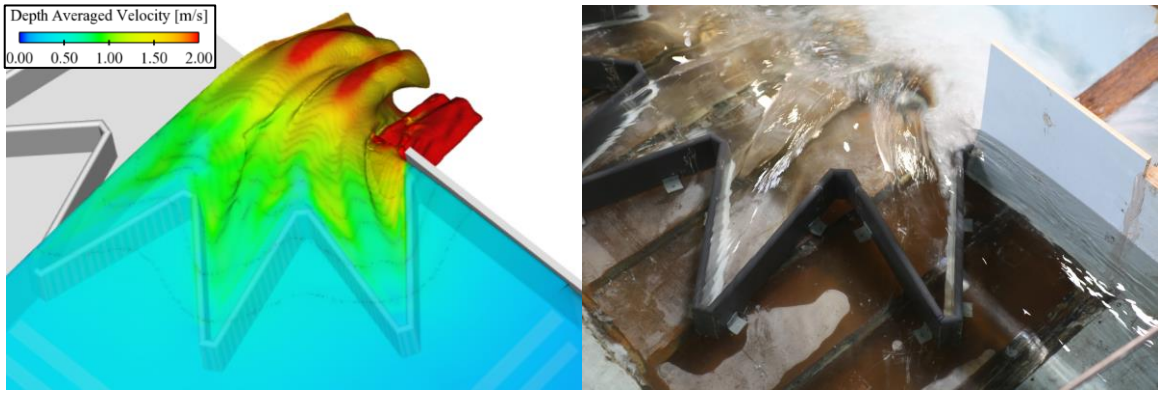

Fig. 26 α=16°: θ=30° H/P=0.8 comparison between numerical and physical tailwater.

For the α=16°: θ=10° weir, the numerical model resolved a partially aerated nappe for $0.3 \geq H/P \geq 0.7$ (air cavities decreased in size and quantity with increasing H). In the physical model at these discharges, the nappe was not aerated; however, flow aeration did occur as flow from cycle sidewalls collided near the downstream apexes. Also, in the physical model, flow surging was observed where the nappe behavior fluctuates

periodically. What is observed is that a forced air cavity would occasionally travel upstream but would then be rapidly filled with water and carried back downstream.

A comparison between the physical and numerical θ=10° models at H/P=0.4 is given in Fig. 27. The differences in nappe behavior between the physical and numerical models for the θ=10° weir are the likely cause for the slightly greater range of relative errors (ε_{C_d} between -2.5% and 2.8%) in the θ=10° numerical model compared to the θ=30° model (ε_{C_d} between -0.4% and 3.6%) for both WM2 mesh configurations at $0.3 \geq H/P \geq 0.7$.

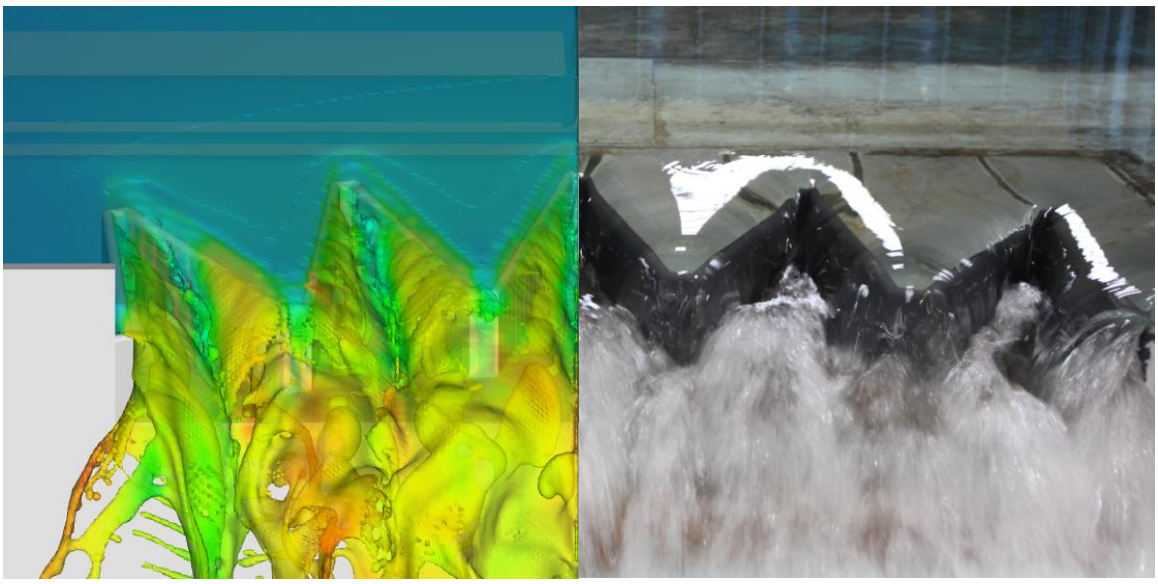

Fig. 27 - α=16°: θ=30° H/P=0.4 comparison between numerical and physical nappe and tailwater aeration.

Arced Labyrinth Weir Cycle Alignment

As mentioned previously, the θ=30° geometries are more hydraulically efficient at H/P<~0.5 than the θ=10° geometries due to better cycle alignment to approaching flow conditions. Using Flow-3D's post-processing tool, FlowSight, streamlines were generated (see Fig. 28) for both the α=16°: θ=10° and 30° arced labyrinth weirs at H/P=0.4 to observe approach flow conditions and cycle alignment

In Fig. 28a, the streamlines paralleling the headbox wall and entering the distal downstream cycle via the distal sidewall are nearly perpendicular to the weir's crest, causing this portion of the weir to be highly efficient. However, this directs flow in the adjacent sidewall to curve around the upstream apex and travel nearly parallel to the weir's crest for half of the sidewall length causing a loss in efficiency locally. Fig. 28a also shows streamlines entering upstream cycle openings at varying approach angles while Fig. 28b shows a more even distribution of flow with streamlines entering nearly perpendicular to each upstream cycle opening.

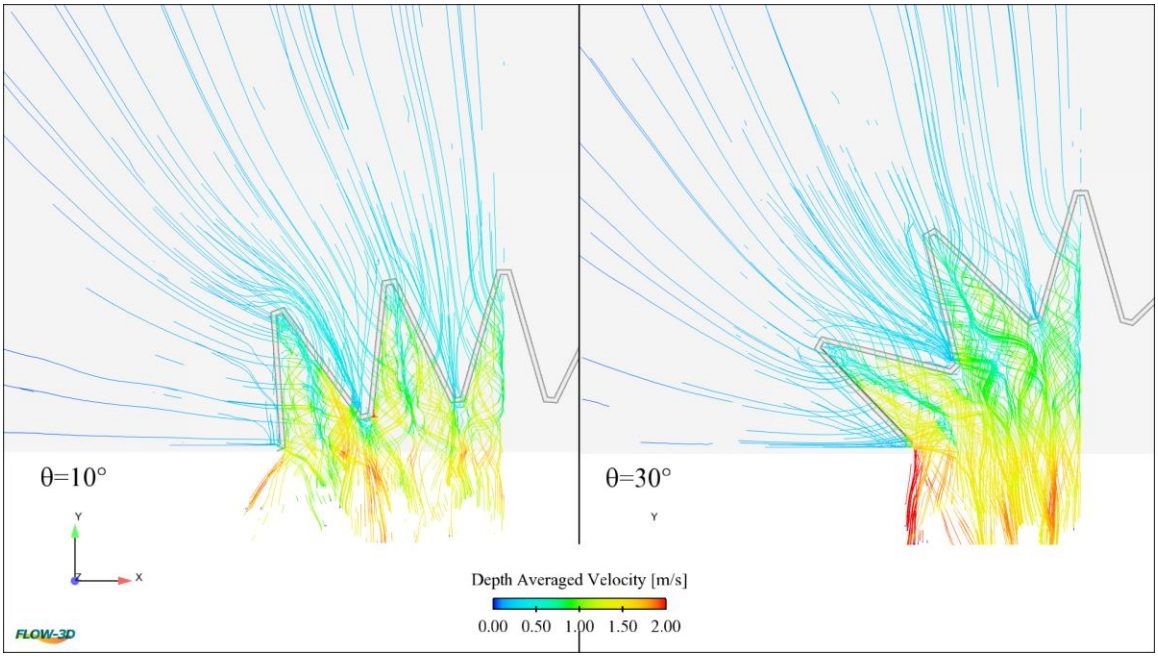

(a) (b)

Fig. 28 Comparison between α=16°: θ=10° (a) and 30° (b) streamlines at H/P=0.4.

While the θ=30° weirs are better aligned to the approach flow at H/P<~0.5, as approach velocity and depth increase streamlines start to align more with the channel opening and not the weir crest (see Fig. 29). Converging flow downstream of the weir also causes the weir to submerge.

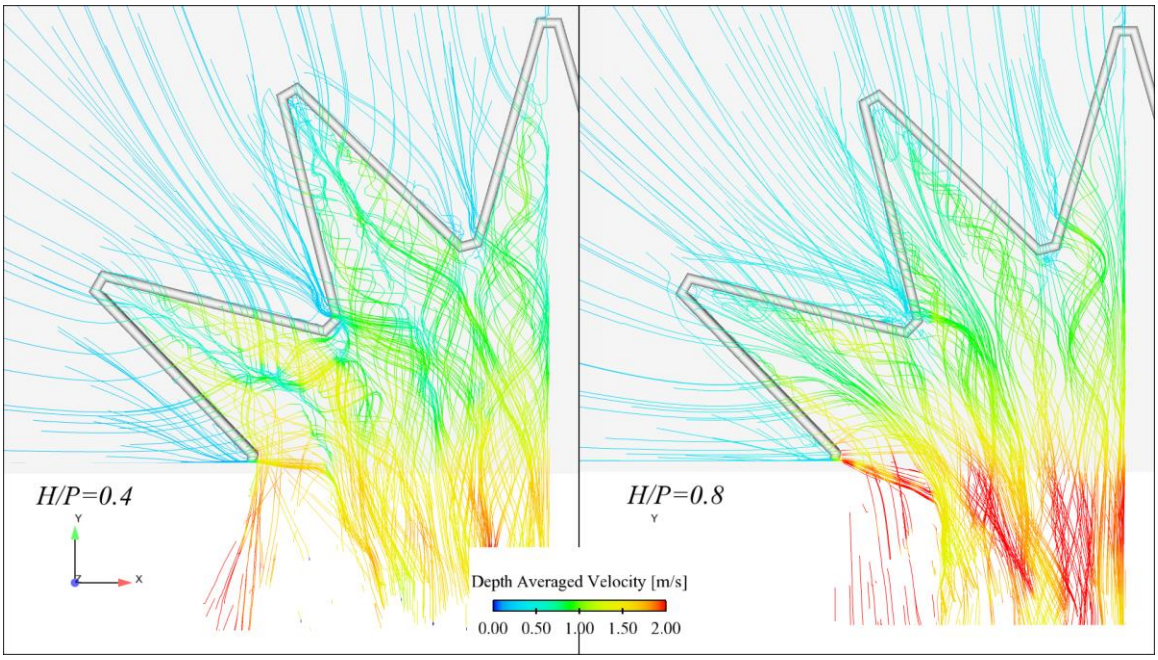

(a) (b)

Fig. 29 α=16°: θ=30° streamline comparison between *H/P*=0.4 (a) and *H/P*=0.8 (b).Submergence Effects

As mentioned in the physical model results, the θ=30° weirs experience more extreme submergence when compared to θ<30°. Due to the shorter arc radius, *R*, and converging flow momentum patterns downstream flow is forced to converge, forming a mound, and causes the weir to submerge. In one-dimensional (1D) open channel hydraulics it is assumed that a control section occurs at the weir crest and the flow transitions from subcritical into supercritical flow. Weir submergence, however, can cause the control point of the weir to shift from the weir's crest to a point further downstream. The Froude Number is equal to one at critical depth ($F = \frac{V}{\sqrt{gy_c}} = 1$); by displaying localized values of the Froude Number in the *x*-*y* plane the shift between control points is apparent for the θ=30° weir (see Fig. 30).

Fig. 30 shows the θ=30° weir at H/P=0.4 and 0.8 with a color scheme indicating values of the Froude Number between 0 and 1. In Fig. 30a the red coloration at the weir crest indicates the location of the critical section; also displayed are areas of local submergence at the upstream apexes (yellow and green coloration). In comparison, Fig. 30b shows that the control section does not occur until the channel exit. This shift in control point is due to increased approach velocity, poor cycle alignment to approach flow (at large discharges) and converging flow downstream of the weir. All of which results in an elevated headwater, which suppresses the formation of a critical section at the crest.

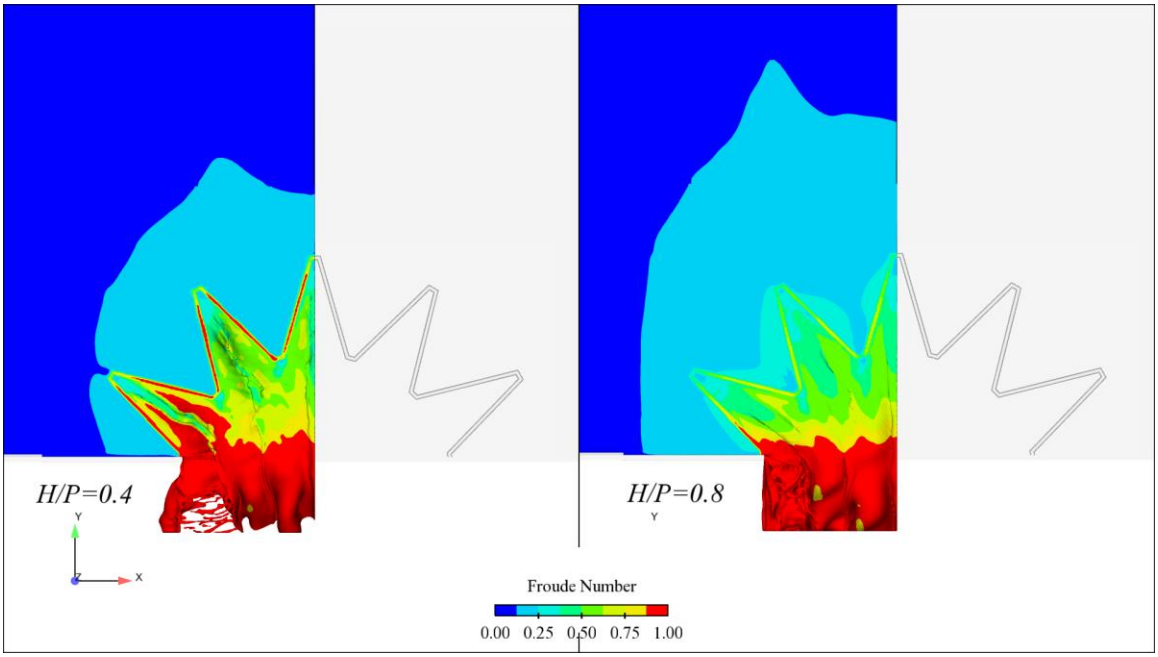

(a) (b)

Fig. 30 α=16°: θ=30° comparison of localized Froude Number for H/P=0.4 (a) and H/P=0.8 (b).

CONCLUSION

The purpose of this study was to further the understanding of the hydraulic behaviors of arced labyrinth weirs in reservoir applications through physical and numerical modeling. Existing arced labyrinth weir research is limited, but designers now have additional reference data and information to aid in the hydraulic design process. From the results of this study the following is concluded:

- α=16° arced labyrinth weirs are more hydraulically efficient than interpolation between α=12° and 20° geometries would suggest. Like the observations of Christensen (2012), it was found that discharge efficiency (quantified by C_d) increases with increasing α.
- In comparing the α=16° arced labyrinth geometries at the three θ values tested, the θ=20° geometry is most efficient at H/P>0.3 and only slightly less efficient than θ=30° at H/P<0.3. The θ=10° was the least efficient at H/P<0.5. Designers must consider at what heads their prototype will operate and choose the best value of θ to fit their design requirements., which may also be constrained to site specific conditions.
- The superior discharge efficiency of the θ=30° arced labyrinth weirs at smaller heads (H/P<0.35) is due to better cycle alignment. However, these benefits quickly diminish (with increasing head) as increased momentum and converging downstream flow patterns submerges the weir at lower H/P values compared to θ<30° (H/P<0.35 for θ=20° and <0.55 for θ=10°). This submergence forms a mound of convergent flow downstream of the weir and

causes the control section to shift from the weir crest to the channel outlet, as supported by the numerical models.

- In the hydraulic design of arced labyrinth weirs, the empirical data herein can provide estimates for rating curve development at various cycle number configurations. However, designers must consider site-specific characteristics that may alter discharge efficiency. To accurately model site-specific conditions the use of physical and CFD modeling is recommended.
- In the numerical models, a mesh independent solution was found as quantified by GCI values less than 2.2%. However, at $H/P>0.6$ the finest mesh (RM1-WM3) diverged due to high flow depths, and a cell size that used more than two grid cells (vertically increasing) to resolve the velocity profile in the viscous sub-layer and log-law estimated turbulent region at the weir crest.
- The numerical models provided good agreement with physical model results with relative errors between -2.5% and 3.6% for the RM0-WM2 and RM1-WM2 mesh configurations. Good agreement was also found for the RM1-WM3 mesh configuration at $H/P<0.6$.
- In comparing the nappe behaviors of the physical and numerical models, the numerical model accurately resolved the nappe for the α=16°: θ=30° arced labyrinth weir. The α=16°: θ=10° numerical model demonstrated small voids of air in the nappe, while the physical model represented a mostly drowned nappe with occasional air voids entering and rapidly being forced downstream.
- Streamlines rendered in post-processing of the numerical models show improved alignment of the α=16°: θ=30° arced labyrinth weir to approach flow

at low heads in comparison to α=16°: θ=10°. Submergence is also accurately modeled for the α=16°: θ=30° weir and shows the shift in control section due to changes in approach velocity alignment and converging flow patterns immediately downstream of the weir.

- It can be concluded that CFD can be a useful tool in the hydraulic design of arced labyrinth weirs when designers ensure their solution is mesh independent. It is stressed that CFD models of arced labyrinth weirs be verified with the empirical data presented herein, or, ideally, a physical model study.

Further arced labyrinth weir research is merited to better understand trends in discharge efficiency for 12°<α<20°, the effects of various approach flow conditions, and downstream channel configurations including the use of an arced apron as opposed to the rectangular apron used in this study.

REFERENCES

ASCE. (2009). “CHAPTER 2 TERMINOLOGY AND BASIC METHODOLOGY.” *Verification and Validation of 3D Free-Surface Flow Models*, 19–44.

ASME. (2006). *ASME PTC 19.1-2005: Test Uncertainty*. *American Society of Mechanical Engineers*, New York, NY.

Christensen, N. A. (2012). “Flow Characteristics of Arced Labyrinth Weirs.” M.S. thesis, Utah State University, Logan, Utah, USA.

Crookston, B. M. (2010). “Labyrinth weirs.” Ph.D. dissertation, Utah State University, Logan, Utah, USA.

Crookston, B. M., Anderson, R. M., and Tullis, B. P. (2018). “Free-flow discharge estimation method for Piano Key weir geometries.” *Journal of Hydro-Environment Research*, Elsevier, 19(4), 160–167.

Crookston, B. M., and Tullis, B. P. (2012). “Arced Labyrinth Weirs.” *Journal of Hydraulic Engineering*, 138(6), 555–562.

Crookston, B. M., and Tullis, B. P. (2013). “Hydraulic Design and Analysis of Labyrinth Weirs. I: Discharge Relationships.” *Journal of Irrigation and Drainage Enineering*, 139(5), 363–370.

Darvas, L. (1971). “Discussion of performance and design of labyrinth weirs, by Hay and Taylor.” *Journal of Hydraulic Engineering*, 97(8), 1246–1251.

Falvey, H. T. (2003). *Hydraulic Design of Labyrinth Weirs*. *ASCE Press*, ASCE, Reston, VA.

Finnemore, E. J., and Franzini, J. B. (2002). *Fluid Mechanics with Engineering Applications*. McGraw-Hill.

Gentilini, B. (1940). “Stramazzi con cresta a planta obliqua e a zig-zag.” *Memorie e Studi dell Instituto di Idraulica e Construzioni Idrauliche del Regil Politecnico di Milano*, No. 48.(in Italian).

Hay, N., and Taylor, G. (1970). “Performance and design of labyrinth weirs.” *Journal of Hydraulic Engineering*, 96(11), 2337–2357.

Hinchliff, D., and Houston, K. (1984). “Hydraulic design and application of labyrinth spillways.” *Proc. of 4th Annual USCOLD Lecture*, Washington, DC, USA.

Hirt, C., and Nichols, B. (1981). “Volume of fluid (VOF) method for the dynamics of free boundaries.” *Journal of Computational Physics*, Academic Press, 39(1), 201–225.

"k-epsilon models." (2011).<https://www.cfd-online.com/Wiki/K-epsilon_models>(Dec. 5, 2019).

Kozák, M., and Sváb, J. (1961). "Tort alaprojzú bukók laboratóriumi vizsgálata." *Hidrológiai Közlöny*, No. 5.(in Hungarian).

Lefebvre, V., Vermeulen, J., and Blancher, B. (2014). "Influence of geometrical parameters on PK-Weirs discharge with 3D numerical analysis." *Labyrinth and Piano Key Weirs II - PKW 2013 - Erpicum et al. (eds)*, Taylor & Fransic Group, London, England, 49–56.

Lopes, R., Matos, J., and Melo, J. (2006). "Discharge capacity and residual energy of labyrinth weirs." *Proc. of the Int. Junior Researcher and Engineer Workshop on Hydraulic Structures (IJREWHS '06),* Montemor-o-Novo, Hydraulic Model Report No. CH61/06, Div. of Civil Engineering, the University of Queensland, Brisbane, Australia, 47–55.

Lopes, R., Matos, J., and Melo, J. (2008). "Characteristic depths and energy dissipation downstream of a labyrinth weir." *Proc. of the Int. Junior Researcher and Engineer Workshop on Hydraulic Structures (IJREWHS '08)*, Pisa, italy.

Lux, F., and Hinchliff, D. (1985). "Design and construction of labyrinth spillways." *15th Congress ICOLD, Vol. IV, Q59-R15*, Lausanne, Switzerland, 249–274.

Magalhães, A., and Lorena, M. (1989). "Hydraulic design of labyrinth weirs." *Report No. 736*, National Laboratory of Civil Engineering, Lisbon, Portugal.

Melo, J., Ramos, C., and Magalhães, A. (2002). "Descarregadores com soleira em labirinto de um ciclo em canais convergentes. Determinação da capacidad de vazão." *Proc. 6° Congresso da Água*, Porto, Portugal. (in Portuguese).

Pralong, J., Montarros, B., Blancher, B., and Laugier, F. (2011). "A sensitivity analysis of Piano Key Weirs geometrical parameters based on 3D numerical modeling." *Labyrinth and Piano Key Weirs - PKW 2011 - Erpicum et al. (eds)*, Taylor & Fransic Group, London, England, 133–139.

Roache, P. J. (1998). *Fundamentals of Computational Fluid Dynamics*. Hermosa Publishers, Albuquerque, NM.

Saad, Y., and Schults, M. H. (1986). "GMRES: A Generalized Minimal Residual Algorithm for Solving Nonsymmetric Linear Systems." *SIAM Journal on Scientific and Statistical Computing*, 7(3), 856–869.

Sangsefidi, Y., Mehraein, M., and Ghodsian, M. (2015). "Numerical simulation of flow over labyrinth spillways." 22(5), 1779–1787.

Savage, B. M., Crookston, B. M., and Paxson, G. S. (2016). "Physical and Numerical

Modeling of Large Headwater Ratios for a 15° Labyrinth Spillway." *Journal of Hydraulic Engineering*, 142(11), 04016046.

Taylor, G. (1968). "The performance of labyrinth weirs." Ph.D. thesis, University of Nottingham, Nottingham, England.

Thompson, E. A., Cox, N. C., Ebner, L. L., and Tullis, B. (2016). "The Hydraulic Design of an Arced Labyrinth Weir at Isabella Dam." *6th International Symposium on Hydraulic Structures: Hydraulic Structures and Water System Management, ISHS 2016*, Portland, OR.

Tullis, B. P., Young, J. C., and Chandler, M. A. (2007). "Head-Discharge Relationships for Submerged Labyrinth Weirs." *Journal of Hydraulic Engineering*, 133(3), 248–254.

Tullis, J. P., Amanian, N., and Waldron, D. (1995). "Design of Labyrinth Spillways." *Journal of Hydraulic Engineering*, 121(3), 247–255.

Willmore, C. M. (2004). "Hydraulic characteristics of labyrinth weirs." Utah State University.

APPENDICES

Appendix A – Weir Model Drawings

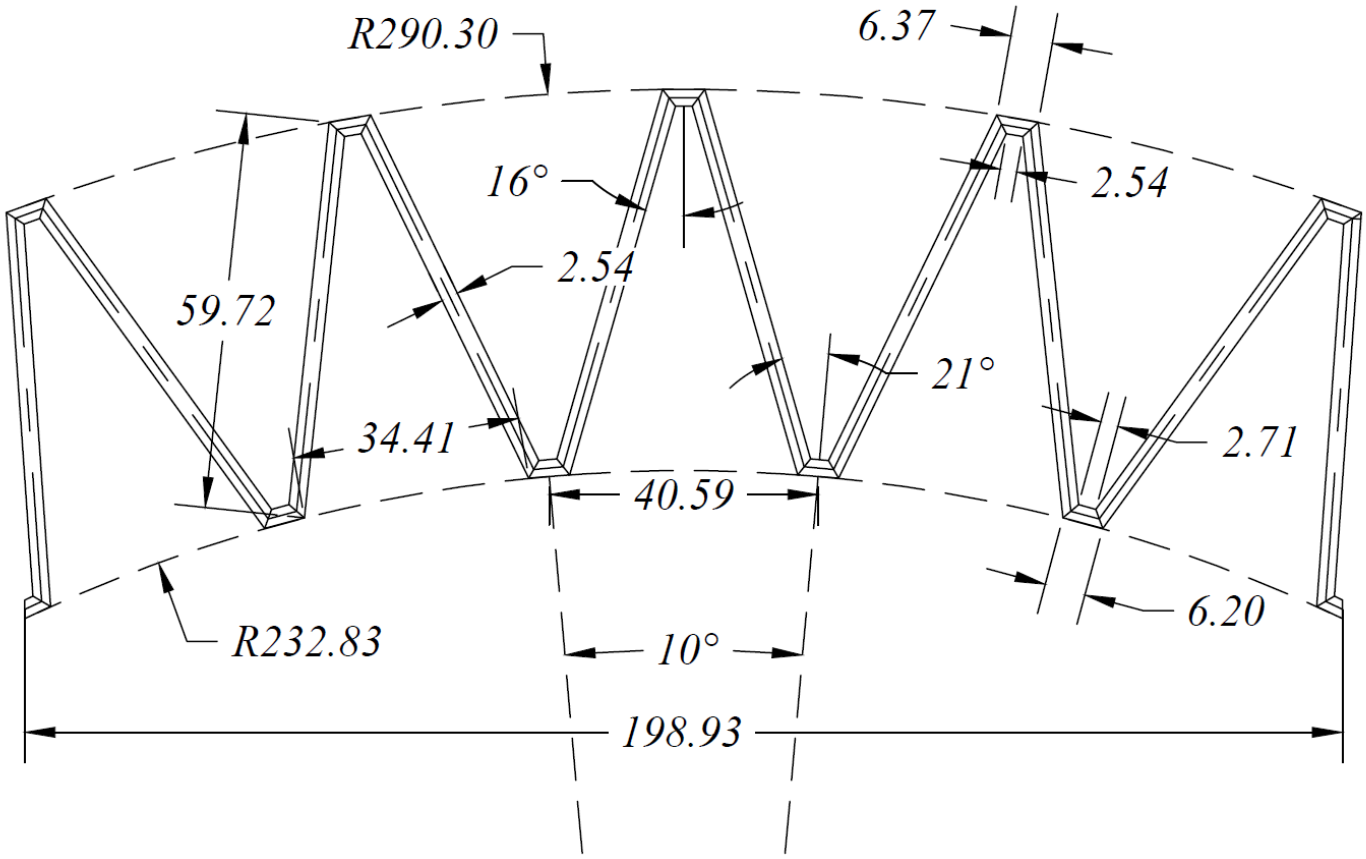

Fig. A1 α=16°, θ=10° weir details (in centimeters).

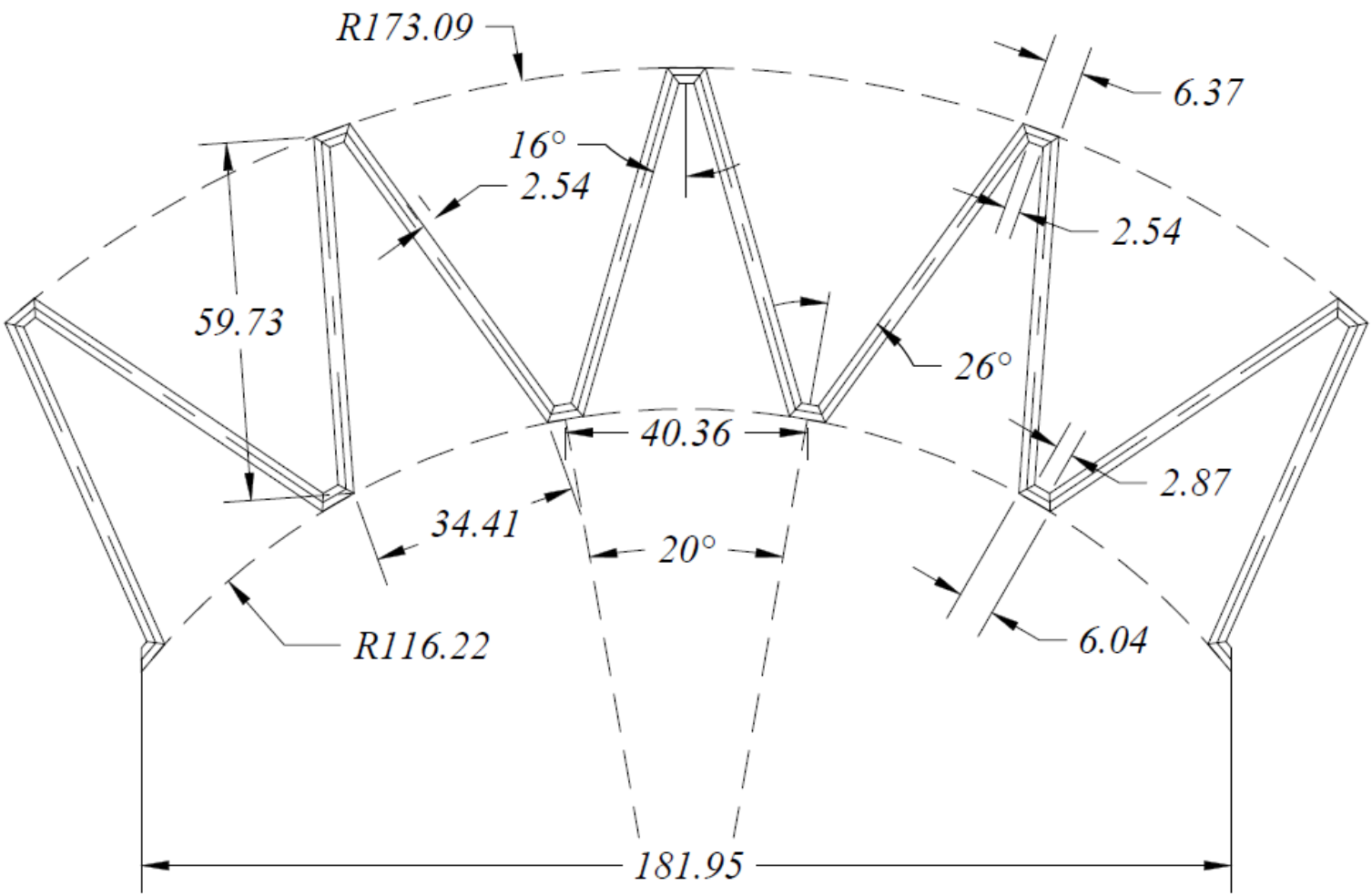

Fig. A2 α=16°, θ=20° weir details (in centimeters).

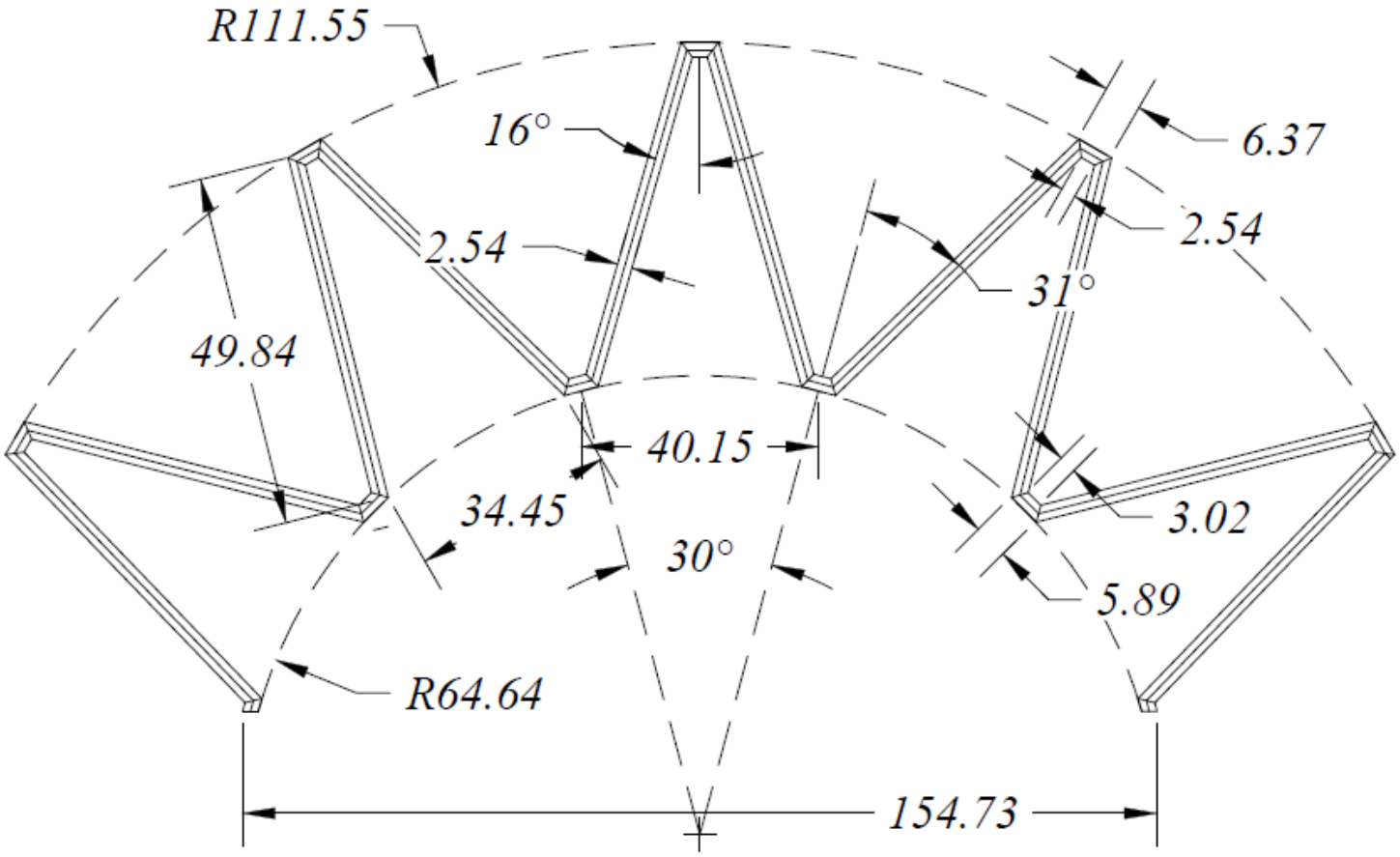

Fig. A3 α=16°, θ=30° weir details (in centimeters).

Appendix B – Tabulated Physical Data

Table B1 α=16°: θ=10° tabulated results from physical model.

Q [L/s]	H [m]	H/P [-]	C_d [-]	$U_{C_{d_{95}}}$ [%]	ε' [-]
19.3	0.015	0.071	0.593	4.16%	1.81
25.2	0.017	0.083	0.615	3.70%	1.88
25.7	0.017	0.083	0.625	3.77%	1.91
29.9	0.018	0.089	0.657	3.69%	2.01
33.8	0.020	0.097	0.651	3.36%	1.99
38.1	0.021	0.104	0.664	3.20%	2.03
38.5	0.021	0.105	0.664	3.18%	2.03
38.6	0.021	0.105	0.666	3.19%	2.03
38.7	0.021	0.104	0.674	3.25%	2.06
43.1	0.023	0.112	0.677	3.05%	2.07
46.2	0.024	0.116	0.684	2.97%	2.09
49.2	0.024	0.119	0.701	2.96%	2.14
51.0	0.025	0.123	0.688	2.81%	2.10
57.1	0.027	0.132	0.694	2.64%	2.12
63.8	0.029	0.141	0.703	2.51%	2.15
76.2	0.032	0.158	0.707	2.26%	2.16
91.5	0.037	0.179	0.710	2.02%	2.17
91.8	0.037	0.179	0.712	2.02%	2.17
104.4	0.040	0.196	0.706	1.84%	2.15
118.3	0.044	0.213	0.705	1.69%	2.15
122.0	0.045	0.219	0.698	1.63%	2.13
137.5	0.049	0.238	0.693	1.49%	2.11
138.0	0.049	0.238	0.695	1.50%	2.12
161.0	0.055	0.267	0.682	1.32%	2.08
161.1	0.055	0.269	0.674	1.30%	2.06
161.2	0.055	0.270	0.672	1.29%	2.05
161.2	0.055	0.270	0.672	1.29%	2.05
168.3	0.057	0.277	0.676	1.27%	2.07
187.6	0.062	0.302	0.661	1.14%	2.02
188.3	0.062	0.302	0.664	1.15%	2.03
204.6	0.066	0.325	0.648	1.05%	1.98
224.5	0.072	0.351	0.633	0.96%	1.93
263.2	0.082	0.402	0.605	0.81%	1.85

Q	H	H/P	C_d	$U_{C_{d_{95}}}$	ε'
268.1	0.084	0.409	0.599	0.79%	1.83
304.7	0.094	0.462	0.569	0.68%	1.74
324.5	0.101	0.491	0.552	0.63%	1.68
338.5	0.105	0.512	0.541	0.59%	1.65
366.0	0.113	0.553	0.521	0.54%	1.59
392.1	0.122	0.594	0.501	0.49%	1.53
394.7	0.122	0.597	0.501	0.49%	1.53
430.9	0.133	0.652	0.479	0.44%	1.46
459.4	0.143	0.698	0.461	0.40%	1.41
464.9	0.145	0.709	0.456	0.39%	1.39
491.8	0.154	0.750	0.443	0.37%	1.35
524.5	0.163	0.797	0.432	0.35%	1.32
547.6	0.170	0.832	0.422	0.33%	1.29

Table B2 α=16°: θ=20° tabulated results from physical model.

Q [L/s]	H [m]	H/P [-]	C_d [-]	$U_{C_{d\,95}}$ [%]	ε' [-]
12.5	0.011	0.056	0.551	4.94%	1.69
17.1	0.014	0.067	0.583	4.41%	1.79
22.4	0.016	0.079	0.594	3.81%	1.82
22.4	0.016	0.078	0.604	3.91%	1.85
25.7	0.017	0.083	0.629	3.81%	1.92
25.8	0.017	0.085	0.615	3.66%	1.88
31.7	0.019	0.094	0.641	3.43%	1.96
37.5	0.021	0.103	0.661	3.23%	2.02
37.7	0.021	0.104	0.658	3.19%	2.01
38.2	0.021	0.104	0.667	3.24%	2.04
38.3	0.021	0.106	0.653	3.13%	2.00
44.5	0.023	0.115	0.672	2.97%	2.06
47.9	0.024	0.119	0.683	2.90%	2.09
50.3	0.025	0.124	0.678	2.78%	2.08
50.5	0.025	0.124	0.681	2.79%	2.08
57.5	0.027	0.133	0.692	2.63%	2.12
62.5	0.028	0.140	0.699	2.53%	2.14
63.4	0.029	0.142	0.698	2.50%	2.14
69.4	0.030	0.149	0.706	2.41%	2.16
76.8	0.032	0.159	0.711	2.28%	2.18
80.2	0.033	0.164	0.707	2.20%	2.16
82.1	0.034	0.165	0.714	2.20%	2.19
82.6	0.034	0.165	0.718	2.21%	2.20
87.6	0.035	0.173	0.713	2.10%	2.18
94.8	0.037	0.182	0.715	2.01%	2.19
94.8	0.037	0.182	0.715	2.01%	2.19
100.7	0.039	0.189	0.715	1.93%	2.19
101.3	0.039	0.189	0.719	1.94%	2.20
101.8	0.039	0.191	0.714	1.91%	2.19
107.2	0.040	0.197	0.718	1.87%	2.20
107.5	0.040	0.197	0.720	1.87%	2.20
113.5	0.041	0.203	0.727	1.84%	2.23
113.6	0.041	0.204	0.724	1.82%	2.21
114.3	0.042	0.205	0.720	1.80%	2.20
119.6	0.043	0.211	0.722	1.76%	2.21
125.3	0.044	0.218	0.721	1.70%	2.21

Q	H	H/P	C_d	$U_{C_{d\,95}}$	ε'
126.4	0.044	0.219	0.724	1.70%	2.22
129.3	0.045	0.222	0.722	1.67%	2.21
135.6	0.047	0.230	0.720	1.61%	2.20
137.7	0.047	0.233	0.717	1.59%	2.19
144.3	0.049	0.240	0.717	1.54%	2.19
145.7	0.049	0.243	0.714	1.52%	2.18
156.0	0.052	0.255	0.708	1.44%	2.17
156.1	0.052	0.255	0.712	1.45%	2.18
168.9	0.055	0.270	0.704	1.35%	2.15
169.1	0.055	0.270	0.705	1.36%	2.16
170.3	0.055	0.272	0.704	1.35%	2.15
180.6	0.057	0.282	0.705	1.30%	2.16
182.3	0.058	0.285	0.700	1.28%	2.14
193.8	0.061	0.299	0.695	1.22%	2.13
194.4	0.061	0.300	0.694	1.22%	2.13
205.0	0.064	0.312	0.688	1.16%	2.11
216.8	0.067	0.327	0.678	1.09%	2.08
229.5	0.070	0.345	0.663	1.02%	2.03
250.2	0.076	0.372	0.645	0.93%	1.97
260.7	0.078	0.385	0.639	0.89%	1.96
271.4	0.082	0.401	0.627	0.85%	1.92
271.8	0.082	0.401	0.628	0.85%	1.92
300.2	0.089	0.438	0.606	0.76%	1.86
322.3	0.096	0.470	0.585	0.69%	1.79
347.2	0.103	0.504	0.568	0.63%	1.74
366.3	0.108	0.531	0.554	0.59%	1.70
367.8	0.109	0.533	0.553	0.59%	1.69
387.1	0.114	0.559	0.542	0.56%	1.66
410.8	0.121	0.594	0.526	0.52%	1.61
415.0	0.121	0.597	0.527	0.52%	1.61
418.7	0.124	0.607	0.518	0.50%	1.59
427.5	0.126	0.621	0.512	0.49%	1.57
445.2	0.132	0.646	0.502	0.46%	1.54
459.4	0.136	0.667	0.494	0.45%	1.51
474.2	0.140	0.690	0.485	0.43%	1.48
476.6	0.141	0.694	0.482	0.42%	1.48
477.8	0.142	0.699	0.479	0.42%	1.47
480.4	0.142	0.699	0.482	0.42%	1.47
484.7	0.144	0.708	0.477	0.41%	1.46

Table B3 α=16°: θ=30° tabulated results from physical model.

Q [L/s]	H [m]	H/P [-]	C_d [-]	$U_{C_{d\,95}}$ [%]	ε' [-]
12.7	0.011	0.056	0.559	0.05	1.71
15.7	0.013	0.063	0.574	0.05	1.75
19.1	0.014	0.070	0.599	0.04	1.83
22.1	0.016	0.076	0.613	0.04	1.87
25.3	0.017	0.082	0.627	0.04	1.91
25.4	0.017	0.082	0.629	0.04	1.92
28.3	0.018	0.087	0.639	0.04	1.95
31.5	0.019	0.092	0.653	0.04	1.99
34.5	0.020	0.097	0.666	0.03	2.03
37.8	0.021	0.102	0.673	0.03	2.05
40.9	0.022	0.106	0.683	0.03	2.08
43.8	0.023	0.111	0.688	0.03	2.10
50.5	0.025	0.120	0.700	0.03	2.14
50.9	0.025	0.122	0.692	0.03	2.11
56.5	0.026	0.129	0.709	0.03	2.16
62.9	0.028	0.137	0.714	0.03	2.18
69.0	0.030	0.146	0.718	0.02	2.19
75.9	0.032	0.154	0.727	0.02	2.22
75.9	0.032	0.155	0.717	0.02	2.19
76.0	0.032	0.155	0.718	0.02	2.19
82.4	0.033	0.163	0.726	0.02	2.21
88.4	0.035	0.169	0.732	0.02	2.24
88.5	0.035	0.170	0.729	0.02	2.22
94.3	0.036	0.177	0.733	0.02	2.24
100.6	0.038	0.184	0.739	0.02	2.26
100.9	0.038	0.184	0.737	0.02	2.25
101.0	0.038	0.185	0.733	0.02	2.24
107.0	0.039	0.192	0.736	0.02	2.25
112.1	0.041	0.198	0.733	0.02	2.24
114.3	0.041	0.200	0.739	0.02	2.26
119.9	0.042	0.207	0.738	0.02	2.25
124.8	0.043	0.212	0.740	0.02	2.26
126.9	0.044	0.215	0.737	0.02	2.25
137.0	0.046	0.226	0.737	0.02	2.25
137.7	0.046	0.227	0.737	0.02	2.25
137.7	0.046	0.227	0.737	0.02	2.25

Q	H	H/P	C_d	$U_{C_{d_{95}}}$	ε'
137.9	0.046	0.227	0.739	0.02	2.25
148.0	0.049	0.239	0.731	0.02	2.23
153.7	0.050	0.245	0.735	0.02	2.24
162.4	0.052	0.255	0.731	0.01	2.23
168.5	0.054	0.262	0.725	0.01	2.21
173.7	0.055	0.268	0.722	0.01	2.20
179.6	0.057	0.277	0.711	0.01	2.17
188.9	0.059	0.288	0.705	0.01	2.15
202.5	0.063	0.307	0.688	0.01	2.10
218.8	0.067	0.326	0.678	0.01	2.07
239.1	0.073	0.355	0.654	0.01	2.00
253.2	0.076	0.373	0.642	0.01	1.96
270.3	0.081	0.398	0.623	0.01	1.90
290.0	0.087	0.423	0.609	0.01	1.86
307.5	0.092	0.450	0.589	0.01	1.80
329.2	0.099	0.484	0.565	0.01	1.72
337.5	0.101	0.495	0.561	0.01	1.71
359.7	0.109	0.533	0.534	0.01	1.63
367.3	0.112	0.547	0.524	0.01	1.60
393.1	0.122	0.596	0.494	0.00	1.51
408.7	0.130	0.634	0.467	0.00	1.43
428.5	0.139	0.679	0.443	0.00	1.35
441.9	0.144	0.704	0.432	0.00	1.32
464.1	0.154	0.754	0.410	0.00	1.25
484.3	0.163	0.795	0.395	0.00	1.20
488.0	0.164	0.803	0.392	0.00	1.20

Appendix C – Numerical Model Time Series Data

Time series plots and data summary for the α=16°: θ=10° arced labyrinth weir.

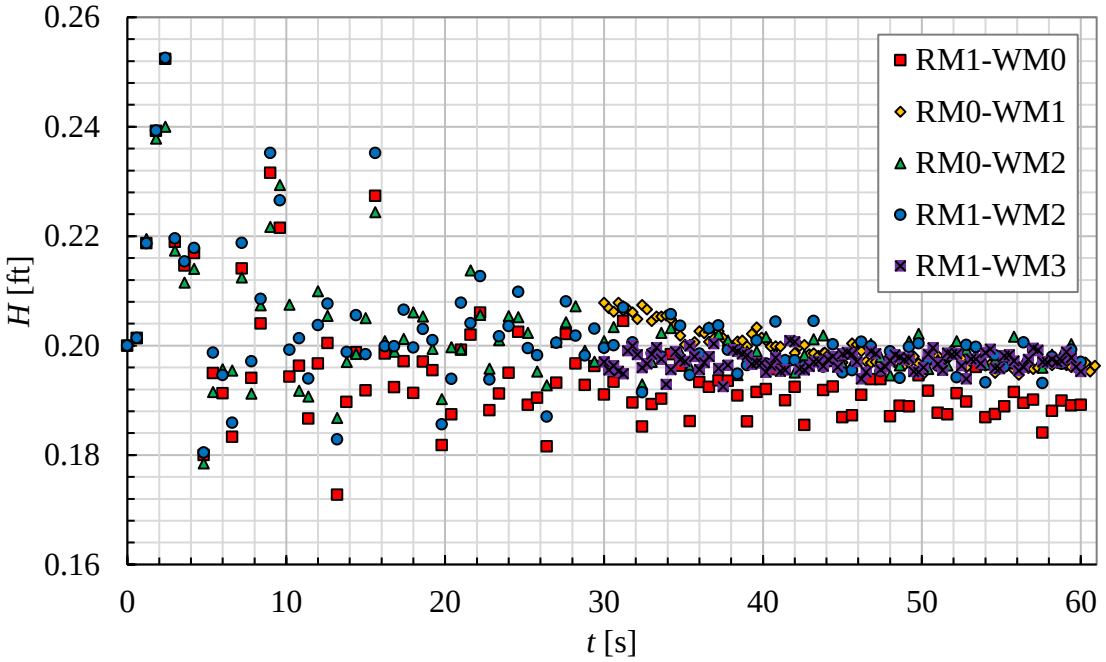

Fig. C1 Numerical H vs t for the α=16°: θ=10° arced labyrinth weir at H/P=0.3 for each mesh configuration tested.

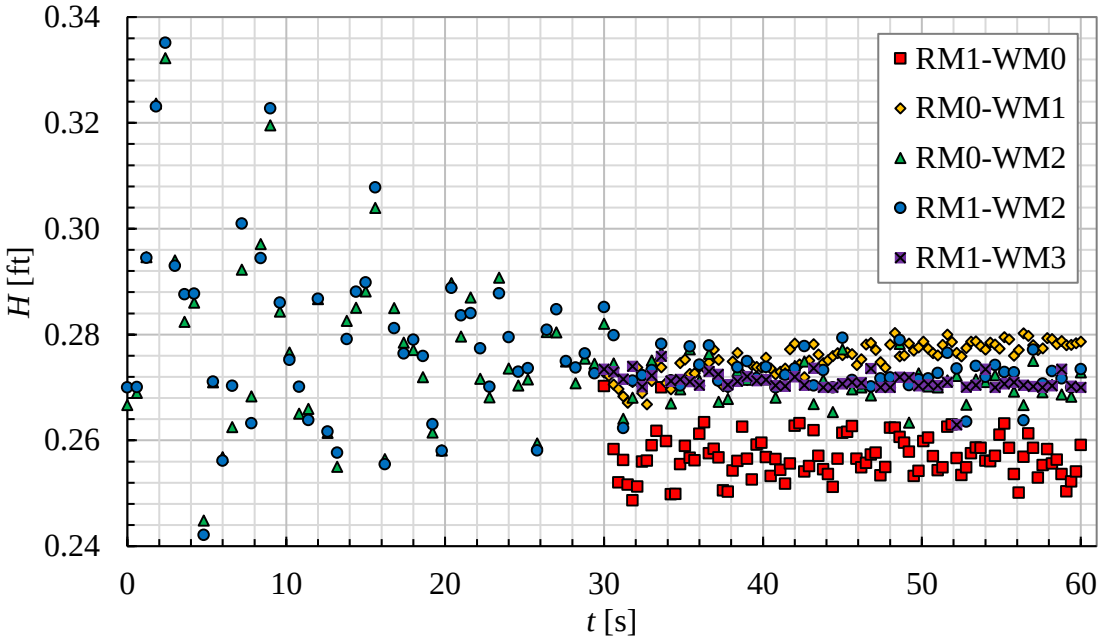

Fig. C2 Numerical H vs t for the α=16°: θ=10° arced labyrinth weir at H/P=0.4 for each mesh configuration tested.

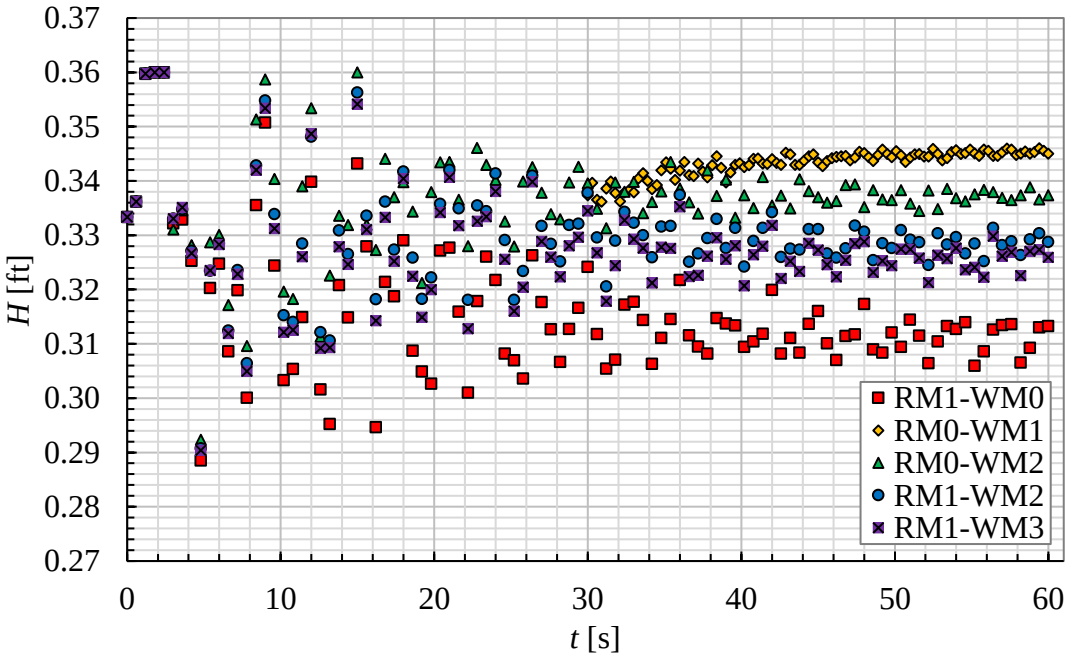

Fig. C3 Numerical H vs t for the α=16°: θ=10° arced labyrinth weir at H/P=0.5 for each mesh configuration tested.

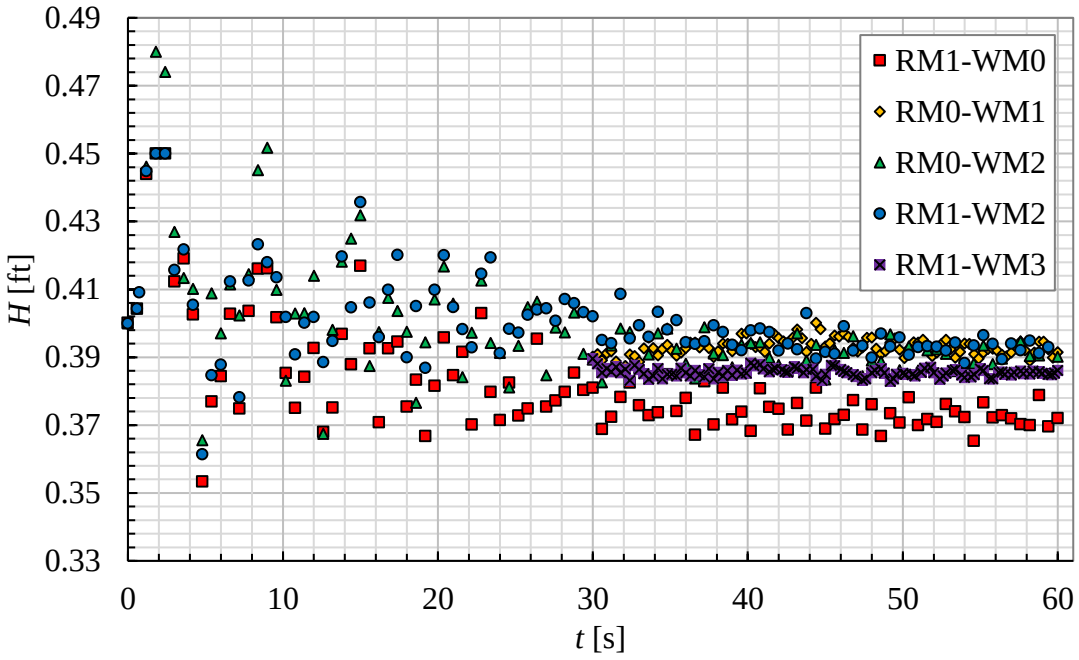

Fig. C4 Numerical H vs t for the α=16°: θ=10° arced labyrinth weir at H/P=0.6 for each mesh configuration tested.

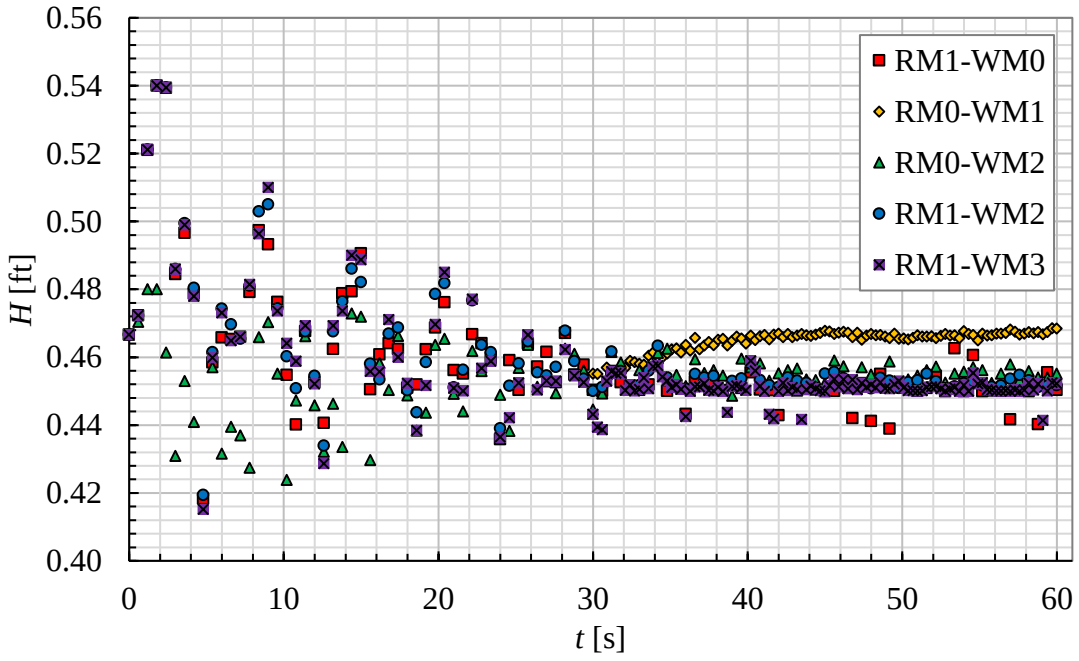

Fig. C5 Numerical H vs t for the α=16°: θ=10° arced labyrinth weir at H/P=0.7 for each mesh configuration tested.

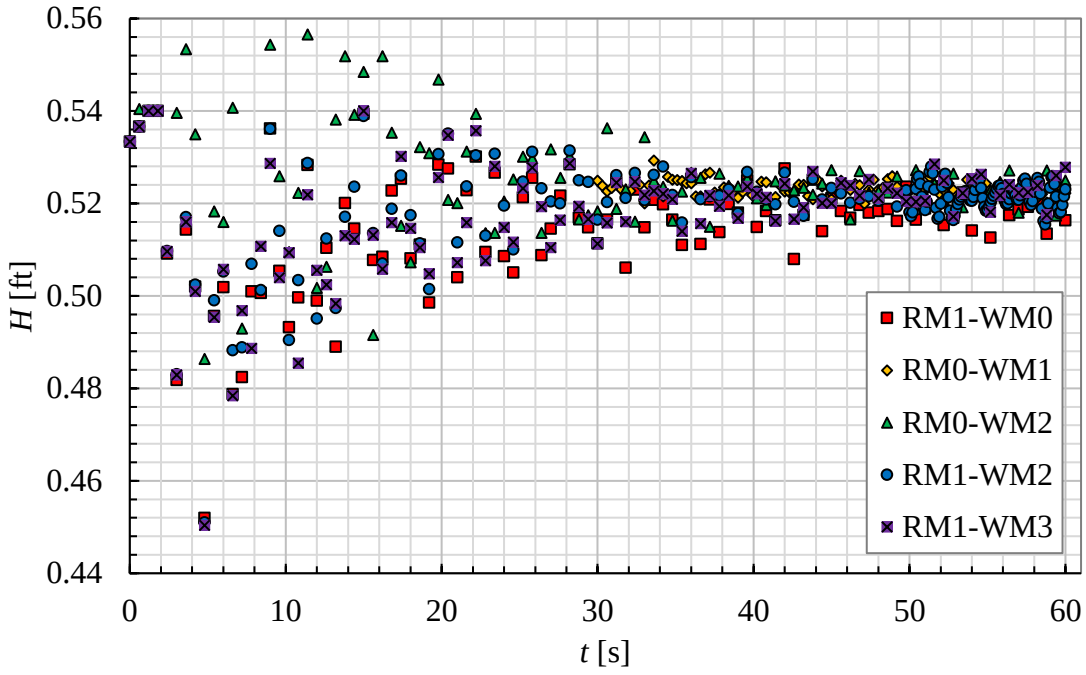

Fig. C6 Numerical H vs t for the α=16°: θ=10° arced labyrinth weir at H/P=0.8 for each mesh configuration tested.

Table C1 Tabulated time series data for the α=16°: θ=10° arced labyrinth weir at H/P=0.3.

RM1-WM0			RM0-WM1			RM0-WM2			RM1-WM2			RM1-WM3		
Cell Count:	1271551		*Cell Count:*	1271992		*Cell Count:*	2581420		*Cell Count:*	2723872		*Cell Count:*	5502679	
Q	90.94	[L/s]	Q	91.28	[L/s]	Q	91.28	[L/s]	Q	90.94	[L/s]	Q	90.94	[L/s]
H	0.058	[m]	H	0.060	[m]	H	0.060	[m]	H	0.060	[m]	H	0.060	[m]
H/P	0.284	[-]	H/P	0.293	[-]	H/P	0.297	[-]	H/P	0.296	[-]	H/P	0.296	[-]
C_d	0.710	[-]	C_d	0.681	[-]	C_d	0.667	[-]	C_d	0.668	[-]	C_d	0.669	[-]
$C_{d\text{-}emp}$	0.671	[-]	$C_{d\text{-}emp}$	0.666	[-]	$C_{d\text{-}emp}$	0.664	[-]	$C_{d\text{-}emp}$	0.664	[-]	$C_{d\text{-}emp}$	0.665	[-]
ε_{Cd}	5.75%	[%]	ε_{Cd}	2.27%	[%]	ε_{Cd}	0.49%	[%]	ε_{Cd}	0.55%	[%]	ε_{Cd}	0.69%	[%]
Time [s]	h [m]	H [m]	Time [s]	h [m]	H [m]	Time [s]	h [m]	H [m]	Time [s]	h [m]	H [m]	Time [s]	h [m]	H [m]
0.00	0.0610	0.0610	30.00	0.0633	0.0634	0.00	0.0610	0.0610	0.00	0.0610	0.0610	30.00	0.0600	0.0601
0.60	0.0614	0.0614	30.30	0.0630	0.0631	0.60	0.0614	0.0614	0.60	0.0614	0.0614	30.30	0.0596	0.0597
1.20	0.0667	0.0667	30.60	0.0628	0.0629	1.20	0.0669	0.0669	1.20	0.0667	0.0667	30.60	0.0598	0.0599
1.80	0.0729	0.0730	30.90	0.0633	0.0634	1.80	0.0725	0.0725	1.80	0.0729	0.0730	30.90	0.0595	0.0596
2.40	0.0769	0.0770	31.20	0.0629	0.0630	2.40	0.0732	0.0732	2.40	0.0770	0.0771	31.20	0.0594	0.0595
3.00	0.0667	0.0670	31.50	0.0630	0.0631	3.00	0.0663	0.0665	3.00	0.0669	0.0672	31.50	0.0607	0.0607
3.60	0.0654	0.0658	31.80	0.0628	0.0629	3.60	0.0645	0.0647	3.60	0.0656	0.0660	31.80	0.0609	0.0610
4.20	0.0661	0.0663	32.10	0.0624	0.0625	4.20	0.0652	0.0655	4.20	0.0664	0.0666	32.10	0.0605	0.0605
4.80	0.0549	0.0552	32.40	0.0632	0.0633	4.80	0.0544	0.0547	4.80	0.0550	0.0553	32.40	0.0597	0.0598
5.40	0.0594	0.0595	32.70	0.0630	0.0631	5.40	0.0584	0.0584	5.40	0.0606	0.0607	32.70	0.0599	0.0600
6.00	0.0583	0.0584	33.00	0.0623	0.0624	6.00	0.0596	0.0597	6.00	0.0593	0.0594	33.00	0.0605	0.0606
6.60	0.0559	0.0559	33.30	0.0626	0.0627	6.60	0.0596	0.0596	6.60	0.0567	0.0567	33.30	0.0609	0.0609
7.20	0.0652	0.0653	33.60	0.0626	0.0627	7.20	0.0648	0.0648	7.20	0.0667	0.0667	33.60	0.0602	0.0603
7.80	0.0592	0.0592	33.90	0.0626	0.0627	7.80	0.0583	0.0583	7.80	0.0601	0.0601	33.90	0.0588	0.0589
8.40	0.0622	0.0622	34.20	0.0624	0.0625	8.40	0.0632	0.0633	8.40	0.0636	0.0636	34.20	0.0596	0.0597

9.00	0.0706	0.0707	34.50	0.0621	0.0622	9.00	0.0676	0.0677	9.00	0.0717	0.0718	34.50	0.0606	0.0607
9.60	0.0675	0.0678	34.80	0.0615	0.0616	9.60	0.0699	0.0701	9.60	0.0690	0.0693	34.80	0.0602	0.0602
10.20	0.0592	0.0593	35.10	0.0610	0.0611	10.20	0.0632	0.0634	10.20	0.0607	0.0609	35.10	0.0601	0.0602
10.80	0.0598	0.0601	35.40	0.0610	0.0611	10.80	0.0584	0.0586	10.80	0.0614	0.0616	35.40	0.0609	0.0610
11.40	0.0569	0.0571	35.70	0.0611	0.0612	11.40	0.0581	0.0583	11.40	0.0591	0.0593	35.70	0.0604	0.0604
12.00	0.0600	0.0601	36.00	0.0618	0.0618	12.00	0.0640	0.0641	12.00	0.0621	0.0622	36.00	0.0596	0.0597
12.60	0.0611	0.0612	36.30	0.0617	0.0617	12.60	0.0626	0.0627	12.60	0.0633	0.0634	36.30	0.0600	0.0601
13.20	0.0526	0.0528	36.60	0.0612	0.0613	13.20	0.0569	0.0570	13.20	0.0557	0.0558	36.60	0.0604	0.0604
13.80	0.0578	0.0579	36.90	0.0613	0.0614	13.80	0.0601	0.0601	13.80	0.0606	0.0606	36.90	0.0611	0.0611
14.40	0.0606	0.0606	37.20	0.0618	0.0618	14.40	0.0605	0.0606	14.40	0.0626	0.0627	37.20	0.0597	0.0598
15.00	0.0585	0.0585	37.50	0.0614	0.0615	15.00	0.0625	0.0625	15.00	0.0605	0.0605	37.50	0.0587	0.0588
15.60	0.0693	0.0694	37.80	0.0611	0.0612	15.60	0.0684	0.0685	15.60	0.0717	0.0718	37.80	0.0599	0.0600
16.20	0.0605	0.0608	38.10	0.0609	0.0610	16.20	0.0612	0.0614	16.20	0.0609	0.0612	38.10	0.0607	0.0608
16.80	0.0586	0.0588	38.40	0.0612	0.0613	16.80	0.0606	0.0607	16.80	0.0609	0.0611	38.40	0.0606	0.0607
17.40	0.0601	0.0602	38.70	0.0613	0.0613	17.40	0.0613	0.0615	17.40	0.0630	0.0631	38.70	0.0605	0.0606
18.00	0.0583	0.0584	39.00	0.0609	0.0610	18.00	0.0628	0.0629	18.00	0.0608	0.0609	39.00	0.0604	0.0605
18.60	0.0601	0.0602	39.30	0.0616	0.0617	18.60	0.0626	0.0627	18.60	0.0619	0.0621	39.30	0.0599	0.0600
19.20	0.0596	0.0597	39.60	0.0620	0.0621	19.20	0.0608	0.0609	19.20	0.0613	0.0614	39.60	0.0600	0.0601
19.80	0.0554	0.0555	39.90	0.0614	0.0615	19.80	0.0580	0.0581	19.80	0.0566	0.0567	39.90	0.0600	0.0601
20.40	0.0571	0.0572	40.20	0.0613	0.0614	20.40	0.0609	0.0609	20.40	0.0591	0.0592	40.20	0.0595	0.0596
21.00	0.0607	0.0608	40.50	0.0609	0.0610	21.00	0.0608	0.0609	21.00	0.0633	0.0634	40.50	0.0599	0.0599
21.60	0.0616	0.0616	40.80	0.0609	0.0610	21.60	0.0651	0.0652	21.60	0.0622	0.0623	40.80	0.0603	0.0604
22.20	0.0628	0.0629	41.10	0.0609	0.0610	22.20	0.0627	0.0628	22.20	0.0648	0.0649	41.10	0.0595	0.0596
22.80	0.0574	0.0575	41.40	0.0602	0.0603	22.80	0.0597	0.0598	22.80	0.0591	0.0592	41.40	0.0596	0.0597
23.40	0.0583	0.0585	41.70	0.0601	0.0602	23.40	0.0613	0.0614	23.40	0.0615	0.0617	41.70	0.0612	0.0613
24.00	0.0594	0.0596	42.00	0.0606	0.0606	24.00	0.0626	0.0627	24.00	0.0620	0.0622	42.00	0.0612	0.0612

24.60	0.0617	0.0618	42.30	0.0609	0.0610	24.60	0.0625	0.0626	24.60	0.0640	0.0641	42.30	0.0597	0.0597
25.20	0.0577	0.0578	42.60	0.0610	0.0611	25.20	0.0617	0.0618	25.20	0.0608	0.0609	42.60	0.0596	0.0597
25.80	0.0580	0.0582	42.90	0.0605	0.0606	25.80	0.0595	0.0597	25.80	0.0604	0.0606	42.90	0.0598	0.0599
26.40	0.0553	0.0555	43.20	0.0605	0.0606	26.40	0.0587	0.0589	26.40	0.0570	0.0571	43.20	0.0601	0.0601
27.00	0.0589	0.0590	43.50	0.0604	0.0605	27.00	0.0611	0.0612	27.00	0.0611	0.0612	43.50	0.0601	0.0602
27.60	0.0616	0.0617	43.80	0.0605	0.0606	27.60	0.0623	0.0623	27.60	0.0634	0.0635	43.80	0.0598	0.0599
28.20	0.0600	0.0601	44.10	0.0604	0.0605	28.20	0.0631	0.0632	28.20	0.0615	0.0616	44.10	0.0602	0.0603
28.80	0.0588	0.0589	44.40	0.0601	0.0602	28.80	0.0607	0.0608	28.80	0.0604	0.0605	44.40	0.0603	0.0604
29.40	0.0598	0.0599	44.70	0.0601	0.0602	29.40	0.0601	0.0602	29.40	0.0619	0.0620	44.70	0.0598	0.0599
30.00	0.0582	0.0583	45.00	0.0600	0.0601	30.00	0.0612	0.0613	30.00	0.0608	0.0609	45.00	0.0605	0.0606
30.60	0.0589	0.0591	45.30	0.0605	0.0606	30.60	0.0620	0.0621	30.60	0.0610	0.0611	45.30	0.0606	0.0607
31.20	0.0623	0.0625	45.60	0.0611	0.0612	31.20	0.0631	0.0633	31.20	0.0631	0.0632	45.60	0.0605	0.0606
31.80	0.0578	0.0579	45.90	0.0610	0.0611	31.80	0.0611	0.0612	31.80	0.0611	0.0613	45.90	0.0601	0.0602
32.40	0.0565	0.0565	46.20	0.0607	0.0607	32.40	0.0588	0.0589	32.40	0.0584	0.0584	46.20	0.0591	0.0592
33.00	0.0577	0.0578	46.50	0.0601	0.0602	33.00	0.0601	0.0602	33.00	0.0605	0.0606	46.50	0.0595	0.0596
33.60	0.0580	0.0581	46.80	0.0600	0.0601	33.60	0.0617	0.0618	33.60	0.0604	0.0605	46.80	0.0606	0.0607
34.20	0.0605	0.0606	47.10	0.0600	0.0601	34.20	0.0619	0.0620	34.20	0.0627	0.0628	47.10	0.0605	0.0606
34.80	0.0598	0.0599	47.40	0.0600	0.0601	34.80	0.0606	0.0607	34.80	0.0621	0.0622	47.40	0.0596	0.0597
35.40	0.0567	0.0569	47.70	0.0601	0.0602	35.40	0.0598	0.0599	35.40	0.0593	0.0594	47.70	0.0598	0.0599
36.00	0.0589	0.0590	48.00	0.0603	0.0604	36.00	0.0605	0.0606	36.00	0.0605	0.0606	48.00	0.0601	0.0602
36.60	0.0587	0.0588	48.30	0.0600	0.0601	36.60	0.0620	0.0621	36.60	0.0619	0.0620	48.30	0.0604	0.0605
37.20	0.0590	0.0591	48.60	0.0603	0.0604	37.20	0.0616	0.0617	37.20	0.0621	0.0622	48.60	0.0603	0.0604
37.80	0.0590	0.0591	48.90	0.0599	0.0600	37.80	0.0612	0.0614	37.80	0.0607	0.0609	48.90	0.0602	0.0603
38.40	0.0582	0.0583	49.20	0.0600	0.0601	38.40	0.0593	0.0594	38.40	0.0594	0.0595	49.20	0.0602	0.0603
39.00	0.0567	0.0569	49.50	0.0604	0.0604	39.00	0.0606	0.0608	39.00	0.0599	0.0600	49.50	0.0595	0.0596
39.60	0.0584	0.0584	49.80	0.0600	0.0600	39.60	0.0606	0.0607	39.60	0.0612	0.0613	49.80	0.0595	0.0596

40.20	0.0585	0.0586	50.10	0.0594	0.0595	40.20	0.0614	0.0615	40.20	0.0600	0.0600	50.10	0.0597	0.0598
40.80	0.0596	0.0597	50.40	0.0601	0.0601	40.80	0.0605	0.0606	40.80	0.0623	0.0624	50.40	0.0605	0.0606
41.40	0.0579	0.0580	50.70	0.0605	0.0606	41.40	0.0602	0.0603	41.40	0.0601	0.0602	50.70	0.0608	0.0609
42.00	0.0587	0.0588	51.00	0.0604	0.0605	42.00	0.0595	0.0595	42.00	0.0601	0.0602	51.00	0.0599	0.0600
42.60	0.0565	0.0566	51.30	0.0598	0.0598	42.60	0.0604	0.0605	42.60	0.0598	0.0599	51.30	0.0596	0.0597
43.20	0.0602	0.0603	51.60	0.0602	0.0603	43.20	0.0613	0.0614	43.20	0.0623	0.0624	51.60	0.0606	0.0606
43.80	0.0585	0.0586	51.90	0.0607	0.0608	43.80	0.0615	0.0616	43.80	0.0598	0.0599	51.90	0.0605	0.0605
44.40	0.0587	0.0588	52.20	0.0605	0.0606	44.40	0.0601	0.0602	44.40	0.0610	0.0611	52.20	0.0605	0.0606
45.00	0.0570	0.0570	52.50	0.0602	0.0603	45.00	0.0600	0.0600	45.00	0.0595	0.0596	52.50	0.0598	0.0599
45.60	0.0571	0.0572	52.80	0.0597	0.0598	45.60	0.0599	0.0600	45.60	0.0596	0.0597	52.80	0.0591	0.0592
46.20	0.0582	0.0583	53.10	0.0601	0.0602	46.20	0.0612	0.0613	46.20	0.0612	0.0613	53.10	0.0602	0.0603
46.80	0.0591	0.0592	53.40	0.0608	0.0609	46.80	0.0610	0.0611	46.80	0.0609	0.0610	53.40	0.0602	0.0603
47.40	0.0591	0.0592	53.70	0.0599	0.0600	47.40	0.0603	0.0604	47.40	0.0595	0.0596	53.70	0.0600	0.0601
48.00	0.0570	0.0571	54.00	0.0598	0.0599	48.00	0.0593	0.0594	48.00	0.0606	0.0607	54.00	0.0606	0.0607
48.60	0.0576	0.0577	54.30	0.0599	0.0600	48.60	0.0599	0.0599	48.60	0.0592	0.0592	54.30	0.0608	0.0608
49.20	0.0576	0.0577	54.60	0.0594	0.0595	49.20	0.0612	0.0613	49.20	0.0609	0.0610	54.60	0.0597	0.0598
49.80	0.0593	0.0594	54.90	0.0597	0.0598	49.80	0.0616	0.0617	49.80	0.0611	0.0611	54.90	0.0597	0.0597
50.40	0.0584	0.0585	55.20	0.0600	0.0601	50.40	0.0597	0.0597	50.40	0.0602	0.0603	55.20	0.0604	0.0605
51.00	0.0572	0.0573	55.50	0.0599	0.0600	51.00	0.0602	0.0602	51.00	0.0598	0.0599	55.50	0.0604	0.0605
51.60	0.0571	0.0572	55.80	0.0596	0.0597	51.60	0.0599	0.0599	51.60	0.0604	0.0605	55.80	0.0601	0.0602
52.20	0.0583	0.0584	56.10	0.0593	0.0594	52.20	0.0612	0.0613	52.20	0.0592	0.0593	56.10	0.0596	0.0597
52.80	0.0578	0.0579	56.40	0.0598	0.0599	52.80	0.0607	0.0608	52.80	0.0610	0.0611	56.40	0.0598	0.0599
53.40	0.0598	0.0598	56.70	0.0597	0.0598	53.40	0.0604	0.0605	53.40	0.0609	0.0610	56.70	0.0602	0.0603
54.00	0.0570	0.0570	57.00	0.0596	0.0597	54.00	0.0599	0.0600	54.00	0.0589	0.0590	57.00	0.0608	0.0609
54.60	0.0571	0.0572	57.30	0.0597	0.0598	54.60	0.0602	0.0602	54.60	0.0604	0.0605	57.30	0.0607	0.0608
55.20	0.0576	0.0576	57.60	0.0600	0.0601	55.20	0.0601	0.0602	55.20	0.0598	0.0598	57.60	0.0600	0.0601

55.80	0.0584	0.0585	57.90	0.0600	0.0601	55.80	0.0615	0.0615	55.80	0.0599	0.0600	57.90	0.0600	0.0601
56.40	0.0578	0.0578	58.20	0.0599	0.0600	56.40	0.0600	0.0601	56.40	0.0611	0.0612	58.20	0.0602	0.0603
57.00	0.0579	0.0580	58.50	0.0600	0.0601	57.00	0.0607	0.0608	57.00	0.0607	0.0608	58.50	0.0601	0.0601
57.60	0.0561	0.0562	58.80	0.0600	0.0601	57.60	0.0597	0.0598	57.60	0.0589	0.0589	58.80	0.0601	0.0602
58.20	0.0573	0.0574	59.10	0.0599	0.0600	58.20	0.0605	0.0605	58.20	0.0603	0.0604	59.10	0.0606	0.0607
58.80	0.0579	0.0580	59.40	0.0598	0.0599	58.80	0.0604	0.0605	58.80	0.0599	0.0600	59.40	0.0603	0.0604
59.40	0.0576	0.0577	59.70	0.0597	0.0598	59.40	0.0610	0.0611	59.40	0.0607	0.0608	59.70	0.0598	0.0599
60.00	0.0577	0.0577	60.00	0.0596	0.0597	60.00	0.0598	0.0599	60.00	0.0600	0.0601	60.00	0.0595	0.0596

Table C2 Tabulated time series data for the α=16°: θ=10° arced labyrinth weir at H/P=0.4.

RM1-WM0			RM0-WM1			RM0-WM2			RM1-WM2			RM1-WM3		
Cell Count:	1326329		*Cell Count:*	1345090		*Cell Count:*	2733565		*Cell Count:*	2845318		*Cell Count:*	5752983	
Q	125.78	[L/s]	*Q*	127.66	[L/s]	*Q*	127.66	[L/s]	*Q*	128.16	[L/s]	*Q*	128.16	[L/s]
H	0.078	[m]	*H*	0.085	[m]	*H*	0.083	[m]	*H*	0.083	[m]	*H*	0.083	[m]
H/P	0.386	[-]	*H/P*	0.417	[-]	*H/P*	0.406	[-]	*H/P*	0.408	[-]	*H/P*	0.407	[-]
C_d	0.621	[-]	C_d	0.561	[-]	C_d	0.584	[-]	C_d	0.581	[-]	C_d	0.585	[-]
$C_{d\text{-}emp}$	0.610	[-]	$C_{d\text{-}emp}$	0.591	[-]	$C_{d\text{-}emp}$	0.598	[-]	$C_{d\text{-}emp}$	0.596	[-]	$C_{d\text{-}emp}$	0.598	[-]
ε_{Cd}	1.85%	[%]	ε_{Cd}	-5.08%	[%]	ε_{Cd}	-2.29%	[%]	ε_{Cd}	-2.54%	[%]	ε_{Cd}	-2.03%	[%]
Time [s]	*h* [m]	*H* [m]	Time [s]	*h* [m]	*H* [m]	Time [s]	*h* [m]	*H* [m]	Time [s]	*h* [m]	*H* [m]	Time [s]	*h* [m]	*H* [m]
30.00	0.0824	0.0826	30.00	0.0832	0.0833	0.00	0.0813	0.0813	0.00	0.0823	0.0823	30.00	0.0834	0.0835
30.30	0.0833	0.0835	30.30	0.0830	0.0831	0.60	0.0820	0.0820	0.60	0.0823	0.0823	30.30	0.0831	0.0832
30.60	0.0787	0.0790	30.60	0.0825	0.0826	1.20	0.0898	0.0899	1.20	0.0898	0.0898	30.60	0.0832	0.0833
30.90	0.0768	0.0770	30.90	0.0822	0.0824	1.80	0.0986	0.0987	1.80	0.0985	0.0985	30.90	0.0828	0.0830
31.20	0.0781	0.0783	31.20	0.0818	0.0820	2.40	0.1013	0.1015	2.40	0.1022	0.1023	31.20	0.0828	0.0829
31.50	0.0767	0.0768	31.50	0.0814	0.0816	3.00	0.0896	0.0902	3.00	0.0893	0.0898	31.50	0.0823	0.0825
31.80	0.0758	0.0759	31.80	0.0826	0.0828	3.60	0.0861	0.0867	3.60	0.0877	0.0883	31.80	0.0835	0.0837
32.10	0.0766	0.0767	32.10	0.0834	0.0836	4.20	0.0872	0.0876	4.20	0.0877	0.0881	32.10	0.0835	0.0837
32.40	0.0780	0.0782	32.40	0.0820	0.0821	4.80	0.0746	0.0751	4.80	0.0738	0.0743	32.40	0.0823	0.0825
32.70	0.0781	0.0783	32.70	0.0813	0.0815	5.40	0.0826	0.0827	5.40	0.0826	0.0828	32.70	0.0823	0.0825
33.00	0.0790	0.0791	33.00	0.0827	0.0828	6.00	0.0783	0.0784	6.00	0.0781	0.0782	33.00	0.0830	0.0831
33.30	0.0798	0.0800	33.30	0.0837	0.0838	6.60	0.0800	0.0801	6.60	0.0824	0.0824	33.30	0.0835	0.0837
33.60	0.0823	0.0825	33.60	0.0835	0.0836	7.20	0.0891	0.0891	7.20	0.0917	0.0918	33.60	0.0841	0.0842
33.90	0.0792	0.0793	33.90	0.0826	0.0827	7.80	0.0818	0.0818	7.80	0.0802	0.0803	33.90	0.0824	0.0826
34.20	0.0761	0.0763	34.20	0.0822	0.0823	8.40	0.0906	0.0907	8.40	0.0897	0.0899	34.20	0.0827	0.0828

34.50	0.0762	0.0763	34.50	0.0827	0.0828	9.00	0.0974	0.0977	9.00	0.0984	0.0987	34.50	0.0826	0.0828
34.80	0.0779	0.0780	34.80	0.0837	0.0838	9.60	0.0867	0.0870	9.60	0.0872	0.0875	34.80	0.0828	0.0829
35.10	0.0789	0.0791	35.10	0.0839	0.0840	10.20	0.0843	0.0845	10.20	0.0839	0.0841	35.10	0.0823	0.0825
35.40	0.0782	0.0784	35.40	0.0831	0.0832	10.80	0.0808	0.0812	10.80	0.0823	0.0828	35.40	0.0826	0.0828
35.70	0.0781	0.0782	35.70	0.0831	0.0833	11.40	0.0811	0.0813	11.40	0.0804	0.0806	35.70	0.0825	0.0827
36.00	0.0796	0.0797	36.00	0.0835	0.0837	12.00	0.0874	0.0876	12.00	0.0874	0.0876	36.00	0.0824	0.0826
36.30	0.0803	0.0804	36.30	0.0834	0.0836	12.60	0.0797	0.0798	12.60	0.0798	0.0799	36.30	0.0823	0.0825
36.60	0.0785	0.0787	36.60	0.0837	0.0839	13.20	0.0777	0.0779	13.20	0.0785	0.0787	36.60	0.0832	0.0834
36.90	0.0787	0.0789	36.90	0.0845	0.0846	13.80	0.0861	0.0862	13.80	0.0851	0.0851	36.90	0.0842	0.0844
37.20	0.0783	0.0784	37.20	0.0839	0.0840	14.40	0.0869	0.0869	14.40	0.0878	0.0879	37.20	0.0830	0.0832
37.50	0.0764	0.0765	37.50	0.0824	0.0825	15.00	0.0878	0.0880	15.00	0.0883	0.0885	37.50	0.0801	0.0803
37.80	0.0763	0.0764	37.80	0.0823	0.0824	15.60	0.0926	0.0931	15.60	0.0938	0.0943	37.80	0.0824	0.0826
38.10	0.0775	0.0776	38.10	0.0838	0.0840	16.20	0.0782	0.0785	16.20	0.0779	0.0782	38.10	0.0824	0.0826
38.40	0.0781	0.0781	38.40	0.0843	0.0845	16.80	0.0869	0.0871	16.80	0.0857	0.0859	38.40	0.0826	0.0828
38.70	0.0800	0.0801	38.70	0.0831	0.0832	17.40	0.0849	0.0851	17.40	0.0843	0.0845	38.70	0.0823	0.0825
39.00	0.0782	0.0783	39.00	0.0827	0.0829	18.00	0.0845	0.0847	18.00	0.0850	0.0852	39.00	0.0829	0.0831
39.30	0.0770	0.0771	39.30	0.0836	0.0837	18.60	0.0829	0.0833	18.60	0.0841	0.0845	39.30	0.0825	0.0827
39.60	0.0790	0.0791	39.60	0.0835	0.0836	19.20	0.0797	0.0798	19.20	0.0802	0.0803	39.60	0.0827	0.0828
39.90	0.0791	0.0792	39.90	0.0834	0.0836	19.80	0.0787	0.0788	19.80	0.0787	0.0788	39.90	0.0833	0.0834
40.20	0.0783	0.0784	40.20	0.0840	0.0841	20.40	0.0883	0.0884	20.40	0.0880	0.0882	40.20	0.0827	0.0829
40.50	0.0772	0.0773	40.50	0.0834	0.0835	21.00	0.0852	0.0854	21.00	0.0865	0.0866	40.50	0.0826	0.0828
40.80	0.0782	0.0783	40.80	0.0831	0.0832	21.60	0.0875	0.0876	21.60	0.0866	0.0867	40.80	0.0824	0.0826
41.10	0.0775	0.0777	41.10	0.0832	0.0834	22.20	0.0828	0.0831	22.20	0.0845	0.0848	41.10	0.0823	0.0825
41.40	0.0768	0.0768	41.40	0.0834	0.0835	22.80	0.0817	0.0820	22.80	0.0823	0.0826	41.40	0.0824	0.0825
41.70	0.0779	0.0780	41.70	0.0845	0.0847	23.40	0.0886	0.0889	23.40	0.0877	0.0880	41.70	0.0830	0.0832
42.00	0.0801	0.0802	42.00	0.0848	0.0850	24.00	0.0834	0.0836	24.00	0.0852	0.0854	42.00	0.0829	0.0831

42.30	0.0802	0.0803	42.30	0.0836	0.0838	24.60	0.0824	0.0826	24.60	0.0832	0.0834	42.30	0.0827	0.0828
42.60	0.0775	0.0776	42.60	0.0829	0.0830	25.20	0.0828	0.0830	25.20	0.0834	0.0836	42.60	0.0824	0.0826
42.90	0.0778	0.0779	42.90	0.0838	0.0840	25.80	0.0791	0.0793	25.80	0.0787	0.0789	42.90	0.0825	0.0827
43.20	0.0798	0.0799	43.20	0.0848	0.0849	26.40	0.0855	0.0856	26.40	0.0856	0.0858	43.20	0.0834	0.0836
43.50	0.0783	0.0785	43.50	0.0842	0.0843	27.00	0.0855	0.0856	27.00	0.0868	0.0870	43.50	0.0825	0.0827
43.80	0.0776	0.0777	43.80	0.0837	0.0838	27.60	0.0838	0.0840	27.60	0.0838	0.0840	43.80	0.0823	0.0825
44.10	0.0773	0.0774	44.10	0.0839	0.0840	28.20	0.0825	0.0827	28.20	0.0834	0.0836	44.10	0.0825	0.0826
44.40	0.0766	0.0767	44.40	0.0841	0.0843	28.80	0.0840	0.0841	28.80	0.0843	0.0844	44.40	0.0823	0.0825
44.70	0.0782	0.0783	44.70	0.0843	0.0844	29.40	0.0837	0.0839	29.40	0.0831	0.0833	44.70	0.0825	0.0827
45.00	0.0797	0.0798	45.00	0.0842	0.0843	30.00	0.0860	0.0862	30.00	0.0869	0.0872	45.00	0.0825	0.0826
45.30	0.0797	0.0799	45.30	0.0843	0.0845	30.60	0.0837	0.0839	30.60	0.0853	0.0855	45.30	0.0827	0.0828
45.60	0.0801	0.0802	45.60	0.0842	0.0844	31.20	0.0805	0.0806	31.20	0.0800	0.0801	45.60	0.0826	0.0828
45.90	0.0782	0.0783	45.90	0.0836	0.0837	31.80	0.0817	0.0818	31.80	0.0827	0.0828	45.90	0.0826	0.0828
46.20	0.0777	0.0778	46.20	0.0839	0.0841	32.40	0.0826	0.0828	32.40	0.0830	0.0832	46.20	0.0826	0.0827
46.50	0.0779	0.0781	46.50	0.0848	0.0849	33.00	0.0838	0.0840	33.00	0.0833	0.0835	46.50	0.0826	0.0828
46.80	0.0784	0.0786	46.80	0.0849	0.0850	33.60	0.0843	0.0844	33.60	0.0848	0.0850	46.80	0.0834	0.0835
47.10	0.0785	0.0787	47.10	0.0845	0.0846	34.20	0.0814	0.0815	34.20	0.0827	0.0828	47.10	0.0824	0.0826
47.40	0.0772	0.0774	47.40	0.0837	0.0839	34.80	0.0822	0.0823	34.80	0.0824	0.0825	47.40	0.0823	0.0825
47.70	0.0777	0.0779	47.70	0.0834	0.0836	35.40	0.0845	0.0846	35.40	0.0847	0.0848	47.70	0.0828	0.0830
48.00	0.0800	0.0801	48.00	0.0848	0.0849	36.00	0.0827	0.0828	36.00	0.0836	0.0837	48.00	0.0823	0.0824
48.30	0.0800	0.0801	48.30	0.0854	0.0856	36.60	0.0842	0.0844	36.60	0.0847	0.0849	48.30	0.0826	0.0827
48.60	0.0794	0.0796	48.60	0.0841	0.0842	37.20	0.0815	0.0817	37.20	0.0827	0.0829	48.60	0.0829	0.0831
48.90	0.0791	0.0792	48.90	0.0841	0.0843	37.80	0.0816	0.0818	37.80	0.0824	0.0825	48.90	0.0826	0.0827
49.20	0.0786	0.0787	49.20	0.0848	0.0850	38.40	0.0832	0.0833	38.40	0.0834	0.0835	49.20	0.0829	0.0830
49.50	0.0772	0.0773	49.50	0.0844	0.0846	39.00	0.0827	0.0828	39.00	0.0838	0.0839	49.50	0.0823	0.0825
49.80	0.0775	0.0776	49.80	0.0846	0.0847	39.60	0.0828	0.0830	39.60	0.0828	0.0830	49.80	0.0824	0.0825

50.10	0.0792	0.0793	50.10	0.0849	0.0851	40.20	0.0828	0.0829	40.20	0.0835	0.0836	50.10	0.0830	0.0831
50.40	0.0794	0.0796	50.40	0.0845	0.0847	40.80	0.0817	0.0818	40.80	0.0823	0.0824	50.40	0.0825	0.0826
50.70	0.0783	0.0785	50.70	0.0843	0.0844	41.40	0.0831	0.0832	41.40	0.0830	0.0831	50.70	0.0823	0.0825
51.00	0.0775	0.0777	51.00	0.0841	0.0843	42.00	0.0835	0.0837	42.00	0.0834	0.0835	51.00	0.0824	0.0826
51.30	0.0777	0.0778	51.30	0.0847	0.0849	42.60	0.0838	0.0839	42.60	0.0847	0.0848	51.30	0.0840	0.0841
51.60	0.0800	0.0802	51.60	0.0853	0.0855	43.20	0.0813	0.0815	43.20	0.0824	0.0825	51.60	0.0826	0.0827
51.90	0.0802	0.0803	51.90	0.0849	0.0851	43.80	0.0827	0.0829	43.80	0.0833	0.0834	51.90	0.0833	0.0834
52.20	0.0782	0.0784	52.20	0.0843	0.0844	44.40	0.0809	0.0810	44.40	0.0823	0.0824	52.20	0.0801	0.0803
52.50	0.0772	0.0774	52.50	0.0841	0.0842	45.00	0.0845	0.0846	45.00	0.0852	0.0853	52.50	0.0825	0.0827
52.80	0.0777	0.0778	52.80	0.0846	0.0847	45.60	0.0822	0.0823	45.60	0.0827	0.0828	52.80	0.0823	0.0825
53.10	0.0785	0.0786	53.10	0.0849	0.0851	46.20	0.0823	0.0824	46.20	0.0825	0.0826	53.10	0.0825	0.0827
53.40	0.0788	0.0790	53.40	0.0849	0.0851	46.80	0.0818	0.0820	46.80	0.0823	0.0825	53.40	0.0824	0.0826
53.70	0.0788	0.0789	53.70	0.0847	0.0848	47.40	0.0825	0.0827	47.40	0.0828	0.0830	53.70	0.0823	0.0825
54.00	0.0781	0.0782	54.00	0.0845	0.0846	48.00	0.0826	0.0827	48.00	0.0829	0.0830	54.00	0.0833	0.0835
54.30	0.0780	0.0782	54.30	0.0849	0.0850	48.60	0.0848	0.0849	48.60	0.0850	0.0852	54.30	0.0823	0.0824
54.60	0.0783	0.0785	54.60	0.0848	0.0849	49.20	0.0803	0.0804	49.20	0.0824	0.0826	54.60	0.0823	0.0824
54.90	0.0796	0.0797	54.90	0.0845	0.0847	49.80	0.0831	0.0833	49.80	0.0828	0.0829	54.90	0.0836	0.0837
55.20	0.0802	0.0804	55.20	0.0852	0.0853	50.40	0.0824	0.0825	50.40	0.0828	0.0830	55.20	0.0825	0.0826
55.50	0.0788	0.0790	55.50	0.0851	0.0852	51.00	0.0823	0.0824	51.00	0.0831	0.0833	55.50	0.0828	0.0830
55.80	0.0773	0.0774	55.80	0.0841	0.0843	51.60	0.0827	0.0829	51.60	0.0843	0.0844	55.80	0.0826	0.0828
56.10	0.0762	0.0764	56.10	0.0844	0.0846	52.20	0.0830	0.0831	52.20	0.0834	0.0835	56.10	0.0826	0.0828
56.40	0.0783	0.0784	56.40	0.0854	0.0856	52.80	0.0813	0.0814	52.80	0.0803	0.0805	56.40	0.0824	0.0826
56.70	0.0796	0.0798	56.70	0.0853	0.0854	53.40	0.0828	0.0829	53.40	0.0835	0.0837	56.70	0.0828	0.0829
57.00	0.0788	0.0790	57.00	0.0847	0.0849	54.00	0.0826	0.0828	54.00	0.0829	0.0831	57.00	0.0824	0.0825
57.30	0.0771	0.0773	57.30	0.0845	0.0846	54.60	0.0830	0.0832	54.60	0.0836	0.0838	57.30	0.0825	0.0827
57.60	0.0778	0.0780	57.60	0.0845	0.0847	55.20	0.0827	0.0828	55.20	0.0832	0.0833	57.60	0.0823	0.0825

57.90	0.0787	0.0789	57.90	0.0851	0.0853	55.80	0.0821	0.0822	55.80	0.0832	0.0833	57.90	0.0831	0.0833
58.20	0.0779	0.0781	58.20	0.0851	0.0852	56.40	0.0813	0.0815	56.40	0.0804	0.0806	58.20	0.0824	0.0825
58.50	0.0781	0.0783	58.50	0.0848	0.0849	57.00	0.0838	0.0840	57.00	0.0845	0.0846	58.50	0.0825	0.0827
58.80	0.0773	0.0775	58.80	0.0850	0.0851	57.60	0.0820	0.0822	57.60	0.0825	0.0827	58.80	0.0833	0.0835
59.10	0.0763	0.0765	59.10	0.0847	0.0849	58.20	0.0824	0.0826	58.20	0.0832	0.0834	59.10	0.0823	0.0825
59.40	0.0769	0.0770	59.40	0.0848	0.0849	58.80	0.0819	0.0821	58.80	0.0828	0.0830	59.40	0.0824	0.0825
59.70	0.0775	0.0776	59.70	0.0848	0.0850	59.40	0.0818	0.0819	59.40	0.0823	0.0824	59.70	0.0834	0.0835
60.00	0.0790	0.0791	60.00	0.0849	0.0851	60.00	0.0832	0.0833	60.00	0.0834	0.0835	60.00	0.0823	0.0825

Table C3 Tabulated time series data for the α=16°: θ=10° arced labyrinth weir at H/P=0.5.

RM1-WM0			RM0-WM1			RM0-WM2			RM1-WM2			RM1-WM3		
Cell Count:	1326329		*Cell Count:*	1345090		*Cell Count:*	2733565		*Cell Count:*	2845318		*Cell Count:*	5752983	
Q	157.06	[L/s]	*Q*	161.51	[L/s]	*Q*	161.51	[L/s]	*Q*	157.06	[L/s]	*Q*	157.06	[L/s]
H	0.095	[m]	*H*	0.105	[m]	*H*	0.103	[m]	*H*	0.100	[m]	*H*	0.099	[m]
H/P	0.467	[-]	*H/P*	0.518	[-]	*H/P*	0.506	[-]	*H/P*	0.493	[-]	*H/P*	0.488	[-]
C_d	0.583	[-]	C_d	0.514	[-]	C_d	0.532	[-]	C_d	0.538	[-]	C_d	0.545	[-]
$C_{d\text{-}emp}$	0.563	[-]	$C_{d\text{-}emp}$	0.536	[-]	$C_{d\text{-}emp}$	0.542	[-]	$C_{d\text{-}emp}$	0.548	[-]	$C_{d\text{-}emp}$	0.551	[-]
ε_{Cd}	3.65%	[%]	ε_{Cd}	-4.09%	[%]	ε_{Cd}	-1.81%	[%]	ε_{Cd}	-1.95%	[%]	ε_{Cd}	-1.09%	[%]
Time [s]	*h* [m]	*H* [m]	Time [s]	*h* [m]	*H* [m]	Time [s]	*h* [m]	*H* [m]	Time [s]	*h* [m]	*H* [m]	Time [s]	*h* [m]	*H* [m]
0.00	0.1016	0.1016	30.00	0.1028	0.1031	0.00	0.1016	0.1016	0.00	0.1016	0.1016	0.00	0.1016	0.1016
0.60	0.1025	0.1025	30.30	0.1035	0.1038	0.60	0.1025	0.1025	0.60	0.1025	0.1025	0.60	0.1025	0.1025
1.20	0.1096	0.1097	30.60	0.1026	0.1028	1.20	0.1096	0.1097	1.20	0.1096	0.1097	1.20	0.1096	0.1097
1.80	0.1097	0.1098	30.90	0.1025	0.1027	1.80	0.1097	0.1098	1.80	0.1097	0.1098	1.80	0.1097	0.1098
2.40	0.1097	0.1098	31.20	0.1032	0.1034	2.40	0.1097	0.1098	2.40	0.1097	0.1098	2.40	0.1097	0.1098
3.00	0.1012	0.1016	31.50	0.1036	0.1038	3.00	0.1009	0.1013	3.00	0.1015	0.1019	3.00	0.1015	0.1019
3.60	0.1015	0.1019	31.80	0.1029	0.1032	3.60	0.1020	0.1024	3.60	0.1020	0.1024	3.60	0.1021	0.1025
4.20	0.0991	0.0996	32.10	0.1025	0.1027	4.20	0.1000	0.1004	4.20	0.0997	0.1001	4.20	0.0996	0.1000
4.80	0.0879	0.0886	32.40	0.1030	0.1032	4.80	0.0891	0.0897	4.80	0.0886	0.0892	4.80	0.0885	0.0891
5.40	0.0976	0.0978	32.70	0.1031	0.1033	5.40	0.1002	0.1004	5.40	0.0986	0.0988	5.40	0.0986	0.0988
6.00	0.0990	0.0992	33.00	0.1030	0.1032	6.00	0.1006	0.1009	6.00	0.1001	0.1004	6.00	0.1001	0.1003
6.60	0.0941	0.0942	33.30	0.1038	0.1040	6.60	0.0967	0.0968	6.60	0.0952	0.0953	6.60	0.0951	0.0952
7.20	0.0975	0.0977	33.60	0.1041	0.1043	7.20	0.0984	0.0986	7.20	0.0986	0.0988	7.20	0.0984	0.0986
7.80	0.0915	0.0916	33.90	0.1036	0.1038	7.80	0.0944	0.0945	7.80	0.0934	0.0935	7.80	0.0929	0.0931

8.40	0.1023	0.1025	34.20	0.1032	0.1034	8.40	0.1071	0.1074	8.40	0.1045	0.1047	8.40	0.1042	0.1045
9.00	0.1069	0.1072	34.50	0.1034	0.1036	9.00	0.1093	0.1097	9.00	0.1081	0.1084	9.00	0.1077	0.1080
9.60	0.0989	0.0992	34.80	0.1042	0.1044	9.60	0.1037	0.1040	9.60	0.1018	0.1020	9.60	0.1010	0.1012
10.20	0.0924	0.0927	35.10	0.1047	0.1049	10.20	0.0974	0.0977	10.20	0.0961	0.0964	10.20	0.0951	0.0954
10.80	0.0931	0.0934	35.40	0.1043	0.1045	10.80	0.0970	0.0974	10.80	0.0957	0.0961	10.80	0.0953	0.0956
11.40	0.0960	0.0964	35.70	0.1037	0.1039	11.40	0.1033	0.1037	11.40	0.1001	0.1005	11.40	0.0994	0.0998
12.00	0.1036	0.1039	36.00	0.1042	0.1044	12.00	0.1077	0.1080	12.00	0.1061	0.1064	12.00	0.1063	0.1066
12.60	0.0919	0.0922	36.30	0.1047	0.1049	12.60	0.0949	0.0952	12.60	0.0951	0.0954	12.60	0.0942	0.0945
13.20	0.0900	0.0902	36.60	0.1040	0.1042	13.20	0.0983	0.0985	13.20	0.0947	0.0949	13.20	0.0943	0.0945
13.80	0.0978	0.0979	36.90	0.1039	0.1041	13.80	0.1017	0.1018	13.80	0.1009	0.1010	13.80	0.0999	0.1001
14.40	0.0960	0.0962	37.20	0.1046	0.1048	14.40	0.1012	0.1013	14.40	0.0995	0.0997	14.40	0.0989	0.0991
15.00	0.1046	0.1048	37.50	0.1042	0.1044	15.00	0.1097	0.1100	15.00	0.1086	0.1088	15.00	0.1079	0.1082
15.60	0.1000	0.1005	37.80	0.1038	0.1041	15.60	0.1012	0.1016	15.60	0.1017	0.1021	15.60	0.1009	0.1014
16.20	0.0898	0.0901	38.10	0.1045	0.1047	16.20	0.0998	0.1000	16.20	0.0970	0.0973	16.20	0.0958	0.0960
16.80	0.0980	0.0983	38.40	0.1050	0.1052	16.80	0.1049	0.1052	16.80	0.1025	0.1028	16.80	0.1016	0.1019
17.40	0.0972	0.0974	38.70	0.1044	0.1046	17.40	0.1027	0.1029	17.40	0.0998	0.1000	17.40	0.0991	0.0993
18.00	0.1003	0.1006	39.00	0.1036	0.1038	18.00	0.1036	0.1040	18.00	0.1042	0.1045	18.00	0.1038	0.1041
18.60	0.0941	0.0946	39.30	0.1041	0.1043	18.60	0.1019	0.1023	18.60	0.0993	0.0998	18.60	0.0983	0.0987
19.20	0.0929	0.0932	39.60	0.1045	0.1047	19.20	0.0979	0.0982	19.20	0.0970	0.0973	19.20	0.0960	0.0962
19.80	0.0922	0.0925	39.90	0.1046	0.1048	19.80	0.1030	0.1032	19.80	0.0982	0.0984	19.80	0.0975	0.0977
20.40	0.0997	0.0999	40.20	0.1044	0.1046	20.40	0.1047	0.1049	20.40	0.1023	0.1025	20.40	0.1018	0.1021
21.00	0.0999	0.1001	40.50	0.1045	0.1047	21.00	0.1047	0.1050	21.00	0.1042	0.1045	21.00	0.1038	0.1041
21.60	0.0963	0.0966	40.80	0.1049	0.1051	21.60	0.1026	0.1029	21.60	0.1021	0.1024	21.60	0.1011	0.1014
22.20	0.0917	0.0921	41.10	0.1049	0.1051	22.20	0.1000	0.1003	22.20	0.0970	0.0973	22.20	0.0953	0.0957
22.80	0.0969	0.0972	41.40	0.1046	0.1048	22.80	0.1055	0.1058	22.80	0.1022	0.1026	22.80	0.1014	0.1017
23.40	0.0994	0.0996	41.70	0.1046	0.1048	23.40	0.1045	0.1048	23.40	0.1019	0.1022	23.40	0.1016	0.1018

24.00	0.0981	0.0983	42.00	0.1048	0.1051	24.00	0.1037	0.1039	24.00	0.1040	0.1043	24.00	0.1030	0.1033
24.60	0.0939	0.0943	42.30	0.1046	0.1049	24.60	0.1014	0.1017	24.60	0.1003	0.1007	24.60	0.0992	0.0996
25.20	0.0935	0.0939	42.60	0.1045	0.1048	25.20	0.0999	0.1003	25.20	0.0969	0.0972	25.20	0.0963	0.0966
25.80	0.0925	0.0928	42.90	0.1052	0.1054	25.80	0.1036	0.1039	25.80	0.0986	0.0989	25.80	0.0977	0.0980
26.40	0.0995	0.0997	43.20	0.1051	0.1053	26.40	0.1044	0.1046	26.40	0.1039	0.1041	26.40	0.1036	0.1038
27.00	0.0968	0.0970	43.50	0.1045	0.1048	27.00	0.1030	0.1032	27.00	0.1011	0.1013	27.00	0.1002	0.1004
27.60	0.0953	0.0956	43.80	0.1045	0.1047	27.60	0.1018	0.1020	27.60	0.1001	0.1003	27.60	0.0994	0.0996
28.20	0.0935	0.0937	44.10	0.1048	0.1050	28.20	0.1015	0.1017	28.20	0.0991	0.0994	28.20	0.0982	0.0985
28.80	0.0953	0.0955	44.40	0.1050	0.1052	28.80	0.1035	0.1038	28.80	0.1011	0.1014	28.80	0.1000	0.1002
29.40	0.0965	0.0967	44.70	0.1051	0.1053	29.40	0.1044	0.1047	29.40	0.1012	0.1015	29.40	0.1005	0.1007
30.00	0.0988	0.0991	45.00	0.1047	0.1049	30.00	0.1035	0.1037	30.00	0.1030	0.1032	30.00	0.1019	0.1022
30.60	0.0950	0.0952	45.30	0.1045	0.1047	30.60	0.1021	0.1023	30.60	0.1005	0.1007	30.60	0.0996	0.0998
31.20	0.0931	0.0933	45.60	0.1047	0.1049	31.20	0.1010	0.1012	31.20	0.0977	0.0979	31.20	0.0969	0.0971
31.80	0.0936	0.0938	45.90	0.1049	0.1051	31.80	0.1035	0.1038	31.80	0.1003	0.1005	31.80	0.0989	0.0991
32.40	0.0967	0.0969	46.20	0.1050	0.1052	32.40	0.1030	0.1032	32.40	0.1019	0.1021	32.40	0.1014	0.1016
33.00	0.0968	0.0970	46.50	0.1050	0.1052	33.00	0.1036	0.1038	33.00	0.1013	0.1015	33.00	0.1004	0.1006
33.60	0.0958	0.0960	46.80	0.1050	0.1053	33.60	0.1018	0.1020	33.60	0.1006	0.1008	33.60	0.0999	0.1000
34.20	0.0934	0.0935	47.10	0.1048	0.1050	34.20	0.1024	0.1026	34.20	0.0993	0.0995	34.20	0.0979	0.0981
34.80	0.0948	0.0950	47.40	0.1049	0.1052	34.80	0.1030	0.1032	34.80	0.1011	0.1012	34.80	0.0999	0.1001
35.40	0.0959	0.0960	47.70	0.1053	0.1055	35.40	0.1047	0.1049	35.40	0.1011	0.1013	35.40	0.0998	0.1000
36.00	0.0981	0.0982	48.00	0.1052	0.1054	36.00	0.1032	0.1034	36.00	0.1029	0.1030	36.00	0.1022	0.1024
36.60	0.0950	0.0952	48.30	0.1050	0.1052	36.60	0.1024	0.1026	36.60	0.0991	0.0993	36.60	0.0983	0.0984
37.20	0.0943	0.0945	48.60	0.1048	0.1050	37.20	0.1018	0.1020	37.20	0.0996	0.0998	37.20	0.0983	0.0985
37.80	0.0939	0.0941	48.90	0.1051	0.1053	37.80	0.1042	0.1044	37.80	0.1004	0.1006	37.80	0.0994	0.0995
38.40	0.0959	0.0961	49.20	0.1054	0.1056	38.40	0.1028	0.1030	38.40	0.1015	0.1016	38.40	0.1004	0.1006
39.00	0.0956	0.0958	49.50	0.1051	0.1054	39.00	0.1037	0.1039	39.00	0.0999	0.1000	39.00	0.0992	0.0994

39.60	0.0955	0.0957	49.80	0.1050	0.1052	39.60	0.1016	0.1018	39.60	0.1010	0.1012	39.60	0.1000	0.1002
40.20	0.0943	0.0945	50.10	0.1053	0.1055	40.20	0.1028	0.1030	40.20	0.0988	0.0990	40.20	0.0977	0.0979
40.80	0.0946	0.0948	50.40	0.1051	0.1053	40.80	0.1021	0.1023	40.80	0.1003	0.1004	40.80	0.0995	0.0996
41.40	0.0951	0.0952	50.70	0.1047	0.1049	41.40	0.1039	0.1040	41.40	0.1010	0.1012	41.40	0.1000	0.1001
42.00	0.0975	0.0977	51.00	0.1049	0.1052	42.00	0.1023	0.1025	42.00	0.1019	0.1021	42.00	0.1011	0.1013
42.60	0.0939	0.0942	51.30	0.1051	0.1053	42.60	0.1028	0.1030	42.60	0.0994	0.0996	42.60	0.0982	0.0984
43.20	0.0948	0.0950	51.60	0.1051	0.1054	43.20	0.1021	0.1023	43.20	0.0998	0.1000	43.20	0.0991	0.0993
43.80	0.0940	0.0942	51.90	0.1050	0.1052	43.80	0.1037	0.1039	43.80	0.0998	0.1000	43.80	0.0986	0.0988
44.40	0.0956	0.0958	52.20	0.1050	0.1052	44.40	0.1031	0.1033	44.40	0.1009	0.1011	44.40	0.1001	0.1003
45.00	0.0963	0.0965	52.50	0.1054	0.1056	45.00	0.1027	0.1029	45.00	0.1009	0.1011	45.00	0.0998	0.1000
45.60	0.0945	0.0947	52.80	0.1051	0.1053	45.60	0.1024	0.1026	45.60	0.0996	0.0998	45.60	0.0989	0.0991
46.20	0.0936	0.0938	53.10	0.1048	0.1050	46.20	0.1025	0.1027	46.20	0.0993	0.0996	46.20	0.0982	0.0985
46.80	0.0949	0.0952	53.40	0.1049	0.1051	46.80	0.1034	0.1036	46.80	0.0999	0.1001	46.80	0.0992	0.0994
47.40	0.0950	0.0952	53.70	0.1052	0.1055	47.40	0.1034	0.1036	47.40	0.1011	0.1013	47.40	0.1001	0.1003
48.00	0.0967	0.0969	54.00	0.1054	0.1056	48.00	0.1022	0.1024	48.00	0.1008	0.1010	48.00	0.1002	0.1004
48.60	0.0942	0.0944	54.30	0.1051	0.1054	48.60	0.1031	0.1033	48.60	0.0992	0.0994	48.60	0.0985	0.0987
49.20	0.0940	0.0942	54.60	0.1052	0.1054	49.20	0.1026	0.1028	49.20	0.1001	0.1004	49.20	0.0991	0.0994
49.80	0.0951	0.0954	54.90	0.1054	0.1056	49.80	0.1026	0.1028	49.80	0.0999	0.1001	49.80	0.0989	0.0991
50.40	0.0943	0.0945	55.20	0.1052	0.1054	50.40	0.1031	0.1033	50.40	0.1009	0.1011	50.40	0.0998	0.1000
51.00	0.0958	0.0960	55.50	0.1050	0.1052	51.00	0.1024	0.1026	51.00	0.1003	0.1005	51.00	0.0998	0.1000
51.60	0.0949	0.0952	55.80	0.1054	0.1056	51.60	0.1019	0.1022	51.60	0.1002	0.1004	51.60	0.0993	0.0995
52.20	0.0934	0.0936	56.10	0.1053	0.1055	52.20	0.1031	0.1033	52.20	0.0989	0.0991	52.20	0.0979	0.0981
52.80	0.0946	0.0948	56.40	0.1050	0.1052	52.80	0.1021	0.1023	52.80	0.1007	0.1009	52.80	0.0995	0.0997
53.40	0.0955	0.0957	56.70	0.1050	0.1052	53.40	0.1032	0.1034	53.40	0.1001	0.1003	53.40	0.0993	0.0995
54.00	0.0953	0.0955	57.00	0.1052	0.1055	54.00	0.1027	0.1029	54.00	0.1005	0.1007	54.00	0.0999	0.1001
54.60	0.0957	0.0959	57.30	0.1055	0.1057	54.60	0.1025	0.1027	54.60	0.0996	0.0998	54.60	0.0986	0.0989

55.20	0.0933	0.0935	57.60	0.1054	0.1056	55.20	0.1029	0.1031	55.20	0.1001	0.1003	55.20	0.0988	0.0990
55.80	0.0941	0.0943	57.90	0.1051	0.1053	55.80	0.1031	0.1034	55.80	0.0991	0.0993	55.80	0.0982	0.0984
56.40	0.0953	0.0955	58.20	0.1052	0.1054	56.40	0.1030	0.1032	56.40	0.1010	0.1012	56.40	0.1005	0.1007
57.00	0.0955	0.0958	58.50	0.1053	0.1055	57.00	0.1027	0.1029	57.00	0.1000	0.1003	57.00	0.0994	0.0996
57.60	0.0956	0.0958	58.80	0.1052	0.1054	57.60	0.1026	0.1028	57.60	0.1002	0.1004	57.60	0.0996	0.0998
58.20	0.0934	0.0937	59.10	0.1052	0.1055	58.20	0.1028	0.1031	58.20	0.0995	0.0997	58.20	0.0983	0.0985
58.80	0.0943	0.0945	59.40	0.1055	0.1057	58.80	0.1033	0.1035	58.80	0.1003	0.1005	58.80	0.0997	0.0999
59.40	0.0954	0.0956	59.70	0.1053	0.1055	59.40	0.1026	0.1028	59.40	0.1007	0.1009	59.40	0.0998	0.1000
60.00	0.0955	0.0957	60.00	0.1052	0.1054	60.00	0.1028	0.1031	60.00	0.1002	0.1004	60.00	0.0993	0.0996

Table C4 Tabulated time series data for the α=16°: θ=10° arced labyrinth weir at H/P=0.6.

RM1-WM0			RM0-WM1			RM0-WM2			RM1-WM2			RM1-WM3		
Cell Count:	1381107		*Cell Count:*	1418188		*Cell Count:*	2885710		*Cell Count:*	2966764		*Cell Count:*	6003287	
Q	189.98	[L/s]	Q	193.88	[L/s]	Q	193.88	[L/s]	Q	194.64	[L/s]	Q	194.64	[L/s]
H	0.113	[m]	H	0.120	[m]	H	0.119	[m]	H	0.120	[m]	H	0.117	[m]
H/P	0.558	[-]	H/P	0.589	[-]	H/P	0.585	[-]	H/P	0.589	[-]	H/P	0.578	[-]
C_d	0.539	[-]	C_d	0.507	[-]	C_d	0.514	[-]	C_d	0.509	[-]	C_d	0.525	[-]
$C_{d\text{-}emp}$	0.516	[-]	$C_{d\text{-}emp}$	0.502	[-]	$C_{d\text{-}emp}$	0.504	[-]	$C_{d\text{-}emp}$	0.502	[-]	$C_{d\text{-}emp}$	0.507	[-]
ε_{Cd}	4.53%	[%]	ε_{Cd}	1.12%	[%]	ε_{Cd}	1.93%	[%]	ε_{Cd}	1.50%	[%]	ε_{Cd}	3.51%	[%]
Time [s]	h [m]	H [m]	Time [s]	h [m]	H [m]	Time [s]	h [m]	H [m]	Time [s]	h [m]	H [m]	Time [s]	h [m]	H [m]
0.00	0.1220	0.1220	30.00	0.1189	0.1192	0.00	0.1219	0.1219	0.00	0.1219	0.1219	30.00	0.1187	0.1190
0.60	0.1232	0.1232	30.30	0.1192	0.1194	0.60	0.1233	0.1233	0.60	0.1232	0.1232	30.30	0.1183	0.1186
1.20	0.1353	0.1355	30.60	0.1186	0.1189	1.20	0.1360	0.1361	0.74	0.1247	0.1247	30.60	0.1175	0.1178
1.80	0.1372	0.1373	30.90	0.1192	0.1195	1.80	0.1463	0.1464	1.20	0.1356	0.1357	30.90	0.1179	0.1181
2.40	0.1372	0.1373	31.20	0.1194	0.1197	2.40	0.1445	0.1447	1.80	0.1372	0.1373	31.20	0.1176	0.1179
3.00	0.1257	0.1263	31.50	0.1185	0.1188	3.00	0.1301	0.1311	2.40	0.1372	0.1373	31.50	0.1180	0.1183
3.60	0.1277	0.1284	31.80	0.1178	0.1181	3.60	0.1260	0.1270	3.00	0.1267	0.1273	31.80	0.1175	0.1178
4.20	0.1227	0.1234	32.10	0.1181	0.1184	4.20	0.1250	0.1258	3.60	0.1286	0.1292	32.10	0.1178	0.1181
4.80	0.1077	0.1084	32.40	0.1191	0.1194	4.80	0.1114	0.1120	4.20	0.1236	0.1242	32.40	0.1168	0.1171
5.40	0.1149	0.1151	32.70	0.1190	0.1193	5.40	0.1246	0.1248	4.80	0.1102	0.1108	32.70	0.1182	0.1185
6.00	0.1172	0.1175	33.00	0.1185	0.1187	6.00	0.1210	0.1213	5.40	0.1173	0.1175	33.00	0.1178	0.1181
6.60	0.1228	0.1229	33.30	0.1197	0.1199	6.60	0.1254	0.1255	6.00	0.1182	0.1186	33.30	0.1174	0.1177
7.20	0.1143	0.1144	33.60	0.1207	0.1209	7.20	0.1226	0.1228	6.60	0.1257	0.1259	33.60	0.1169	0.1172
7.80	0.1230	0.1232	33.90	0.1197	0.1200	7.80	0.1263	0.1264	7.20	0.1153	0.1154	33.90	0.1172	0.1175

8.40	0.1268	0.1271	34.20	0.1190	0.1193	8.40	0.1357	0.1362	7.80	0.1257	0.1259	34.20	0.1179	0.1181
9.00	0.1268	0.1273	34.50	0.1196	0.1199	9.00	0.1377	0.1382	8.40	0.1290	0.1294	34.50	0.1169	0.1172
9.60	0.1225	0.1230	34.80	0.1200	0.1203	9.60	0.1249	0.1255	9.00	0.1274	0.1278	34.80	0.1173	0.1176
10.20	0.1174	0.1179	35.10	0.1195	0.1197	10.20	0.1168	0.1174	9.60	0.1260	0.1265	35.40	0.1172	0.1175
10.80	0.1143	0.1149	35.40	0.1190	0.1193	10.80	0.1228	0.1234	10.20	0.1225	0.1230	35.70	0.1179	0.1182
11.40	0.1171	0.1177	35.70	0.1193	0.1196	11.40	0.1228	0.1232	10.80	0.1191	0.1197	36.00	0.1175	0.1178
12.00	0.1197	0.1199	36.00	0.1197	0.1200	12.00	0.1262	0.1265	11.40	0.1220	0.1225	36.30	0.1172	0.1175
12.60	0.1122	0.1125	36.30	0.1202	0.1205	12.60	0.1120	0.1123	12.00	0.1225	0.1227	36.60	0.1177	0.1180
13.20	0.1143	0.1146	36.60	0.1202	0.1205	13.20	0.1213	0.1216	12.60	0.1184	0.1189	36.90	0.1173	0.1176
13.80	0.1210	0.1212	36.90	0.1198	0.1200	13.80	0.1274	0.1276	13.20	0.1203	0.1207	37.20	0.1171	0.1174
14.40	0.1182	0.1185	37.20	0.1202	0.1205	14.40	0.1295	0.1298	13.80	0.1279	0.1281	37.50	0.1178	0.1181
15.00	0.1271	0.1275	37.50	0.1197	0.1200	15.00	0.1316	0.1322	14.40	0.1234	0.1236	37.80	0.1169	0.1172
15.60	0.1197	0.1202	37.80	0.1189	0.1192	15.60	0.1181	0.1188	15.00	0.1328	0.1332	38.10	0.1175	0.1178
16.20	0.1130	0.1134	38.10	0.1194	0.1197	16.20	0.1211	0.1215	15.60	0.1238	0.1243	38.40	0.1172	0.1175
16.80	0.1197	0.1202	38.40	0.1201	0.1204	16.80	0.1242	0.1247	16.20	0.1207	0.1210	38.70	0.1177	0.1180
17.40	0.1203	0.1206	38.70	0.1201	0.1204	17.40	0.1230	0.1235	16.80	0.1249	0.1254	39.00	0.1172	0.1175
18.00	0.1144	0.1150	39.00	0.1194	0.1197	18.00	0.1212	0.1216	17.40	0.1281	0.1284	39.30	0.1177	0.1180
18.60	0.1168	0.1171	39.30	0.1198	0.1200	18.60	0.1148	0.1152	18.00	0.1189	0.1195	39.60	0.1174	0.1177
19.20	0.1118	0.1121	39.60	0.1210	0.1213	19.20	0.1202	0.1204	18.60	0.1235	0.1237	39.90	0.1174	0.1177
19.80	0.1163	0.1165	39.90	0.1210	0.1213	19.80	0.1241	0.1244	19.20	0.1179	0.1183	40.20	0.1183	0.1186
20.40	0.1206	0.1210	40.20	0.1201	0.1204	20.40	0.1270	0.1273	19.80	0.1249	0.1252	40.40	0.1181	0.1184
21.00	0.1173	0.1175	40.50	0.1198	0.1201	21.00	0.1237	0.1240	20.40	0.1280	0.1284	40.80	0.1182	0.1186
21.60	0.1193	0.1197	40.80	0.1198	0.1201	21.60	0.1171	0.1175	21.00	0.1234	0.1237	41.00	0.1178	0.1181
22.20	0.1128	0.1133	41.10	0.1194	0.1197	22.20	0.1211	0.1216	21.60	0.1214	0.1217	41.40	0.1176	0.1179
22.80	0.1228	0.1232	41.40	0.1201	0.1204	22.80	0.1258	0.1261	22.20	0.1197	0.1202	41.60	0.1178	0.1181
23.40	0.1158	0.1161	41.70	0.1210	0.1213	23.40	0.1202	0.1204	22.80	0.1264	0.1267	41.80	0.1179	0.1181

24.00	0.1132	0.1137	42.00	0.1206	0.1209	24.00	0.1193	0.1196	23.40	0.1278	0.1281	42.20	0.1177	0.1180
24.60	0.1166	0.1169	42.30	0.1203	0.1206	24.60	0.1162	0.1165	24.00	0.1192	0.1196	42.40	0.1176	0.1179
25.20	0.1136	0.1139	42.60	0.1201	0.1204	25.20	0.1199	0.1201	24.60	0.1214	0.1218	42.60	0.1175	0.1178
25.80	0.1143	0.1145	42.90	0.1206	0.1209	25.80	0.1234	0.1236	25.20	0.1211	0.1213	43.00	0.1180	0.1183
26.40	0.1205	0.1208	43.20	0.1214	0.1217	26.40	0.1239	0.1241	25.80	0.1227	0.1229	43.20	0.1179	0.1182
27.00	0.1144	0.1147	43.50	0.1206	0.1209	27.00	0.1173	0.1175	26.40	0.1231	0.1234	43.60	0.1175	0.1178
27.60	0.1150	0.1153	43.80	0.1193	0.1196	27.60	0.1215	0.1218	27.00	0.1233	0.1235	43.80	0.1178	0.1181
28.20	0.1158	0.1160	44.10	0.1201	0.1204	28.20	0.1211	0.1214	27.60	0.1221	0.1224	44.40	0.1172	0.1175
28.80	0.1175	0.1177	44.40	0.1220	0.1222	28.80	0.1229	0.1232	28.20	0.1241	0.1243	44.80	0.1168	0.1171
29.40	0.1159	0.1162	44.70	0.1214	0.1217	29.40	0.1192	0.1195	28.80	0.1237	0.1240	45.00	0.1173	0.1176
30.00	0.1161	0.1164	45.00	0.1198	0.1201	30.00	0.1187	0.1189	29.40	0.1229	0.1232	45.40	0.1182	0.1185
30.60	0.1124	0.1126	45.30	0.1201	0.1204	30.60	0.1166	0.1168	30.00	0.1225	0.1228	45.60	0.1181	0.1184
31.20	0.1135	0.1138	45.60	0.1208	0.1211	31.20	0.1199	0.1201	30.60	0.1204	0.1206	46.00	0.1178	0.1181
31.80	0.1153	0.1155	45.90	0.1207	0.1211	31.80	0.1214	0.1217	31.20	0.1201	0.1204	46.20	0.1176	0.1179
32.40	0.1166	0.1168	46.20	0.1210	0.1213	32.40	0.1211	0.1214	31.80	0.1246	0.1248	46.40	0.1175	0.1177
33.00	0.1146	0.1148	46.50	0.1207	0.1210	33.00	0.1180	0.1182	32.40	0.1205	0.1207	46.80	0.1173	0.1176
33.60	0.1137	0.1139	46.80	0.1197	0.1200	33.60	0.1191	0.1194	33.00	0.1217	0.1220	47.00	0.1171	0.1175
34.20	0.1139	0.1142	47.10	0.1194	0.1197	34.20	0.1210	0.1213	33.60	0.1207	0.1210	47.40	0.1168	0.1171
34.80	0.1173	0.1176	47.40	0.1198	0.1200	34.80	0.1215	0.1217	34.20	0.1229	0.1232	47.60	0.1169	0.1173
35.40	0.1140	0.1143	47.70	0.1206	0.1209	35.40	0.1196	0.1200	34.80	0.1214	0.1216	48.00	0.1175	0.1178
36.00	0.1152	0.1155	48.00	0.1207	0.1210	36.00	0.1183	0.1186	35.40	0.1222	0.1225	48.20	0.1177	0.1180
36.60	0.1119	0.1122	48.30	0.1196	0.1200	36.60	0.1170	0.1173	36.00	0.1202	0.1205	48.60	0.1178	0.1181
37.20	0.1167	0.1170	48.60	0.1192	0.1195	37.20	0.1216	0.1218	36.60	0.1201	0.1203	48.80	0.1175	0.1177
37.80	0.1128	0.1131	48.90	0.1194	0.1197	37.80	0.1192	0.1195	37.20	0.1203	0.1206	49.20	0.1167	0.1170
38.40	0.1161	0.1164	49.20	0.1202	0.1205	38.40	0.1191	0.1194	37.80	0.1217	0.1220	49.40	0.1169	0.1172
39.00	0.1133	0.1136	49.50	0.1206	0.1208	39.00	0.1180	0.1183	38.40	0.1211	0.1215	49.60	0.1173	0.1176

39.60	0.1140	0.1143	49.80	0.1195	0.1198	39.60	0.1200	0.1202	39.00	0.1200	0.1203	50.00	0.1174	0.1177
40.20	0.1122	0.1125	50.10	0.1188	0.1191	40.20	0.1202	0.1204	39.60	0.1195	0.1197	50.20	0.1173	0.1176
40.80	0.1161	0.1164	50.40	0.1196	0.1199	40.80	0.1202	0.1206	40.20	0.1213	0.1216	50.60	0.1173	0.1176
41.40	0.1144	0.1147	50.70	0.1202	0.1205	41.40	0.1188	0.1192	40.80	0.1214	0.1218	50.80	0.1172	0.1175
42.00	0.1142	0.1145	51.00	0.1202	0.1205	42.00	0.1182	0.1185	41.40	0.1211	0.1214	51.40	0.1179	0.1182
42.60	0.1124	0.1127	51.30	0.1204	0.1207	42.60	0.1177	0.1180	42.00	0.1195	0.1198	51.80	0.1180	0.1183
43.20	0.1148	0.1151	51.60	0.1198	0.1201	43.20	0.1210	0.1213	42.60	0.1201	0.1204	52.00	0.1175	0.1178
43.80	0.1132	0.1135	51.90	0.1190	0.1193	43.80	0.1186	0.1189	43.20	0.1196	0.1199	52.40	0.1169	0.1172
44.40	0.1161	0.1164	52.20	0.1193	0.1196	44.40	0.1200	0.1203	43.80	0.1228	0.1231	52.60	0.1172	0.1175
45.00	0.1125	0.1127	52.50	0.1201	0.1204	45.00	0.1169	0.1172	44.40	0.1187	0.1190	52.80	0.1175	0.1178
45.60	0.1133	0.1136	52.80	0.1204	0.1207	45.60	0.1195	0.1198	45.00	0.1193	0.1197	53.20	0.1177	0.1180
46.20	0.1137	0.1140	53.10	0.1196	0.1199	46.20	0.1193	0.1196	45.60	0.1192	0.1195	53.40	0.1177	0.1180
46.80	0.1150	0.1153	53.40	0.1188	0.1191	46.80	0.1208	0.1210	46.20	0.1217	0.1220	53.80	0.1173	0.1176
47.40	0.1124	0.1126	53.70	0.1193	0.1196	47.40	0.1172	0.1175	46.80	0.1195	0.1197	54.00	0.1170	0.1173
48.00	0.1146	0.1150	54.00	0.1201	0.1204	48.00	0.1186	0.1189	47.40	0.1199	0.1202	54.40	0.1171	0.1174
48.60	0.1118	0.1121	54.30	0.1201	0.1203	48.60	0.1185	0.1188	48.00	0.1188	0.1191	54.60	0.1173	0.1176
49.20	0.1138	0.1141	54.60	0.1192	0.1195	49.20	0.1209	0.1212	48.60	0.1210	0.1212	55.00	0.1178	0.1181
49.80	0.1130	0.1133	54.90	0.1188	0.1191	49.80	0.1177	0.1180	49.20	0.1198	0.1201	55.20	0.1177	0.1180
50.40	0.1153	0.1156	55.20	0.1193	0.1196	50.40	0.1198	0.1201	49.80	0.1207	0.1210	55.60	0.1169	0.1172
51.00	0.1128	0.1130	55.50	0.1196	0.1199	51.00	0.1177	0.1180	50.40	0.1191	0.1194	55.80	0.1169	0.1172
51.60	0.1133	0.1136	55.80	0.1196	0.1199	51.60	0.1195	0.1198	51.00	0.1198	0.1201	56.20	0.1175	0.1178
52.20	0.1130	0.1133	56.10	0.1195	0.1198	52.20	0.1196	0.1199	51.60	0.1199	0.1202	56.40	0.1175	0.1178
52.80	0.1147	0.1150	56.40	0.1191	0.1194	52.80	0.1192	0.1195	52.20	0.1198	0.1201	56.60	0.1174	0.1176
53.40	0.1140	0.1143	56.70	0.1190	0.1192	53.40	0.1176	0.1179	52.80	0.1195	0.1198	57.00	0.1173	0.1176
54.00	0.1135	0.1138	57.00	0.1193	0.1196	54.00	0.1183	0.1186	53.40	0.1202	0.1205	57.20	0.1175	0.1178
54.60	0.1114	0.1116	57.30	0.1198	0.1201	54.60	0.1183	0.1186	54.00	0.1183	0.1186	57.60	0.1176	0.1179

55.20	0.1148	0.1151	57.60	0.1203	0.1205	55.20	0.1199	0.1202	54.60	0.1199	0.1202	57.80	0.1174	0.1177
55.80	0.1135	0.1138	57.90	0.1195	0.1198	55.80	0.1183	0.1186	55.20	0.1209	0.1212	58.20	0.1174	0.1177
56.40	0.1137	0.1139	58.20	0.1186	0.1188	56.40	0.1187	0.1190	55.80	0.1201	0.1204	58.40	0.1176	0.1179
57.00	0.1134	0.1137	58.50	0.1193	0.1196	57.00	0.1175	0.1178	56.40	0.1187	0.1190	58.80	0.1176	0.1178
57.60	0.1129	0.1132	58.80	0.1203	0.1206	57.60	0.1203	0.1206	57.00	0.1201	0.1204	59.00	0.1174	0.1177
58.20	0.1128	0.1130	59.10	0.1203	0.1206	58.20	0.1190	0.1193	57.60	0.1195	0.1198	59.40	0.1173	0.1176
58.80	0.1155	0.1157	59.40	0.1196	0.1199	58.80	0.1190	0.1194	58.20	0.1203	0.1206	59.60	0.1173	0.1176
59.40	0.1126	0.1130	59.70	0.1188	0.1191	59.40	0.1174	0.1177	58.80	0.1192	0.1196	59.80	0.1174	0.1177
60.00	0.1134	0.1137	60.00	0.1193	0.1196	60.00	0.1189	0.1192	59.40	0.1198	0.1201	60.00	0.1177	0.1180

Table C5 Tabulated time series data for the α=16°: θ=10° arced labyrinth weir at H/P=0.7.

RM1-WM0			RM0-WM1			RM0-WM2			RM1-WM2			RM1-WM3		
Cell Count:	1435885		*Cell Count:*	1418188		*Cell Count:*	2885710		*Cell Count:*	3088210		*Cell Count:*	6253591	
Q	227.11	[L/s]	Q	226.23	[L/s]	Q	226.23	[L/s]	Q	227.11	[L/s]	Q	227.11	[L/s]
H	0.137	[m]	H	0.142	[m]	H	0.139	[m]	H	0.138	[m]	H	0.137	[m]
H/P	0.675	[-]	H/P	0.700	[-]	H/P	0.683	[-]	H/P	0.679	[-]	H/P	0.677	[-]
C_d	0.485	[-]	C_d	0.457	[-]	C_d	0.475	[-]	C_d	0.481	[-]	C_d	0.483	[-]
$C_{d\text{-}emp}$	0.469	[-]	$C_{d\text{-}emp}$	0.460	[-]	$C_{d\text{-}emp}$	0.466	[-]	$C_{d\text{-}emp}$	0.467	[-]	$C_{d\text{-}emp}$	0.468	[-]
ε_{Cd}	3.44%	[%]	ε_{Cd}	-0.74%	[%]	ε_{Cd}	1.87%	[%]	ε_{Cd}	2.83%	[%]	ε_{Cd}	3.21%	[%]
Time [s]	h [m]	H [m]	Time [s]	h [m]	H [m]	Time [s]	h [m]	H [m]	Time [s]	h [m]	H [m]	Time [s]	h [m]	H [m]
0.00	0.1422	0.1422	30.00	0.1387	0.1391	0.00	0.1422	0.1422	0.00	0.1422	0.1422	30.00	0.1351	0.1354
0.60	0.1440	0.1440	30.30	0.1387	0.1391	0.60	0.1434	0.1434	0.60	0.1440	0.1440	30.30	0.1339	0.1342
1.20	0.1588	0.1590	30.60	0.1376	0.1379	1.20	0.1463	0.1463	1.20	0.1589	0.1590	30.60	0.1337	0.1341
1.80	0.1646	0.1648	30.90	0.1393	0.1397	1.80	0.1463	0.1463	1.80	0.1646	0.1648	30.90	0.1381	0.1385
2.40	0.1644	0.1646	31.20	0.1387	0.1390	2.40	0.1406	0.1408	2.40	0.1644	0.1647	31.20	0.1389	0.1393
3.00	0.1477	0.1487	31.50	0.1390	0.1393	3.00	0.1313	0.1319	3.00	0.1481	0.1491	31.50	0.1388	0.1391
3.60	0.1514	0.1524	31.80	0.1388	0.1391	3.60	0.1381	0.1386	3.60	0.1522	0.1532	31.80	0.1388	0.1391
4.20	0.1459	0.1468	32.10	0.1392	0.1396	4.20	0.1344	0.1350	4.20	0.1464	0.1473	32.10	0.1372	0.1376
4.80	0.1275	0.1282	32.40	0.1399	0.1403	4.80	0.1180	0.1188	4.80	0.1278	0.1285	32.40	0.1377	0.1381
5.40	0.1397	0.1401	32.70	0.1398	0.1401	5.40	0.1393	0.1397	5.40	0.1406	0.1409	32.70	0.1372	0.1375
6.00	0.1420	0.1422	33.00	0.1396	0.1400	6.00	0.1315	0.1318	6.00	0.1446	0.1448	33.00	0.1373	0.1377
6.60	0.1418	0.1420	33.30	0.1395	0.1399	6.60	0.1340	0.1343	6.60	0.1432	0.1433	33.30	0.1384	0.1387
7.20	0.1420	0.1422	33.60	0.1403	0.1407	7.20	0.1332	0.1336	7.20	0.1419	0.1420	33.60	0.1374	0.1377
7.80	0.1461	0.1464	33.90	0.1406	0.1410	7.80	0.1303	0.1305	7.80	0.1466	0.1469	33.90	0.1394	0.1397
8.40	0.1516	0.1519	34.20	0.1398	0.1401	8.40	0.1420	0.1424	8.40	0.1533	0.1537	34.20	0.1395	0.1398

9.00	0.1503	0.1511	34.50	0.1402	0.1406	9.00	0.1434	0.1438	9.00	0.1539	0.1546	34.50	0.1384	0.1388
9.60	0.1452	0.1458	34.80	0.1405	0.1409	9.60	0.1387	0.1392	9.60	0.1446	0.1454	34.80	0.1381	0.1385
10.20	0.1386	0.1394	35.10	0.1409	0.1413	10.20	0.1292	0.1297	10.20	0.1403	0.1410	35.10	0.1375	0.1380
10.80	0.1342	0.1347	35.40	0.1410	0.1413	10.80	0.1363	0.1369	10.80	0.1374	0.1380	35.40	0.1378	0.1382
11.40	0.1425	0.1431	35.70	0.1406	0.1410	11.40	0.1421	0.1426	11.40	0.1425	0.1431	35.70	0.1373	0.1377
12.00	0.1379	0.1383	36.00	0.1413	0.1417	12.00	0.1359	0.1364	12.00	0.1385	0.1389	36.00	0.1349	0.1353
12.60	0.1343	0.1349	36.30	0.1408	0.1411	12.60	0.1317	0.1323	12.60	0.1323	0.1327	36.30	0.1372	0.1375
13.20	0.1410	0.1412	36.60	0.1419	0.1423	13.20	0.1360	0.1363	13.20	0.1425	0.1428	36.60	0.1375	0.1379
13.80	0.1459	0.1462	36.90	0.1409	0.1413	13.80	0.1321	0.1325	13.80	0.1452	0.1455	36.90	0.1375	0.1379
14.40	0.1461	0.1465	37.20	0.1413	0.1416	14.40	0.1441	0.1446	14.40	0.1482	0.1486	37.20	0.1379	0.1382
15.00	0.1495	0.1502	37.50	0.1416	0.1419	15.00	0.1439	0.1444	15.00	0.1469	0.1477	37.50	0.1372	0.1376
15.60	0.1373	0.1379	37.80	0.1413	0.1416	15.60	0.1310	0.1315	15.60	0.1396	0.1402	37.80	0.1372	0.1376
16.20	0.1405	0.1409	38.10	0.1418	0.1421	16.20	0.1397	0.1402	16.20	0.1382	0.1387	38.10	0.1375	0.1379
16.80	0.1415	0.1421	38.40	0.1419	0.1422	16.80	0.1373	0.1377	16.80	0.1423	0.1429	38.40	0.1372	0.1375
17.40	0.1409	0.1414	38.70	0.1413	0.1416	17.40	0.1421	0.1426	17.40	0.1429	0.1433	38.70	0.1353	0.1356
18.00	0.1375	0.1381	39.00	0.1417	0.1421	18.00	0.1368	0.1375	18.00	0.1372	0.1378	39.00	0.1376	0.1379
18.60	0.1378	0.1380	39.30	0.1421	0.1424	18.60	0.1336	0.1340	18.60	0.1353	0.1356	39.30	0.1376	0.1380
19.20	0.1409	0.1413	39.60	0.1419	0.1422	19.20	0.1352	0.1357	19.20	0.1398	0.1401	39.60	0.1375	0.1378
19.80	0.1429	0.1432	39.90	0.1414	0.1418	19.80	0.1413	0.1416	19.80	0.1459	0.1462	39.90	0.1372	0.1376
20.40	0.1451	0.1455	40.20	0.1422	0.1425	20.40	0.1419	0.1423	20.40	0.1468	0.1472	40.20	0.1399	0.1402
21.00	0.1391	0.1394	40.50	0.1417	0.1421	21.00	0.1369	0.1374	21.00	0.1375	0.1380	40.50	0.1390	0.1393
21.60	0.1387	0.1392	40.80	0.1421	0.1424	21.60	0.1354	0.1359	21.60	0.1391	0.1395	40.80	0.1376	0.1380
22.20	0.1423	0.1427	41.10	0.1422	0.1426	22.20	0.1408	0.1411	22.20	0.1453	0.1457	41.10	0.1372	0.1375
22.80	0.1415	0.1418	41.40	0.1418	0.1422	22.80	0.1390	0.1393	22.80	0.1413	0.1416	41.40	0.1351	0.1355
23.40	0.1402	0.1406	41.70	0.1423	0.1426	23.40	0.1401	0.1405	23.40	0.1407	0.1411	41.70	0.1347	0.1351
24.00	0.1328	0.1333	42.00	0.1423	0.1427	24.00	0.1368	0.1373	24.00	0.1338	0.1343	42.00	0.1372	0.1376

24.60	0.1399	0.1402	42.30	0.1420	0.1424	24.60	0.1336	0.1340	24.60	0.1376	0.1380	42.30	0.1379	0.1383
25.20	0.1373	0.1375	42.60	0.1423	0.1427	25.20	0.1393	0.1396	25.20	0.1396	0.1399	42.60	0.1372	0.1376
25.80	0.1414	0.1417	42.90	0.1420	0.1424	25.80	0.1413	0.1416	25.80	0.1416	0.1419	42.90	0.1375	0.1379
26.40	0.1394	0.1396	43.20	0.1421	0.1425	26.40	0.1376	0.1378	26.40	0.1388	0.1391	43.20	0.1373	0.1377
27.00	0.1407	0.1410	43.50	0.1423	0.1427	27.00	0.1380	0.1384	27.00	0.1386	0.1388	43.50	0.1346	0.1349
27.60	0.1380	0.1382	43.80	0.1422	0.1425	27.60	0.1370	0.1373	27.60	0.1393	0.1396	43.80	0.1373	0.1376
28.20	0.1424	0.1427	44.10	0.1421	0.1425	28.20	0.1410	0.1413	28.20	0.1426	0.1429	44.10	0.1376	0.1380
28.80	0.1386	0.1390	44.40	0.1422	0.1426	28.80	0.1405	0.1408	28.80	0.1398	0.1402	44.40	0.1374	0.1378
29.40	0.1395	0.1399	44.70	0.1424	0.1427	29.40	0.1390	0.1393	29.40	0.1383	0.1386	44.70	0.1372	0.1376
30.00	0.1373	0.1375	45.00	0.1426	0.1429	30.00	0.1355	0.1358	30.00	0.1372	0.1375	45.00	0.1372	0.1375
30.60	0.1372	0.1375	45.30	0.1425	0.1429	30.60	0.1369	0.1373	30.60	0.1375	0.1378	45.30	0.1377	0.1380
31.20	0.1390	0.1393	45.60	0.1423	0.1427	31.20	0.1407	0.1410	31.20	0.1407	0.1411	45.60	0.1382	0.1386
31.80	0.1380	0.1383	45.90	0.1424	0.1428	31.80	0.1397	0.1400	31.80	0.1390	0.1393	45.90	0.1376	0.1379
32.40	0.1376	0.1380	46.20	0.1425	0.1429	32.40	0.1375	0.1378	32.40	0.1376	0.1379	46.20	0.1382	0.1385
33.00	0.1373	0.1377	46.50	0.1424	0.1428	33.00	0.1390	0.1393	33.00	0.1377	0.1381	46.50	0.1374	0.1377
33.60	0.1378	0.1381	46.80	0.1420	0.1424	33.60	0.1394	0.1397	33.60	0.1390	0.1393	46.80	0.1382	0.1386
34.20	0.1401	0.1405	47.10	0.1424	0.1428	34.20	0.1406	0.1410	34.20	0.1412	0.1416	47.10	0.1373	0.1377
34.80	0.1372	0.1375	47.40	0.1418	0.1422	34.80	0.1410	0.1413	34.80	0.1384	0.1388	47.40	0.1379	0.1382
35.40	0.1377	0.1381	47.70	0.1421	0.1425	35.40	0.1386	0.1390	35.40	0.1375	0.1379	47.70	0.1375	0.1379
36.00	0.1351	0.1354	48.00	0.1423	0.1426	36.00	0.1376	0.1380	36.00	0.1374	0.1378	48.00	0.1377	0.1381
36.60	0.1380	0.1383	48.30	0.1422	0.1425	36.60	0.1400	0.1404	36.60	0.1387	0.1390	48.30	0.1375	0.1378
37.20	0.1380	0.1383	48.60	0.1422	0.1425	37.20	0.1388	0.1392	37.20	0.1384	0.1387	48.60	0.1379	0.1383
37.80	0.1377	0.1381	48.90	0.1421	0.1424	37.80	0.1390	0.1395	37.80	0.1385	0.1389	48.90	0.1374	0.1378
38.40	0.1372	0.1376	49.20	0.1419	0.1423	38.40	0.1386	0.1389	38.40	0.1372	0.1376	49.20	0.1374	0.1378
39.00	0.1378	0.1382	49.50	0.1423	0.1427	39.00	0.1367	0.1371	39.00	0.1381	0.1384	49.50	0.1378	0.1382
39.60	0.1374	0.1378	49.80	0.1419	0.1422	39.60	0.1401	0.1404	39.60	0.1383	0.1386	49.80	0.1381	0.1384

40.20	0.1389	0.1393	50.10	0.1419	0.1422	40.20	0.1393	0.1397	40.20	0.1396	0.1400	50.10	0.1375	0.1378
40.80	0.1373	0.1377	50.40	0.1418	0.1422	40.80	0.1396	0.1400	40.80	0.1382	0.1385	50.40	0.1372	0.1376
41.40	0.1372	0.1376	50.70	0.1420	0.1423	41.40	0.1381	0.1385	41.40	0.1377	0.1381	50.70	0.1372	0.1376
42.00	0.1350	0.1354	51.00	0.1422	0.1425	42.00	0.1388	0.1392	42.00	0.1375	0.1379	51.00	0.1372	0.1376
42.60	0.1381	0.1385	51.30	0.1421	0.1424	42.60	0.1391	0.1394	42.60	0.1384	0.1387	51.30	0.1372	0.1376
43.20	0.1372	0.1376	51.60	0.1421	0.1424	43.20	0.1392	0.1396	43.20	0.1381	0.1384	51.60	0.1375	0.1379
43.80	0.1375	0.1378	51.90	0.1421	0.1425	43.80	0.1382	0.1386	43.80	0.1379	0.1382	51.90	0.1376	0.1379
44.40	0.1373	0.1377	52.20	0.1419	0.1423	44.40	0.1382	0.1386	44.40	0.1375	0.1378	52.20	0.1376	0.1379
45.00	0.1372	0.1375	52.50	0.1421	0.1425	45.00	0.1379	0.1382	45.00	0.1387	0.1391	52.50	0.1374	0.1377
45.60	0.1372	0.1375	52.80	0.1423	0.1427	45.60	0.1399	0.1402	45.60	0.1389	0.1392	52.80	0.1372	0.1375
46.20	0.1376	0.1380	53.10	0.1421	0.1425	46.20	0.1394	0.1397	46.20	0.1383	0.1387	53.10	0.1373	0.1377
46.80	0.1347	0.1352	53.40	0.1422	0.1425	46.80	0.1382	0.1385	46.80	0.1379	0.1383	53.40	0.1375	0.1378
47.40	0.1379	0.1382	53.70	0.1419	0.1423	47.40	0.1393	0.1397	47.40	0.1376	0.1380	53.70	0.1372	0.1375
48.00	0.1345	0.1349	54.00	0.1425	0.1429	48.00	0.1387	0.1390	48.00	0.1374	0.1378	54.00	0.1377	0.1381
48.60	0.1387	0.1391	54.30	0.1423	0.1427	48.60	0.1380	0.1384	48.60	0.1384	0.1387	54.30	0.1372	0.1375
49.20	0.1338	0.1342	54.60	0.1422	0.1426	49.20	0.1398	0.1402	49.20	0.1381	0.1385	54.60	0.1388	0.1391
49.80	0.1375	0.1379	54.90	0.1417	0.1421	49.80	0.1380	0.1383	49.80	0.1374	0.1378	54.90	0.1378	0.1382
50.40	0.1376	0.1379	55.20	0.1423	0.1427	50.40	0.1382	0.1386	50.40	0.1379	0.1383	55.20	0.1379	0.1383
51.00	0.1372	0.1375	55.50	0.1422	0.1425	51.00	0.1386	0.1389	51.00	0.1381	0.1385	55.50	0.1373	0.1377
51.60	0.1374	0.1378	55.80	0.1422	0.1425	51.60	0.1390	0.1394	51.60	0.1387	0.1391	55.80	0.1373	0.1377
52.20	0.1385	0.1389	56.10	0.1423	0.1427	52.20	0.1394	0.1397	52.20	0.1380	0.1384	56.10	0.1372	0.1376
52.80	0.1372	0.1375	56.40	0.1423	0.1427	52.80	0.1379	0.1383	52.80	0.1374	0.1378	56.40	0.1372	0.1376
53.40	0.1410	0.1413	56.70	0.1424	0.1427	53.40	0.1387	0.1391	53.40	0.1376	0.1380	56.70	0.1372	0.1376
54.00	0.1372	0.1375	57.00	0.1427	0.1431	54.00	0.1389	0.1393	54.00	0.1379	0.1382	57.00	0.1372	0.1375
54.60	0.1404	0.1407	57.30	0.1425	0.1429	54.60	0.1393	0.1397	54.60	0.1380	0.1384	57.30	0.1373	0.1376
55.20	0.1372	0.1376	57.60	0.1422	0.1426	55.20	0.1390	0.1394	55.20	0.1377	0.1380	57.60	0.1372	0.1375

55.80	0.1372	0.1376	57.90	0.1423	0.1427	55.80	0.1379	0.1383	55.80	0.1376	0.1379	57.90	0.1373	0.1376
56.40	0.1372	0.1375	58.20	0.1425	0.1428	56.40	0.1387	0.1391	56.40	0.1377	0.1380	58.20	0.1379	0.1383
57.00	0.1346	0.1350	58.50	0.1423	0.1427	57.00	0.1396	0.1399	57.00	0.1383	0.1386	58.50	0.1373	0.1377
57.60	0.1372	0.1376	58.80	0.1425	0.1428	57.60	0.1382	0.1385	57.60	0.1386	0.1390	58.80	0.1378	0.1382
58.20	0.1372	0.1375	59.10	0.1423	0.1426	58.20	0.1389	0.1393	58.20	0.1381	0.1385	59.10	0.1345	0.1349
58.80	0.1342	0.1346	59.40	0.1425	0.1428	58.80	0.1384	0.1387	58.80	0.1375	0.1379	59.40	0.1372	0.1375
59.40	0.1388	0.1392	59.70	0.1428	0.1432	59.40	0.1384	0.1387	59.40	0.1376	0.1380	59.70	0.1379	0.1383
60.00	0.1373	0.1376	60.00	0.1428	0.1431	60.00	0.1387	0.1391	60.00	0.1377	0.1381	60.00	0.1379	0.1382

Table C6 Tabulated time series data for the α=16°: θ=10° arced labyrinth weir at H/P=0.8

RM1-WM0			RM0-WM1			RM0-WM2			RM1-WM2			RM1-WM3		
Cell Count:	1435885		*Cell Count:*	1491286		*Cell Count:*	3037855		*Cell Count:*	3088210		*Cell Count:*	6253591	
Q	260.96	[L/s]	Q	259.94	[L/s]	Q	259.94	[L/s]	Q	260.96	[L/s]	Q	260.96	[L/s]
H	0.158	[m]	H	0.159	[m]	H	0.159	[m]	H	0.159	[m]	H	0.159	[m]
H/P	0.778	[-]	H/P	0.785	[-]	H/P	0.785	[-]	H/P	0.782	[-]	H/P	0.784	[-]
C_d	0.450	[-]	C_d	0.443	[-]	C_d	0.443	[-]	C_d	0.447	[-]	C_d	0.445	[-]
$C_{d\text{-}emp}$	0.438	[-]	$C_{d\text{-}emp}$	0.437	[-]	$C_{d\text{-}emp}$	0.437	[-]	$C_{d\text{-}emp}$	0.437	[-]	$C_{d\text{-}emp}$	0.437	[-]
ε_{Cd}	2.71%	[%]	ε_{Cd}	1.40%	[%]	ε_{Cd}	1.36%	[%]	ε_{Cd}	2.12%	[%]	ε_{Cd}	1.87%	[%]
Time [s]	h [m]	H [m]	Time [s]	h [m]	H [m]	Time [s]	h [m]	H [m]	Time [s]	h [m]	H [m]	Time [s]	h [m]	H [m]
0.00	0.1626	0.1626	30.00	0.1600	0.1604	0.00	0.1626	0.1626	0.00	0.1626	0.1626	0.00	0.1626	0.1626
0.60	0.1636	0.1636	30.30	0.1596	0.1601	0.60	0.1647	0.1647	0.60	0.1636	0.1636	0.60	0.1636	0.1636
1.20	0.1646	0.1646	30.60	0.1593	0.1597	1.20	0.1818	0.1820	1.20	0.1646	0.1646	1.20	0.1646	0.1646
1.80	0.1646	0.1646	30.90	0.1595	0.1599	1.80	0.1829	0.1831	1.80	0.1646	0.1646	1.80	0.1646	0.1646
2.40	0.1552	0.1554	31.20	0.1599	0.1603	2.40	0.1828	0.1831	2.40	0.1554	0.1555	2.40	0.1553	0.1555
3.00	0.1468	0.1476	31.50	0.1594	0.1599	3.00	0.1645	0.1657	3.00	0.1472	0.1479	3.00	0.1472	0.1479
3.60	0.1568	0.1574	31.80	0.1592	0.1596	3.60	0.1687	0.1698	3.60	0.1576	0.1581	3.60	0.1573	0.1578
4.20	0.1530	0.1536	32.10	0.1593	0.1598	4.20	0.1631	0.1640	4.20	0.1531	0.1537	4.20	0.1527	0.1533
4.80	0.1378	0.1386	32.40	0.1599	0.1603	4.80	0.1482	0.1488	4.80	0.1375	0.1383	4.80	0.1373	0.1382
5.40	0.1511	0.1517	32.70	0.1597	0.1602	5.40	0.1580	0.1584	5.40	0.1521	0.1528	5.40	0.1510	0.1517
6.00	0.1530	0.1534	33.00	0.1585	0.1589	6.00	0.1573	0.1578	6.00	0.1540	0.1544	6.00	0.1541	0.1545
6.60	0.1459	0.1465	33.30	0.1597	0.1601	6.60	0.1648	0.1650	6.60	0.1488	0.1492	6.60	0.1458	0.1462
7.20	0.1470	0.1475	33.60	0.1613	0.1617	7.20	0.1502	0.1505	7.20	0.1490	0.1494	7.20	0.1514	0.1518
7.80	0.1527	0.1531	33.90	0.1594	0.1598	7.80	0.1714	0.1717	7.80	0.1545	0.1550	7.80	0.1489	0.1495

8.40	0.1526	0.1529	34.20	0.1590	0.1594	8.40	0.1710	0.1717	8.40	0.1528	0.1531	8.40	0.1557	0.1559
9.00	0.1634	0.1641	34.50	0.1603	0.1607	9.00	0.1690	0.1696	9.00	0.1634	0.1640	9.00	0.1611	0.1618
9.60	0.1540	0.1547	34.80	0.1601	0.1605	9.60	0.1603	0.1611	9.60	0.1567	0.1573	9.60	0.1536	0.1542
10.20	0.1503	0.1509	35.10	0.1600	0.1605	10.20	0.1553	0.1562	10.20	0.1495	0.1501	10.20	0.1552	0.1558
10.80	0.1523	0.1529	35.40	0.1600	0.1604	10.80	0.1592	0.1600	10.80	0.1534	0.1541	10.80	0.1480	0.1487
11.40	0.1610	0.1616	35.70	0.1598	0.1602	11.40	0.1696	0.1701	11.40	0.1611	0.1618	11.40	0.1591	0.1597
12.00	0.1521	0.1527	36.00	0.1598	0.1603	12.00	0.1529	0.1534	12.00	0.1509	0.1516	12.00	0.1541	0.1548
12.60	0.1556	0.1563	36.30	0.1590	0.1594	12.60	0.1543	0.1550	12.60	0.1562	0.1568	12.60	0.1531	0.1538
13.20	0.1490	0.1494	36.60	0.1590	0.1594	13.20	0.1640	0.1643	13.20	0.1516	0.1519	13.20	0.1519	0.1522
13.80	0.1585	0.1590	36.90	0.1604	0.1609	13.80	0.1682	0.1686	13.80	0.1576	0.1580	13.80	0.1564	0.1568
14.40	0.1568	0.1574	37.20	0.1605	0.1610	14.40	0.1643	0.1651	14.40	0.1596	0.1601	14.40	0.1561	0.1568
15.00	0.1644	0.1650	37.50	0.1592	0.1596	15.00	0.1672	0.1680	15.00	0.1643	0.1648	15.00	0.1646	0.1651
15.60	0.1548	0.1553	37.80	0.1591	0.1595	15.60	0.1498	0.1504	15.60	0.1565	0.1571	15.60	0.1564	0.1569
16.20	0.1550	0.1556	38.10	0.1595	0.1600	16.20	0.1682	0.1688	16.20	0.1545	0.1551	16.20	0.1542	0.1548
16.80	0.1593	0.1600	38.40	0.1596	0.1600	16.80	0.1632	0.1639	16.80	0.1581	0.1588	16.80	0.1572	0.1579
17.40	0.1601	0.1606	38.70	0.1593	0.1597	17.40	0.1570	0.1576	17.40	0.1603	0.1608	17.40	0.1616	0.1621
18.00	0.1549	0.1556	39.00	0.1589	0.1593	18.00	0.1546	0.1552	18.00	0.1577	0.1584	18.00	0.1569	0.1575
18.60	0.1558	0.1563	39.30	0.1593	0.1597	18.60	0.1622	0.1625	18.60	0.1559	0.1563	18.60	0.1556	0.1561
19.20	0.1520	0.1525	39.60	0.1600	0.1604	19.20	0.1618	0.1623	19.20	0.1528	0.1534	19.20	0.1539	0.1544
19.80	0.1610	0.1614	39.90	0.1590	0.1595	19.80	0.1667	0.1671	19.80	0.1617	0.1621	19.80	0.1602	0.1606
20.40	0.1608	0.1613	40.20	0.1591	0.1595	20.40	0.1587	0.1592	20.40	0.1631	0.1635	20.40	0.1630	0.1635
21.00	0.1536	0.1541	40.50	0.1599	0.1604	21.00	0.1585	0.1590	21.00	0.1559	0.1564	21.00	0.1546	0.1552
21.60	0.1594	0.1599	40.80	0.1599	0.1603	21.60	0.1619	0.1625	21.60	0.1596	0.1602	21.60	0.1572	0.1578
22.20	0.1616	0.1619	41.10	0.1586	0.1591	22.20	0.1644	0.1648	22.20	0.1617	0.1620	22.20	0.1633	0.1636
22.80	0.1553	0.1558	41.40	0.1589	0.1594	22.80	0.1565	0.1569	22.80	0.1564	0.1568	22.80	0.1547	0.1552
23.40	0.1605	0.1610	41.70	0.1597	0.1601	23.40	0.1566	0.1570	23.40	0.1618	0.1622	23.40	0.1609	0.1615

24.00	0.1550	0.1554	42.00	0.1593	0.1597	24.00	0.1586	0.1590	24.00	0.1583	0.1588	24.00	0.1569	0.1574
24.60	0.1539	0.1543	42.30	0.1592	0.1596	24.60	0.1601	0.1603	24.60	0.1555	0.1558	24.60	0.1559	0.1563
25.20	0.1589	0.1593	42.60	0.1592	0.1597	25.20	0.1616	0.1619	25.20	0.1599	0.1603	25.20	0.1595	0.1599
25.80	0.1602	0.1606	42.90	0.1598	0.1602	25.80	0.1615	0.1618	25.80	0.1619	0.1622	25.80	0.1609	0.1612
26.40	0.1551	0.1554	43.20	0.1597	0.1602	26.40	0.1565	0.1569	26.40	0.1595	0.1598	26.40	0.1583	0.1586
27.00	0.1568	0.1572	43.50	0.1590	0.1594	27.00	0.1621	0.1624	27.00	0.1586	0.1590	27.00	0.1556	0.1560
27.60	0.1590	0.1593	43.80	0.1588	0.1592	27.60	0.1602	0.1605	27.60	0.1585	0.1588	27.60	0.1574	0.1578
28.20	0.1611	0.1614	44.10	0.1600	0.1605	28.20	0.1616	0.1621	28.20	0.1620	0.1624	28.20	0.1611	0.1615
28.80	0.1576	0.1580	44.40	0.1596	0.1600	28.80	0.1574	0.1579	28.80	0.1600	0.1604	28.80	0.1583	0.1586
29.40	0.1569	0.1573	44.70	0.1588	0.1592	29.40	0.1577	0.1581	29.40	0.1599	0.1603	29.40	0.1575	0.1578
30.00	0.1559	0.1563	45.00	0.1588	0.1592	30.00	0.1580	0.1584	30.00	0.1574	0.1578	30.00	0.1558	0.1562
30.60	0.1574	0.1578	45.30	0.1594	0.1598	30.60	0.1634	0.1639	30.60	0.1586	0.1590	30.60	0.1572	0.1576
31.20	0.1599	0.1602	45.60	0.1600	0.1604	31.20	0.1581	0.1585	31.20	0.1604	0.1607	31.20	0.1599	0.1602
31.80	0.1542	0.1547	45.90	0.1596	0.1601	31.80	0.1594	0.1598	31.80	0.1589	0.1593	31.80	0.1573	0.1576
32.40	0.1594	0.1599	46.20	0.1594	0.1598	32.40	0.1573	0.1578	32.40	0.1605	0.1609	32.40	0.1599	0.1604
33.00	0.1569	0.1573	46.50	0.1598	0.1602	33.00	0.1629	0.1633	33.00	0.1587	0.1591	33.00	0.1590	0.1594
33.60	0.1587	0.1591	46.80	0.1597	0.1601	33.60	0.1600	0.1604	33.60	0.1604	0.1608	33.60	0.1593	0.1597
34.20	0.1584	0.1589	47.10	0.1585	0.1589	34.20	0.1596	0.1601	34.20	0.1609	0.1614	34.20	0.1591	0.1596
34.80	0.1574	0.1579	47.40	0.1594	0.1598	34.80	0.1574	0.1578	34.80	0.1590	0.1595	34.80	0.1588	0.1592
35.40	0.1558	0.1562	47.70	0.1601	0.1605	35.40	0.1593	0.1597	35.40	0.1572	0.1577	35.40	0.1567	0.1571
36.00	0.1601	0.1606	48.00	0.1594	0.1598	36.00	0.1605	0.1609	36.00	0.1602	0.1607	36.00	0.1605	0.1609
36.60	0.1558	0.1563	48.30	0.1595	0.1599	36.60	0.1602	0.1606	36.60	0.1588	0.1592	36.60	0.1572	0.1576
37.20	0.1587	0.1592	48.60	0.1601	0.1605	37.20	0.1570	0.1575	37.20	0.1590	0.1594	37.20	0.1590	0.1595
37.80	0.1566	0.1570	48.90	0.1603	0.1607	37.80	0.1605	0.1609	37.80	0.1590	0.1595	37.80	0.1583	0.1587
38.40	0.1584	0.1588	49.20	0.1596	0.1600	38.40	0.1597	0.1600	38.40	0.1594	0.1598	38.40	0.1590	0.1594
39.00	0.1579	0.1584	49.50	0.1593	0.1597	39.00	0.1596	0.1600	39.00	0.1578	0.1583	39.00	0.1575	0.1580

39.60	0.1600	0.1605	49.80	0.1591	0.1595	39.60	0.1602	0.1607	39.60	0.1606	0.1610	39.60	0.1596	0.1601
40.20	0.1569	0.1574	50.10	0.1594	0.1599	40.20	0.1588	0.1593	40.20	0.1593	0.1597	40.20	0.1591	0.1596
40.80	0.1580	0.1584	50.40	0.1595	0.1600	40.80	0.1584	0.1588	40.80	0.1588	0.1592	40.80	0.1589	0.1594
41.40	0.1574	0.1578	50.70	0.1595	0.1600	41.40	0.1600	0.1604	41.40	0.1584	0.1589	41.40	0.1573	0.1578
42.00	0.1608	0.1612	51.00	0.1594	0.1598	42.00	0.1597	0.1601	42.00	0.1605	0.1609	42.00	0.1598	0.1602
42.60	0.1548	0.1553	51.30	0.1602	0.1606	42.60	0.1594	0.1598	42.60	0.1586	0.1590	42.60	0.1575	0.1579
43.20	0.1577	0.1582	51.60	0.1595	0.1599	43.20	0.1595	0.1600	43.20	0.1577	0.1581	43.20	0.1582	0.1587
43.80	0.1601	0.1605	51.90	0.1592	0.1596	43.80	0.1591	0.1595	43.80	0.1601	0.1606	43.80	0.1606	0.1611
44.40	0.1567	0.1571	52.20	0.1594	0.1598	44.40	0.1598	0.1603	44.40	0.1588	0.1592	44.40	0.1585	0.1589
45.00	0.1588	0.1593	52.50	0.1598	0.1603	45.00	0.1607	0.1611	45.00	0.1595	0.1599	45.00	0.1585	0.1589
45.60	0.1580	0.1585	52.80	0.1594	0.1598	45.60	0.1595	0.1600	45.60	0.1592	0.1596	45.60	0.1598	0.1603
46.20	0.1575	0.1580	53.10	0.1591	0.1595	46.20	0.1574	0.1579	46.20	0.1585	0.1590	46.20	0.1597	0.1601
46.80	0.1584	0.1588	53.40	0.1592	0.1596	46.80	0.1606	0.1611	46.80	0.1588	0.1593	46.80	0.1590	0.1594
47.40	0.1579	0.1583	53.70	0.1601	0.1605	47.40	0.1592	0.1596	47.40	0.1590	0.1594	47.40	0.1601	0.1605
48.00	0.1580	0.1585	54.00	0.1597	0.1601	48.00	0.1593	0.1597	48.00	0.1587	0.1591	48.00	0.1588	0.1593
48.60	0.1581	0.1586	54.30	0.1595	0.1600	48.60	0.1592	0.1597	48.60	0.1595	0.1600	48.60	0.1595	0.1600
49.20	0.1573	0.1577	54.60	0.1599	0.1604	49.20	0.1603	0.1607	49.20	0.1583	0.1587	49.20	0.1592	0.1596
49.80	0.1596	0.1600	54.90	0.1598	0.1602	49.80	0.1591	0.1595	49.80	0.1594	0.1598	49.80	0.1586	0.1590
50.40	0.1574	0.1579	55.20	0.1592	0.1596	50.40	0.1607	0.1611	50.40	0.1594	0.1599	50.40	0.1586	0.1590
51.00	0.1582	0.1586	55.50	0.1594	0.1598	51.00	0.1591	0.1596	51.00	0.1580	0.1585	51.00	0.1587	0.1591
51.60	0.1596	0.1600	55.80	0.1597	0.1601	51.60	0.1598	0.1603	51.60	0.1594	0.1598	51.60	0.1611	0.1615
52.20	0.1571	0.1575	56.10	0.1596	0.1601	52.20	0.1587	0.1591	52.20	0.1604	0.1608	52.20	0.1600	0.1605
52.80	0.1575	0.1580	56.40	0.1593	0.1598	52.80	0.1605	0.1609	52.80	0.1574	0.1579	52.80	0.1576	0.1581
53.40	0.1592	0.1597	56.70	0.1589	0.1593	53.40	0.1583	0.1587	53.40	0.1591	0.1596	53.40	0.1592	0.1596
54.00	0.1567	0.1571	57.00	0.1589	0.1594	54.00	0.1601	0.1605	54.00	0.1587	0.1591	54.00	0.1601	0.1606
54.60	0.1593	0.1598	57.30	0.1598	0.1602	54.60	0.1590	0.1594	54.60	0.1595	0.1599	54.60	0.1604	0.1609

55.20	0.1562	0.1567	57.60	0.1596	0.1600	55.20	0.1594	0.1598	55.20	0.1586	0.1590	55.20	0.1579	0.1584
55.80	0.1592	0.1597	57.90	0.1589	0.1594	55.80	0.1599	0.1603	55.80	0.1597	0.1601	55.80	0.1590	0.1595
56.40	0.1577	0.1581	58.20	0.1589	0.1593	56.40	0.1607	0.1611	56.40	0.1588	0.1592	56.40	0.1597	0.1602
57.00	0.1581	0.1586	58.50	0.1591	0.1595	57.00	0.1579	0.1583	57.00	0.1587	0.1592	57.00	0.1592	0.1596
57.60	0.1583	0.1587	58.80	0.1586	0.1590	57.60	0.1601	0.1605	57.60	0.1592	0.1596	57.60	0.1592	0.1597
58.20	0.1586	0.1590	59.10	0.1586	0.1591	58.20	0.1592	0.1596	58.20	0.1602	0.1606	58.20	0.1597	0.1601
58.80	0.1565	0.1569	59.40	0.1596	0.1601	58.80	0.1607	0.1611	58.80	0.1575	0.1579	58.80	0.1577	0.1581
59.40	0.1598	0.1603	59.70	0.1595	0.1600	59.40	0.1577	0.1581	59.40	0.1589	0.1594	59.40	0.1603	0.1608
60.00	0.1574	0.1578	60.00	0.1592	0.1596	60.00	0.1600	0.1604	60.00	0.1594	0.1599	60.00	0.1609	0.1613

Time series plots and data summary for the α=16°: θ=30° arced labyrinth weir.

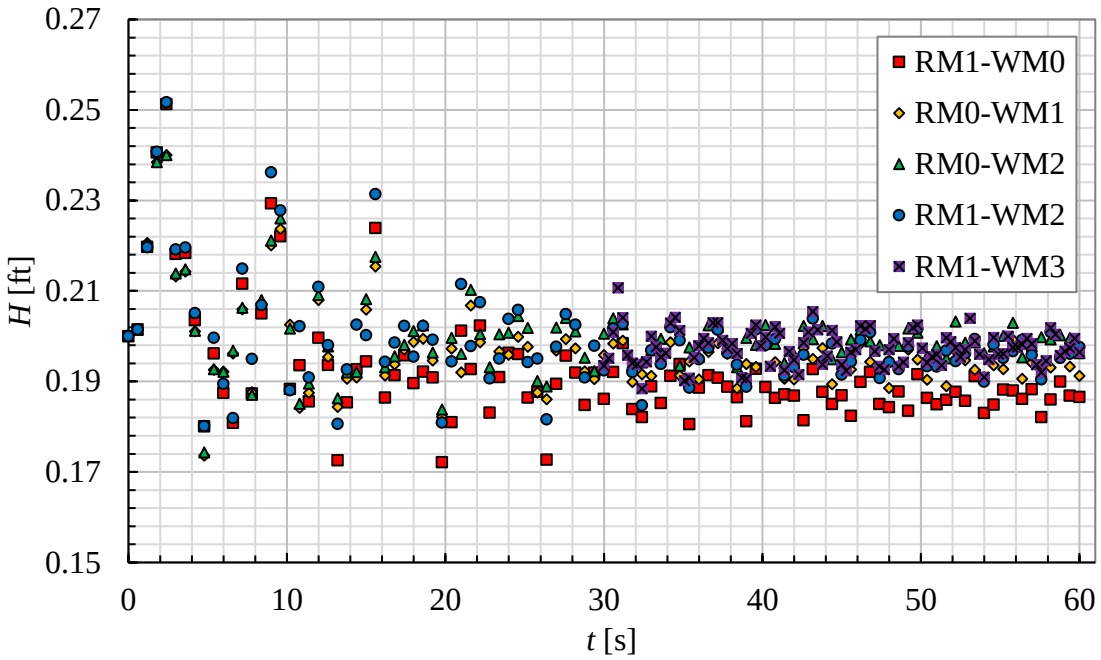

Fig. C7 Numerical H vs t for the α=16°: θ=30° arced labyrinth weir at H/P=0.3 for each mesh configuration tested.

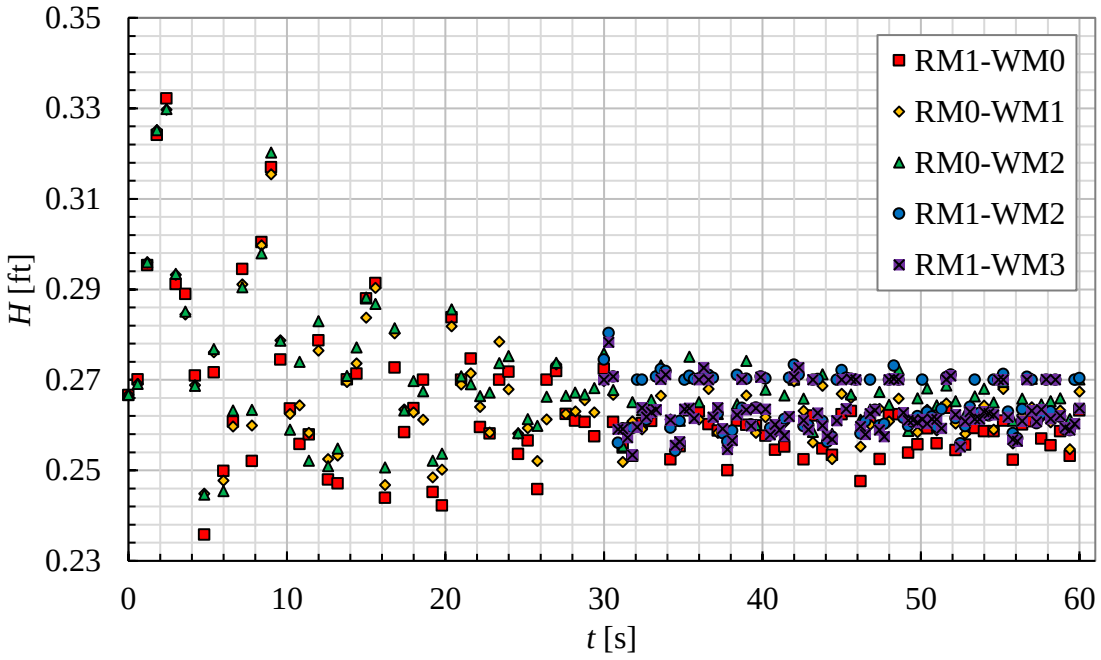

Fig. C8 Numerical H vs t for the α=16°: θ=30° arced labyrinth weir at H/P=0.4 for each mesh configuration tested.

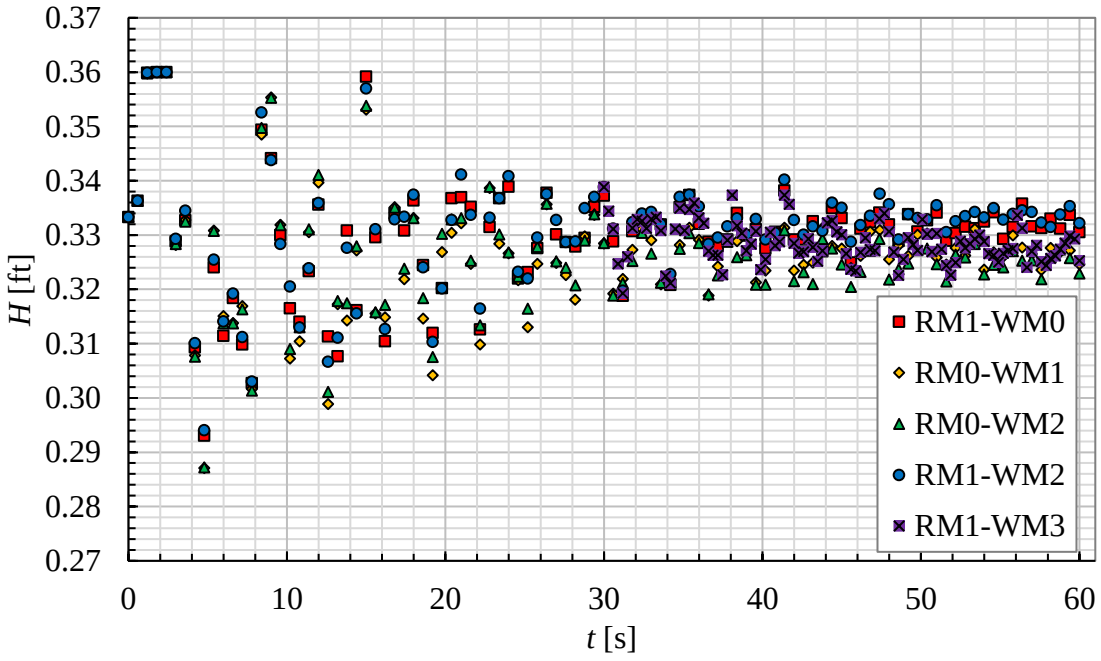

Fig. C9 Numerical H vs t for the α=16°: θ=30° arced labyrinth weir at H/P=0.5 for each mesh configuration tested.

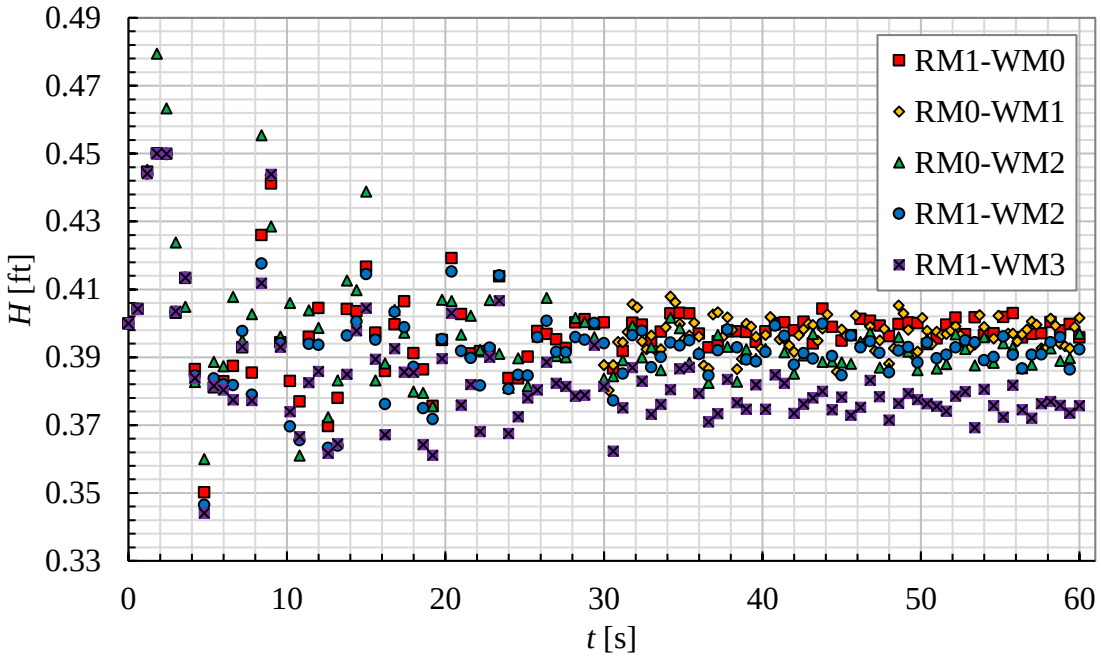

Fig. C10 Numerical H vs t for the α=16°: θ=30° arced labyrinth weir at H/P=0.6 for each mesh configuration tested.

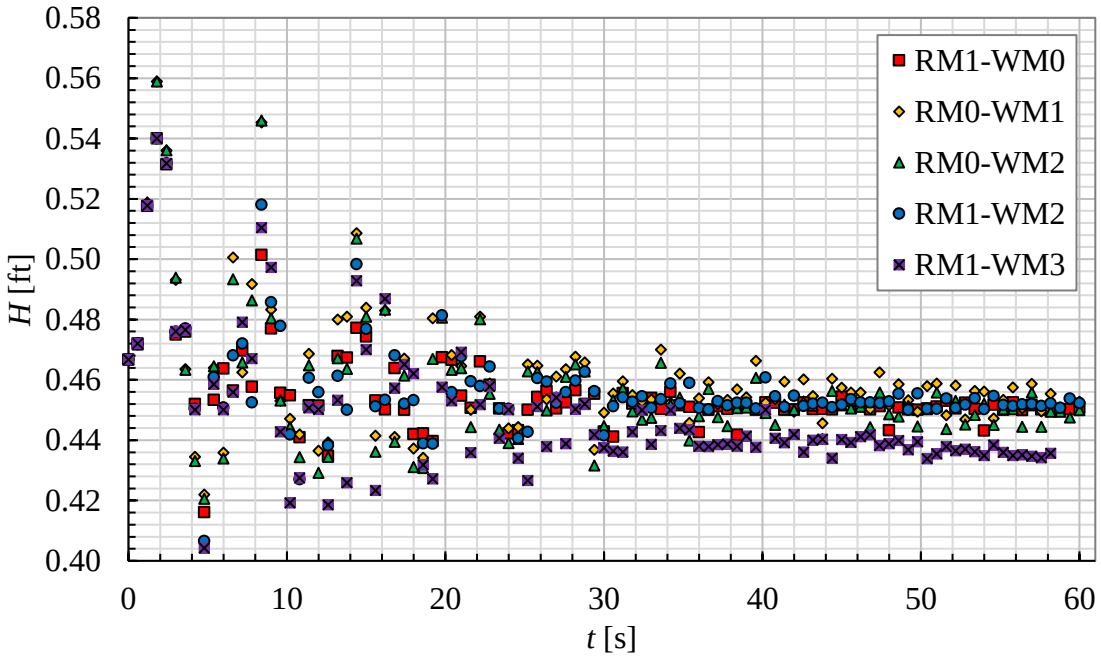

Fig. C11 Numerical H vs t for the α=16°: θ=30° arced labyrinth weir at H/P=0.7 for each mesh configuration tested.

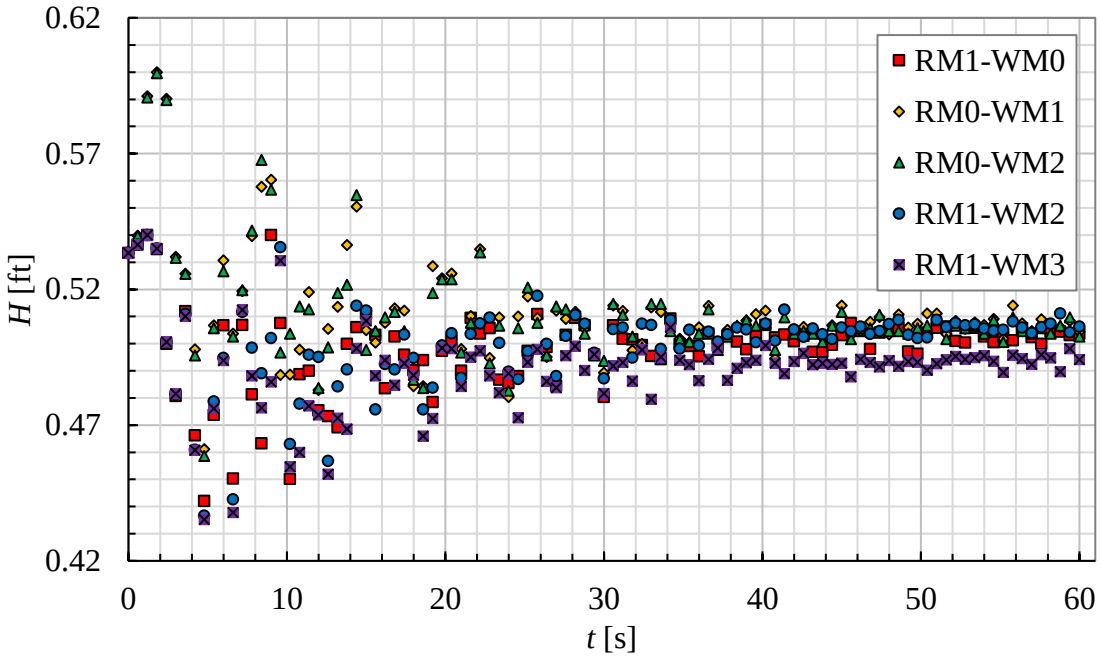

Fig. C12 Numerical H vs t for the α=16°: θ=30° arced labyrinth weir at H/P=0.8 for each mesh configuration tested.

Table C7 Tabulated time series data for the α=16°: θ=30° arced labyrinth weir at H/P=0.3

RM1-WM0			RM0-WM1			RM0-WM2			RM1-WM2			RM1-WM3		
Cell Count:	1375051		*Cell Count:*	1350940		*Cell Count:*	2764732		*Cell Count:*	3062452		*Cell Count:*	6292639	
Q	95.68	[L/s]	*Q*	96.46	[L/s]	*Q*	96.46	[L/s]	*Q*	95.68	[L/s]	*Q*	95.68	[L/s]
H	0.057	[m]	*H*	0.059	[m]	*H*	0.061	[m]	*H*	0.060	[m]	*H*	0.060	[m]
H/P	0.280	[-]	*H/P*	0.290	[-]	*H/P*	0.298	[-]	*H/P*	0.294	[-]	*H/P*	0.296	[-]
C_d	0.763	[-]	C_d	0.731	[-]	C_d	0.702	[-]	C_d	0.711	[-]	C_d	0.704	[-]
$C_{d\text{-}emp}$	0.711	[-]	$C_{d\text{-}emp}$	0.705	[-]	$C_{d\text{-}emp}$	0.700	[-]	$C_{d\text{-}emp}$	0.703	[-]	$C_{d\text{-}emp}$	0.702	[-]
ε_{Cd}	7.44%	[%]	ε_{Cd}	3.62%	[%]	ε_{Cd}	0.20%	[%]	ε_{Cd}	1.14%	[%]	ε_{Cd}	0.28%	[%]
Time [s]	*h* [m]	*H* [m]	Time [s]	*h* [m]	*H* [m]	Time [s]	*h* [m]	*H* [m]	Time [s]	*h* [m]	*H* [m]	Time [s]	*h* [m]	*H* [m]
0.00	0.0610	0.0610	0.00	0.0610	0.0610	0.00	0.0610	0.0610	0.00	0.0610	0.0610	30.00	0.0590	0.0591
0.60	0.0614	0.0614	0.60	0.0614	0.0614	0.60	0.0614	0.0614	0.60	0.0614	0.0614	30.30	0.0595	0.0596
1.20	0.0670	0.0670	1.20	0.0672	0.0673	1.20	0.0672	0.0673	1.20	0.0670	0.0670	30.60	0.0612	0.0614
1.80	0.0733	0.0734	1.80	0.0727	0.0727	1.80	0.0727	0.0727	1.80	0.0734	0.0734	30.90	0.0642	0.0644
2.40	0.0766	0.0767	2.40	0.0732	0.0732	2.40	0.0732	0.0732	2.40	0.0767	0.0768	31.20	0.0622	0.0624
3.00	0.0665	0.0669	3.00	0.0650	0.0653	3.00	0.0652	0.0655	3.00	0.0668	0.0672	31.50	0.0597	0.0599
3.60	0.0666	0.0669	3.60	0.0653	0.0656	3.60	0.0655	0.0657	3.60	0.0669	0.0672	31.80	0.0591	0.0593
4.20	0.0620	0.0624	4.20	0.0613	0.0617	4.20	0.0613	0.0617	4.20	0.0625	0.0628	32.10	0.0591	0.0592
4.80	0.0549	0.0552	4.80	0.0529	0.0533	4.80	0.0531	0.0535	4.80	0.0549	0.0552	32.40	0.0574	0.0575
5.40	0.0598	0.0599	5.40	0.0587	0.0588	5.40	0.0587	0.0588	5.40	0.0608	0.0610	32.70	0.0592	0.0594
6.00	0.0571	0.0572	6.00	0.0586	0.0586	6.00	0.0586	0.0586	6.00	0.0578	0.0578	33.00	0.0610	0.0611
6.60	0.0551	0.0552	6.60	0.0598	0.0599	6.60	0.0600	0.0600	6.60	0.0554	0.0555	33.30	0.0602	0.0604
7.20	0.0645	0.0645	7.20	0.0628	0.0628	7.20	0.0629	0.0629	7.20	0.0655	0.0655	33.60	0.0596	0.0597
7.80	0.0571	0.0571	7.80	0.0572	0.0572	7.80	0.0570	0.0570	7.80	0.0594	0.0594	33.90	0.0598	0.0599
8.40	0.0625	0.0626	8.40	0.0632	0.0632	8.40	0.0634	0.0635	8.40	0.0630	0.0632	34.20	0.0618	0.0620

9.00	0.0699	0.0701	9.00	0.0671	0.0672	9.00	0.0674	0.0676	9.00	0.0720	0.0721	34.50	0.0622	0.0624
9.60	0.0677	0.0680	9.60	0.0682	0.0684	9.60	0.0689	0.0691	9.60	0.0694	0.0697	34.80	0.0613	0.0614
10.20	0.0574	0.0575	10.20	0.0617	0.0619	10.20	0.0615	0.0616	10.20	0.0573	0.0575	35.10	0.0580	0.0581
10.80	0.0590	0.0593	10.80	0.0561	0.0563	10.80	0.0564	0.0566	10.80	0.0616	0.0619	35.40	0.0581	0.0583
11.40	0.0566	0.0567	11.40	0.0571	0.0573	11.40	0.0578	0.0580	11.40	0.0582	0.0583	35.70	0.0595	0.0596
12.00	0.0608	0.0610	12.00	0.0634	0.0636	12.00	0.0637	0.0639	12.00	0.0643	0.0644	36.00	0.0603	0.0604
12.60	0.0590	0.0592	12.60	0.0595	0.0597	12.60	0.0603	0.0604	12.60	0.0603	0.0605	36.30	0.0608	0.0609
13.20	0.0526	0.0527	13.20	0.0562	0.0563	13.20	0.0568	0.0569	13.20	0.0550	0.0552	36.60	0.0605	0.0606
13.80	0.0565	0.0566	13.80	0.0581	0.0582	13.80	0.0585	0.0586	13.80	0.0587	0.0588	36.90	0.0619	0.0620
14.40	0.0587	0.0588	14.40	0.0582	0.0583	14.40	0.0585	0.0586	14.40	0.0617	0.0618	37.20	0.0619	0.0620
15.00	0.0593	0.0593	15.00	0.0627	0.0628	15.00	0.0635	0.0635	15.00	0.0610	0.0611	37.50	0.0607	0.0608
15.60	0.0682	0.0684	15.60	0.0657	0.0658	15.60	0.0663	0.0665	15.60	0.0705	0.0707	37.80	0.0601	0.0602
16.20	0.0568	0.0571	16.20	0.0583	0.0585	16.20	0.0589	0.0590	16.20	0.0592	0.0595	38.10	0.0605	0.0606
16.80	0.0583	0.0585	16.80	0.0591	0.0593	16.80	0.0596	0.0598	16.80	0.0605	0.0607	38.40	0.0598	0.0599
17.40	0.0597	0.0599	17.40	0.0601	0.0602	17.40	0.0604	0.0605	17.40	0.0616	0.0618	38.70	0.0581	0.0583
18.00	0.0578	0.0579	18.00	0.0606	0.0607	18.00	0.0613	0.0614	18.00	0.0596	0.0597	39.00	0.0581	0.0582
18.60	0.0586	0.0588	18.60	0.0608	0.0610	18.60	0.0617	0.0619	18.60	0.0617	0.0618	39.30	0.0612	0.0612
19.20	0.0582	0.0583	19.20	0.0593	0.0595	19.20	0.0599	0.0601	19.20	0.0607	0.0609	39.60	0.0617	0.0618
19.80	0.0525	0.0526	19.80	0.0555	0.0557	19.80	0.0560	0.0562	19.80	0.0551	0.0552	39.90	0.0603	0.0604
20.40	0.0552	0.0553	20.40	0.0601	0.0602	20.40	0.0608	0.0609	20.40	0.0593	0.0593	40.20	0.0609	0.0610
21.00	0.0613	0.0614	21.00	0.0585	0.0586	21.00	0.0598	0.0599	21.00	0.0645	0.0646	40.50	0.0589	0.0590
21.60	0.0587	0.0588	21.60	0.0630	0.0631	21.60	0.0641	0.0642	21.60	0.0603	0.0604	40.80	0.0616	0.0617
22.20	0.0617	0.0618	22.20	0.0606	0.0607	22.20	0.0611	0.0612	22.20	0.0632	0.0633	41.10	0.0611	0.0613
22.80	0.0558	0.0559	22.80	0.0582	0.0583	22.80	0.0589	0.0590	22.80	0.0581	0.0583	41.40	0.0587	0.0588
23.40	0.0582	0.0584	23.40	0.0599	0.0601	23.40	0.0611	0.0613	23.40	0.0595	0.0596	41.70	0.0599	0.0600
24.00	0.0598	0.0600	24.00	0.0597	0.0599	24.00	0.0612	0.0613	24.00	0.0621	0.0623	42.00	0.0594	0.0594

24.60	0.0598	0.0599	24.60	0.0609	0.0611	24.60	0.0623	0.0625	24.60	0.0627	0.0629	42.30	0.0584	0.0584
25.20	0.0568	0.0570	25.20	0.0602	0.0604	25.20	0.0615	0.0616	25.20	0.0592	0.0593	42.60	0.0605	0.0606
25.80	0.0572	0.0573	25.80	0.0572	0.0573	25.80	0.0579	0.0581	25.80	0.0594	0.0596	42.90	0.0612	0.0613
26.40	0.0526	0.0528	26.40	0.0567	0.0569	26.40	0.0576	0.0577	26.40	0.0554	0.0555	43.20	0.0626	0.0627
27.00	0.0577	0.0578	27.00	0.0600	0.0601	27.00	0.0615	0.0616	27.00	0.0602	0.0603	43.50	0.0614	0.0615
27.60	0.0596	0.0597	27.60	0.0608	0.0609	27.60	0.0622	0.0623	27.60	0.0624	0.0625	43.80	0.0591	0.0591
28.20	0.0585	0.0586	28.20	0.0601	0.0603	28.20	0.0613	0.0614	28.20	0.0617	0.0619	44.10	0.0596	0.0597
28.80	0.0563	0.0564	28.80	0.0586	0.0587	28.80	0.0595	0.0597	28.80	0.0582	0.0583	44.40	0.0613	0.0614
29.40	0.0585	0.0586	29.40	0.0581	0.0582	29.40	0.0586	0.0587	29.40	0.0603	0.0604	44.70	0.0606	0.0607
30.00	0.0567	0.0568	30.00	0.0597	0.0598	30.00	0.0611	0.0612	30.00	0.0587	0.0588	45.00	0.0590	0.0591
30.60	0.0585	0.0587	30.60	0.0605	0.0606	30.60	0.0622	0.0623	30.60	0.0615	0.0616	45.30	0.0586	0.0587
31.20	0.0605	0.0607	31.20	0.0606	0.0608	31.20	0.0618	0.0619	31.20	0.0618	0.0620	45.60	0.0599	0.0600
31.80	0.0560	0.0562	31.80	0.0579	0.0580	31.80	0.0591	0.0592	31.80	0.0585	0.0587	45.90	0.0600	0.0601
32.40	0.0555	0.0556	32.40	0.0584	0.0585	32.40	0.0592	0.0593	32.40	0.0563	0.0564	46.20	0.0616	0.0617
33.00	0.0576	0.0577	33.00	0.0583	0.0584	33.00	0.0600	0.0601	33.00	0.0600	0.0601	46.50	0.0615	0.0615
33.60	0.0564	0.0566	33.60	0.0595	0.0596	33.60	0.0608	0.0609	33.60	0.0591	0.0592	46.80	0.0617	0.0617
34.20	0.0583	0.0584	34.20	0.0606	0.0607	34.20	0.0621	0.0622	34.20	0.0616	0.0617	47.10	0.0599	0.0600
34.80	0.0591	0.0592	34.80	0.0583	0.0584	34.80	0.0590	0.0591	34.80	0.0607	0.0608	47.40	0.0589	0.0590
35.40	0.0550	0.0552	35.40	0.0593	0.0594	35.40	0.0602	0.0603	35.40	0.0575	0.0576	47.70	0.0587	0.0588
36.00	0.0575	0.0576	36.00	0.0580	0.0581	36.00	0.0596	0.0597	36.00	0.0594	0.0595	48.00	0.0601	0.0601
36.60	0.0583	0.0584	36.60	0.0599	0.0600	36.60	0.0617	0.0618	36.60	0.0602	0.0603	48.30	0.0608	0.0609
37.20	0.0582	0.0583	37.20	0.0605	0.0606	37.20	0.0616	0.0617	37.20	0.0614	0.0615	48.60	0.0589	0.0590
37.80	0.0576	0.0577	37.80	0.0598	0.0599	37.80	0.0605	0.0606	37.80	0.0598	0.0600	48.90	0.0592	0.0593
38.40	0.0568	0.0570	38.40	0.0575	0.0576	38.40	0.0589	0.0590	38.40	0.0590	0.0592	49.20	0.0605	0.0606
39.00	0.0552	0.0554	39.00	0.0591	0.0592	39.00	0.0608	0.0610	39.00	0.0576	0.0577	49.50	0.0615	0.0616
39.60	0.0587	0.0588	39.60	0.0589	0.0590	39.60	0.0604	0.0605	39.60	0.0614	0.0615	49.80	0.0617	0.0618

40.20	0.0575	0.0576	40.20	0.0603	0.0604	40.20	0.0617	0.0618	40.20	0.0604	0.0604	50.10	0.0602	0.0602
40.80	0.0568	0.0569	40.80	0.0592	0.0593	40.80	0.0604	0.0605	40.80	0.0608	0.0609	50.40	0.0592	0.0592
41.40	0.0570	0.0572	41.40	0.0581	0.0582	41.40	0.0592	0.0593	41.40	0.0583	0.0584	50.70	0.0596	0.0597
42.00	0.0570	0.0571	42.00	0.0580	0.0582	42.00	0.0597	0.0598	42.00	0.0589	0.0590	51.00	0.0597	0.0598
42.60	0.0553	0.0554	42.60	0.0602	0.0602	42.60	0.0616	0.0617	42.60	0.0597	0.0598	51.30	0.0590	0.0591
43.20	0.0587	0.0588	43.20	0.0594	0.0595	43.20	0.0608	0.0609	43.20	0.0622	0.0622	51.60	0.0608	0.0609
43.80	0.0572	0.0573	43.80	0.0602	0.0603	43.80	0.0617	0.0618	43.80	0.0592	0.0593	51.90	0.0606	0.0607
44.40	0.0564	0.0565	44.40	0.0577	0.0578	44.40	0.0594	0.0595	44.40	0.0605	0.0606	52.20	0.0602	0.0603
45.00	0.0570	0.0570	45.00	0.0584	0.0585	45.00	0.0599	0.0600	45.00	0.0584	0.0585	52.50	0.0596	0.0596
45.60	0.0556	0.0557	45.60	0.0587	0.0588	45.60	0.0608	0.0608	45.60	0.0592	0.0593	52.80	0.0601	0.0601
46.20	0.0579	0.0580	46.20	0.0605	0.0605	46.20	0.0614	0.0615	46.20	0.0607	0.0608	53.10	0.0622	0.0622
46.80	0.0585	0.0586	46.80	0.0592	0.0593	46.80	0.0606	0.0607	46.80	0.0612	0.0613	53.40	0.0606	0.0607
47.40	0.0564	0.0565	47.40	0.0587	0.0588	47.40	0.0604	0.0604	47.40	0.0581	0.0582	53.70	0.0597	0.0598
48.00	0.0562	0.0562	48.00	0.0575	0.0575	48.00	0.0594	0.0594	48.00	0.0592	0.0593	54.00	0.0582	0.0583
48.60	0.0572	0.0573	48.60	0.0588	0.0589	48.60	0.0603	0.0604	48.60	0.0587	0.0588	54.30	0.0594	0.0595
49.20	0.0559	0.0560	49.20	0.0601	0.0601	49.20	0.0615	0.0616	49.20	0.0603	0.0603	54.60	0.0609	0.0609
49.80	0.0584	0.0585	49.80	0.0594	0.0595	49.80	0.0612	0.0613	49.80	0.0614	0.0615	54.90	0.0597	0.0598
50.40	0.0568	0.0569	50.40	0.0580	0.0581	50.40	0.0596	0.0597	50.40	0.0589	0.0590	55.20	0.0598	0.0598
51.00	0.0564	0.0564	51.00	0.0590	0.0591	51.00	0.0603	0.0604	51.00	0.0589	0.0590	55.50	0.0610	0.0610
51.60	0.0567	0.0568	51.60	0.0576	0.0577	51.60	0.0595	0.0595	51.60	0.0600	0.0601	55.80	0.0602	0.0603
52.20	0.0572	0.0573	52.20	0.0600	0.0600	52.20	0.0619	0.0620	52.20	0.0593	0.0593	56.10	0.0602	0.0603
52.80	0.0566	0.0567	52.80	0.0593	0.0594	52.80	0.0605	0.0606	52.80	0.0598	0.0599	56.40	0.0604	0.0605
53.40	0.0583	0.0583	53.40	0.0587	0.0588	53.40	0.0606	0.0606	53.40	0.0608	0.0608	56.70	0.0608	0.0609
54.00	0.0558	0.0559	54.00	0.0582	0.0583	54.00	0.0598	0.0599	54.00	0.0579	0.0580	57.00	0.0604	0.0605
54.60	0.0563	0.0564	54.60	0.0590	0.0591	54.60	0.0603	0.0603	54.60	0.0604	0.0605	57.30	0.0590	0.0591
55.20	0.0574	0.0574	55.20	0.0587	0.0588	55.20	0.0610	0.0611	55.20	0.0595	0.0596	57.60	0.0585	0.0586

55.80	0.0573	0.0574	55.80	0.0607	0.0608	55.80	0.0619	0.0620	55.80	0.0600	0.0600	57.90	0.0593	0.0594
56.40	0.0567	0.0568	56.40	0.0581	0.0582	56.40	0.0595	0.0596	56.40	0.0607	0.0608	58.20	0.0615	0.0616
57.00	0.0574	0.0575	57.00	0.0592	0.0593	57.00	0.0603	0.0604	57.00	0.0597	0.0598	58.50	0.0611	0.0612
57.60	0.0555	0.0556	57.60	0.0587	0.0588	57.60	0.0609	0.0610	57.60	0.0580	0.0581	58.80	0.0597	0.0598
58.20	0.0567	0.0568	58.20	0.0589	0.0589	58.20	0.0607	0.0608	58.20	0.0612	0.0613	59.10	0.0599	0.0600
58.80	0.0579	0.0580	58.80	0.0597	0.0598	58.80	0.0610	0.0611	58.80	0.0595	0.0596	59.40	0.0602	0.0603
59.40	0.0569	0.0570	59.40	0.0589	0.0590	59.40	0.0608	0.0609	59.40	0.0598	0.0599	59.70	0.0608	0.0609
60.00	0.0569	0.0570	60.00	0.0583	0.0584	60.00	0.0598	0.0599	60.00	0.0602	0.0603	60.00	0.0599	0.0600

Table C8 Tabulated time series data for the α=16°: θ=30° arced labyrinth weir at H/P=0.4

RM1-WM0			RM0-WM1			RM0-WM2			RM1-WM2			RM1-WM3		
Cell Count:	1434429		*Cell Count:*	1428682		*Cell Count:*	2927821		*Cell Count:*	3199288		*Cell Count:*	6579263	
Q	133.24	[L/s]	Q	133.62	[L/s]	Q	133.62	[L/s]	Q	133.24	[L/s]	Q	133.24	[L/s]
H	0.079	[m]	H	0.080	[m]	H	0.081	[m]	H	0.081	[m]	H	0.080	[m]
H/P	0.387	[-]	H/P	0.393	[-]	H/P	0.399	[-]	H/P	0.397	[-]	H/P	0.395	[-]
C_d	0.654	[-]	C_d	0.642	[-]	C_d	0.628	[-]	C_d	0.629	[-]	C_d	0.635	[-]
$C_{d\text{-}emp}$	0.639	[-]	$C_{d\text{-}emp}$	0.635	[-]	$C_{d\text{-}emp}$	0.630	[-]	$C_{d\text{-}emp}$	0.631	[-]	$C_{d\text{-}emp}$	0.633	[-]
ε_{Cd}	2.46%	[%]	ε_{Cd}	1.23%	[%]	ε_{Cd}	-0.38%	[%]	ε_{Cd}	-0.29%	[%]	ε_{Cd}	0.37%	[%]
Time [s]	h [m]	H [m]	Time [s]	h [m]	H [m]	Time [s]	h [m]	H [m]	Time [s]	h [m]	H [m]	Time [s]	h [m]	H [m]
0.00	0.0813	0.0813	0.00	0.0813	0.0813	0.00	0.0813	0.0813	30.00	0.0837	0.0839	30.00	0.0823	0.0825
0.60	0.0823	0.0823	0.60	0.0820	0.0820	0.60	0.0820	0.0820	30.30	0.0854	0.0857	30.30	0.0848	0.0851
1.20	0.0900	0.0901	1.20	0.0902	0.0903	1.20	0.0902	0.0903	30.60	0.0825	0.0827	30.60	0.0825	0.0827
1.80	0.0988	0.0989	1.80	0.0991	0.0992	1.80	0.0991	0.0992	30.90	0.0781	0.0783	30.90	0.0790	0.0792
2.40	0.1012	0.1015	2.40	0.1005	0.1007	2.40	0.1005	0.1008	31.20	0.0790	0.0792	31.20	0.0790	0.0792
3.00	0.0888	0.0894	3.00	0.0894	0.0900	3.00	0.0894	0.0901	31.50	0.0790	0.0792	31.50	0.0784	0.0786
3.60	0.0881	0.0887	3.60	0.0867	0.0873	3.60	0.0869	0.0875	31.80	0.0790	0.0792	31.80	0.0772	0.0774
4.20	0.0826	0.0831	4.20	0.0819	0.0825	4.20	0.0819	0.0824	32.10	0.0823	0.0825	32.10	0.0791	0.0793
4.80	0.0719	0.0724	4.80	0.0746	0.0751	4.80	0.0746	0.0750	32.40	0.0823	0.0824	32.40	0.0804	0.0806
5.40	0.0828	0.0829	5.40	0.0842	0.0843	5.40	0.0844	0.0845	32.70	0.0796	0.0798	32.70	0.0798	0.0800
6.00	0.0762	0.0763	6.00	0.0755	0.0756	6.00	0.0748	0.0749	33.00	0.0801	0.0802	33.00	0.0801	0.0803
6.60	0.0795	0.0795	6.60	0.0792	0.0792	6.60	0.0802	0.0803	33.30	0.0825	0.0827	33.30	0.0803	0.0804
7.20	0.0898	0.0898	7.20	0.0887	0.0888	7.20	0.0885	0.0886	33.60	0.0830	0.0832	33.60	0.0823	0.0825
7.80	0.0768	0.0769	7.80	0.0792	0.0793	7.80	0.0803	0.0803	33.90	0.0829	0.0830	33.90	0.0826	0.0828
8.40	0.0916	0.0918	8.40	0.0914	0.0916	8.40	0.0908	0.0911	34.20	0.0791	0.0792	34.20	0.0796	0.0797

9.00	0.0966	0.0970	9.00	0.0961	0.0965	9.00	0.0976	0.0979	34.50	0.0775	0.0777	34.50	0.0779	0.0780
9.60	0.0837	0.0841	9.60	0.0850	0.0854	9.60	0.0849	0.0854	34.80	0.0795	0.0797	34.80	0.0781	0.0783
10.20	0.0804	0.0806	10.20	0.0800	0.0803	10.20	0.0789	0.0792	35.10	0.0823	0.0824	35.10	0.0803	0.0805
10.80	0.0780	0.0784	10.80	0.0806	0.0811	10.80	0.0835	0.0840	35.40	0.0826	0.0827	35.40	0.0804	0.0805
11.40	0.0786	0.0789	11.40	0.0787	0.0790	11.40	0.0769	0.0771	35.70	0.0824	0.0825	35.70	0.0797	0.0798
12.00	0.0850	0.0852	12.00	0.0843	0.0845	12.00	0.0862	0.0865	36.00	0.0824	0.0825	36.00	0.0823	0.0824
12.60	0.0756	0.0758	12.60	0.0770	0.0771	12.60	0.0765	0.0767	36.30	0.0825	0.0826	36.30	0.0831	0.0832
13.20	0.0753	0.0755	13.20	0.0772	0.0773	13.20	0.0777	0.0778	36.60	0.0826	0.0828	36.60	0.0823	0.0824
13.80	0.0823	0.0824	13.80	0.0822	0.0822	13.80	0.0826	0.0827	36.90	0.0824	0.0826	36.90	0.0798	0.0799
14.40	0.0827	0.0828	14.40	0.0834	0.0835	14.40	0.0845	0.0846	37.20	0.0800	0.0802	37.20	0.0804	0.0806
15.00	0.0878	0.0880	15.00	0.0865	0.0866	15.00	0.0878	0.0880	37.50	0.0787	0.0789	37.50	0.0790	0.0792
15.60	0.0888	0.0893	15.60	0.0885	0.0889	15.60	0.0874	0.0879	37.80	0.0781	0.0783	37.80	0.0776	0.0778
16.20	0.0743	0.0746	16.20	0.0752	0.0756	16.20	0.0764	0.0767	38.10	0.0789	0.0790	38.10	0.0782	0.0783
16.80	0.0831	0.0834	16.80	0.0854	0.0857	16.80	0.0858	0.0860	38.40	0.0826	0.0827	38.40	0.0799	0.0800
17.40	0.0788	0.0790	17.40	0.0803	0.0805	17.40	0.0802	0.0805	38.70	0.0804	0.0805	38.70	0.0823	0.0824
18.00	0.0804	0.0806	18.00	0.0801	0.0804	18.00	0.0822	0.0824	39.00	0.0824	0.0825	39.00	0.0803	0.0804
18.60	0.0823	0.0827	18.60	0.0796	0.0800	18.60	0.0815	0.0819	39.30	0.0793	0.0794	39.30	0.0792	0.0793
19.20	0.0747	0.0749	19.20	0.0757	0.0759	19.20	0.0768	0.0770	39.60	0.0804	0.0806	39.60	0.0804	0.0805
19.80	0.0738	0.0740	19.80	0.0762	0.0764	19.80	0.0773	0.0775	39.90	0.0825	0.0827	39.90	0.0825	0.0826
20.40	0.0865	0.0867	20.40	0.0859	0.0860	20.40	0.0870	0.0872	40.20	0.0824	0.0825	40.20	0.0803	0.0805
21.00	0.0823	0.0824	21.00	0.0820	0.0821	21.00	0.0825	0.0827	40.50	0.0791	0.0792	40.50	0.0786	0.0787
21.60	0.0837	0.0839	21.60	0.0827	0.0829	21.60	0.0820	0.0822	40.80	0.0789	0.0791	40.80	0.0793	0.0794
22.20	0.0791	0.0794	22.20	0.0805	0.0807	22.20	0.0812	0.0815	41.10	0.0792	0.0794	41.10	0.0789	0.0790
22.80	0.0787	0.0790	22.80	0.0787	0.0790	22.80	0.0814	0.0817	41.40	0.0797	0.0798	41.40	0.0785	0.0787
23.40	0.0823	0.0826	23.40	0.0849	0.0852	23.40	0.0834	0.0837	41.70	0.0824	0.0825	41.70	0.0798	0.0800
24.00	0.0828	0.0831	24.00	0.0817	0.0819	24.00	0.0839	0.0841	42.00	0.0833	0.0834	42.00	0.0825	0.0826

24.60	0.0773	0.0775	24.60	0.0787	0.0789	24.60	0.0787	0.0789	42.30	0.0827	0.0828	42.30	0.0831	0.0832
25.20	0.0782	0.0785	25.20	0.0790	0.0793	25.20	0.0796	0.0799	42.60	0.0792	0.0793	42.60	0.0796	0.0797
25.80	0.0749	0.0752	25.80	0.0768	0.0771	25.80	0.0792	0.0794	42.90	0.0793	0.0794	42.90	0.0789	0.0791
26.40	0.0823	0.0825	26.40	0.0796	0.0798	26.40	0.0812	0.0813	43.20	0.0823	0.0825	43.20	0.0823	0.0824
27.00	0.0829	0.0831	27.00	0.0833	0.0835	27.00	0.0834	0.0836	43.50	0.0823	0.0825	43.50	0.0801	0.0802
27.60	0.0800	0.0802	27.60	0.0800	0.0802	27.60	0.0812	0.0814	43.80	0.0795	0.0797	43.80	0.0792	0.0794
28.20	0.0795	0.0797	28.20	0.0802	0.0804	28.20	0.0814	0.0816	44.10	0.0781	0.0783	44.10	0.0785	0.0787
28.80	0.0795	0.0796	28.80	0.0809	0.0811	28.80	0.0813	0.0815	44.40	0.0785	0.0786	44.40	0.0783	0.0784
29.40	0.0785	0.0787	29.40	0.0801	0.0803	29.40	0.0818	0.0820	44.70	0.0823	0.0825	44.70	0.0796	0.0797
30.00	0.0830	0.0833	30.00	0.0822	0.0825	30.00	0.0841	0.0843	45.00	0.0829	0.0831	45.00	0.0823	0.0825
30.60	0.0795	0.0797	30.60	0.0813	0.0815	30.60	0.0816	0.0819	45.30	0.0824	0.0826	45.30	0.0803	0.0805
31.20	0.0777	0.0779	31.20	0.0768	0.0769	31.20	0.0778	0.0780	45.60	0.0824	0.0825	45.60	0.0824	0.0825
31.80	0.0772	0.0773	31.80	0.0795	0.0796	31.80	0.0808	0.0809	45.90	0.0823	0.0824	45.90	0.0823	0.0824
32.40	0.0794	0.0795	32.40	0.0790	0.0791	32.40	0.0803	0.0804	46.20	0.0787	0.0788	46.20	0.0792	0.0793
33.00	0.0795	0.0797	33.00	0.0804	0.0806	33.00	0.0809	0.0811	46.50	0.0795	0.0797	46.50	0.0786	0.0788
33.60	0.0825	0.0827	33.60	0.0812	0.0814	33.60	0.0833	0.0834	46.80	0.0823	0.0825	46.80	0.0800	0.0802
34.20	0.0769	0.0771	34.20	0.0796	0.0798	34.20	0.0793	0.0794	47.10	0.0803	0.0805	47.10	0.0802	0.0804
34.80	0.0778	0.0780	34.80	0.0779	0.0780	34.80	0.0795	0.0797	47.40	0.0792	0.0794	47.40	0.0789	0.0791
35.40	0.0802	0.0804	35.40	0.0824	0.0826	35.40	0.0839	0.0840	47.70	0.0793	0.0795	47.70	0.0785	0.0786
36.00	0.0802	0.0803	36.00	0.0796	0.0798	36.00	0.0808	0.0809	48.00	0.0823	0.0825	48.00	0.0823	0.0825
36.60	0.0793	0.0795	36.60	0.0817	0.0818	36.60	0.0826	0.0827	48.30	0.0832	0.0834	48.30	0.0824	0.0825
37.20	0.0789	0.0791	37.20	0.0787	0.0789	37.20	0.0800	0.0802	48.60	0.0823	0.0825	48.60	0.0823	0.0825
37.80	0.0762	0.0763	37.80	0.0777	0.0779	37.80	0.0789	0.0790	48.90	0.0797	0.0799	48.90	0.0801	0.0803
38.40	0.0795	0.0796	38.40	0.0803	0.0804	38.40	0.0807	0.0808	49.20	0.0792	0.0794	49.20	0.0796	0.0797
39.00	0.0793	0.0794	39.00	0.0813	0.0814	39.00	0.0836	0.0837	49.50	0.0795	0.0796	49.50	0.0796	0.0798
39.60	0.0792	0.0794	39.60	0.0787	0.0789	39.60	0.0793	0.0794	49.80	0.0799	0.0800	49.80	0.0794	0.0796

40.20	0.0785	0.0787	40.20	0.0798	0.0799	40.20	0.0816	0.0818	50.10	0.0823	0.0825	50.10	0.0796	0.0798
40.80	0.0776	0.0777	40.80	0.0788	0.0789	40.80	0.0790	0.0791	50.40	0.0801	0.0803	50.40	0.0793	0.0795
41.40	0.0778	0.0779	41.40	0.0794	0.0795	41.40	0.0812	0.0814	50.70	0.0798	0.0800	50.70	0.0797	0.0798
42.00	0.0823	0.0824	42.00	0.0822	0.0823	42.00	0.0829	0.0830	51.00	0.0791	0.0793	51.00	0.0796	0.0798
42.60	0.0769	0.0771	42.60	0.0802	0.0804	42.60	0.0810	0.0812	51.30	0.0803	0.0805	51.30	0.0790	0.0792
43.20	0.0799	0.0800	43.20	0.0781	0.0782	43.20	0.0788	0.0789	51.60	0.0825	0.0826	51.60	0.0823	0.0825
43.80	0.0777	0.0778	43.80	0.0819	0.0820	43.80	0.0827	0.0828	51.90	0.0826	0.0828	51.90	0.0826	0.0827
44.40	0.0772	0.0774	44.40	0.0769	0.0771	44.40	0.0787	0.0788	52.20	0.0797	0.0799	52.20	0.0799	0.0801
45.00	0.0800	0.0801	45.00	0.0814	0.0815	45.00	0.0826	0.0827	52.50	0.0780	0.0782	52.50	0.0778	0.0780
45.60	0.0802	0.0803	45.60	0.0811	0.0812	45.60	0.0813	0.0815	52.80	0.0792	0.0793	52.80	0.0795	0.0797
46.20	0.0755	0.0756	46.20	0.0778	0.0779	46.20	0.0796	0.0797	53.10	0.0805	0.0806	53.10	0.0802	0.0803
46.80	0.0797	0.0799	46.80	0.0793	0.0794	46.80	0.0803	0.0805	53.40	0.0823	0.0825	53.40	0.0797	0.0798
47.40	0.0770	0.0771	47.40	0.0803	0.0805	47.40	0.0815	0.0817	53.70	0.0801	0.0802	53.70	0.0796	0.0798
48.00	0.0800	0.0801	48.00	0.0795	0.0797	48.00	0.0806	0.0808	54.00	0.0799	0.0801	54.00	0.0802	0.0803
48.60	0.0800	0.0801	48.60	0.0810	0.0812	48.60	0.0830	0.0831	54.30	0.0799	0.0801	54.30	0.0800	0.0802
49.20	0.0774	0.0775	49.20	0.0793	0.0795	49.20	0.0789	0.0790	54.60	0.0823	0.0825	54.60	0.0799	0.0801
49.80	0.0780	0.0781	49.80	0.0788	0.0789	49.80	0.0811	0.0812	54.90	0.0823	0.0825	54.90	0.0823	0.0825
50.40	0.0790	0.0792	50.40	0.0803	0.0804	50.40	0.0817	0.0819	55.20	0.0827	0.0829	55.20	0.0823	0.0825
51.00	0.0780	0.0782	51.00	0.0789	0.0791	51.00	0.0806	0.0807	55.50	0.0802	0.0803	55.50	0.0798	0.0800
51.60	0.0804	0.0806	51.60	0.0807	0.0809	51.60	0.0819	0.0821	55.80	0.0787	0.0789	55.80	0.0783	0.0784
52.20	0.0776	0.0777	52.20	0.0793	0.0795	52.20	0.0809	0.0811	56.10	0.0784	0.0785	56.10	0.0782	0.0783
52.80	0.0779	0.0781	52.80	0.0787	0.0788	52.80	0.0799	0.0801	56.40	0.0803	0.0805	56.40	0.0795	0.0797
53.40	0.0790	0.0792	53.40	0.0801	0.0802	53.40	0.0812	0.0813	56.70	0.0825	0.0827	56.70	0.0823	0.0825
54.00	0.0788	0.0790	54.00	0.0806	0.0807	54.00	0.0817	0.0819	57.00	0.0823	0.0825	57.00	0.0802	0.0804
54.60	0.0788	0.0790	54.60	0.0789	0.0791	54.60	0.0808	0.0810	57.30	0.0794	0.0795	57.30	0.0795	0.0797
55.20	0.0795	0.0797	55.20	0.0817	0.0819	55.20	0.0822	0.0823	57.60	0.0800	0.0802	57.60	0.0803	0.0805

55.80	0.0769	0.0771	55.80	0.0780	0.0782	55.80	0.0795	0.0797	57.90	0.0823	0.0825	57.90	0.0823	0.0825
56.40	0.0793	0.0794	56.40	0.0799	0.0801	56.40	0.0810	0.0812	58.20	0.0802	0.0803	58.20	0.0797	0.0798
57.00	0.0795	0.0797	57.00	0.0805	0.0806	57.00	0.0824	0.0826	58.50	0.0823	0.0825	58.50	0.0823	0.0825
57.60	0.0783	0.0785	57.60	0.0798	0.0800	57.60	0.0806	0.0808	58.80	0.0798	0.0800	58.80	0.0799	0.0801
58.20	0.0779	0.0781	58.20	0.0794	0.0796	58.20	0.0809	0.0810	59.10	0.0790	0.0791	59.10	0.0791	0.0793
58.80	0.0788	0.0790	58.80	0.0802	0.0804	58.80	0.0811	0.0812	59.40	0.0789	0.0791	59.40	0.0789	0.0791
59.40	0.0772	0.0773	59.40	0.0776	0.0778	59.40	0.0796	0.0798	59.70	0.0823	0.0825	59.70	0.0793	0.0795
60.00	0.0802	0.0804	60.00	0.0815	0.0817	60.00	0.0823	0.0825	60.00	0.0824	0.0826	60.00	0.0804	0.0805

Table C9 Tabulated time series data for the α=16°: θ=30° arced labyrinth weir at H/P=0.5

RM1-WM0			RM0-WM1			RM0-WM2			RM1-WM2			RM1-WM3		
Cell Count:	1434429		*Cell Count:*	1428682		*Cell Count:*	2927821		*Cell Count:*	3199288		*Cell Count:*	6579263	
Q	167.66	[L/s]	Q	164.71	[L/s]	Q	164.71	[L/s]	Q	167.66	[L/s]	Q	165.35	[L/s]
H	0.101	[m]	H	0.100	[m]	H	0.099	[m]	H	0.102	[m]	H	0.100	[m]
H/P	0.498	[-]	H/P	0.491	[-]	H/P	0.487	[-]	H/P	0.500	[-]	H/P	0.491	[-]
C_d	0.565	[-]	C_d	0.567	[-]	C_d	0.573	[-]	C_d	0.561	[-]	C_d	0.568	[-]
$C_{d\text{-}emp}$	0.557	[-]	$C_{d\text{-}emp}$	0.562	[-]	$C_{d\text{-}emp}$	0.564	[-]	$C_{d\text{-}emp}$	0.555	[-]	$C_{d\text{-}emp}$	0.561	[-]
ε_{Cd}	1.54%	[%]	ε_{Cd}	0.95%	[%]	ε_{Cd}	1.54%	[%]	ε_{Cd}	1.11%	[%]	ε_{Cd}	1.21%	[%]
Time [s]	h [m]	H [m]	Time [s]	h [m]	H [m]	Time [s]	h [m]	H [m]	Time [s]	h [m]	H [m]	Time [s]	h [m]	H [m]
0.00	0.1016	0.1016	0.00	0.1016	0.1016	0.00	0.1016	0.1016	0.00	0.1016	0.1016	30.00	0.1033	0.1035
0.60	0.1025	0.1025	0.60	0.1025	0.1025	0.60	0.1025	0.1025	0.60	0.1025	0.1025	30.30	0.1019	0.1022
1.20	0.1097	0.1097	1.20	0.1096	0.1097	1.20	0.1096	0.1097	1.20	0.1097	0.1097	30.60	0.1009	0.1012
1.80	0.1097	0.1098	1.80	0.1097	0.1098	1.80	0.1097	0.1098	1.80	0.1097	0.1098	30.90	0.0990	0.0992
2.40	0.1097	0.1098	2.40	0.1097	0.1098	2.40	0.1097	0.1098	2.40	0.1097	0.1098	31.20	0.0973	0.0975
3.00	0.1002	0.1007	3.00	0.1000	0.1005	3.00	0.1001	0.1005	3.00	0.1004	0.1008	31.50	0.0994	0.0996
3.60	0.1014	0.1018	3.60	0.1014	0.1018	3.60	0.1013	0.1018	3.60	0.1019	0.1023	31.80	0.1010	0.1012
4.20	0.0943	0.0949	4.20	0.0938	0.0945	4.20	0.0938	0.0944	4.20	0.0945	0.0951	32.10	0.1015	0.1017
4.80	0.0893	0.0899	4.80	0.0875	0.0881	4.80	0.0875	0.0881	4.80	0.0896	0.0902	32.40	0.1014	0.1016
5.40	0.0988	0.0990	5.40	0.1008	0.1010	5.40	0.1008	0.1010	5.40	0.0992	0.0994	32.70	0.1010	0.1012
6.00	0.0949	0.0952	6.00	0.0960	0.0962	6.00	0.0956	0.0958	6.00	0.0957	0.0960	33.00	0.1015	0.1017
6.60	0.0970	0.0972	6.60	0.0956	0.0958	6.60	0.0956	0.0958	6.60	0.0973	0.0975	33.30	0.1016	0.1018
7.20	0.0944	0.0946	7.20	0.0966	0.0968	7.20	0.0964	0.0966	7.20	0.0949	0.0950	33.60	0.1008	0.1010
7.80	0.0923	0.0924	7.80	0.0919	0.0920	7.80	0.0919	0.0920	7.80	0.0923	0.0925	33.90	0.0983	0.0985
8.40	0.1065	0.1068	8.40	0.1062	0.1066	8.40	0.1066	0.1069	8.40	0.1075	0.1078	34.20	0.0979	0.0981

9.00	0.1049	0.1052	9.00	0.1083	0.1087	9.00	0.1083	0.1086	9.00	0.1048	0.1052	34.50	0.1009	0.1011
9.60	0.1006	0.1009	9.60	0.1012	0.1015	9.60	0.1011	0.1015	9.60	0.1001	0.1004	34.80	0.1021	0.1023
10.20	0.0965	0.0967	10.20	0.0937	0.0940	10.20	0.0942	0.0945	10.20	0.0977	0.0980	35.10	0.1008	0.1010
10.80	0.0957	0.0961	10.80	0.0946	0.0951	10.80	0.0954	0.0959	10.80	0.0954	0.0958	35.40	0.1020	0.1022
11.40	0.0985	0.0990	11.40	0.1007	0.1011	11.40	0.1009	0.1013	11.40	0.0987	0.0992	35.70	0.1024	0.1026
12.00	0.1023	0.1026	12.00	0.1035	0.1039	12.00	0.1040	0.1043	12.00	0.1024	0.1027	36.00	0.1016	0.1017
12.60	0.0949	0.0952	12.60	0.0911	0.0914	12.60	0.0918	0.0921	12.60	0.0935	0.0938	36.30	0.1012	0.1014
13.20	0.0938	0.0940	13.20	0.0967	0.0969	13.20	0.0969	0.0971	13.20	0.0948	0.0951	36.60	0.0997	0.0999
13.80	0.1008	0.1010	13.80	0.0958	0.0960	13.80	0.0968	0.0969	13.80	0.0999	0.1000	36.90	0.0994	0.0997
14.40	0.0964	0.0965	14.40	0.0997	0.0999	14.40	0.0999	0.1002	14.40	0.0962	0.0964	37.20	0.0994	0.0997
15.00	0.1095	0.1097	15.00	0.1076	0.1080	15.00	0.1078	0.1082	15.00	0.1088	0.1091	37.50	0.0984	0.0985
15.60	0.1005	0.1009	15.60	0.0962	0.0967	15.60	0.0962	0.0967	15.60	0.1009	0.1014	37.80	0.1003	0.1004
16.20	0.0946	0.0949	16.20	0.0960	0.0962	16.20	0.0967	0.0970	16.20	0.0953	0.0956	38.10	0.1028	0.1030
16.80	0.1018	0.1022	16.80	0.1021	0.1025	16.80	0.1021	0.1025	16.80	0.1015	0.1018	38.40	0.1011	0.1013
17.40	0.1008	0.1010	17.40	0.0981	0.0983	17.40	0.0987	0.0989	17.40	0.1016	0.1018	38.70	0.1007	0.1009
18.00	0.1025	0.1029	18.00	0.1015	0.1020	18.00	0.1015	0.1020	18.00	0.1028	0.1033	39.00	0.0997	0.0999
18.60	0.0989	0.0993	18.60	0.0959	0.0963	18.60	0.0970	0.0974	18.60	0.0988	0.0992	39.30	0.1001	0.1003
19.20	0.0951	0.0954	19.20	0.0927	0.0930	19.20	0.0937	0.0940	19.20	0.0946	0.0949	39.60	0.1008	0.1010
19.80	0.0976	0.0978	19.80	0.0996	0.0999	19.80	0.1007	0.1009	19.80	0.0976	0.0978	39.90	0.0986	0.0989
20.40	0.1026	0.1029	20.40	0.1007	0.1009	20.40	0.1015	0.1017	20.40	0.1014	0.1017	40.20	0.0992	0.0994
21.00	0.1027	0.1030	21.00	0.1012	0.1015	21.00	0.1015	0.1018	21.00	0.1040	0.1043	40.50	0.1007	0.1009
21.60	0.1022	0.1024	21.60	0.0990	0.0993	21.60	0.0992	0.0995	21.60	0.1017	0.1020	40.80	0.1000	0.1002
22.20	0.0953	0.0956	22.20	0.0944	0.0948	22.20	0.0955	0.0959	22.20	0.0964	0.0968	41.10	0.1002	0.1004
22.80	0.1010	0.1014	22.80	0.1032	0.1036	22.80	0.1033	0.1036	22.80	0.1016	0.1019	41.40	0.1028	0.1030
23.40	0.1026	0.1029	23.40	0.1001	0.1004	23.40	0.1006	0.1009	23.40	0.1027	0.1029	41.70	0.1023	0.1025
24.00	0.1033	0.1036	24.00	0.0995	0.0998	24.00	0.0996	0.0999	24.00	0.1039	0.1042	42.00	0.1001	0.1004

24.60	0.0981	0.0985	24.60	0.0981	0.0984	24.60	0.0982	0.0986	24.60	0.0985	0.0989	42.30	0.0996	0.0998
25.20	0.0985	0.0988	25.20	0.0954	0.0957	25.20	0.0965	0.0968	25.20	0.0981	0.0985	42.60	0.0996	0.0999
25.80	0.0998	0.1001	25.80	0.0990	0.0993	25.80	0.0999	0.1002	25.80	0.1004	0.1007	42.90	0.1004	0.1006
26.40	0.1029	0.1032	26.40	0.1023	0.1025	26.40	0.1023	0.1026	26.40	0.1029	0.1031	43.20	0.0999	0.1001
27.00	0.1006	0.1009	27.00	0.0990	0.0993	27.00	0.0991	0.0993	27.00	0.1014	0.1017	43.50	0.0991	0.0993
27.60	0.1002	0.1004	27.60	0.0983	0.0986	27.60	0.0987	0.0990	27.60	0.1002	0.1004	43.80	0.0997	0.0999
28.20	0.0999	0.1002	28.20	0.0970	0.0972	28.20	0.0978	0.0980	28.20	0.1002	0.1005	44.10	0.1013	0.1015
28.80	0.1004	0.1006	28.80	0.1005	0.1007	28.80	0.1003	0.1005	28.80	0.1021	0.1023	44.40	0.1014	0.1016
29.40	0.1022	0.1024	29.40	0.1017	0.1020	29.40	0.1017	0.1020	29.40	0.1027	0.1030	44.70	0.1008	0.1010
30.00	0.1028	0.1031	30.00	0.1001	0.1004	30.00	0.1001	0.1004	30.00	0.1033	0.1036	45.00	0.1006	0.1008
30.60	0.1002	0.1004	30.60	0.0973	0.0975	30.60	0.0972	0.0974	30.60	0.1009	0.1012	45.30	0.0995	0.0998
31.20	0.0972	0.0974	31.20	0.0981	0.0983	31.20	0.0979	0.0981	31.20	0.0975	0.0977	45.60	0.0987	0.0989
31.80	0.1008	0.1010	31.80	0.0998	0.1000	31.80	0.0991	0.0993	31.80	0.1013	0.1015	45.90	0.0986	0.0988
32.40	0.1014	0.1016	32.40	0.1009	0.1012	32.40	0.1007	0.1009	32.40	0.1018	0.1020	46.20	0.0996	0.0999
33.00	0.1015	0.1017	33.00	0.1003	0.1005	33.00	0.0995	0.0997	33.00	0.1019	0.1021	46.50	0.1004	0.1007
33.60	0.1012	0.1013	33.60	0.0978	0.0980	33.60	0.0979	0.0981	33.60	0.1012	0.1014	46.80	0.0998	0.1000
34.20	0.0978	0.0979	34.20	0.0981	0.0982	34.20	0.0979	0.0981	34.20	0.0984	0.0986	47.10	0.0997	0.0999
34.80	0.1021	0.1023	34.80	0.1000	0.1002	34.80	0.0998	0.1000	34.80	0.1027	0.1029	47.40	0.1015	0.1017
35.40	0.1028	0.1030	35.40	0.1010	0.1012	35.40	0.1007	0.1009	35.40	0.1028	0.1030	47.70	0.1018	0.1020
36.00	0.1012	0.1014	36.00	0.1003	0.1005	36.00	0.1001	0.1003	36.00	0.1022	0.1024	48.00	0.1008	0.1010
36.60	0.1002	0.1004	36.60	0.0972	0.0974	36.60	0.0973	0.0975	36.60	0.1001	0.1003	48.30	0.0996	0.0999
37.20	0.1000	0.1002	37.20	0.0988	0.0990	37.20	0.0983	0.0985	37.20	0.1004	0.1007	48.60	0.0983	0.0986
37.80	0.1003	0.1005	37.80	0.1003	0.1005	37.80	0.1002	0.1004	37.80	0.1011	0.1012	48.90	0.0992	0.0995
38.40	0.1018	0.1020	38.40	0.1002	0.1004	38.40	0.0993	0.0995	38.40	0.1015	0.1017	49.20	0.1004	0.1007
39.00	0.1005	0.1008	39.00	0.0995	0.0997	39.00	0.0995	0.0997	39.00	0.1006	0.1008	49.50	0.1000	0.1003
39.60	0.1009	0.1011	39.60	0.0979	0.0982	39.60	0.0978	0.0980	39.60	0.1015	0.1017	49.80	0.0997	0.1000

40.20	0.0998	0.1000	40.20	0.0986	0.0988	40.20	0.0978	0.0980	40.20	0.1003	0.1005	50.10	0.1015	0.1017
40.80	0.1008	0.1009	40.80	0.1007	0.1009	40.80	0.1002	0.1003	40.80	0.1007	0.1009	50.40	0.1006	0.1009
41.40	0.1031	0.1033	41.40	0.1010	0.1012	41.40	0.1008	0.1011	41.40	0.1037	0.1039	50.70	0.0996	0.0999
42.00	0.1003	0.1006	42.00	0.0986	0.0988	42.00	0.0980	0.0982	42.00	0.1014	0.1017	51.00	0.1007	0.1009
42.60	0.1003	0.1006	42.60	0.0989	0.0992	42.60	0.0985	0.0987	42.60	0.1006	0.1008	51.30	0.0998	0.1001
43.20	0.1014	0.1016	43.20	0.0990	0.0993	43.20	0.0978	0.0981	43.20	0.1011	0.1013	51.60	0.0989	0.0991
43.80	0.0997	0.0999	43.80	0.1010	0.1012	43.80	0.1004	0.1006	43.80	0.1008	0.1011	51.90	0.0983	0.0986
44.40	0.1021	0.1023	44.40	0.1000	0.1002	44.40	0.0998	0.1001	44.40	0.1024	0.1026	52.20	0.0990	0.0993
45.00	0.1015	0.1018	45.00	0.0998	0.1001	45.00	0.0989	0.0991	45.00	0.1021	0.1023	52.50	0.1002	0.1004
45.60	0.0990	0.0993	45.60	0.0987	0.0990	45.60	0.0977	0.0979	45.60	0.1002	0.1004	52.80	0.0999	0.1001
46.20	0.1009	0.1012	46.20	0.0994	0.0997	46.20	0.0985	0.0988	46.20	0.1011	0.1014	53.10	0.1001	0.1003
46.80	0.1013	0.1015	46.80	0.1008	0.1010	46.80	0.0997	0.1000	46.80	0.1017	0.1019	53.40	0.1004	0.1006
47.40	0.1018	0.1020	47.40	0.1009	0.1011	47.40	0.1004	0.1006	47.40	0.1029	0.1031	53.70	0.1006	0.1008
48.00	0.1012	0.1014	48.00	0.0992	0.0994	48.00	0.0981	0.0983	48.00	0.1023	0.1025	54.00	0.1002	0.1005
48.60	0.1002	0.1005	48.60	0.1000	0.1002	48.60	0.0987	0.0989	48.60	0.1003	0.1006	54.30	0.0995	0.0998
49.20	0.1017	0.1020	49.20	0.0994	0.0997	49.20	0.0990	0.0992	49.20	0.1017	0.1020	54.60	0.0994	0.0997
49.80	0.1008	0.1010	49.80	0.1006	0.1008	49.80	0.0997	0.1000	49.80	0.1015	0.1018	54.90	0.0991	0.0993
50.40	0.1014	0.1017	50.40	0.1007	0.1009	50.40	0.0998	0.1001	50.40	0.1015	0.1017	55.20	0.0995	0.0998
51.00	0.1018	0.1021	51.00	0.0993	0.0996	51.00	0.0989	0.0992	51.00	0.1022	0.1025	55.50	0.0997	0.0999
51.60	0.1003	0.1005	51.60	0.0989	0.0992	51.60	0.0980	0.0982	51.60	0.1007	0.1010	55.80	0.0998	0.1001
52.20	0.1007	0.1009	52.20	0.0999	0.1001	52.20	0.0995	0.0997	52.20	0.1013	0.1016	56.10	0.1017	0.1020
52.80	0.1010	0.1013	52.80	0.0994	0.0997	52.80	0.0993	0.0996	52.80	0.1016	0.1019	56.40	0.1010	0.1012
53.40	0.1010	0.1012	53.40	0.1009	0.1012	53.40	0.1001	0.1003	53.40	0.1019	0.1021	56.70	0.0988	0.0990
54.00	0.1013	0.1016	54.00	0.0986	0.0989	54.00	0.0984	0.0986	54.00	0.1016	0.1018	57.00	0.0997	0.0999
54.60	0.1019	0.1021	54.60	0.0996	0.0998	54.60	0.0989	0.0991	54.60	0.1021	0.1023	57.30	0.1000	0.1002
55.20	0.1004	0.1006	55.20	0.0994	0.0996	55.20	0.0988	0.0990	55.20	0.1014	0.1017	57.60	0.0991	0.0993

55.80	0.1010	0.1013	55.80	0.1006	0.1008	55.80	0.0997	0.0999	55.80	0.1018	0.1020	57.90	0.0989	0.0991
56.40	0.1023	0.1026	56.40	0.0999	0.1001	56.40	0.0992	0.0994	56.40	0.1020	0.1022	58.20	0.0993	0.0995
57.00	0.1011	0.1013	57.00	0.0995	0.0998	57.00	0.0992	0.0994	57.00	0.1019	0.1021	58.50	0.0994	0.0997
57.60	0.1010	0.1012	57.60	0.0986	0.0989	57.60	0.0981	0.0983	57.60	0.1013	0.1015	58.80	0.0998	0.1000
58.20	0.1015	0.1017	58.20	0.0999	0.1001	58.20	0.0993	0.0996	58.20	0.1010	0.1013	59.10	0.1001	0.1004
58.80	0.1009	0.1012	58.80	0.0996	0.0999	58.80	0.0998	0.1000	58.80	0.1017	0.1020	59.40	0.1005	0.1007
59.40	0.1017	0.1019	59.40	0.0997	0.1000	59.40	0.0993	0.0995	59.40	0.1022	0.1024	59.70	0.1004	0.1006
60.00	0.1007	0.1010	60.00	0.0989	0.0992	60.00	0.0984	0.0987	60.00	0.1012	0.1015	60.00	0.0991	0.0994

Table C10 Tabulated time series data for the α=16°: θ=30° arced labyrinth weir at H/P=0.6

RM1-WM0			RM0-WM1			RM0-WM2			RM1-WM2			RM1-WM3		
Cell Count:	1493807		*Cell Count:*	1506424		*Cell Count:*	3090910		*Cell Count:*	3336124		*Cell Count:*	6865887	
Q	194.06	[L/s]	*Q*	190.62	[L/s]	*Q*	190.62	[L/s]	*Q*	191.36	[L/s]	*Q*	191.36	[L/s]
H	0.121	[m]	*H*	0.121	[m]	*H*	0.119	[m]	*H*	0.119	[m]	*H*	0.115	[m]
H/P	0.598	[-]	*H/P*	0.595	[-]	*H/P*	0.587	[-]	*H/P*	0.587	[-]	*H/P*	0.564	[-]
C_d	0.497	[-]	C_d	0.491	[-]	C_d	0.502	[-]	C_d	0.503	[-]	C_d	0.534	[-]
$C_{d\text{-}emp}$	0.490	[-]	$C_{d\text{-}emp}$	0.492	[-]	$C_{d\text{-}emp}$	0.497	[-]	$C_{d\text{-}emp}$	0.496	[-]	$C_{d\text{-}emp}$	0.511	[-]
ε_{Cd}	1.42%	[%]	ε_{Cd}	-0.03%	[%]	ε_{Cd}	1.04%	[%]	ε_{Cd}	1.35%	[%]	ε_{Cd}	4.52%	[%]
Time [s]	*h* [m]	*H* [m]	Time [s]	*h* [m]	*H* [m]	Time [s]	*h* [m]	*H* [m]	Time [s]	*h* [m]	*H* [m]	Time [s]	*h* [m]	*H* [m]
0.00	0.1219	0.1219	30.00	0.1182	0.1184	0.00	0.1219	0.1219	0.00	0.1219	0.1219	0.00	0.1219	0.1219
0.60	0.1232	0.1232	30.30	0.1159	0.1161	0.60	0.1232	0.1232	0.60	0.1232	0.1232	0.60	0.1232	0.1232
1.20	0.1355	0.1357	30.60	0.1182	0.1183	1.20	0.1357	0.1358	1.20	0.1353	0.1355	1.20	0.1353	0.1355
1.80	0.1372	0.1373	30.90	0.1202	0.1205	1.80	0.1461	0.1463	1.80	0.1372	0.1373	1.80	0.1372	0.1373
2.40	0.1371	0.1373	31.20	0.1202	0.1205	2.40	0.1412	0.1415	2.40	0.1371	0.1373	2.40	0.1371	0.1373
3.00	0.1228	0.1237	31.50	0.1211	0.1214	3.00	0.1292	0.1302	3.00	0.1229	0.1237	3.00	0.1230	0.1238
3.60	0.1260	0.1267	31.80	0.1236	0.1239	3.60	0.1234	0.1244	3.60	0.1260	0.1267	3.60	0.1260	0.1268
4.20	0.1178	0.1187	32.10	0.1233	0.1235	4.20	0.1166	0.1176	4.20	0.1172	0.1182	4.20	0.1170	0.1180
4.80	0.1067	0.1073	32.40	0.1203	0.1205	4.80	0.1097	0.1103	4.80	0.1056	0.1063	4.80	0.1049	0.1056
5.40	0.1162	0.1164	32.70	0.1196	0.1198	5.40	0.1185	0.1187	5.40	0.1170	0.1172	5.40	0.1163	0.1166
6.00	0.1167	0.1168	33.00	0.1208	0.1210	6.00	0.1181	0.1182	6.00	0.1164	0.1166	6.00	0.1159	0.1161
6.60	0.1181	0.1183	33.30	0.1195	0.1197	6.60	0.1243	0.1243	6.60	0.1164	0.1166	6.60	0.1150	0.1152
7.20	0.1198	0.1198	33.60	0.1196	0.1198	7.20	0.1204	0.1205	7.20	0.1212	0.1213	7.20	0.1198	0.1199
7.80	0.1175	0.1177	33.90	0.1216	0.1218	7.80	0.1227	0.1229	7.80	0.1155	0.1158	7.80	0.1150	0.1152
8.40	0.1299	0.1301	34.20	0.1243	0.1246	8.40	0.1388	0.1391	8.40	0.1273	0.1275	8.40	0.1255	0.1258

9.00	0.1345	0.1350	34.50	0.1238	0.1240	9.00	0.1306	0.1313	9.00	0.1352	0.1357	9.00	0.1353	0.1358
9.60	0.1202	0.1207	34.80	0.1219	0.1221	9.60	0.1207	0.1213	9.60	0.1201	0.1207	9.60	0.1198	0.1204
10.20	0.1167	0.1173	35.10	0.1205	0.1208	10.20	0.1238	0.1244	10.20	0.1127	0.1132	10.20	0.1140	0.1145
10.80	0.1149	0.1155	35.40	0.1208	0.1212	10.80	0.1100	0.1107	10.80	0.1114	0.1120	10.80	0.1117	0.1123
11.40	0.1207	0.1212	35.70	0.1220	0.1223	11.40	0.1231	0.1236	11.40	0.1201	0.1205	11.40	0.1166	0.1171
12.00	0.1233	0.1236	36.00	0.1207	0.1210	12.00	0.1215	0.1217	12.00	0.1200	0.1203	12.00	0.1176	0.1180
12.60	0.1127	0.1130	36.30	0.1181	0.1184	12.60	0.1135	0.1138	12.60	0.1107	0.1111	12.60	0.1102	0.1106
13.20	0.1152	0.1154	36.60	0.1178	0.1181	13.20	0.1168	0.1170	13.20	0.1109	0.1111	13.20	0.1111	0.1113
13.80	0.1232	0.1235	36.90	0.1227	0.1229	13.80	0.1257	0.1258	13.80	0.1208	0.1210	13.80	0.1173	0.1176
14.40	0.1230	0.1232	37.20	0.1229	0.1231	14.40	0.1249	0.1252	14.40	0.1221	0.1223	14.40	0.1212	0.1215
15.00	0.1270	0.1275	37.50	0.1207	0.1209	15.00	0.1337	0.1344	15.00	0.1263	0.1268	15.00	0.1233	0.1238
15.60	0.1211	0.1215	37.80	0.1224	0.1227	15.60	0.1168	0.1174	15.60	0.1204	0.1209	15.60	0.1187	0.1192
16.20	0.1176	0.1180	38.10	0.1213	0.1216	16.20	0.1183	0.1187	16.20	0.1147	0.1150	16.20	0.1119	0.1123
16.80	0.1218	0.1223	38.40	0.1178	0.1182	16.80	0.1231	0.1236	16.80	0.1229	0.1234	16.80	0.1196	0.1201
17.40	0.1239	0.1243	38.70	0.1187	0.1190	17.40	0.1211	0.1214	17.40	0.1216	0.1219	17.40	0.1175	0.1180
18.00	0.1192	0.1198	39.00	0.1219	0.1222	18.00	0.1158	0.1164	18.00	0.1180	0.1186	18.00	0.1175	0.1180
18.60	0.1178	0.1181	39.30	0.1216	0.1219	18.60	0.1157	0.1160	18.60	0.1143	0.1147	18.60	0.1110	0.1114
19.20	0.1145	0.1148	39.60	0.1207	0.1209	19.20	0.1145	0.1147	19.20	0.1133	0.1136	19.20	0.1101	0.1103
19.80	0.1204	0.1206	39.90	0.1197	0.1199	19.80	0.1240	0.1242	19.80	0.1205	0.1207	19.80	0.1187	0.1189
20.40	0.1278	0.1281	40.20	0.1209	0.1211	20.40	0.1239	0.1242	20.40	0.1266	0.1268	20.40	0.1228	0.1231
21.00	0.1227	0.1231	40.50	0.1225	0.1228	21.00	0.1209	0.1211	21.00	0.1194	0.1198	21.00	0.1146	0.1150
21.60	0.1192	0.1196	40.80	0.1219	0.1222	21.60	0.1226	0.1231	21.60	0.1188	0.1192	21.60	0.1164	0.1167
22.20	0.1194	0.1198	41.10	0.1205	0.1208	22.20	0.1195	0.1200	22.20	0.1163	0.1168	22.20	0.1122	0.1127
22.80	0.1195	0.1198	41.40	0.1205	0.1208	22.80	0.1240	0.1243	22.80	0.1197	0.1201	22.80	0.1189	0.1192
23.40	0.1261	0.1264	41.70	0.1199	0.1202	23.40	0.1192	0.1195	23.40	0.1262	0.1265	23.40	0.1240	0.1242
24.00	0.1170	0.1174	42.00	0.1193	0.1196	24.00	0.1161	0.1166	24.00	0.1160	0.1164	24.00	0.1120	0.1124

24.60	0.1170	0.1174	42.30	0.1208	0.1211	24.60	0.1188	0.1191	24.60	0.1173	0.1177	24.60	0.1135	0.1139
25.20	0.1189	0.1192	42.60	0.1214	0.1217	25.20	0.1163	0.1165	25.20	0.1172	0.1175	25.20	0.1152	0.1154
25.80	0.1212	0.1214	42.90	0.1219	0.1222	25.80	0.1207	0.1209	25.80	0.1207	0.1209	25.80	0.1159	0.1162
26.40	0.1210	0.1212	43.20	0.1218	0.1220	26.40	0.1242	0.1244	26.40	0.1221	0.1224	26.40	0.1184	0.1187
27.00	0.1205	0.1207	43.50	0.1203	0.1206	27.00	0.1190	0.1192	27.00	0.1193	0.1196	27.00	0.1165	0.1167
27.60	0.1197	0.1199	43.80	0.1214	0.1217	27.60	0.1189	0.1191	27.60	0.1193	0.1196	27.60	0.1163	0.1165
28.20	0.1220	0.1223	44.10	0.1227	0.1230	28.20	0.1224	0.1226	28.20	0.1207	0.1209	28.20	0.1154	0.1157
28.80	0.1223	0.1225	44.40	0.1189	0.1192	28.80	0.1220	0.1223	28.80	0.1204	0.1207	28.80	0.1155	0.1157
29.40	0.1218	0.1221	44.70	0.1176	0.1179	29.40	0.1207	0.1210	29.40	0.1219	0.1222	29.40	0.1200	0.1202
30.00	0.1220	0.1222	45.00	0.1214	0.1217	30.00	0.1169	0.1172	30.00	0.1201	0.1204	30.00	0.1162	0.1165
30.60	0.1179	0.1181	45.30	0.1208	0.1211	30.60	0.1172	0.1173	30.60	0.1150	0.1152	30.60	0.1104	0.1107
31.20	0.1194	0.1197	45.60	0.1209	0.1212	31.20	0.1186	0.1188	31.20	0.1174	0.1176	31.20	0.1143	0.1145
31.80	0.1220	0.1222	45.90	0.1226	0.1229	31.80	0.1217	0.1220	31.80	0.1208	0.1211	31.80	0.1179	0.1182
32.40	0.1218	0.1220	46.20	0.1201	0.1203	32.40	0.1189	0.1191	32.40	0.1213	0.1215	32.40	0.1167	0.1169
33.00	0.1203	0.1205	46.50	0.1202	0.1205	33.00	0.1198	0.1200	33.00	0.1180	0.1182	33.00	0.1137	0.1140
33.60	0.1211	0.1214	46.80	0.1216	0.1219	33.60	0.1177	0.1179	33.60	0.1189	0.1191	33.60	0.1146	0.1148
34.20	0.1228	0.1231	47.10	0.1194	0.1197	34.20	0.1224	0.1227	34.20	0.1202	0.1204	34.20	0.1160	0.1162
34.80	0.1229	0.1231	47.40	0.1204	0.1207	34.80	0.1215	0.1218	34.80	0.1199	0.1202	34.80	0.1178	0.1181
35.40	0.1228	0.1231	47.70	0.1214	0.1217	35.40	0.1184	0.1187	35.40	0.1204	0.1207	35.40	0.1180	0.1183
36.00	0.1210	0.1213	48.00	0.1183	0.1186	36.00	0.1193	0.1196	36.00	0.1191	0.1194	36.00	0.1156	0.1159
36.60	0.1197	0.1200	48.30	0.1197	0.1200	36.60	0.1166	0.1168	36.60	0.1172	0.1175	36.60	0.1131	0.1134
37.20	0.1203	0.1206	48.60	0.1235	0.1238	37.20	0.1209	0.1211	37.20	0.1195	0.1198	37.20	0.1138	0.1141
37.80	0.1212	0.1215	48.90	0.1228	0.1231	37.80	0.1198	0.1201	37.80	0.1214	0.1216	37.80	0.1169	0.1171
38.40	0.1212	0.1215	49.20	0.1213	0.1216	38.40	0.1167	0.1170	38.40	0.1197	0.1200	38.40	0.1148	0.1151
39.00	0.1211	0.1214	49.50	0.1191	0.1194	39.00	0.1196	0.1199	39.00	0.1187	0.1190	39.00	0.1142	0.1145
39.60	0.1202	0.1205	49.80	0.1194	0.1197	39.60	0.1187	0.1189	39.60	0.1185	0.1187	39.60	0.1164	0.1166

40.20	0.1212	0.1214	50.10	0.1224	0.1227	40.20	0.1196	0.1198	40.20	0.1193	0.1196	40.20	0.1142	0.1145
40.80	0.1219	0.1222	50.40	0.1213	0.1215	40.80	0.1218	0.1221	40.80	0.1217	0.1220	40.80	0.1173	0.1176
41.40	0.1220	0.1223	50.70	0.1201	0.1203	41.40	0.1193	0.1196	41.40	0.1208	0.1211	41.40	0.1165	0.1169
42.00	0.1213	0.1216	51.00	0.1212	0.1214	42.00	0.1174	0.1177	42.00	0.1182	0.1185	42.00	0.1138	0.1142
42.60	0.1220	0.1223	51.30	0.1209	0.1211	42.60	0.1190	0.1194	42.60	0.1192	0.1195	42.60	0.1147	0.1150
43.20	0.1201	0.1204	51.60	0.1210	0.1213	43.20	0.1210	0.1213	43.20	0.1187	0.1190	43.20	0.1152	0.1155
43.80	0.1232	0.1235	51.90	0.1213	0.1216	43.80	0.1185	0.1187	43.80	0.1219	0.1221	43.80	0.1158	0.1161
44.40	0.1216	0.1219	52.20	0.1217	0.1220	44.40	0.1185	0.1187	44.40	0.1190	0.1192	44.40	0.1142	0.1144
45.00	0.1204	0.1206	52.50	0.1208	0.1212	45.00	0.1184	0.1187	45.00	0.1173	0.1176	45.00	0.1153	0.1156
45.60	0.1208	0.1211	52.80	0.1200	0.1203	45.60	0.1183	0.1186	45.60	0.1208	0.1211	45.60	0.1137	0.1140
46.20	0.1223	0.1226	53.10	0.1197	0.1200	46.20	0.1203	0.1205	46.20	0.1198	0.1200	46.20	0.1144	0.1147
46.80	0.1221	0.1224	53.40	0.1200	0.1202	46.80	0.1211	0.1213	46.80	0.1203	0.1206	46.80	0.1168	0.1171
47.40	0.1217	0.1220	53.70	0.1227	0.1229	47.40	0.1179	0.1182	47.40	0.1193	0.1195	47.40	0.1153	0.1156
48.00	0.1207	0.1211	54.00	0.1216	0.1219	48.00	0.1178	0.1182	48.00	0.1175	0.1178	48.00	0.1132	0.1135
48.60	0.1218	0.1221	54.30	0.1184	0.1187	48.60	0.1207	0.1210	48.60	0.1195	0.1197	48.60	0.1147	0.1150
49.20	0.1220	0.1223	54.60	0.1206	0.1209	49.20	0.1194	0.1197	49.20	0.1198	0.1201	49.20	0.1156	0.1159
49.80	0.1219	0.1222	54.90	0.1226	0.1229	49.80	0.1177	0.1180	49.80	0.1184	0.1187	49.80	0.1151	0.1154
50.40	0.1201	0.1204	55.20	0.1207	0.1210	50.40	0.1205	0.1208	50.40	0.1202	0.1205	50.40	0.1147	0.1150
51.00	0.1205	0.1208	55.50	0.1210	0.1212	51.00	0.1179	0.1181	51.00	0.1188	0.1190	51.00	0.1145	0.1148
51.60	0.1218	0.1221	55.80	0.1210	0.1213	51.60	0.1183	0.1185	51.60	0.1191	0.1194	51.60	0.1140	0.1143
52.20	0.1224	0.1227	56.10	0.1203	0.1206	52.20	0.1209	0.1212	52.20	0.1197	0.1200	52.20	0.1154	0.1157
52.80	0.1209	0.1212	56.40	0.1209	0.1212	52.80	0.1196	0.1199	52.80	0.1204	0.1207	52.80	0.1158	0.1161
53.40	0.1225	0.1227	56.70	0.1214	0.1217	53.40	0.1181	0.1184	53.40	0.1202	0.1205	53.40	0.1125	0.1128
54.00	0.1209	0.1212	57.00	0.1221	0.1224	54.00	0.1207	0.1209	54.00	0.1186	0.1189	54.00	0.1160	0.1163
54.60	0.1210	0.1213	57.30	0.1218	0.1221	54.60	0.1184	0.1187	54.60	0.1189	0.1192	54.60	0.1145	0.1148
55.20	0.1225	0.1228	57.60	0.1197	0.1200	55.20	0.1201	0.1204	55.20	0.1207	0.1210	55.20	0.1135	0.1138

55.80	0.1228	0.1231	57.90	0.1197	0.1200	55.80	0.1198	0.1201	55.80	0.1191	0.1194	55.80	0.1164	0.1167
56.40	0.1206	0.1209	58.20	0.1223	0.1226	56.40	0.1179	0.1182	56.40	0.1178	0.1181	56.40	0.1142	0.1144
57.00	0.1210	0.1213	58.50	0.1217	0.1220	57.00	0.1182	0.1185	57.00	0.1191	0.1194	57.00	0.1134	0.1137
57.60	0.1210	0.1213	58.80	0.1201	0.1204	57.60	0.1195	0.1197	57.60	0.1191	0.1194	57.60	0.1147	0.1150
58.20	0.1220	0.1223	59.10	0.1199	0.1202	58.20	0.1197	0.1199	58.20	0.1202	0.1205	58.20	0.1149	0.1152
58.80	0.1213	0.1215	59.40	0.1197	0.1199	58.80	0.1185	0.1188	58.80	0.1207	0.1210	58.80	0.1145	0.1148
59.40	0.1219	0.1221	59.70	0.1216	0.1219	59.40	0.1188	0.1191	59.40	0.1178	0.1181	59.40	0.1139	0.1142
60.00	0.1207	0.1209	60.00	0.1224	0.1227	60.00	0.1210	0.1213	60.00	0.1196	0.1199	60.00	0.1145	0.1148

Table C11 Tabulated time series data for the α=16°: θ=30° arced labyrinth weir at H/P=0.7

RM1-WM0			RM0-WM1			RM0-WM2			RM1-WM2			RM1-WM3		
Cell Count:	1553185		*Cell Count:*	1584166		*Cell Count:*	3253999		*Cell Count:*	3472960		*Cell Count:*	7152511	
Q	214.10	[L/s]	*Q*	213.27	[L/s]	*Q*	213.27	[L/s]	*Q*	214.10	[L/s]	*Q*	214.10	[L/s]
H	0.137	[m]	*H*	0.138	[m]	*H*	0.137	[m]	*H*	0.138	[m]	*H*	0.133	[m]
H/P	0.676	[-]	*H/P*	0.681	[-]	*H/P*	0.674	[-]	*H/P*	0.678	[-]	*H/P*	0.656	[-]
C_d	0.456	[-]	C_d	0.449	[-]	C_d	0.456	[-]	C_d	0.453	[-]	C_d	0.477	[-]
$C_{d\text{-}emp}$	0.446	[-]	$C_{d\text{-}emp}$	0.443	[-]	$C_{d\text{-}emp}$	0.447	[-]	$C_{d\text{-}emp}$	0.445	[-]	$C_{d\text{-}emp}$	0.456	[-]
ε_{Cd}	2.26%	[%]	ε_{Cd}	1.28%	[%]	ε_{Cd}	2.06%	[%]	ε_{Cd}	1.97%	[%]	ε_{Cd}	4.47%	[%]
Time [s]	*h* [m]	*H* [m]	Time [s]	*h* [m]	*H* [m]	Time [s]	*h* [m]	*H* [m]	Time [s]	*h* [m]	*H* [m]	Time [s]	*h* [m]	*H* [m]
0.00	0.1422	0.1422	0.00	0.1422	0.1422	0.00	0.1422	0.1422	0.00	0.1422	0.1422	0.00	0.1422	0.1422
0.60	0.1439	0.1439	0.60	0.1438	0.1438	0.60	0.1438	0.1438	0.60	0.1439	0.1439	0.60	0.1439	0.1439
1.20	0.1578	0.1579	1.20	0.1581	0.1583	1.20	0.1581	0.1583	1.20	0.1578	0.1580	1.20	0.1578	0.1580
1.80	0.1646	0.1648	1.80	0.1704	0.1705	1.80	0.1703	0.1705	1.80	0.1646	0.1648	1.80	0.1646	0.1648
2.40	0.1620	0.1623	2.40	0.1634	0.1641	2.40	0.1634	0.1641	2.40	0.1621	0.1624	2.40	0.1621	0.1624
3.00	0.1448	0.1460	3.00	0.1503	0.1518	3.00	0.1505	0.1520	3.00	0.1451	0.1463	3.00	0.1451	0.1463
3.60	0.1451	0.1462	3.60	0.1413	0.1425	3.60	0.1412	0.1425	3.60	0.1454	0.1465	3.60	0.1453	0.1464
4.20	0.1378	0.1387	4.20	0.1324	0.1335	4.20	0.1320	0.1331	4.20	0.1373	0.1383	4.20	0.1372	0.1383
4.80	0.1268	0.1274	4.80	0.1286	0.1293	4.80	0.1282	0.1289	4.80	0.1239	0.1246	4.80	0.1232	0.1239
5.40	0.1382	0.1385	5.40	0.1414	0.1415	5.40	0.1416	0.1417	5.40	0.1405	0.1408	5.40	0.1398	0.1400
6.00	0.1414	0.1416	6.00	0.1328	0.1330	6.00	0.1323	0.1324	6.00	0.1374	0.1375	6.00	0.1372	0.1372
6.60	0.1391	0.1392	6.60	0.1526	0.1526	6.60	0.1504	0.1504	6.60	0.1427	0.1428	6.60	0.1390	0.1391
7.20	0.1432	0.1433	7.20	0.1410	0.1411	7.20	0.1420	0.1421	7.20	0.1439	0.1440	7.20	0.1460	0.1462
7.80	0.1395	0.1398	7.80	0.1499	0.1502	7.80	0.1482	0.1485	7.80	0.1379	0.1382	7.80	0.1423	0.1426
8.40	0.1528	0.1532	8.40	0.1662	0.1670	8.40	0.1664	0.1672	8.40	0.1579	0.1583	8.40	0.1556	0.1561

9.00	0.1454	0.1460	9.00	0.1473	0.1479	9.00	0.1464	0.1471	9.00	0.1481	0.1487	9.00	0.1516	0.1522
9.60	0.1389	0.1396	9.60	0.1381	0.1389	9.60	0.1381	0.1389	9.60	0.1456	0.1463	9.60	0.1350	0.1356
10.20	0.1386	0.1394	10.20	0.1363	0.1371	10.20	0.1354	0.1363	10.20	0.1347	0.1355	10.20	0.1278	0.1285
10.80	0.1344	0.1350	10.80	0.1347	0.1354	10.80	0.1324	0.1331	10.80	0.1302	0.1309	10.80	0.1303	0.1312
11.40	0.1376	0.1380	11.40	0.1428	0.1433	11.40	0.1417	0.1422	11.40	0.1404	0.1409	11.40	0.1374	0.1378
12.00	0.1376	0.1380	12.00	0.1331	0.1334	12.00	0.1308	0.1311	12.00	0.1390	0.1393	12.00	0.1372	0.1376
12.60	0.1325	0.1330	12.60	0.1339	0.1340	12.60	0.1324	0.1325	12.60	0.1336	0.1339	12.60	0.1276	0.1279
13.20	0.1426	0.1428	13.20	0.1463	0.1464	13.20	0.1424	0.1424	13.20	0.1406	0.1407	13.20	0.1381	0.1383
13.80	0.1425	0.1427	13.80	0.1466	0.1469	13.80	0.1413	0.1416	13.80	0.1372	0.1373	13.80	0.1298	0.1300
14.40	0.1455	0.1458	14.40	0.1550	0.1557	14.40	0.1545	0.1551	14.40	0.1519	0.1523	14.40	0.1502	0.1505
15.00	0.1446	0.1454	15.00	0.1475	0.1483	15.00	0.1466	0.1474	15.00	0.1454	0.1460	15.00	0.1433	0.1440
15.60	0.1381	0.1386	15.60	0.1346	0.1351	15.60	0.1329	0.1334	15.60	0.1375	0.1381	15.60	0.1290	0.1298
16.20	0.1372	0.1378	16.20	0.1472	0.1477	16.20	0.1473	0.1478	16.20	0.1382	0.1387	16.20	0.1484	0.1491
16.80	0.1414	0.1419	16.80	0.1344	0.1351	16.80	0.1340	0.1346	16.80	0.1427	0.1432	16.80	0.1394	0.1400
17.40	0.1372	0.1377	17.40	0.1423	0.1430	17.40	0.1407	0.1413	17.40	0.1378	0.1384	17.40	0.1418	0.1426
18.00	0.1347	0.1351	18.00	0.1333	0.1337	18.00	0.1314	0.1319	18.00	0.1381	0.1386	18.00	0.1408	0.1416
18.60	0.1348	0.1351	18.60	0.1323	0.1325	18.60	0.1313	0.1315	18.60	0.1338	0.1342	18.60	0.1316	0.1323
19.20	0.1340	0.1343	19.20	0.1464	0.1466	19.20	0.1423	0.1425	19.20	0.1337	0.1340	19.20	0.1302	0.1306
19.80	0.1425	0.1427	19.80	0.1467	0.1468	19.80	0.1465	0.1467	19.80	0.1467	0.1469	19.80	0.1395	0.1398
20.40	0.1422	0.1424	20.40	0.1427	0.1431	20.40	0.1412	0.1416	20.40	0.1390	0.1392	20.40	0.1381	0.1384
21.00	0.1386	0.1389	21.00	0.1416	0.1423	21.00	0.1414	0.1420	21.00	0.1426	0.1429	21.00	0.1430	0.1436
21.60	0.1374	0.1378	21.60	0.1372	0.1377	21.60	0.1354	0.1360	21.60	0.1401	0.1406	21.60	0.1329	0.1337
22.20	0.1421	0.1424	22.20	0.1466	0.1469	22.20	0.1463	0.1467	22.20	0.1396	0.1400	22.20	0.1377	0.1383
22.80	0.1397	0.1399	22.80	0.1398	0.1402	22.80	0.1388	0.1391	22.80	0.1416	0.1420	22.80	0.1395	0.1402
23.40	0.1373	0.1377	23.40	0.1348	0.1352	23.40	0.1352	0.1356	23.40	0.1373	0.1377	23.40	0.1343	0.1348
24.00	0.1348	0.1352	24.00	0.1353	0.1357	24.00	0.1338	0.1342	24.00	0.1373	0.1378	24.00	0.1372	0.1377

24.60	0.1351	0.1354	24.60	0.1354	0.1357	24.60	0.1342	0.1345	24.60	0.1343	0.1347	24.60	0.1323	0.1328
25.20	0.1372	0.1374	25.20	0.1418	0.1419	25.20	0.1411	0.1413	25.20	0.1349	0.1353	25.20	0.1300	0.1305
25.80	0.1385	0.1387	25.80	0.1416	0.1418	25.80	0.1410	0.1412	25.80	0.1404	0.1407	25.80	0.1375	0.1379
26.40	0.1391	0.1394	26.40	0.1382	0.1385	26.40	0.1371	0.1373	26.40	0.1400	0.1403	26.40	0.1334	0.1338
27.00	0.1373	0.1376	27.00	0.1405	0.1408	27.00	0.1384	0.1387	27.00	0.1379	0.1381	27.00	0.1384	0.1386
27.60	0.1379	0.1382	27.60	0.1413	0.1417	27.60	0.1405	0.1409	27.60	0.1390	0.1393	27.60	0.1337	0.1341
28.20	0.1392	0.1395	28.20	0.1426	0.1429	28.20	0.1418	0.1421	28.20	0.1401	0.1405	28.20	0.1372	0.1376
28.80	0.1377	0.1381	28.80	0.1420	0.1423	28.80	0.1411	0.1414	28.80	0.1410	0.1413	28.80	0.1378	0.1383
29.40	0.1388	0.1391	29.40	0.1331	0.1334	29.40	0.1315	0.1318	29.40	0.1390	0.1393	29.40	0.1347	0.1350
30.00	0.1350	0.1352	30.00	0.1369	0.1372	30.00	0.1355	0.1358	30.00	0.1346	0.1348	30.00	0.1333	0.1337
30.60	0.1344	0.1347	30.60	0.1388	0.1391	30.60	0.1382	0.1385	30.60	0.1375	0.1377	30.60	0.1330	0.1333
31.20	0.1388	0.1391	31.20	0.1400	0.1403	31.20	0.1393	0.1396	31.20	0.1384	0.1387	31.20	0.1329	0.1332
31.80	0.1378	0.1379	31.80	0.1386	0.1389	31.80	0.1370	0.1373	31.80	0.1380	0.1381	31.80	0.1349	0.1352
32.40	0.1372	0.1373	32.40	0.1380	0.1382	32.40	0.1362	0.1364	32.40	0.1385	0.1387	32.40	0.1372	0.1375
33.00	0.1384	0.1386	33.00	0.1382	0.1385	33.00	0.1364	0.1366	33.00	0.1374	0.1375	33.00	0.1337	0.1340
33.60	0.1373	0.1374	33.60	0.1433	0.1436	33.60	0.1419	0.1422	33.60	0.1383	0.1384	33.60	0.1351	0.1353
34.20	0.1390	0.1391	34.20	0.1379	0.1383	34.20	0.1377	0.1381	34.20	0.1398	0.1400	34.20	0.1372	0.1374
34.80	0.1376	0.1379	34.80	0.1408	0.1412	34.80	0.1384	0.1388	34.80	0.1378	0.1381	34.80	0.1353	0.1356
35.40	0.1375	0.1378	35.40	0.1359	0.1362	35.40	0.1341	0.1344	35.40	0.1399	0.1401	35.40	0.1352	0.1355
36.00	0.1349	0.1352	36.00	0.1383	0.1386	36.00	0.1365	0.1368	36.00	0.1374	0.1376	36.00	0.1335	0.1338
36.60	0.1372	0.1374	36.60	0.1400	0.1403	36.60	0.1393	0.1396	36.60	0.1372	0.1374	36.60	0.1335	0.1337
37.20	0.1375	0.1378	37.20	0.1377	0.1381	37.20	0.1364	0.1368	37.20	0.1380	0.1383	37.20	0.1337	0.1339
37.80	0.1373	0.1376	37.80	0.1382	0.1385	37.80	0.1355	0.1359	37.80	0.1376	0.1379	37.80	0.1337	0.1340
38.40	0.1346	0.1350	38.40	0.1392	0.1395	38.40	0.1373	0.1376	38.40	0.1379	0.1382	38.40	0.1335	0.1337
39.00	0.1376	0.1379	39.00	0.1384	0.1387	39.00	0.1374	0.1377	39.00	0.1379	0.1382	39.00	0.1345	0.1348
39.60	0.1372	0.1375	39.60	0.1421	0.1424	39.60	0.1404	0.1407	39.60	0.1373	0.1376	39.60	0.1334	0.1336

40.20	0.1379	0.1383	40.20	0.1379	0.1383	40.20	0.1369	0.1372	40.20	0.1405	0.1407	40.20	0.1372	0.1374
40.80	0.1379	0.1382	40.80	0.1382	0.1386	40.80	0.1357	0.1360	40.80	0.1385	0.1388	40.80	0.1343	0.1345
41.40	0.1372	0.1375	41.40	0.1400	0.1404	41.40	0.1377	0.1380	41.40	0.1375	0.1379	41.40	0.1339	0.1341
42.00	0.1372	0.1376	42.00	0.1370	0.1373	42.00	0.1372	0.1375	42.00	0.1386	0.1390	42.00	0.1347	0.1350
42.60	0.1379	0.1383	42.60	0.1403	0.1405	42.60	0.1380	0.1383	42.60	0.1376	0.1379	42.60	0.1329	0.1332
43.20	0.1372	0.1376	43.20	0.1386	0.1389	43.20	0.1376	0.1379	43.20	0.1378	0.1381	43.20	0.1341	0.1343
43.80	0.1373	0.1376	43.80	0.1358	0.1362	43.80	0.1342	0.1346	43.80	0.1379	0.1382	43.80	0.1342	0.1344
44.40	0.1372	0.1376	44.40	0.1403	0.1407	44.40	0.1391	0.1394	44.40	0.1374	0.1378	44.40	0.1323	0.1326
45.00	0.1385	0.1388	45.00	0.1394	0.1397	45.00	0.1376	0.1380	45.00	0.1377	0.1380	45.00	0.1342	0.1345
45.60	0.1381	0.1384	45.60	0.1389	0.1392	45.60	0.1373	0.1376	45.60	0.1382	0.1386	45.60	0.1339	0.1341
46.20	0.1375	0.1378	46.20	0.1389	0.1392	46.20	0.1375	0.1378	46.20	0.1379	0.1382	46.20	0.1345	0.1347
46.80	0.1372	0.1376	46.80	0.1373	0.1376	46.80	0.1354	0.1358	46.80	0.1379	0.1383	46.80	0.1347	0.1349
47.40	0.1375	0.1379	47.40	0.1409	0.1413	47.40	0.1389	0.1393	47.40	0.1379	0.1382	47.40	0.1336	0.1339
48.00	0.1351	0.1354	48.00	0.1376	0.1380	48.00	0.1367	0.1371	48.00	0.1380	0.1384	48.00	0.1337	0.1341
48.60	0.1374	0.1377	48.60	0.1398	0.1401	48.60	0.1365	0.1368	48.60	0.1388	0.1392	48.60	0.1341	0.1344
49.20	0.1372	0.1376	49.20	0.1382	0.1384	49.20	0.1376	0.1379	49.20	0.1372	0.1375	49.20	0.1331	0.1335
49.80	0.1372	0.1375	49.80	0.1370	0.1373	49.80	0.1355	0.1358	49.80	0.1388	0.1391	49.80	0.1339	0.1342
50.40	0.1373	0.1376	50.40	0.1396	0.1399	50.40	0.1372	0.1376	50.40	0.1373	0.1376	50.40	0.1322	0.1325
51.00	0.1375	0.1378	51.00	0.1398	0.1402	51.00	0.1389	0.1393	51.00	0.1373	0.1376	51.00	0.1327	0.1330
51.60	0.1381	0.1384	51.60	0.1366	0.1370	51.60	0.1353	0.1356	51.60	0.1383	0.1387	51.60	0.1335	0.1338
52.20	0.1373	0.1376	52.20	0.1396	0.1399	52.20	0.1381	0.1384	52.20	0.1374	0.1377	52.20	0.1330	0.1334
52.80	0.1379	0.1382	52.80	0.1362	0.1365	52.80	0.1357	0.1360	52.80	0.1377	0.1380	52.80	0.1332	0.1335
53.40	0.1373	0.1376	53.40	0.1391	0.1394	53.40	0.1367	0.1370	53.40	0.1383	0.1386	53.40	0.1330	0.1333
54.00	0.1351	0.1354	54.00	0.1390	0.1394	54.00	0.1378	0.1381	54.00	0.1373	0.1376	54.00	0.1325	0.1329
54.60	0.1377	0.1380	54.60	0.1363	0.1366	54.60	0.1356	0.1360	54.60	0.1386	0.1389	54.60	0.1336	0.1340
55.20	0.1372	0.1375	55.20	0.1382	0.1385	55.20	0.1372	0.1376	55.20	0.1377	0.1380	55.20	0.1329	0.1332

55.80	0.1379	0.1383	55.80	0.1395	0.1397	55.80	0.1372	0.1376	55.80	0.1376	0.1379	55.80	0.1326	0.1329
56.40	0.1372	0.1375	56.40	0.1373	0.1376	56.40	0.1355	0.1358	56.40	0.1377	0.1381	56.40	0.1326	0.1330
57.00	0.1376	0.1379	57.00	0.1398	0.1402	57.00	0.1389	0.1393	57.00	0.1378	0.1381	57.00	0.1325	0.1328
57.60	0.1372	0.1375	57.60	0.1370	0.1374	57.60	0.1355	0.1358	57.60	0.1376	0.1379	57.60	0.1323	0.1327
58.20	0.1372	0.1375	58.20	0.1388	0.1391	58.20	0.1370	0.1373	58.20	0.1378	0.1382	58.20	0.1328	0.1331
58.80	0.1372	0.1375	58.80	0.1374	0.1377	58.80	0.1370	0.1373	58.80	0.1374	0.1377			
59.40	0.1373	0.1375	59.40	0.1382	0.1386	59.40	0.1364	0.1367	59.40	0.1383	0.1386			
60.00	0.1374	0.1377	60.00	0.1380	0.1383	60.00	0.1372	0.1375	60.00	0.1378	0.1381			

Table C12 Tabulated time series data for the α=16°: θ=30° arced labyrinth weir at H/P=0.8

RM1-WM0			RM0-WM1			RM0-WM2			RM1-WM2			RM1-WM3		
Cell Count:	1553185		*Cell Count:*	1584166		*Cell Count:*	3253999		*Cell Count:*	3609796		*Cell Count:*	7152511	
Q	235.54	[L/s]	Q	234.62	[L/s]	Q	234.62	[L/s]	Q	235.54	[L/s]	Q	235.54	[L/s]
H	0.153	[m]	H	0.155	[m]	H	0.154	[m]	H	0.154	[m]	H	0.150	[m]
H/P	0.754	[-]	H/P	0.761	[-]	H/P	0.759	[-]	H/P	0.759	[-]	H/P	0.740	[-]
C_d	0.425	[-]	C_d	0.418	[-]	C_d	0.420	[-]	C_d	0.421	[-]	C_d	0.438	[-]
$C_{d\text{-}emp}$	0.409	[-]	$C_{d\text{-}emp}$	0.406	[-]	$C_{d\text{-}emp}$	0.407	[-]	$C_{d\text{-}emp}$	0.407	[-]	$C_{d\text{-}emp}$	0.415	[-]
ε_{Cd}	4.01%	[%]	ε_{Cd}	2.95%	[%]	ε_{Cd}	3.19%	[%]	ε_{Cd}	3.57%	[%]	ε_{Cd}	5.45%	[%]
Time [s]	h [m]	H [m]	Time [s]	h [m]	H [m]	Time [s]	h [m]	H [m]	Time [s]	h [m]	H [m]	Time [s]	h [m]	H [m]
0.00	0.1626	0.1626	0.00	0.1626	0.1626	0.00	0.1627	0.1627	0.00	0.1626	0.1626	0.00	0.1626	0.1626
0.60	0.1635	0.1635	0.60	0.1645	0.1645	0.60	0.1645	0.1645	0.60	0.1635	0.1635	0.60	0.1635	0.1635
1.20	0.1646	0.1646	1.20	0.1802	0.1804	1.20	0.1800	0.1803	1.20	0.1646	0.1646	1.20	0.1646	0.1646
1.80	0.1630	0.1630	1.80	0.1829	0.1831	1.80	0.1828	0.1831	1.80	0.1631	0.1631	1.80	0.1631	0.1631
2.40	0.1524	0.1527	2.40	0.1799	0.1803	2.40	0.1797	0.1803	2.40	0.1525	0.1528	2.40	0.1526	0.1529
3.00	0.1465	0.1473	3.00	0.1621	0.1635	3.00	0.1621	0.1636	3.00	0.1467	0.1475	3.00	0.1468	0.1475
3.60	0.1560	0.1567	3.60	0.1602	0.1616	3.60	0.1602	0.1614	3.60	0.1557	0.1564	3.60	0.1555	0.1561
4.20	0.1421	0.1428	4.20	0.1518	0.1528	4.20	0.1511	0.1520	4.20	0.1405	0.1413	4.20	0.1404	0.1413
4.80	0.1347	0.1356	4.80	0.1406	0.1411	4.80	0.1398	0.1404	4.80	0.1331	0.1340	4.80	0.1326	0.1336
5.40	0.1444	0.1449	5.40	0.1544	0.1547	5.40	0.1541	0.1544	5.40	0.1459	0.1463	5.40	0.1451	0.1455
6.00	0.1544	0.1546	6.00	0.1618	0.1619	6.00	0.1605	0.1605	6.00	0.1508	0.1510	6.00	0.1505	0.1507
6.60	0.1373	0.1376	6.60	0.1535	0.1537	6.60	0.1532	0.1535	6.60	0.1349	0.1351	6.60	0.1334	0.1337
7.20	0.1545	0.1548	7.20	0.1583	0.1585	7.20	0.1584	0.1587	7.20	0.1560	0.1565	7.20	0.1562	0.1566
7.80	0.1467	0.1471	7.80	0.1645	0.1650	7.80	0.1651	0.1657	7.80	0.1520	0.1524	7.80	0.1488	0.1493
8.40	0.1412	0.1415	8.40	0.1700	0.1703	8.40	0.1730	0.1733	8.40	0.1491	0.1495	8.40	0.1452	0.1456

9.00	0.1646	0.1650	9.00	0.1708	0.1716	9.00	0.1697	0.1703	9.00	0.1530	0.1534	9.00	0.1481	0.1485
9.60	0.1547	0.1553	9.60	0.1489	0.1499	9.60	0.1514	0.1523	9.60	0.1632	0.1637	9.60	0.1617	0.1622
10.20	0.1372	0.1379	10.20	0.1489	0.1496	10.20	0.1535	0.1541	10.20	0.1411	0.1417	10.20	0.1386	0.1391
10.80	0.1489	0.1496	10.80	0.1517	0.1525	10.80	0.1566	0.1575	10.80	0.1456	0.1463	10.80	0.1402	0.1410
11.40	0.1494	0.1498	11.40	0.1582	0.1585	11.40	0.1563	0.1566	11.40	0.1511	0.1516	11.40	0.1454	0.1459
12.00	0.1449	0.1454	12.00	0.1472	0.1477	12.00	0.1474	0.1477	12.00	0.1509	0.1514	12.00	0.1444	0.1449
12.60	0.1443	0.1447	12.60	0.1541	0.1543	12.60	0.1520	0.1523	12.60	0.1392	0.1395	12.60	0.1378	0.1381
13.20	0.1430	0.1433	13.20	0.1565	0.1568	13.20	0.1581	0.1584	13.20	0.1476	0.1479	13.20	0.1440	0.1444
13.80	0.1524	0.1527	13.80	0.1635	0.1639	13.80	0.1590	0.1596	13.80	0.1495	0.1498	13.80	0.1428	0.1431
14.40	0.1542	0.1548	14.40	0.1678	0.1684	14.40	0.1691	0.1697	14.40	0.1566	0.1572	14.40	0.1519	0.1523
15.00	0.1558	0.1563	15.00	0.1539	0.1545	15.00	0.1517	0.1523	15.00	0.1561	0.1565	15.00	0.1550	0.1554
15.60	0.1534	0.1539	15.60	0.1525	0.1531	15.60	0.1538	0.1541	15.60	0.1450	0.1455	15.60	0.1488	0.1493
16.20	0.1474	0.1478	16.20	0.1547	0.1553	16.20	0.1553	0.1563	16.20	0.1501	0.1505	16.20	0.1505	0.1510
16.80	0.1532	0.1538	16.80	0.1564	0.1571	16.80	0.1560	0.1566	16.80	0.1495	0.1501	16.80	0.1477	0.1483
17.40	0.1512	0.1517	17.40	0.1561	0.1566	17.40	0.1538	0.1544	17.40	0.1534	0.1540	17.40	0.1502	0.1506
18.00	0.1494	0.1499	18.00	0.1476	0.1481	18.00	0.1483	0.1486	18.00	0.1508	0.1514	18.00	0.1488	0.1493
18.60	0.1505	0.1509	18.60	0.1476	0.1480	18.60	0.1474	0.1477	18.60	0.1450	0.1454	18.60	0.1420	0.1424
19.20	0.1458	0.1462	19.20	0.1611	0.1613	19.20	0.1581	0.1584	19.20	0.1474	0.1478	19.20	0.1440	0.1443
19.80	0.1516	0.1519	19.80	0.1597	0.1600	19.80	0.1596	0.1599	19.80	0.1522	0.1525	19.80	0.1519	0.1521
20.40	0.1528	0.1532	20.40	0.1603	0.1608	20.40	0.1596	0.1602	20.40	0.1535	0.1539	20.40	0.1518	0.1521
21.00	0.1493	0.1499	21.00	0.1518	0.1523	21.00	0.1514	0.1520	21.00	0.1486	0.1492	21.00	0.1476	0.1480
21.60	0.1553	0.1558	21.60	0.1555	0.1559	21.60	0.1547	0.1550	21.60	0.1535	0.1540	21.60	0.1509	0.1514
22.20	0.1535	0.1538	22.20	0.1630	0.1634	22.20	0.1627	0.1630	22.20	0.1547	0.1550	22.20	0.1516	0.1519
22.80	0.1541	0.1545	22.80	0.1508	0.1513	22.80	0.1502	0.1508	22.80	0.1553	0.1557	22.80	0.1488	0.1492
23.40	0.1483	0.1489	23.40	0.1553	0.1558	23.40	0.1544	0.1547	23.40	0.1525	0.1531	23.40	0.1469	0.1474
24.00	0.1480	0.1484	24.00	0.1464	0.1468	24.00	0.1471	0.1474	24.00	0.1493	0.1497	24.00	0.1491	0.1495

24.60	0.1487	0.1491	24.60	0.1555	0.1557	24.60	0.1541	0.1544	24.60	0.1484	0.1488	24.60	0.1441	0.1445
25.20	0.1516	0.1519	25.20	0.1577	0.1579	25.20	0.1587	0.1587	25.20	0.1516	0.1519	25.20	0.1503	0.1506
25.80	0.1557	0.1560	25.80	0.1553	0.1556	25.80	0.1547	0.1550	25.80	0.1578	0.1580	25.80	0.1518	0.1520
26.40	0.1520	0.1523	26.40	0.1509	0.1512	26.40	0.1511	0.1511	26.40	0.1524	0.1527	26.40	0.1482	0.1485
27.00	0.1477	0.1480	27.00	0.1561	0.1564	27.00	0.1566	0.1569	27.00	0.1487	0.1491	27.00	0.1474	0.1478
27.60	0.1534	0.1537	27.60	0.1552	0.1555	27.60	0.1563	0.1566	27.60	0.1533	0.1536	27.60	0.1511	0.1514
28.20	0.1553	0.1556	28.20	0.1560	0.1563	28.20	0.1560	0.1563	28.20	0.1556	0.1559	28.20	0.1521	0.1525
28.80	0.1545	0.1547	28.80	0.1541	0.1544	28.80	0.1535	0.1538	28.80	0.1547	0.1549	28.80	0.1494	0.1497
29.40	0.1512	0.1515	29.40	0.1513	0.1516	29.40	0.1511	0.1514	29.40	0.1514	0.1516	29.40	0.1512	0.1515
30.00	0.1464	0.1468	30.00	0.1491	0.1495	30.00	0.1505	0.1508	30.00	0.1485	0.1488	30.00	0.1468	0.1472
30.60	0.1545	0.1548	30.60	0.1567	0.1570	30.60	0.1569	0.1572	30.60	0.1540	0.1543	30.60	0.1499	0.1502
31.20	0.1530	0.1532	31.20	0.1561	0.1564	31.20	0.1557	0.1560	31.20	0.1542	0.1544	31.20	0.1503	0.1505
31.80	0.1529	0.1531	31.80	0.1516	0.1520	31.80	0.1532	0.1535	31.80	0.1508	0.1510	31.80	0.1482	0.1485
32.40	0.1522	0.1525	32.40	0.1524	0.1527	32.40	0.1520	0.1526	32.40	0.1546	0.1548	32.40	0.1517	0.1519
33.00	0.1510	0.1513	33.00	0.1565	0.1568	33.00	0.1569	0.1572	33.00	0.1545	0.1547	33.00	0.1462	0.1464
33.60	0.1507	0.1510	33.60	0.1560	0.1563	33.60	0.1569	0.1572	33.60	0.1518	0.1520	33.60	0.1509	0.1511
34.20	0.1552	0.1556	34.20	0.1546	0.1550	34.20	0.1538	0.1541	34.20	0.1551	0.1554	34.20	0.1542	0.1545
34.80	0.1524	0.1528	34.80	0.1530	0.1534	34.80	0.1529	0.1532	34.80	0.1518	0.1521	34.80	0.1505	0.1508
35.40	0.1521	0.1525	35.40	0.1525	0.1528	35.40	0.1526	0.1529	35.40	0.1539	0.1542	35.40	0.1500	0.1503
36.00	0.1510	0.1513	36.00	0.1542	0.1546	36.00	0.1535	0.1538	36.00	0.1522	0.1525	36.00	0.1483	0.1485
36.60	0.1535	0.1539	36.60	0.1566	0.1570	36.60	0.1563	0.1569	36.60	0.1537	0.1541	36.60	0.1506	0.1509
37.20	0.1522	0.1526	37.20	0.1519	0.1523	37.20	0.1517	0.1523	37.20	0.1526	0.1530	37.20	0.1519	0.1522
37.80	0.1533	0.1536	37.80	0.1539	0.1543	37.80	0.1532	0.1538	37.80	0.1535	0.1538	37.80	0.1483	0.1485
38.40	0.1526	0.1529	38.40	0.1542	0.1545	38.40	0.1544	0.1547	38.40	0.1542	0.1545	38.40	0.1497	0.1499
39.00	0.1517	0.1520	39.00	0.1550	0.1553	39.00	0.1550	0.1553	39.00	0.1540	0.1542	39.00	0.1503	0.1505
39.60	0.1533	0.1536	39.60	0.1557	0.1561	39.60	0.1544	0.1547	39.60	0.1526	0.1529	39.60	0.1505	0.1508

40.20	0.1545	0.1548	40.20	0.1561	0.1565	40.20	0.1547	0.1553	40.20	0.1546	0.1549	40.20	0.1522	0.1525
40.80	0.1531	0.1534	40.80	0.1507	0.1511	40.80	0.1517	0.1520	40.80	0.1527	0.1531	40.80	0.1502	0.1505
41.40	0.1534	0.1537	41.40	0.1561	0.1565	41.40	0.1553	0.1557	41.40	0.1562	0.1565	41.40	0.1490	0.1493
42.00	0.1527	0.1530	42.00	0.1539	0.1543	42.00	0.1535	0.1538	42.00	0.1540	0.1543	42.00	0.1504	0.1507
42.60	0.1533	0.1536	42.60	0.1543	0.1546	42.60	0.1538	0.1541	42.60	0.1532	0.1535	42.60	0.1513	0.1516
43.20	0.1515	0.1519	43.20	0.1539	0.1543	43.20	0.1535	0.1541	43.20	0.1541	0.1545	43.20	0.1500	0.1504
43.80	0.1515	0.1519	43.80	0.1531	0.1535	43.80	0.1526	0.1532	43.80	0.1535	0.1539	43.80	0.1502	0.1506
44.40	0.1523	0.1526	44.40	0.1545	0.1548	44.40	0.1544	0.1547	44.40	0.1529	0.1533	44.40	0.1501	0.1505
45.00	0.1533	0.1537	45.00	0.1567	0.1570	45.00	0.1560	0.1563	45.00	0.1542	0.1546	45.00	0.1502	0.1506
45.60	0.1547	0.1550	45.60	0.1534	0.1537	45.60	0.1529	0.1532	45.60	0.1538	0.1542	45.60	0.1487	0.1490
46.20	0.1538	0.1542	46.20	0.1538	0.1542	46.20	0.1541	0.1544	46.20	0.1543	0.1547	46.20	0.1506	0.1510
46.80	0.1518	0.1522	46.80	0.1549	0.1553	46.80	0.1541	0.1544	46.80	0.1535	0.1539	46.80	0.1503	0.1507
47.40	0.1536	0.1540	47.40	0.1554	0.1557	47.40	0.1557	0.1560	47.40	0.1538	0.1542	47.40	0.1498	0.1502
48.00	0.1539	0.1543	48.00	0.1535	0.1538	48.00	0.1538	0.1541	48.00	0.1546	0.1550	48.00	0.1505	0.1509
48.60	0.1542	0.1545	48.60	0.1557	0.1560	48.60	0.1538	0.1541	48.60	0.1551	0.1554	48.60	0.1498	0.1502
49.20	0.1515	0.1519	49.20	0.1542	0.1545	49.20	0.1535	0.1538	49.20	0.1534	0.1537	49.20	0.1504	0.1508
49.80	0.1513	0.1516	49.80	0.1546	0.1550	49.80	0.1541	0.1544	49.80	0.1530	0.1534	49.80	0.1503	0.1507
50.40	0.1536	0.1540	50.40	0.1558	0.1562	50.40	0.1544	0.1547	50.40	0.1531	0.1535	50.40	0.1494	0.1498
51.00	0.1542	0.1545	51.00	0.1558	0.1562	51.00	0.1550	0.1553	51.00	0.1551	0.1554	51.00	0.1502	0.1505
51.60	0.1543	0.1546	51.60	0.1535	0.1538	51.60	0.1529	0.1532	51.60	0.1543	0.1546	51.60	0.1506	0.1509
52.20	0.1527	0.1531	52.20	0.1550	0.1553	52.20	0.1544	0.1547	52.20	0.1547	0.1550	52.20	0.1510	0.1513
52.80	0.1525	0.1529	52.80	0.1541	0.1544	52.80	0.1541	0.1547	52.80	0.1544	0.1548	52.80	0.1506	0.1510
53.40	0.1542	0.1546	53.40	0.1548	0.1552	53.40	0.1544	0.1547	53.40	0.1546	0.1549	53.40	0.1508	0.1512
54.00	0.1532	0.1536	54.00	0.1545	0.1548	54.00	0.1535	0.1538	54.00	0.1541	0.1545	54.00	0.1510	0.1514
54.60	0.1525	0.1529	54.60	0.1552	0.1555	54.60	0.1550	0.1553	54.60	0.1538	0.1542	54.60	0.1504	0.1508
55.20	0.1532	0.1536	55.20	0.1529	0.1533	55.20	0.1526	0.1529	55.20	0.1540	0.1543	55.20	0.1492	0.1495

55.80	0.1528	0.1531	55.80	0.1567	0.1571	55.80	0.1553	0.1557	55.80	0.1549	0.1552	55.80	0.1511	0.1515
56.40	0.1541	0.1545	5.40	0.1547	0.1550	56.40	0.1538	0.1541	56.40	0.1542	0.1546	56.40	0.1507	0.1511
57.00	0.1531	0.1535	57.00	0.1538	0.1542	57.00	0.1535	0.1538	57.00	0.1536	0.1540	57.00	0.1501	0.1504
57.60	0.1524	0.1527	57.60	0.1551	0.1556	57.60	0.1541	0.1547	57.60	0.1543	0.1546	57.60	0.1512	0.1515
58.20	0.1538	0.1541	58.20	0.1545	0.1548	58.20	0.1535	0.1538	58.20	0.1546	0.1549	58.20	0.1508	0.1511
58.80	0.1537	0.1541	58.80	0.1543	0.1546	58.80	0.1544	0.1547	58.80	0.1558	0.1561	58.80	0.1493	0.1496
59.40	0.1533	0.1538	59.40	0.1549	0.1553	59.40	0.1553	0.1557	59.40	0.1537	0.1541	59.40	0.1518	0.1522
60.00	0.1535	0.1539	60.00	0.1537	0.1541	60.00	0.1532	0.1535	60.00	0.1543	0.1547	60.00	0.1506	0.1510